Queen Mary
University of London

THESIS SUBMITTED FOR THE DEGREE OF
DOCTOR OF PHILOSOPHY

Insights into Black Hole Microstates from AdS$_3$ Holography

MARCEL R. R. HUGHES

Supervisor

DR RODOLFO RUSSO

July 28, 2021

Centre for Research in String Theory
School of Physics and Astronomy
Queen Mary University of London

The brushwood we gather – stack it together, it makes a hut; pull it apart, a field once more. We find beauty not in the thing itself but in the patterns of shadows, the light and the darkness, that one thing against another creates. Were it not for shadows, there would be no beauty.

– Junichirō Tanizaki, *In praise of shadows*

One day I will find the right words, and they will be simple.

– Jack Kerouac, *The Dharma Bums*

Declaration

I, Marcel R. R. Hughes, confirm that the research included within this thesis is my own work or that where it has been carried out in collaboration with, or supported by others, that this is duly acknowledged below and my contribution indicated. Previously published material is also acknowledged below.

I attest that I have exercised reasonable care to ensure that the work is original, and does not to the best of my knowledge break any UK law, infringe any third party's copyright or other Intellectual Property Right, or contain any confidential material.

I accept that the College has the right to use plagiarism detection software to check the electronic version of the thesis.

I confirm that this thesis has not been previously submitted for the award of a degree by this or any other university.

The copyright of this thesis rests with the author and no quotation from it or information derived from it may be published without the prior written consent of the author.

Signature:

Date: July 28, 2021

Details of collaboration and publications:

This thesis describes research carried out with my supervisor Rodolfo Russo and Stefano Giusto, which was published in [1] and [2] with the latter being also in collaboration with Nejc Čeplak. This thesis also describes research carried out solely in collaboration with Nejc Čeplak, published in [3]. It also contains some unpublished material. Where other sources have been used, they are cited in the bibliography.

Abstract

In contrast to the more standard approach of furthering the program of black hole microstates using holography, this thesis instead uses developments in black hole microstates to learn about questions of holography.

We derive the connected tree-level part of 4-point holographic correlators in AdS$_3 \times S^3 \times \mathcal{M}^4$ (where $\mathcal{M}^4$ is T^4 or $K3$) involving two multi-trace and two single-trace operators. These connected correlators are obtained by studying a heavy-heavy-light-light (HHLL) correlation function in the formal limit where the heavy operators become light (LLLL). These results provide a window into higher-point holographic correlators of single-particle operators. We find that the correlators involving multi-trace operators are compactly written in terms of Bloch-Wigner-Ramakrishnan functions. We also extract anomalous dimensions and 3-point couplings for the non-BPS minimal twist double-trace operators at order $1/c$ and find some positive anomalous dimensions at spin zero and two in the K3 case.

This is followed by a study of the Regge limit of various HHLL and LLLL AdS$_3$ holographic 4-point correlators, in the tree-level supergravity approximation, providing explicit checks of the relation between bulk eikonal phases and anomalous dimensions of certain double-trace operators. The pure heavy operators considered, dual to asymptotically AdS$_3 \times S^3$ regular geometries, have conformal dimensions proportional to the central charge. Deviation from AdS$_3 \times S^3$ is parametrised by a scale μ, related to the heavy operator's conformal dimension. We work perturbatively in μ and derive all-order relations between the bulk phase shift and the Regge limit OPE data of a class of heavy-light multi-trace operators exchanged in the cross-channel. Specifically, we show that the minimal solution to the crossing equations relevant for the conical defect geometries is different to that for the microstate geometries dual to pure states.

Acknowledgements

The mountains are calling and I must go.

– John Muir

Contents

Chapter 1

Introduction

1.1 What is a black hole?

Solving the gravitational field equations exactly was likely to be impossible, Albert Einstein concluded on completing the theory of general relativity (GR). Having only found approximate solutions himself, just over a month after publishing the paper detailing their final form, Karl Schwarzschild released an exact solution to the vacuum Einstein field equations in four dimensions[1]

$$ds^2 = -\left(1 - \frac{2G_N M}{r}\right) dt^2 + \left(1 - \frac{2G_N M}{r}\right)^{-1} dr^2 + r^2 \left(d\theta^2 + \sin^2\theta \, d\phi^2\right) , \qquad (1.1)$$

for a mass M at the origin $r = 0$ (using spherical coordinates θ, ϕ). Decades later, it was understood that the Schwarzschild solution describes not only the spacetime around a point mass, but also a black hole. Coined in the late 60s by John Wheeler, this term refers to a body with enough mass to gravitationally trap light within a region, which for the Schwarzschild black hole is

$$r < r_H = 2G_N M . \qquad (1.2)$$

The global (causal) structure of the Schwarzschild solution, and other black hole solutions subsequently discovered, rigorously defines the concept of such event horizons [4,5] – at which (1.1) suggests something special should happen. For a local observer, however, the horizon of a large enough black hole in general relativity is an unremarkable place despite the sealed fate of such an intrepid (or daft) explorer. The condition on the size of the black hole is to remove the separate issue of tidal forces at horizon scales of small black holes – this is because such tidal stretching and compression scales [4] as $\sim r_H^{-2}$. Despite the diverging nature of one of the metric components in

---

[1]Throughout this thesis, the mostly plus convention for the metric is used, along with units in which $c = \hbar = k_B = 1$.

(1.1), it is suggested from the Kretschmann quadratic invariant – one particular gauge-invariant measure of curvature – that there is no region of diverging curvature around the Schwarzschild horizon

$$\mathcal{K} \equiv R^{\mu\nu\sigma\rho} R_{\mu\nu\sigma\rho} \sim \frac{G_N^2 M^2}{r^6} \ , \tag{1.3}$$

and the diverging of metric components of (1.1) at $r = r_H$ is only symptomatic of poorly chosen coordinates with which to describe the geometry. Despite this reassuring discovery, the origin at $r = 0$ in (1.1) *is* a place of divergent curvature – a true curvature singularity. In spite of the ominous nature of singularities in spacetime, from an effective field theory perspective it is not surprising that such singularities exist in GR – and due to various singularity theorems [5], are inevitable. Since the regime of validity of GR breaks down near the predicted singularity, where curvatures become of the order[2] $1/\ell_{pl}^2$, it is expected that they are resolved in any consistent theory of quantum gravitational phenomena.

One approach to this problem is string theory, which at the most basic level, aims at generalising quantum field theory (QFT) to a theory of extended strings rather than point particles (see [6–8] for an introduction, here we give simply some qualitative facts relevant to black holes in string theory). The length scale at which string effects become important is the string length $\ell_s = \alpha'^{1/2} \sim T_{\text{F1}}^{-1/2}$ where T_{F1} is the fundamental string (F1) tension and α' is know as the Regge slope or inverse tension parameter. String theory does not a priori set a (fixed) hierarchy between the string and Planck scales though they are expected to be of similar orders. By considering graviton scattering one finds that the strength of gravity in 10-dimensions scales as $G_N^{(10)} \sim g_s^2 \alpha'^4$ where g_s is the string coupling[3] and so the tension scales as $T_{\text{F1}} \sim g_s^{1/2} (G_N^{(10)})^{-1/4}$. The perturbative string description of string theory (valid[4] for small α' and small g_s) was later supplemented by the discovery of non-perturbative (p+1)-dimensional extended objects called Dp-branes. Unlike the energy of fundamental strings, D-branes have an energy (or tension) scaling with[5] g_s^{-1} and so within perturbative string theory they are very massive. D-branes are thus solitonic in nature, not visible as intermediate states in perturbative string scattering (hence why they were missed for many years),

---

[2]The natural scale with dimensions of length at which quantum gravitational phenomena become important is the Planck length, defined in terms of other fundamental constants as $\ell_{pl} = \sqrt{\frac{G_N \hbar}{c^3}} \sim 10^{-35} m$ or in the natural units adopted here $\ell_{pl} = G_N^{1/2}$. Equivalently, one can use the energy scale of the Planck mass $M_{pl} = G_N^{-1/2}$.

[3]Note that g_s is not a free parameter of the theory since it is set by the background value of the dilaton scalar field ϕ_0 via $g_s = e^{\phi_0}$.

[4]The expansion in g_s is a "loop" expansion and that in α' controls the massive higher string mode excitations.

[5]The full scaling of the physical Dp-brane tension depends on the value of p, *i.e.* the number of spatial dimensions in which the brane is extended, and is given by $T_p \sim g_s^{-1} \alpha'^{-(p+1)/2}$.

but change the background around which one does perturbation theory if placed in a system. Supergravity becomes a good low energy effective description of the massless degrees of freedom of perturbative string theory when the massive string modes and string loops are neglectable – this is the case for $g_s \ll 1$ and energies much lower than the scale of α'. In this regime, the induced theory on the world volume of a D-brane (or a bound state of many coincident branes) is a gauge theory (the gauge group depends on the number and type of branes forming the bound state). Being very massive in this regime, a stack of many D-branes will backreact on the background spacetime in which they are placed producing a black hole metric. The black hole will generically have a number of charges associated to the various background gauge fields that couple to the D-branes used. Thus it is that black holes can be studied in string theory, though not just at the level of the classical metric. We will be interested in a particular black hole, arising from the bound state of two types of D-branes, after a brief detour to the semi-classical entropy of black holes.

1.1.1 Black hole entropy and the information problem

In the early 1970s, a picture of black holes was emerging that they could be thought of as thermodynamic objects. Some gravitational quantities appeared to behave like particular thermodynamic counterparts, as emphasised in the laws of black hole mechanics [9]. Most notably, the surface gravity of the black hole (a measure of the non-affine parametrisation of the null geodesics generating the horizon) behaved as a temperature (*i.e.* it is constant over the horizon) and the horizon area (which is non-decreasing in any process, shown for the Kerr black hole in [10]) as a thermodynamical entropy. These analogies were further solidified in 1975 with Hawking's semi-classical computation in [11] of a scalar quantum field propagating in a collapsing black hole background. This demonstrated that, due to the formation of a smooth classical horizon, an asymptotic observer sees an approximately thermal flux of particles from the region around the black hole horizon. Thus, the black hole has a physical temperature and so from [9], an intrinsic entropy

$$S = \frac{A}{4G_N} \ , \tag{1.4}$$

for a horizon surface area A. Two interesting comments on this result are: firstly, this entropy does not scale with the size (volume) of the system as is expected from a thermodynamically extrinsic quantity, and secondly, when solving the equations of a theory exactly, it is not expected that there will be an entropy associated to it. From the statistical mechanics point of view the immediate question is: where are the corresponding e^S microstates of this system, a coarse-graining of which yields the entropy (1.4)? The no-hair theorems in GR appear to contradict this observation, since they demand that

a black hole can only be described by its mass, angular momentum and charges; certainly this doesn't allow for e^S states. Another consequence of Hawking's calculation is that a black hole is not black; it radiates and through this so-called Hawking process, the black hole will lose mass, albeit slowly.

Thus it seems that classical black hole solutions of general relativity predict their own (ill) fortune; not only due to the presence of a singularity indicating a breakdown of the theory, but also by the existence of a horizon which necessarily yields Hawking radiation. This latter point, however, gives rise to potentially a far greater problem than loss of control over our effective theory. Assuming semi-classical local physics in the region around a smooth horizon, it then appears that the process of black hole formation from a prepared pure state of matter, followed by evaporation of the black hole via the Hawking process into a thermal state of radiation (a mixed state), is not unitary [12]. A natural conjecture is then that, since quantum gravity effects become important in the late stages of collapse, a consistent quantum gravitational analysis would generate corrections to the semi-classical result of Hawking. In fact, by the small corrections theorem of [13], it transpires that exactly these types of corrections cannot be sufficient to resolve the issue at hand. With these points in mind, it is natural to expect that in the UV-complete theory something steps in to make *large* corrections to the story outlined above.

Paradigms of resolution to this issue are generally via the use of non-local phenomena (see for instance [14–16] and references therein), or by appealing to remnants[6] of various kinds (see for instance [17] for a review of some of these ideas). All proposed resolutions to date have issues and critiques, some of which can be found in [18, 19].

1.2 The fuzzball paradigm

Another such method of resolution is that of the fuzzball paradigm [20]. It argues that the classical black hole is instead replaced by a string theory motivated "compact object" at a scale slightly above horizon scales, which is stable by dint of non-trivial topology. In this framework, the classical black hole is treated as a thermal ensemble of fuzzballs – these act as microstates to the black hole. The introduction of horizon-scale microstructure in general relativity would always be in tension with the Buchdahl inequality [21, 22] which states that, under 'reasonable' assumptions, a spherically-symmetric and static distribution of matter will collapse to a black hole for radii

$$r < r_B = \frac{9}{4} G_N M \ . \tag{1.5}$$

---

[6]A remnant refers to a wide class of ideas that somehow stabilise the evaporating black hole once it nears the end point of this process, or otherwise argues for the final state having a subsystem containing the information of the initial collapse that formed the black hole.

By comparison with (1.2), this Buchdahl radius r_B is larger than the Schwarzschild radius with $r_B - r_H = \frac{1}{4}G_N M$ – certainly as compared with the fuzzball length scale

$$r_{\text{fuzzball}} - r_H \sim G_N \ell_{pl} \; , \tag{1.6}$$

where $\ell_{pl} \sim 10^{-35} m$ is the Planck length. Of course, as with all theorems, the applicability of the Buchdahl bound hangs on the validity of its assumptions. Being a proposal within the framework of string theory, not GR, the fuzzball paradigm is able to escape the clutches of the Buchdahl theorem.

Emerging from string theory, fuzzballs are inherently quantum in nature and so do not admit a nice semi-classical description. However, certain coherent state-like objects will be well approximated by a solution to the relevant low energy effective theory: these states are generally referred to as microstate geometries and should have the asymptotic charges of the classical black hole and be horizon-less and non-singular.

1.2.1   The microstate geometry program

The best studied example in which to apply this framework is that of the D1-D5-P system in Figure 1.1. The general overarching setting is type IIB string theory on $\mathbb{R}^{1,4} \times S^1_y \times \mathcal{M}^4$ where the radius of the S^1_y is left unfixed and the four compact directions of $\mathcal{M}^4$ are taken to be string scale (one can consider either $\mathcal{M}^4 = T^4$ or $K3$). We use the coordinates (t, x^a) for the $\mathbb{R}^{1,4}$, y for the S^1_y and z^i for the $\mathcal{M}^4$. In this background are placed n_1 D1-branes and n_p units of momentum on the S^1_y, along with n_5 D5-branes on $S^1_y \times \mathcal{M}^4$. This system is 1/8-BPS[7] relative to the 32 real supercharges of the parent string theory – the two types of D-branes are each 1/2-BPS and the left-moving momentum excitations breaks half of what remains. The metric part of the supergravity solution describing this system is given in 6D by[8]

$$ds^2 = \frac{1}{\sqrt{Z_1 Z_5}} \left(- Z_p^- dt^2 + Z_p^+ dy^2 + \frac{2Q_p}{r^2} dt dy \right) + \sqrt{Z_1 Z_5} \, ds^2_{\mathbb{R}^4} \; ,$$
$$Z_1 = 1 + \frac{Q_1}{r^2} \quad , \quad Z_5 = 1 + \frac{Q_5}{r^2} \quad , \quad Z_p^\pm = 1 \pm \frac{Q_p}{r^2} \; , \tag{1.7}$$

where $ds^2_{\mathbb{R}^4}$ is the flat metric on $\mathbb{R}^4$ and the supergravity charges Q_1, Q_5 and Q_p are related to the number of D1-branes, D5-branes and units of momentum via

$$Q_1 = n_1 \frac{g_s \, \alpha'^3}{V_4} \quad , \quad Q_5 = n_5 \, g_s \, \alpha' \quad , \quad Q_p = n_p \, g_s^2 \, \alpha'^4 \; , \tag{1.8}$$

---

[7]This is shorthand for the state saturating the Bogomol'nyi–Prasad–Sommerfeld bound for 1/8 of the supersymmetries of the theory. This fraction of the supersymmetries are not spontaneously broken by the state.

[8]We neglect the four compact directions of $\mathcal{M}^4$ since all quantities we consider will not depend on them.
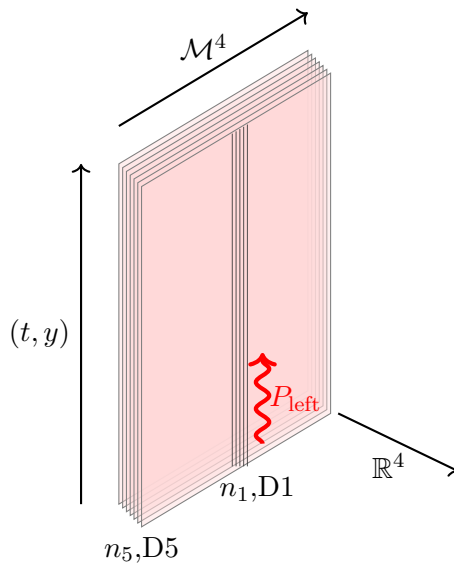
Figure 1.1: The D1-D5-P system in type IIB string theory compactified on $\mathbb{R}^{1,4} \times S_y^1 \times \mathcal{M}^4$ consists of many stacked D1- and D5-branes, both of which are wrapped along the macroscopic S_y^1 and the latter of which are also wrapped on the microscopic $\mathcal{M}^4$ directions. Left-moving momentum excitations are also added along the S_y^1 direction.

where V_4 is the volume of the compact 4-manifold $\mathcal{M}^4$. The asymptotically flat metric (1.7) will be referred to as the 3-charge black hole and yields the 5-dimensional 3-charge Strominger-Vafa extremal[9] black hole after a Kaluza-Klein (KK) reduction on the S_y^1 giving

$$ds^2 = -\left(Z_1 Z_5 Z_p^+\right)^{-\frac{2}{3}} dt^2 + \left(Z_1 Z_5 Z_p^+\right)^{\frac{1}{3}} \left(dr^2 + r^2 d\Omega_3^2\right) . \tag{1.9}$$

The 3-charge black hole (1.7) has a finite-sized horizon for $Q_p \neq 0$, which in these coordinates is located at $r = 0$.

In [23] Strominger and Vafa counted the BPS microstates of the D1-D5 brane system from the world volume gauge theory and matched this exactly to the entropy computed using (1.4) from the area of black hole in (1.9). This is a fundamental result in string theory and significantly motivated the study of these microstates that were counted (the method of counting used is via a protected index which simply counts states without requiring or yielding knowledge of what is being counted).

A long-standing effort to construct microstate geometries for the D1-D5-P system (equally, of the Strominger-Vafa black hole) has led to the discovery of large classes of horizon-less solutions to supergravity having the same asymptotic structure as the black hole, but with different infrared (IR) behaviours encoding microscopic details of the states (see for instance [24–27] and [28] for a recent review). Compared with the infinite AdS$_2$ (anti-de Sitter) throat of the black hole, the constructed microstate geometries have a finite throat, ending in a smooth "cap" above horizon scales. Despite

---

[9]Extremal here is in the sense that it has mass equal to angular momentum (in suitable units).

these families of solutions not covering the whole ensemble of the Strominger-Vafa black hole, they do provide an explicit semi-classical mechanism with which to replace the naive horizon with microscopic structure consistent with unitarity [13, 29].

From the point of view of an infalling massless probe, it has been shown [30, 31] in certain explicit example microstate geometries that the time taken to reach the cap and return to the asymptotic AdS region is $t \sim n_1 n_5$. Thus despite the lack of a horizon, for microstate geometries towards the black hole limit (those with a long throat) a probe appears to get trapped until very long time scales [32]. In fact, the story is richer yet still. The tidal forces exerted on the infalling probe become very large (Planck scale) after a proper time of the order $t \sim \sqrt{n_1 n_5}$, well before reaching the horizon scale microstructure [33]. At this point, the simple geodesic approximation to propagation breaks down and the stringy nature of the probe should be considered. The conclusions of [32, 34] are that an infalling massless probe is excited by the strong tidal forces, developing massive stringy modes and becoming trapped in (or absorbed by) the microstructure. Emission from the relaxation of the probe-fuzzball system, whilst being able to escape, will be highly redshifted.

As dictated by statistical mechanics, a typical microstate will return an expectation value for a given observable exponentially close (in the entropy of the system) to the expectation value for the black hole (the ensemble average). The explicit microstate geometries that we currently have access to are, however, not so close to typicality. In fact they are particularly *atypical* states of the ensemble, generally having properties that differ significantly from the black hole. In the framework of the fuzzball proposal [20, 35], such geometries are considered to be at least a subset of the aforementioned black hole's microstates and one can hope that, by asking carefully chosen questions, universal behaviours of fuzzballs may still be deduced from these explicit solutions. For some work on more typical microstate geometries see [36] and on more general fuzzballs see [37–39].

1.3 AdS/CFT as a tool to study microstates

Following [40], the D1-D5 system described above in the near-brane (or decoupling) limit has an equivalent description in terms of a two-dimensional $\mathcal{N} = (4, 4)$ supersymmetric conformal field theory[10] (CFT) with $SU(2)_L \times SU(2)_R$ R-symmetry and central charge $c = 6n_1 n_5$. This can be seen from the IR regime of the world volume theory of the D5-branes [41] and is a particular instance of the famed AdS/CFT conjecture. We are interested in the supergravity limit of this duality where, as the name suggests, the

---

[10]Some basic facts about conformally invariant field theories will be considered in Section 2.1.

bulk is described in terms of classical supergravity in the decoupling limit

$$\sqrt{Q_1}\,,\sqrt{Q_5} \gg r\,, \tag{1.10}$$

where the metric (1.7) becomes[11] asymptotically $\text{AdS}_3 \times S^3 \times \mathcal{M}^4$ with radii $R_{\text{AdS}} = R_{S^3} = (Q_1 Q_5)^{1/4}$, and the dual CFT is strongly coupled with a large central charge[12]. It is (strongly) believed that this D1-D5 CFT has a region in its moduli space, an infinite distance from the region described by supergravity, at which it is described by a symmetric group (S_N) orbifold of a sigma model with $\mathcal{M}^4$ target space. This description of the CFT is variously referred to as the free point or the free orbifold point.

As a particular example of dual quantities, a gravitational solution with AdS asymptotics has a microscopic description via holography in terms of a state of the dual CFT. However, the logic that this thesis more aspires to is of the inverse type: starting from known states of the CFT, what can be understood about the bulk description. In particular, this duality allows us to describe scattering processes in AdS_3 by using correlation functions in the CFT [42–45].

1.3.1 Large N CFTs and heavy operators

Holographic dualities provide a powerful tool with which to study correlators in strongly coupled CFTs in the limit where the number of degrees of freedom becomes large. This regime is usually called the large N limit in reference to the theory of $SU(N)$ $\mathcal{N} = 4$ supersymmetric Yang-Mills (SYM) which contains fields in the adjoint representation and so the number of degrees of freedom of the theory scale with the rank of the gauge group, that is $c \sim N^2$. In this limit, it is possible to separate primary operators into a class of "light" states, whose conformal dimensions do not grow as N becomes large, and various types of "heavy" states, whose conformal weights scale with some power of N. Another characterisation of the operator spectrum, relevant for holographic theories at large N, is the distinction between single- and multi-particle states. As indicated by their names, this distinction is more readily understood in the dual gravitational description where operators of the first type are dual to single-particle bulk states, while the second class of operators is dual to composite objects of elementary bulk fields. In the best studied example of holographic dualities – that of $\mathcal{N} = 4$ SYM and $\text{AdS}_5 \times S^5$ [40, 46]– the CFT description of single-particle states at leading order in N corresponds to single-trace composite operators and multi-particle states correspond to multi-trace operators (with the trace being over the $SU(N)$ indices). Due to this example, it is

---

[11]This has the effect of dropping the 1's from the Z_1, Z_5 and $Z_p^{\pm}$ of (1.7) yielding a metric describing the product extremal $\text{BTZ} \times S^3$.

[12]From the relation $c = 6N$ we see that the large c limit is equivalent to taking the large N limit and we use the two limits interchangeably throughout the text.

common to use the same nomenclature also in the case of other holographic dualities such as that of $\text{AdS}_3/\text{CFT}_2$ (where in the free orbifold description, the trace is over the S_N indices), which will be the focus of this thesis. It is important to note here that beyond the leading order in N, there is mixing between single- and multi-trace operators in the single-particle spectrum (see for instance [47,48] in AdS_5 and [49–51] in the AdS_3 case.

In this thesis, the term "heavy" when referring to an operator or state will mean that its scaling dimension scales linearly with the central charge, that is

$$\Delta_H \sim c \quad \text{as} \quad c \to \infty \ . \tag{1.11}$$

In the literature there are many types of states that are termed "heavy" in which the dimension scales with some other power of the central charge, however, we will not consider those here.

The heavy states $\mathcal{O}_H$ we consider are multi-particle operators composed of a large number N_b of mutually BPS light operators $\mathcal{O}_L$ that are specific 1/2-BPS chiral primary operators (CPO) and 1/4-BPS operators. For reasons of simplicity, we take all constituents of the $\mathcal{O}_H$ to be identical – that is $\mathcal{O}_H \sim \mathcal{O}_L^{N_b}$ (hence their very atypical nature). In order to have a heavy state, in the sense introduced above, it is necessary to keep the ratio N_b/N finite when taking the large N limit. Even in this heavy setup, N_b/N is a free parameter and so following [52,53], we can often take this ratio to be small and use a perturbative approach in whatever physics is being addressed. These heavy states are atypical in the statistical ensemble of states of fixed conserved quantum numbers; however, the advantage is that a precise dual description in terms of asymptotically $\text{AdS}_3 \times S^3 \times \mathcal{M}^4$ microstate geometries is known [26,27,54,55].

1.3.2 Computing holographic correlators

Ever since the early days of their study, the approach of Witten diagrams [56] provided an explicit avenue for the calculation of holographic correlators among light single-trace operators and several results were obtained for 4-point correlators in the important example of $\mathcal{N} = 4$ SYM theory [57–62]. More recently, knowledge of this class of correlators has been substantially expanded by using a variety of new ideas including: the Mellin space representation [45,63], the position-space approach introduced in [64–66], the use of the large spin expansion [67] and the Lorentzian inversion formula of [68, 69]. Yet one more method for computing holographic correlators is the approach based on "microstate geometries" [70–72], which was used in [73–76] to derive holographic 4-point correlators between singe-particle states in the case of $\text{AdS}_3/\text{CFT}_2$.

The basic idea of this approach is to start from a correlator where a pair of conjugate single-trace operators is made heavy by considering their multi-trace versions,

obtained by taking a large number of identical elementary constituents. It is then possible to exploit several known asymptotically $\text{AdS}_3 \times S^3$ smooth solutions of type IIB supergravity [26, 54, 55, 77] dual to this class of heavy states. The metric part of these smooth supergravity solutions are examples of the microstate geometries discussed above. Specifically, from quadratic fluctuations around these supergravity solutions it is possible – by using the standard AdS/CFT dictionary – to derive so-called heavy-heavy-light-light (HHLL) 4-point correlators with two heavy states corresponding to the geometry and two light states corresponding to the fluctuations. The geometries describing these microstates depend on a set of parameters which quantify the deviation from pure $\text{AdS}_3 \times S^3$. In the language of the dual CFT, these specify the number and type of constituents forming the heavy states. While such an approach to calculating HHLL correlators avoids the use of Witten diagrams – which cannot currently be evaluated in this case – analytic results are often limited to only linear perturbations in the ratio N_b/N discussed above[13] (several explicit examples are known [70–72, 80, 81]). However, an observation of [73–75] is that it is possible to take a "light" limit by formally setting the number of constituents of the heavy states to one and – despite bringing the smooth solutions outside the regime of validity of supergravity – the limit is smooth at the level of correlators and produces results that have all the expected features of 4-point $\text{AdS}_3/\text{CFT}_2$ correlators among single-particle states. Some of these correlators were calculated in [66] by different techniques, providing an independent cross-check of the approach discussed above.

1.4 Flat space eikonal regime

The scattering of two objects is arguably one of the simplest physical experiments that can be thought up. Despite apparent conceptual simplicity, the details of such a process contain a wealth of information about the nature of interactions between the scattering bodies and their internal structure. In order to isolate particular behaviours, it is common to resort to certain approximations or kinematical regimes to simplify the analysis (from the generic case in which all Feynman diagrams contribute, as illustrated in Figure 1.2 for $2 \to 2$ scattering). In the parameter space of $2 \to 2$ scattering of a gravitational theory, clear distinct regions can be identified based on limits of the impact parameter L (or equivalently t) and the centre-of-mass energy s. Here s and t are the Mandelstam variables defined in terms of external particle momenta $\mathbf{P}_i$ as

$$s \equiv (\mathbf{P}_1 + \mathbf{P}_2)^2 \ , \quad t \equiv -(\mathbf{P}_1 - \mathbf{P}_3)^2 = -|\mathbf{q}|^2 \ , \tag{1.12}$$

---

[13]For finite values of N_b/N the calculation of the correlators in the 1/4-BPS states requires some approximation: a WKB approach was used in [78, 79].

and $\mathbf{q}$ is the momentum exchanged in the interaction. The universal regions of such a theorised gravitational S-matrix was described in [82]. One such region is that of large
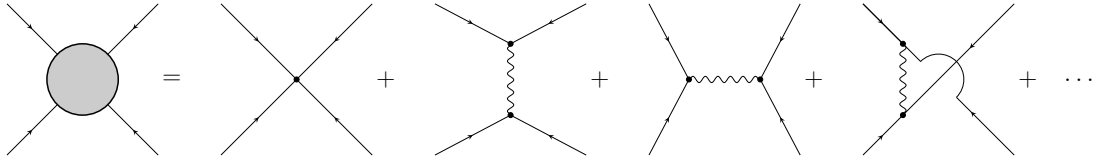
Figure 1.2: Generically, in any particular theory all valid Feynman diagrams contribute to a given scattering process. These can be organised as a perturbative series in the (small) coupling constant g, the leading terms are termed "tree-level" and scale as g^2. The various channels tree-level diagrams of different channels are written explicitly, with diagrams containing loops coming at higher orders.

impact parameter, or small momentum exchange; this is the so-called Born region in which scattering is dominated by a single graviton exchange. Such a tree level scattering amplitude would be proportional to $G_N s^2/t$ for the massless graviton, along with soft graviton contributions. With increasing centre-of-mass energy the multi-graviton exchange processes become non-negligible, requiring supplementation by all the ladder diagrams (shown in Figure 1.3). In this "eikonal regime" of gravitational scattering, defined by

$$s \gg |t| \, , \tag{1.13}$$

it was shown that the leading UV divergences at each order in perturbation theory in flat space can be resummed to a phase [83]. Non-perturbative eikonal considerations have also been shown to soften the UV divergences of perturbative amplitudes [84]. This so-called eikonal phase shift $\delta(s, L)$, allows the eikonal approximation to the full
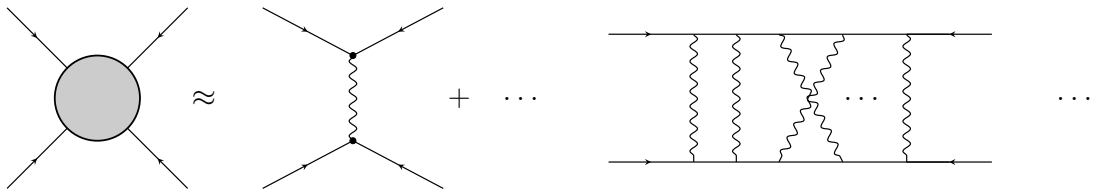
Figure 1.3: In the eikonal regime of $2 \to 2$ scattering the dominant Feynman diagrams at each loop order are the "ladder" diagrams given here. These terms have a regular form and were shown to exponentiate to a phase. Thus, what are independently diverging diagrams (diverging for large energy) become a phase.

scattering amplitude to be written as a Fourier transform of the phase $e^{i\delta(s,L)}$ over the space transverse to the interaction

$$A(s,t) \approx \int_{\mathbb{R}^{d-1}} d\mathbf{x} \; e^{-i\mathbf{q}\cdot\mathbf{x}} e^{i\delta(s,L)} \, , \tag{1.14}$$

valid at large s and small t. Assuming an exponentiated form, the leading eikonal approximation to a scattering amplitude can then be reproduced from the Fourier

transform of the tree-level result. The eikonal regime thus provides an interesting laboratory in which to analyse different gravitational theories in a quantitative way. For elastic scattering processes, the phase shift is real and the eikonal region can be thought of as describing the semiclassical regime. The transition between the Born and eikonal regions, in the $(2+1)$-dimensional case that is of interest here, occurs when $L \sim s$ and $q \sim L^{-1}$. On the other hand if the very high energy limit is taken, at some point the perturbative expansion in G_N will break down, giving rise to the strong gravity region in which inelastic processes such as black hole production dominate. This transition is signalled by the eikonal phase becoming complex.

In a more generic theory, the phase shift can be shown to have an s dependence of

$$\delta(s, L) \approx s^{J-1} f(L) , \tag{1.15}$$

where J is the spin of the exchanged particle. Thus, in the eikonal limit δ is dominated by the graviton contribution and as such the universal piece is proportional to s for all theories containing gravity. In the context of perturbative string theory, the study was initiated in [85, 86] where a stringy eikonal operator was derived from four-point amplitudes (at tree and loop level) with external massless states. A complementary geometric description of the same process is in terms of a particle propagating in a shock wave background (the Aichelburg-Sexl metric [87]), representing the other (highly boosted) particle [88].

1.5 CFT Regge limit

More recently, it was shown that the majority of the above properties of scattering amplitudes in the eikonal limit carry over to AdS spaces. The notable difference is that the phase shift is given instead by the convolution of a 4-point correlation function with wavefunctions for each operator. This eikonal problem was studied in the setting of AdS/CFT, starting from [89–91]: in this case the observables playing the role of the four-point amplitudes are CFT four-point correlators of primary operators in a particular kinematic limit – the Regge limit. This regime of holographic four-point correlators was further studied from different points of view in [92–97].

A slightly different setup is to consider a fixed-target experiment in which a highly energetic particle scatters off a classical object whose mass is much larger than the energy of the incident test particle. A black hole is a prototypical example of such a heavy object. An interesting possibility, one that arises when considering a UV complete theory of gravity, is to consider a specific heavy *pure* state in place of the black hole. For instance, in the context of flat space type II string theories, the target

can be represented by a stack of N Dp-branes [98] and the Regge limit defined in a similar fashion to that of light $2 \to 2$ scattering. A detailed comparison can then be made between the eikonal obtained from an amplitude approach and the dynamics of an energetic string probe propagating in the geometry produced by the Dp-branes. In the AdS/CFT setup, the fixed-target version of the Regge limit was first studied in [52,53], with the bulk heavy object represented by an asymptotically AdS$_{d+1}$ black hole – or for $d = 2$, a conical defect. On the CFT side, the heavy object is described by a heavy state of the type discussed above, and the key observable in this case is a HHLL four-point CFT correlator. The analysis of [52,53] shows explicitly that in order to reproduce the result of the bulk calculation in the presence of a black hole, it is sufficient to characterise the heavy state by its couplings with the stress tensor and its multi-particle ("multi-trace") versions. In the setting of the AdS/CFT correspondence, the phase shift becomes a quantity linking CFT methods to black hole physics; potentially at microscopic scales.

In [52], this setup was used to extract the eikonal phase for AdS black holes and conical defects, which in the case of two-dimensional CFTs was then matched to the behaviour of the HHLL Virasoro vacuum block [99,100] in the Regge limit, emphasising the dominance of the stress tensor sector in this kinematic regime. The bootstrap relations in the Regge limit and their implications for bulk physics were considered variously in [53,93,94,96,97,101,102], while stringy corrections were considered in [103–106].

1.6 Chaos in thermal quantum systems

A somewhat surprisingly related set of questions which utilise similar techniques to access wildly different physics is that of probes of chaos – something which has seen a fair amount of interest in recent years. Exponential sensitivity to initial conditions is a common signal for the presence of chaos, as was originally discovered in the context of classical non-linear systems [107]. The following thought experiment motivates the commonly used measure of chaos in thermal quantum systems. Consider an equilibrium thermal state $|\beta\rangle$ of a quantum theory perturbed by an operator V at time $t = 0$. This is described by the state $V|\beta\rangle$. If the system in this state is evolved to some later time t and the initial perturbation by V was small enough, the system will re-thermalise. That is, if t is large enough, $e^{-iHt}V|\beta\rangle \sim |\beta\rangle$, where H is a time independent Hamiltonian and $e^{-iHt}V|\beta\rangle$ should be thought of here as a new state in the Fock space of the theory rather than a time dependent state. Clearly the action of e^{iHt} on this state reproduces the perturbed thermal state at $t = 0$. If however, at time t the system is again perturbed, this time by the operator W, the state at time t will be $We^{-iHt}V|\beta\rangle$. If the system were not chaotic, evolving back to $t = 0$ would recover the thermal state

perturbed by V, with the W perturbation thermalising. For a system exhibiting strong chaos this does not occur and in fact $e^{iHt} W e^{-iHt} V|\beta\rangle \equiv W(t)V|\beta\rangle \nsim V|\beta\rangle$. This thought experiment thus suggests as a measure of strong chaos the quantity

$$\left\langle -\big[V, W(t)\big]^2 \right\rangle_\beta , \tag{1.16}$$

where V and W are Hermitian operators and $\langle \cdots \rangle_\beta$ is a thermal expectation value in the state $|\beta\rangle$. Properties of this correlator have been discussed in many spin-chain systems and their bulk duals, see for instance [108–111], and in gauge theories and CFTs, for instance in [112–117]. The correlator in (1.16) is theorised to have the very late-time behaviour

$$\left\langle -\big[V, W(t)\big]^2 \right\rangle_\beta \to 2 \left\langle VV \right\rangle_\beta \langle W(t)W(t) \rangle_\beta , \tag{1.17}$$

in any system of a chaotic enough nature, independently of exactly the form of the operators V and W [115]. The universal exponential growth of (1.16) (of the form $e^{\lambda_L t}$) for intermediate times, around which chaotic phenomena start to become significant, is driven by the out-of-time-ordered correlator (OTOC)

$$\left\langle V\, W(t) V\, W(t) \right\rangle_\beta , \tag{1.18}$$

which should have a corresponding period of exponential decay. In [118] it was argued that for thermal quantum systems, there is a hard bound on the rate of exponential decay of (1.18), translating to the Lyapunov exponent satisfying

$$\lambda_L \leq \frac{2\pi}{\beta} . \tag{1.19}$$

Holographic theories, it was conjectured, saturate this bound. This is related to the idea of black holes being the fastest scramblers of information [119] (classical black holes being dual to thermal states). It turns out that in the special case of $d = 2$, vacuum correlators of a CFT_2 on the cylinder $\mathbb{R}_t \times \mathbb{S}_y^1$ of radius R_y can be used to ask questions about thermal correlators with temperature β^{-1} on the cylinder $\mathbb{S}_\tau^1 \times \mathbb{R}_x$, where τ is a Euclidean time with radius $\frac{\beta}{2\pi}$. It turns out that the relevant analytic continuation to obtain the OTOC (1.18) from the associated Euclidean correlator is precisely the Regge limit prescription for the vacuum correlator. We use this fact in Section 4.4.4 to briefly consider this Lyapunov growth at intermediate times in an example $\mathrm{AdS}_3 \times S^3$ holographic correlator.

1.7 Chapter outline

The structure of this thesis is now outlined below.

In Chapter 2 we generally review various background topics that are required throughout the main body of the thesis. This begins in Section 2.1 with a basic (and brief) discussion of two-dimensional CFTs, with a particular focus on the operator content of such theories and the bootstrap philosophy of describing a theory through its dynamical data and determining them from symmetry constraints. This is followed in Section 2.1.1 by a somewhat detailed review of 4-point CFT correlation functions and their decomposition into contributions from individual conformal families of operators, with Appendix A containing some relevant derivations. This section also introduces the crossing constraints for 4-point functions and give an example of their power, relevant for holographic CFTs at infinite central charge. Section 2.2 briefly reviews the D1-D5 system in the gravity picture, with a focus on the D1-D5-P 3-charge black hole and a class of its microstates given by the $(1, 0, n)$ superstrata. The D1-D5 CFT and the description of the heavy pure states dual to the $(1, 0, n)$ family of solutions is then given in Section 2.2.2. A discussion of the relation between the various expansion parameters used throughout the thesis is then contained in Section 2.2.3. Section 2.3 reviews the computation of holographic 4-point correlators with two heavy and two light operator insertions, using the $(1, 0, 0)$ case as an example. This chapter closes out with a look at the Regge limit in asymptotically AdS spacetimes – in Section 2.4 – with a form of the bulk phase shift derived.

In Chapter 3 we examine the formal limit of certain HHLL holographic correlators as the dimension of the heavy operators becomes light. Section 3.2 introduces the multi-trace 4-point functions that we will be concerned with in this chapter and presents the general idea of their extraction from supergravity HHLL correlators computed using asymptotically $\mathrm{AdS}_3 \times S^3$ supergravity solutions. Appendix B.1 provides details of the resummation process from which our correlators are derived. In Section 3.3 we detail explicit correlators involving two n-trace operators for low values of n and explain the connection to correlators involving multi-trace operators with an interpretation as a particular limit of higher-point functions. We also collect the main definitions and properties of the Bloch-Wigner-Ramakrishnan functions in terms of which these correlation functions are naturally written. This is then followed in Section 3.4 by an analysis of various kinematic limits of the $n = 2$ correlator to demonstrate that they yield the behaviour expected from its identification with the connected correlator between two single-trace and two double-trace operators. We analyse both protected and non-protected quantities. Focusing instead on the standard 4-point functions with single-traces ($n = 1$), we show that the full mixing problem in flavour space can be solved and we find the anomalous dimensions for the lowest twist non-BPS double-trace

operators in any flavour representation, with Appendix B.4 detailing a simple method of extraction. We note that flavour-singlet operators of spin 0 and 2 have positive anomalous dimensions for the theory compactified on $K3$. Appendix B.2 gives the explicit form of $n = 1$ correlators used in the unmixing of Section 3.4.2 and Appendix C summarises the derivation of the double-trace OPE data from the inversion formula.

In Chapter 4 we analyse holographic correlators, primarily of the HHLL type, in the Regge limit. Section 3.2 sees a summary of the background material useful for making contact between the eikonal derived in the geometric approach of Section 2.4 and in the holographic CFT language, where one employs the four-point correlators. A derivation is given of formulae connecting explicitly the bulk phase shift and CFT data of particular double-trace operators, eventually to all orders in the perturbative expansion used. In Section 4.3 we review and further analyse the result of [52] where the heavy states represent the conical defect AdS_3 geometries. In Section 4.4 we consider a simple, yet non-trivial, class of 1/2-BPS states. We also discuss in this explicit example how the Regge limit involving the HHLL correlator and the purely light case of Section 4.4.3 differ; showing why the conformal data obtained in the two cases are not the same (Appendix D justifies this difference). In both of these examples, the analysis is first performed at first order in perturbation theory, followed by a partial extension to higher orders (a further example is given briefly in Appendix F). Section 4.4.4 makes a detour to demonstrate the connection between these LLLL holographic correlators and chaotic behaviour in quantum thermal systems. In Section 4.5 we apply the same approach to a class of 1/4-BPS states relevant for the 3-charge D1-D5-P system. Initially in Section 4.5.2 we follow the first order discussions of [1], but then in Section 4.5.3 make a first pass at considering the bulk phase shift for 3-charge microstate geometries in the black hole limit – not attainable from the previous perturbative approach. The Appendix E gives details on the computations of integrals necessary in the CFT analysis of the HHLL and LLLL correlators in Sections 4.4 and 4.5.

A summary of our results and their possible extensions are outlined in the concluding Section 5.

Chapter 2

Background Material

2.1 Conformal field theory

The goal of this section is to spell out some basic facts and results of two-dimensional conformal field theories. Of particular importance in this thesis are the description of local operators and their correlation functions. The general philosophy used throughout for this topic may be described as bootstrap-esque. As evidenced by the physical size of the standard reference [120], the background material and literature for CFTs is vast and this section by no means tries to be an introduction to the subject. Instead it should be viewed as a collection of CFT facts to be assumed later on.

In general dimensions the conformal group serves as an extension to the usual Poincaré spacetime symmetries. A conformal transformation is a transformation of coordinates

$$x^\mu \to \tilde{x}^\mu(x^\nu) \; , \tag{2.1}$$

such that the metric (Minkowski here) transforms as

$$\eta_{\mu\nu} \to \tilde{g}_{\mu\nu} = \frac{1}{\Omega^2} \, \eta_{\mu\nu} \; , \tag{2.2}$$

with Ω being a coordinate dependent conformal factor. In other words, a conformal transformation is a diffeomorphism whose action on the metric can be undone by a Weyl transformation. The set of transformations (2.1) for which this occurs depends on the number of dimensions. In $d > 2$ they form the group $SO(2,d)$ in Lorentzian signatures and are generated by Poincaré, scaling and special conformal transformations. In $d = 2$, this is massively enhanced as seen below.

Considering a CFT$_2$ with a circular spatial direction and coordinates

$$x^0 = t \quad , \quad x^1 = y \quad , \quad y \sim y + 2\pi R_y \; , \tag{2.3}$$

one may define the left-/right-moving lightcone coordinates

$$\sigma^+ \equiv t + y \quad , \quad \sigma^- \equiv t - y \ . \tag{2.4}$$

If t is analytically continued to complex values, purely real values give Lorentzian time and purely imaginary values yields precisely the Wick rotation to Euclidean signature

$$t \to -i\tau_E \quad \text{with} \quad \tau_E \in \mathbb{R} \ . \tag{2.5}$$

In terms of the coordinates (2.4), the transformations satisfying (2.2) are simply

$$\sigma^+ \to \tilde{\sigma}^+(\sigma^+) \quad , \quad \sigma^- \to \tilde{\sigma}^-(\sigma^-) \ , \tag{2.6}$$

since the metric becomes

$$ds^2 = -dt^2 + dy^2 = -d\sigma^+ d\sigma^- = -\underbrace{\frac{d\sigma^+}{d\tilde{\sigma}^+}\frac{d\sigma^-}{d\tilde{\sigma}^-}}_{\Omega^{-2}} d\tilde{\sigma}^+ d\tilde{\sigma}^- \ . \tag{2.7}$$

It is convenient when studying a CFT$_2$ to make a conformal transformation from the (Wick rotated) cylinder to the complex plane (more precisely the Riemann sphere $\mathbb{C} \cup \{\infty\}$) using the map

$$z = e^{\frac{1}{R_y}(\tau_E - iy)} \quad , \quad \bar{z} = e^{\frac{1}{R_y}(\tau_E + iy)} \ . \tag{2.8}$$

For $\tau_E \in \mathbb{R}$, the coordinates $z, \bar{z}$ are complex conjugates, however, often it is useful to treat z and $\bar{z}$ as independent complex coordinates. This, for instance, will be the case for the Regge limit considered in Chapter 4. Conformal transformations on the complex plane are then the holomorphic maps

$$z \to f(z) \quad , \quad \bar{z} \to \bar{f}(\bar{z}) \ . \tag{2.9}$$

Under the conformal map (2.8), constant time slices of the cylinder are mapped to constant radius slices, with the infinite past mapping to the origin and time evolution being an increase in radius. The usual equal-time quantisation on the cylinder becomes radial quantisation on the plane.

In any conformal field theory there exists a stress tensor, which on the plane naturally splits into a holomorphic and an anti-holomorphic field $T(z)$, $\bar{T}(\bar{z})$ admitting the mode expansion

$$T(z) = \sum_{n \in \mathbb{Z}} L_n z^{-2-n} \quad \longleftrightarrow \quad L_n = \oint \frac{dz}{2\pi i} T(z) z^{1+n} \ , \tag{2.10}$$

and likewise for the anti-holomorphic modes $\bar{L}_n$. The Virasoro modes L_n and $\bar{L}_n$ generate the holomorphic and anti-holomorphic conformal transformations respectively. The mode algebra that the L_n satisfy is the Virasoro algebra

$$\left[L_n, L_m\right] = (n - m)L_{n+m} + \frac{c}{12}n(n^2 - 1)\delta_{n+m,0} \ , \tag{2.11}$$

and similarly for the $\bar{L}_n$ modes. The central charge c provides a central extension of the classical Witt algebra and can be thought of as a measure of the number of degrees of freedom in the theory. This is the basic symmetry algebra for a conformal field theory, on top of which other conserved currents may be added – this will be the case in Section 2.2.2 where the theory has additional $U(1)$ and supersymmetry generators. The mode algebra (2.11) has a finite subalgebra of modes that are globally defined on the Riemann sphere, the non-zero commutators of which are given by

$$\left[L_0, L_1\right] = -L_1 \quad , \quad \left[L_0, L_{-1}\right] = L_{-1} \quad , \quad \left[L_1, L_{-1}\right] = 2L_0 \ . \tag{2.12}$$

The global subalgebra (2.12) forms an $\mathfrak{sl}(2)$ and along with that formed from the modes $\{\bar{L}_0, \bar{L}_1, \bar{L}_{-1}\}$ this gives the algebra $\mathfrak{so}(2,2)$ which is simply the "naïve" guess from the higher-dimensional point of view.

The spectrum of local operators[14] in the theory can be classified by their conformal dimensions $h, \bar{h}$ given by the eigenvalue under L_0 and $\bar{L}_0$ respectively. From these, the sum and difference are the total scaling dimension Δ and the spin ℓ given by

$$\Delta = h + \bar{h} \quad , \quad \ell = \left|h - \bar{h}\right| \ . \tag{2.13}$$

Since the dilatation operator $D = L_0 + \bar{L}_0$ acts as the Hamiltonian for the radially-quantised theory on the plane, the total dimension is the analogue of the energy of a state or operator. Key landmarks in the spectrum of a CFT$_2$ are the primary states. These are states that are annihilated by all of the positive Virasoro modes

$$L_n \left|\mathcal{O}_{h,\bar{h}}\right\rangle = \bar{L}_n \left|\mathcal{O}_{h,\bar{h}}\right\rangle = 0 \quad \text{for} \quad n > 0 \ , \tag{2.14}$$

the existence of which is due to the constraint $h, \bar{h} \geq 0$ in $d = 2$ imposed by unitarity. The unique global conformally-invariant vacuum state $|0\rangle$ (for which the associated operator is simply the identity) saturates this unitarity bound in both the left and right sectors, having $h = \bar{h} = 0$. Primary states are the lowest-weight states of a conformal multiplet, which can be filled out by the action of the modes L_{-n} with $n > 0$, acting as raising operators. As a point of nomenclature, all operators in the

---

[14]Due to the state-operator correspondence, we use the operators and states interchangeably. The correspondence says that a local operator $\mathcal{O}(z, \bar{z})$ on the complex plane, where the insertion point is taken to the origin $|z| \to 0$, can be mapped to an initial state $|\mathcal{O}\rangle = \lim_{z \to 0} \mathcal{O}(z) |0\rangle$.

tower of a given primary are referred to as (Virasoro) descendants. A primary operator of dimension $(h, \bar{h})$ transforms under a conformal map (2.9) as a rank $(h, \bar{h})$ tensor

$$\mathcal{O}(z, \bar{z}) \to \mathcal{O}'\Big(f(z), \bar{f}(\bar{z})\Big) = (\partial f)^{-h} (\bar{\partial}\bar{f})^{-\bar{h}} \mathcal{O}(z, \bar{z}) , \qquad (2.15)$$

where we use the common shorthand $\partial \equiv \frac{\partial}{\partial z}$ and $\bar{\partial} \equiv \frac{\partial}{\partial \bar{z}}$. In particular, under the conformal map from the cylinder to the plane (2.8) a primary operator transforms as (where we set $R_y = 1$ here)

$$\mathcal{O}_{\text{cyl}}(\tau, y) \to \mathcal{O}_{\text{pl}}(z, \bar{z}) = z^{-h} \bar{z}^{-\bar{h}} \mathcal{O}(\tau, y) . \qquad (2.16)$$

We will from now on, drop the cylinder and plane labels and distinguish them purely by their coordinate dependence to avoid the cluttering of notation, i.e. $\mathcal{O}_{\text{cyl}}(\tau, y) \equiv \mathcal{O}(\tau, y)$ and $\mathcal{O}_{\text{pl}}(z, \bar{z}) \equiv \mathcal{O}(z, \bar{z})$. The spectrum may alternatively be grouped into towers of states generated by the action of the global conformal modes $L_{-1}, \bar{L}_{-1}$ on a quasi-primary state – this is a state satisfying the definition (2.14) restricted to the global modes, i.e.

$$L_1 \left| \mathcal{O}_{h, \bar{h}} \right\rangle = \bar{L}_1 \left| \mathcal{O}_{h, \bar{h}} \right\rangle = 0 . \qquad (2.17)$$

These descendant states of a quasi-primary are often called global descendants. Clearly all primaries are also quasi-primaries, but the converse is not true. For instance, the holomorphic stress tensor operator $T(z)$ is a quasi-primary of dimension $h = 2$, $\bar{h} = 0$ but is not a primary for a theory with a non-zero central charge. The stress tensor is actually a descendent of the identity operator, being given by $L_{-2} \left| 0 \right\rangle$. Equivalent statements hold for the anti-holomorphic stress tensor $\bar{T}(\bar{z})$.

2.1.1 Correlation functions

In conformal field theories, the conserved currents associated with being conformally invariant impose significant constraints, via the associated Ward identities, on the form of correlation functions. For instance, the functional form of the 2- and 3-point functions of properly normalised primary operators are completely fixed to

$$\langle \mathcal{O}_1(z_1, \bar{z}_1) \mathcal{O}_2(z_2, \bar{z}_2) \rangle = \delta_{12} \, z_{12}^{-h_1-h_2} \bar{z}_{12}^{-\bar{h}_1-\bar{h}_2} , \qquad (2.18a)$$

$$\langle \mathcal{O}_1(z_1, \bar{z}_1) \mathcal{O}_2(z_2, \bar{z}_2) \mathcal{O}_3(z_3, \bar{z}_3) \rangle = C_{123} \, z_{12}^{h_3-h_1-h_2} z_{23}^{h_1-h_2-h_3} z_{13}^{h_2-h_1-h_3}$$
$$\times \bar{z}_{12}^{\bar{h}_3-\bar{h}_1-\bar{h}_2} \bar{z}_{23}^{\bar{h}_1-\bar{h}_2-\bar{h}_3} \bar{z}_{13}^{\bar{h}_2-\bar{h}_1-\bar{h}_3} , \qquad (2.18b)$$

where $\mathcal{O}_i$ has dimensions $h_i, \bar{h}_i$ and $z_{ij} \equiv z_i - z_j$. In the form of the 3-point function (2.18b), there is an overall conformal dimension dependant factor C_{123} that is not fixed

by symmetry. These OPE coefficients[15] represent *dynamical data* specific to a given theory.

Four point functions have their functional form fixed by symmetry only up to a function of conformally invariant cross-ratios of the operator insertion points z_i given by

$$z = \frac{z_{14}z_{23}}{z_{13}z_{24}} \quad , \quad \bar{z} = \frac{\bar{z}_{14}\bar{z}_{23}}{\bar{z}_{13}\bar{z}_{24}} \ . \tag{2.19}$$

A 4-point function then takes the form

$$\langle \mathcal{O}_1(z_1,\bar{z}_1)\mathcal{O}_2(z_2,\bar{z}_2)\mathcal{O}_3(z_3,\bar{z}_3)\mathcal{O}(z_4,\bar{z}_4)\rangle = K_s \bar{K}_s\, G(z,\bar{z}) \ , \tag{2.20}$$

with the prefactor $K_s \bar{K}_s$ is defined in order to transform like the 4-point function under conformal transformations. Here we use the choice

$$K_s = K(z_1, z_2, z_3, z_4) \equiv \frac{z_{23}^{-h_2-h_3+h_4+h_1} z_{24}^{h_3-h_4}}{z_{21}^{h_1+h_2} z_{34}^{h_3+h_4} z_{31}^{h_1-h_2}} \ , \tag{2.21}$$

and likewise for $\bar{K}_s$. To check that this choice of K transforms correctly under global conformal transformations, using the transformations of primaries (2.15), it is enough to simply check scalings and inversions:

- Under the scaling $z_i \to a z_i$, $\bar{z}_i \to \bar{a}\bar{z}_i$ the correlator transforms as

$$\langle \mathcal{O}_1\mathcal{O}_2\mathcal{O}_3\mathcal{O}_4\rangle \to a^{-(h_1+h_2+h_3+h_4)}\, \bar{a}^{-(\bar{h}_1+\bar{h}_2+\bar{h}_3+\bar{h}_4)} \langle \mathcal{O}_1\mathcal{O}_2\mathcal{O}_3\mathcal{O}_4\rangle \tag{2.22}$$

  and from (2.21) K_s transforms as

$$K_s \to a^{-(h_1+h_2+h_3+h_4)} K_s(z_i) \ , \tag{2.23}$$

  correctly matching the correlator once $\bar{K}_s$ is included.

- Under the inversion $z_i \to -\frac{1}{\bar{z}_i}$, $\bar{z}_i \to -\frac{1}{z_i}$ the correlator transforms as

$$\langle \mathcal{O}_1\mathcal{O}_2\mathcal{O}_3\mathcal{O}_4\rangle \to z_1^{2\bar{h}_1}\bar{z}_1^{2h_1} z_2^{2\bar{h}_2}\bar{z}_2^{2h_2} z_3^{2\bar{h}_3}\bar{z}_3^{2h_3} z_4^{2\bar{h}_4}\bar{z}_4^{2h_4} \langle \mathcal{O}_1\mathcal{O}_2\mathcal{O}_3\mathcal{O}_4\rangle \tag{2.24}$$

  and after some algebra, K_s transforms as

$$K_s \to \bar{z}_1^{2h_1}\bar{z}_2^{2h_2}\bar{z}_3^{2h_3}\bar{z}_4^{2h_4} \bar{K}_s(\bar{z}_i) \ , \tag{2.25}$$

---

[15]On the plane, inserting an operator $\mathcal{O}_\Delta$ at a radius r defines a state on a circle of radius $R > r$. If two operators $\mathcal{O}_1$, $\mathcal{O}_2$ are inserted then a state can still be defined on a circle encompassing both. The operator product expansion (OPE) is the statement that this state can be expanded in the complete basis of eigenstates of the dilatation operator, yielding the relation between operators $\mathcal{O}_1 \times \mathcal{O}_2 = \sum_\Delta C_{12\Delta}\mathcal{O}_\Delta$ with a radius of convergence equal to the distance to the nearest other operator insertion. The coefficients in the expansion can be shown to be equal the those appearing in the related 3-point functions.

which again matches the correlator when multiplied by the equivalent transformation of $\bar{K}_s$.

Thus our choice of prefactor K is justified. A useful tool is to use global conformal symmetry to "gauge fix" three operator insertion points, for example to

$$z_1 = 0 \,, \quad z_2 \to \infty \,, \quad z_3 = 1 \quad \Rightarrow \quad z_4 = z \,, \tag{2.26}$$

and likewise for the $\bar{z}_i$. In gauge-fixed form, the 3-point function (2.18b) becomes simply

$$\langle \mathcal{O}_1(\infty)\mathcal{O}_2(1)\mathcal{O}_3(0) \rangle = C_{123} \,. \tag{2.27}$$

For all explicit 4-point correlators considered in thesis, we will have two pairs of conjugate operators with $h_1 = h_2$ and $h_3 = h_4$, and likewise for the anti-holomorphic dimensions. The gauge-fixed correlator of this type then takes the form

$$C(z,\bar{z}) \equiv \langle \bar{\mathcal{O}}_1(0)\mathcal{O}_1(\infty)\mathcal{O}_2(1)\bar{\mathcal{O}}_2(z,\bar{z}) \rangle = (1-z)^{-2h_2}(1-\bar{z})^{-2\bar{h}_2}\, G(z,\bar{z}) \,, \tag{2.28}$$

where $\mathcal{O}(\infty)$ is defined such that the Belavin–Polyakov–Zamolodchikov (BPZ) conjugate state is

$$\langle \mathcal{O}| = \langle 0|\mathcal{O}(\infty) \equiv \lim_{z_1,\bar{z}_1 \to \infty} z_1^{2h_1}\bar{z}_1^{2\bar{h}_1}\langle 0|\mathcal{O}(z_1,\bar{z}_1) \,. \tag{2.29}$$

Below, we consider the decomposition of the conformally-invariant function G in a basis of functions called global conformal blocks. This amounts to organising the spectrum of local operators into towers of global descendants on top of each quasi-primary as discussed around Equation (2.17). Each global conformal block contains the contributions to a 4-point function from a quasi-primary and all of its global descendants, which are fixed by symmetry in terms of the quasi-primary contribution. One can do this in various equivalent ways for a four-point function, corresponding to channels where different pairs of operators are brought together and their OPE expansions used. Our conventions for these different channels in which the 4-point correlator can be expanded are given by:

$$\text{S-channel/direct-channel is } z_3 \to z_4 \text{ or } z \to 1 \tag{2.30}$$

$$\text{T-channel/cross-channel is } z_1 \to z_4 \text{ or } z \to 0 \tag{2.31}$$

These two different expansions of $C(z,\bar{z})$ can be written as a sum over quasi-primary

(a) the direct channel ($z \to 1$)

(b) the cross channel ($z \to 0$)
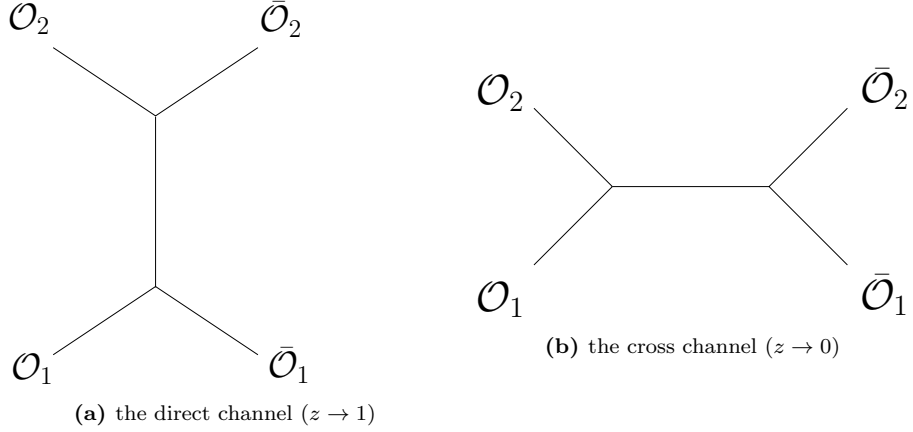
operators exchanged as

$$C(z, \bar{z}) = \sum_{\mathcal{O}'} \frac{C_{11\mathcal{O}'} C_{\bar{\mathcal{O}}'22}}{(1-z)^{2h_2}(1-\bar{z})^{2\bar{h}_2}} \, g_{h,\bar{h}}^{0,0}(1-z, 1-\bar{z}) = \sum_{\mathcal{O}} \frac{C_{12\mathcal{O}} C_{\bar{\mathcal{O}}21}}{z^{h_1+h_2} \bar{z}^{\bar{h}_1+\bar{h}_2}} \, g_{h,\bar{h}}^{h_{12},\bar{h}_{12}}(z, \bar{z}) \ ,$$

$$(2.32)$$

where $h_{ij} \equiv h_i - h_j$ and $C_{ij\mathcal{O}}$ is the three-point function between the operators $\mathcal{O}_i$, $\mathcal{O}_j$ and $\mathcal{O}$ given in (2.27). In these two different channels, the operators exchanged – over which the sum runs – are generically different, hence the different symbols $\mathcal{O}, \mathcal{O}'$ used. The global conformal block for a quasi-primary with conformal dimensions $(h, \bar{h})$ is given by

$$g_{h,\bar{h}}^{a,\bar{a}}(z, \bar{z}) = z^h \bar{z}^{\bar{h}} \,_2F_1\big(h-a, h-a; 2h; z\big) \,_2F_1\big(\bar{h}-\bar{a}, \bar{h}-\bar{a}; 2\bar{h}; \bar{z}\big) \ . \qquad (2.33)$$

Sometimes it will be useful to use the holomorphic and anti-holomorphic parts of conformal block separately, for which we use the notation $g_{h,\bar{h}}^{a,\bar{a}}(z, \bar{z}) = \mathcal{V}_h^{(0)}(z) \bar{\mathcal{V}}_{\bar{h}}^{(0)}(\bar{z})$. In Appendix A we derive this form of the global conformal blocks using two different methods; firstly using a particular projection operator to project the sum in (2.32) onto the contribution of one quasi-primary and explicitly resumming the contributions of its descendants; and secondly utilising the quadratic Casimir of SL(2) instead.

It should be noted that, since we are working in $d = 2$, we are free to organise the spectrum of operators into towers of Virasoro descendants above primary operators. Again, the contribution of this tower of states to a four-point function can be encapsulated in a conformal block – now the much larger Virasoro blocks. Whilst very specific examples have been found [121–124], no known closed form expression exists for general external operator dimensions [125], several results exist in the $1/c$ expansion of a holographic CFT. In the strict $c \to \infty$ limit, the Virasoro block of a primary reduces simply to its global block since the norm of descendants $L_{-n} |\mathcal{O}\rangle$ with $n > 1$ are suppressed in $1/c$ relative to the global descendant $L_{-1} |\mathcal{O}\rangle$. At order $1/c$ Virasoro blocks in various regimes, including with zero, two or three heavy operators, were stud-

ied in [99, 100, 126–133] amongst others. Another general approach to Virasoro blocks includes those with large exchanged operator dimensions [134].

Crossing relations, such as (2.32), coming from the equivalent expansions of correlation functions into conformal blocks in different channels, schematically

$$\langle \bar{\mathcal{O}}_1 \mathcal{O}_2 \, \mathcal{O}_3 \bar{\mathcal{O}}_4 \rangle = \langle \bar{\mathcal{O}}_1 \, \mathcal{O}_2 \mathcal{O}_3 \, \bar{\mathcal{O}}_4 \rangle \ . \tag{2.34}$$

impose significant constraints on the spectrum and dynamical data of a theory and leads to the "bootstrap program" [135–138]. The philosophy of this program is to use symmetry and other physical consistency conditions (such as unitarity) to constrain as much as possible a theory – in some cases this is sufficient to solve the theory entirely [139, 140].

In this thesis we will be focusing on a particular two-dimensional holographic CFT in the gravity regime, i.e. at large values of the central charge $c = 6N$ at strong coupling – see the discussion to come in Section 2.2.2. While the set of sufficient conditions for a CFT to have a classical bulk dual are not known, some necessary conditions appear to be the existence of a large N expansion and a gap $\Delta_{\text{gap}} \sim c$ in its single-particle spectrum. As discussed in Section 1.3.1, holographic CFTs at large N naturally admit a distinguished subset in their spectrum of operators dual to single-particle supergravity modes. At leading order in large N, the single-particle operators are single-trace operators. This nomenclature for operators in the supergravity regime of a holographic CFT originates from the well-studied example of $\mathcal{N} = 4$ super Yang-Mills [141]. In this theory, the operators that are dual to the single-particle modes of the dual type IIB supergravity on AdS$_5 \times S^5$ are of the form $\text{Tr}\, Z^2$, where Z^2 is some complex combination of the basic scalars of $\mathcal{N} = 4$. Operators dual to multi-particle excitations in the bulk will then contain the product of multiple such single-trace constituents. Despite this exact trace structure not holding in general theories, the terminology is used universally. For instance, in the D1-D5 CFT of Section 2.2.2 a trace will be a sum over S_N indices. From single-trace quasi-primary operators, for instance $\mathcal{O}_i$ and $\mathcal{O}_j$, one can then construct a family of quasi-primary double-trace operators that we write schematically as

$$\mathcal{O}_{ij} \equiv \, : \mathcal{O}_i \, \partial^m \bar{\partial}^{\bar{m}} \mathcal{O}_j : \, , \tag{2.35}$$

where $: \cdots :$ denotes that at each level we should take a combination of derivatives that give a quasi-primary. These operators are labelled by the non-negative integers $m, \bar{m}$ and have conformal dimensions of the form

$$h = h_i + h_j + m + \frac{1}{2}\gamma_{m,\bar{m}} \ , \qquad \bar{h} = \bar{h}_i + \bar{h}_j + \bar{m} + \frac{1}{2}\gamma_{m,\bar{m}} \ , \tag{2.36}$$

where $\gamma_{m,\bar{m}}$ are the anomalous dimensions that are generically present when $\mathcal{O}_{ij}$ is not globally BPS – even if the two single-particle constituents are individually protected. In the supergravity limit, the anomalous dimensions are suppressed in $1/N$ and so are small when compared to the leading contribution in (2.36): this is the starting point for the usual perturbative approach discussed below. In analogy with the higher dimensional case, we will often denote the "spin" of the double-trace operators $\mathcal{O}_{ij}$ by

$$\ell \equiv \left| h - \bar{h} \right| = |m - \bar{m}| \ , \tag{2.37}$$

while the number of boxes ($\square = \partial\bar{\partial}$) is given by $\min(m, \bar{m})$. An important detail here is that there is generically a degeneracy in the leading order spectrum which is (partially) lifted by the first order anomalous dimensions. In Chapter 3 we study how this lifting works for a particular example set of double-trace operators. In this present chapter, along with Chapter 4, we will use also γ to indicate the average anomalous dimension of a set of degenerate operators that appear in the OPE decomposition as discussed below.

Early on it was understood that the strict limit of large central charge of holographic CFTs is a generalised free theory (GFT) point [142]. In a GFT, all correlation functions are given simply by a finite sum of all possible Wick contractions – 2-point functions – as in a free theory, however, operators need not have dimensions equal to their free dimensions. As well as the infinite N point of holographic CFTs, GFTs also appear in the context of CFTs at large spin [67, 143, 144]. One can then consider the crossing relations (2.32) in a perturbative expansion in large N; here we discuss the case of the correlator with two pairs of conjugate operators $\langle \bar{\mathcal{O}}_1 \mathcal{O}_1 \mathcal{O}_2 \bar{\mathcal{O}}_2 \rangle$. At this generalised free point, the correlator decomposed in the direct channel (where $\bar{\mathcal{O}}_1$ fuses with $\mathcal{O}_1$ and $\mathcal{O}_2$ with $\bar{\mathcal{O}}_2$) will contain only the contribution of the identity operator, whereas in the cross channel there will be an infinite family of double-trace operators $\mathcal{O}_{12}$ of the form (2.35) with $i = 1$, $j = 2$. The crossing relation for this correlator at order N^0 in the large N expansion, using the explicit global blocks (2.33), then reads [145]

$$(1-z)^{-2h_2}(1-\bar{z})^{-2\bar{h}_2} = z^{-h_1-h_2}\bar{z}^{-\bar{h}_1-\bar{h}_2} \sum_{m,\bar{m}=0}^{\infty} c_{(0)}^2(m,\bar{m}) \, g_{h,\bar{h}}^{h_{12},\bar{h}_{12}}(z,\bar{z})$$

$$= \sum_{m,\bar{m}=0}^{\infty} c_{(0)}^2(m,\bar{m}) z^m {}_2F_1\big(2h_2 + m, 2h_2 + m; 2(h_1 + h_2 + m); z\big)$$

$$\times \bar{z}^{\bar{m}} {}_2F_1\big(2\bar{h}_2 + \bar{m}, 2\bar{h}_2 + \bar{m}; 2(\bar{h}_1 + \bar{h}_2 + \bar{m}); \bar{z}\big) \ , \tag{2.38}$$

where here $c_{(0)}^2(m,\bar{m})$ is the product of the order N^0 cross-channel OPE coefficients between the external operators and exchanged double-trace operator. In the second

line of (2.38), the explicit conformal dimensions (2.36) of the double-trace operators were used along with the cross-channel global blocks from (A.16). Thus we see that the order N^0 crossing relations constrain the OPE coefficients at this order. To solve for these OPE coefficients, one may use the orthogonality relation between solutions of the differential equation (A.25)

$$
\delta_{m,m'} = \oint_0 \frac{dz}{2\pi i} z^{m-m'-1} {}_2F_1\big(A+m, A+m; 2(B+m); z\big)
$$
$$
\times {}_2F_1\big(1-A-m', 1-A-m'; 2(1-B-m'); z\big) , \quad (2.39)
$$

by multiplying both sides of (2.38) by the factor

$$
F_{\mu,\bar\mu} \equiv \frac{z^{-\mu-1}\bar z^{-\bar\mu-1}}{(2\pi i)^2} {}_2F_1\Big(1-2h_2-\mu, 1-2h_2-\mu; 2(1-h_1-h_2-\mu); z\Big)
$$
$$
\times {}_2F_1\Big(1-2\bar h_2-\bar\mu, 1-2\bar h_2-\bar\mu; 2(1-\bar h_1-\bar h_2-\bar\mu); \bar z\Big) , \quad (2.40)
$$

and integrating around a contour centred at $z, \bar z = 0$

$$
\oint_0 \oint_0 \frac{dz d\bar z}{(1-z)^{2h_2}(1-\bar z)^{2\bar h_2}} F_{\mu,\bar\mu}(z,\bar z) = \sum_{m,\bar m=0}^{\infty} c_{(0)}^2(m,\bar m)\,\delta_{m,\mu}\,\delta_{\bar m,\bar\mu} = c_{(0)}^2(\mu,\bar\mu) . \quad (2.41)
$$

Performing the integrals on the left-hand side of (2.41) and relabelling $(\mu,\bar\mu) \to (m,\bar m)$ gives

$$
c_{(0)}^2(m,\bar m) = \frac{\Gamma(2h_1+m)\,\Gamma(2h_2+m)\,\Gamma(2h_1+2h_2+m-1)}{m!\,\Gamma(2h_1)\,\Gamma(2h_2)\,\Gamma(2h_1+2h_2+2m-1)}
$$
$$
\times \frac{\Gamma(2\bar h_1+\bar m)\,\Gamma(2\bar h_2+\bar m)\,\Gamma(2\bar h_1+2\bar h_2+\bar m-1)}{\bar m!\,\Gamma(2\bar h_1)\,\Gamma(2\bar h_2)\,\Gamma(2\bar h_1+2\bar h_2+2\bar m-1)} . \quad (2.42)
$$

The crossing relations can be analysed at higher orders in the $1/N$ expansion [145], where the direct channel will gain contributions from single-trace operators such as the stress tensor and any currents (along with multi-trace composites made from them), and the cross channel will include contributions from $1/N$ corrections to both the OPE coefficients and dimensions of the double-trace operators $\mathcal{O}_{12}$. An analysis at first order in $1/N$ will be performed in Section 4.4.3 and in the majority of Chapter 4 to higher orders in the related parameter μ in the case of one pair of operators being heavy. In both cases the Regge limit is used as a tool to disentangle the various new CFT data contributions at each order.

2.2 A class of superstrata

Superstrata are a type of microstate geometries that are dual to coherent superpositions of microstates of the Strominger-Vafa black hole discussed in the introduction. Just as with their parent class, the microstate geometries, these solitonic-like solutions to the bosonic part of supergravity are smooth and without horizons, whilst having the asymptotic structure of a given black hole. These are of course special states in the black hole's ensemble, however, their advantage is that there is a reasonably well-understood method of construction as an explicit solution of supergravity. For reviews of the construction of superstrata see [28, 146].

2.2.1 Supergravity description

In the context of the D1-D5 system discussed in Section 1.2.1, the idea is to look for solutions to the $\mathcal{N} = (2,0)$ six-dimensional supergravity theory coupled to 5 (21) tensor multiplets[16] that can be obtained from the reduction of type IIB supergravity on $\mathbb{R}^{1,4} \times S_y^1 \times \mathcal{M}^4$ with a string scale $\mathcal{M}^4 = T^4$ (K3)[17]. Since we are interested in solutions preserving a fraction of the supersymmetries of the theory, instead of attempting to solve directly the Einstein equations of motion for the various supergravity fields (second order, non-linear equations), it is significantly simpler to solve the relevant BPS equations [141, 148]. It was shown in [149–152] that the BPS equations can be organised into a system of layered first order and most importantly *linear* equations, once certain data is chosen[18]. If one simply demands a solution with the correct D1 and D5 charges (1.8) then what is obtained is just the 2-charge black hole, described by the metric (1.7) with $Q_p = 0$. This solution represents the low energy description of a bound state of n_1 D1-branes and n_5 D5-branes extended in the macroscopic S_y^1 but point-like in the transverse $\mathbb{R}^4$. Clearly this unique, singular supergravity solution is disappointing from the microstate geometry program point of view. However, it was observed in [24, 153, 154] that Kaluza-Klein monopole and angular momentum dipole charges can be added in such a way so as not to break any more supersymmetries[19].

---

[16]A simple reduction of type IIB supergravity on T^4 yields the maximal $\mathcal{N} = (2,2)$ 6D theory which still has 32 real supersymmetries. With the goal in mind of describing the D1-D5 system, which is 1/4-BPS, we choose to consider the chiral half-maximal $\mathcal{N} = (2,0)$ theory mentioned in the text, and then break a further half to get $\mathcal{N} = (1,0)$ supergravity with 8 real supersymmetries. This $\mathcal{N} = (1,0)$ theory can have between 1 and 5 tensor multiplets depending on the exact process of reduction [141]. By looking for 1/2-BPS solutions to the $\mathcal{N} = (2,0)$ theory we are effectively considering the $\mathcal{N} = (1,0)$ theory.

[17]Note that here we only discuss superstrata with no dependence on the internal $\mathcal{M}^4$ coordinates. This allows for any solutions in 6D to be trivially uplifted to 10D. For examples of superstrata with dependence on this compact 4-manifold, see [26, 147].

[18]In most cases some input from one component of the Einstein equations is needed to supplement the BPS equations [28, 152].

[19]Requiring that the 8 supersymmetries are still preserved constrains the Kaluza-Klein monopole and angular momentum dipole charges in terms of the D1- and D5-brane charges.

This has the effect of expanding the D1-D5 brane system to lie along a curve in the transverse $\mathbb{R}^4$ which can have an arbitrary shape, whilst still preserving 8 real supersymmetries. These *smooth* 2-charge backgrounds (referred to as the Lunin-Mathur geometries) are in 1-to-1 correspondence with Ramond-Ramond (RR) ground states of the dual CFT and can be shown to give rise to the correct e^S number of microstates for the 2-charge black hole [155].

This 2-charge story is a fascinating explicit construction of the microstates of an extremal black hole, however, we would like to go beyond this to the 3-charge system. While the 3-charge black hole (1.7) has a large classical horizon, the horizon of the 2-charge black hole has degenerated to a point at the origin. Thus in order to disentangle black hole physics of the horizon and singularity scales, it is preferable to discuss the D1-D5-P system. The third charge is from the momentum excitations placed along the S_y^1 direction in the D1-D5 system (see Figure 1.1). Superstrata of this 3-charge system are then the gravity description of large coherent momentum excitations travelling in one direction (left-moving by convention) along the S_y^1, after backreacting on the 2-charge backgrounds. These solutions are only a fraction of the total e^S number of microstates of the 3-charge black hole [156,157], yielding an entropy scaling as $S_{\text{strata}} \sim Q^{5/4}$ rather than $S_{\text{BH}} \sim Q^{3/2}$ (where $Q_1 = Q_5 = Q_p = Q$).

In order to discuss the various superstrata geometries we first introduce the general 6D metric ansatz used when solving the BPS equations:

$$ds_6^2 = -\frac{2}{\sqrt{\mathcal{P}}}\big(dv + \beta\big)\bigg[du + \omega + \frac{\mathcal{F}}{2}\big(dv + \beta\big)\bigg] + \sqrt{\mathcal{P}}\,ds_4^2 \,, \qquad (2.43)$$

where y is periodic with period $2\pi R_y$, ds_4^2 is the metric on the base space B and u and v are the null coordinates

$$u = \frac{1}{\sqrt{2}}(t - y) \quad , \quad v = \frac{1}{\sqrt{2}}(t + y) \,. \qquad (2.44)$$

In the ansatz (2.43), the one assumption used is that ∂_u is a null Killing vector[20], which is the case here due to the presence of Killing spinors from the preserved supersymmetries [158]. Therefore, all ansatz quantities are independent of u, but generically depend on the remaining 5 coordinates (v, x^μ) with x^μ being the coordinates on the base B. In (2.43), $\mathcal{P}$ is the warp factor, β describes the fibration over the base B and ω and $\mathcal{F}$ control the angular momentum and momentum of the solution. For the tensor gauge fields of the 6D supergravity theory one also writes an ansatz, which depends on the "electric potentials" Z_I and "magnetic potential" 2-forms Θ_I with $I = 1, 2, 4$.

---

[20]In fact, the coordinate u is chosen to be the coordinate defined by the obtained Killing vector. This Killing vector can generally be timelike or null depending on the dimension – in six dimensions it is null [158].

We can now give a general qualitative description of the BPS equations. In [149,150] it was shown that the BPS equations for the general ansatz described above can be organised into three layers; the so-called "zeroth order equations" essentially constrain the fibration and the metric on the base space. Making the simplifying assumption that these are independent[21] of v, the zeroth layer dictates that the base is hyper-Kähler and that the exterior derivative of β is self-dual. This layer is non-linear, however, if one views the choice of base space and fibration (subject to the above conditions) as an input to the problem then all of the remaining layers are linear. All known superstrata are over a base $B = \mathbb{R}^4$ since these are the simplest to construct. The first layer is a set of homogeneous and linear equations for the Z_I and Θ_I, which in turn fix the warp factor in (2.43) to be

$$\mathcal{P} = Z_1 Z_2 - Z_4^2 \ . \tag{2.45}$$

The second layer is again linear, however, with the solutions to the first layer quadratically sourcing these equations. This final layer fixes $\mathcal{F}$ and ω. Despite the huge simplification of linearity, these equations are still formidable to solve and there are many subtleties that are not discussed here. For a full account see the reviews [28,146] or the papers in which the known superstrata were originally constructed [27,54,55,159–164].

Before describing the class of superstrata used in this thesis, we first note that the 3-charge black hole (1.7) is a very simple solution of this form, with the ansatz quantities

$$\mathcal{F} = -\frac{2Q_p}{r^2} \ , \ Z_1 = 1 + \frac{Q_1}{r^2} \ , \ Z_2 = 1 + \frac{Q_5}{r^2} \ , \ Z_4 = 0 \ , \ \beta = \omega = 0 \ , \ \Theta_I = 0 \ , \tag{2.46}$$

where spherical coordinates with radius r have been used on $B = \mathbb{R}^4$. The interesting thing from the microscopic perspective is that in the same class of supergravity solutions as the singular black hole, there is a huge number of smooth solutions with the same charges and preserving the same supersymmetries. The 2-charge microstate geometries discussed above have $\mathcal{F} = Z_4 = 0$, $\Theta_I = 0$ and the flat metric on $B = \mathbb{R}^4$ and the remaining ansatz quantities are fixed by the Lunin-Mathur profile of a curve in $\mathbb{R}^4$. The charges of the solution are smeared around this curve, the simplest profile for which is a circle and this yields global $\mathrm{AdS}_3 \times S^3$. More complicated profiles yield deformations of global $\mathrm{AdS}_3 \times S^3$.

To get 3-charge superstrata, the 2-charge solutions are used as seed solutions on which one acts with the symmetry generators to generate more complicated solutions. The first and second layer BPS equations are re-solved using the seed as input, generating (with many details omitted) solutions which depend on two arbitrary functions

---

[21]Note that we assume the metric on the base space and β are v-independent; all other ansatz quantities in the 3-charge case can, and should depend on v since the momentum excitations on S_y^1 are along this direction.

of three variables. The general single-mode[22] 3-charge superstrata are labelled by the integers[23] (k, m, n) satisfying $n \geq 0$, $0 \leq m \leq k$ from the requirement of smoothness. This nomenclature and the smoothness conditions appear arbitrary from the gravity perspective, however, in the CFT language of the dual states discussed below they emerge very naturally [51, 55]. The "workhorse" family of superstrata are the $(1, 0, n)$ solutions, depending on the three parameters[24] (a, b, n), and which have the following ansatz quantities (using the notation of [27]):

$$Z_1 = 1 + \frac{Q_1}{\Sigma} + \frac{R_y^2 \, b^2}{2Q_5 \Sigma} \Delta_{2,0,2n} \cos \chi_{2,0,2n} \; , \quad Z_2 = 1 + \frac{Q_5}{\Sigma} \; , \quad Z_4 = \frac{R_y \, b}{\Sigma} \Delta_{1,0,n} \cos \chi_{1,0,n}$$

$$\mathcal{F} = -2F_n(r) \equiv -\frac{b^2}{a^2}\left(1 - \frac{r^{2n}}{(r^2 + a^2)^n}\right) \; , \quad \omega = \omega_0 + \omega_{1,0,n} \; , \quad \Sigma \equiv r^2 + a^2 \cos^2\theta$$

$$\beta = \frac{R_y \, a^2}{\sqrt{2} \, \Sigma}\left(\sin^2\theta \, d\phi_1 - \cos^2\theta \, d\phi_2\right) \; , \quad \omega_0 = \frac{R_y \, a^2}{\sqrt{2} \, \Sigma}\left(\sin^2\theta \, d\phi_1 + \cos^2\theta \, d\phi_2\right) \; ,$$

$$\omega_{1,0,n} = \frac{\sqrt{2} \, a^2 R_y}{\Sigma} F_n(r) \sin^2\theta \, d\phi_1 \; , \quad \chi_{1,0,n} = \frac{\chi_{2,0,2n}}{2} = \frac{\sqrt{2}}{R_y} n v + \phi_1$$

$$\Delta_{1,0,n} = \sqrt{\Delta_{2,0,2n}} = \frac{a \, r^n}{(r^2 + a^2)^{(n+1)/2}} \sin \theta \tag{2.47}$$

where on the $\mathbb{R}^4$ we have used the oblate spherical coordinates $(r, \theta, \phi_1, \phi_2)$ adapted to disk sources, which can be obtained from the Cartesian coordinates x^μ $(\mu = 1, \ldots, 4)$ via

$$x_1 + ix_2 = \sqrt{r^2 + a^2} \, \sin\theta \, e^{i\phi_1} \quad , \quad x_3 + ix_4 = r \cos\theta \, e^{i\phi_2} \; . \tag{2.48}$$

This gives the flat metric on $\mathbb{R}^4$ as

$$ds_4^2 = \Sigma\left(\frac{dr^2}{r^2 + a^2} + d\theta^2\right) + (r^2 + a^2)\sin^2\theta \, d\phi_1^2 + r^2 \cos^2\theta \, d\phi_2^2 \; , \tag{2.49}$$

with the coordinates $(r, \theta, \phi_1, \phi_2)$ having the ranges

$$r \geq 0 \quad , \quad 0 \leq \theta \leq \frac{\pi}{2} \quad , \quad 0 \leq \phi_1, \phi_2 < 2\pi \; . \tag{2.50}$$

---

[22]Since the BPS equations are linear, a general solution can be written as a sum over arbitrary modes of this form. We discuss only single-mode superstrata [163].

[23]In full generality there will be an additional integer q which relate to the fermionic generators used in the construction of the superstrata [161]. We focus on superstrata that used only the bosonic generators in their construction, defining $(k, m, n, q = 0) \equiv (k, m, n)$.

[24]Note that setting $n = 0$ reduces this family of 3-charge superstrata to a family for the 2-charge black hole. We will also use this $(1, 0, 0)$ family in this thesis.

Demanding smoothness of the solution[25] then imposes the relation

$$\frac{Q_1 Q_5}{R_y^2} = a^2 + \frac{b^2}{2} \equiv a_0^2 \, , \tag{2.51}$$

and the conserved charges are the angular momenta and momentum

$$J_L = J_R = \frac{R_y a^2}{2} \quad , \quad Q_p = \frac{1}{2} n b^2 \, . \tag{2.52}$$

Despite not being at all close to a typical state of the ensemble of the 3-charge black hole, this family of solutions does contain a surprising amount of structure. The general structure of this $(1, 0, n)$ family of solution is the following. At very large distances from the centre $r \gg a, b, Q_1^{1/2}, Q_5^{1/2}$ the geometry is flat, however, upon taking the decoupling limit (1.10) (effectively dropping the 1's in Z_1 and Z_2) the solution becomes "asymptotically" $\mathrm{AdS}_3 \times S^3$ with equal radii

$$R_{\mathrm{AdS}} = R_{S^3} = \left(Q_1 Q_5 \right)^{1/4} \, . \tag{2.53}$$

In this region the radius of the S_y^1 decreases for decreasing r (in keeping with being part of an AdS_3) until it stabilises to a fixed radius, signifying the start of a BTZ-like $\mathrm{AdS}_2 \times S_y^1 \times S^3$ throat at $r \sim \sqrt{Q_p}$. The length of this throat is controlled by the ratio $\frac{b}{a}$ and it transitions to a region where the momentum excitations are localised at $r \sim a\sqrt{n}$ before smoothly capping off in another AdS_3 region (though the S^3 smoothly pinches off here). This general structure lends the name of "smoothly capped geometries" to this class of solutions. It should be noted that (in the decoupling limit) whilst setting $a = 0$ in the $(1, 0, n)$ geometry gives the extremal BTZ metric, this value is not part of the ensemble and there is a minimal value of a. One of the interesting features of this geometry manifests itself when written in the form of an S^3 fibration

$$ds_6^2 \equiv \widetilde{g}_{MN} dx^M dx^N = V^{-2} g_{\mu\nu} dx^\mu dx^\nu + G_{\alpha\beta} \left(dx^\alpha + A_\mu^\alpha dx^\mu \right) \left(dx^\beta + A_\nu^\beta dx^\nu \right) , \tag{2.54}$$

where M, N run over $(u, v, r, \theta, \phi_1, \phi_2)$, α, β run over the S^3 coordinates (θ, ϕ_1, ϕ_2), and μ, ν are over (u, v, r). The prefactor V in (2.54) is given by

$$V^2 \equiv \frac{\det G_{\alpha\beta}}{\det \Omega_{\alpha\beta}} \, , \tag{2.55}$$

where $\Omega_{\alpha\beta}$ is $\sqrt{Q_1 Q_5}$ times the round metric on the 3-sphere at infinity. The extracted metric $g_{\mu\nu}$ turns out to be independent of the S^3 coordinates, signifying a consistent reduction to three dimensions. We will use this fact in Chapter 4 to reduce a 6D

---

[25] We note that conditions from demanding flat asymptotics and the absence of closed timelike curves have also been used to constrain the ansatz data (2.47).

geodesic problem down to a 3D one.

2.2.2   Superstrata in the D1-D5 CFT

In this section we give a basic description of the D1-D5 CFT, dual to the D1-D5 brane system in the decoupling limit, at the free orbifold point in its moduli space. This is by no means a complete or thorough exposition of this theory; most details of the orbifold CFT are not required for the material presented in this thesis and so the aim of this section is simply to motivate the dual CFT description of the superstrata discussed in the previous section. For more details see [165–167].

We give here the general idea of an orbifold theory: given a seed CFT $\mathfrak{B}$ with central charge $\tilde{c}$, the tensor product theory $\mathfrak{B}^N$ with central charge $c = \tilde{c}N$ is defined by taking N non-interacting copies of the seed. By imposing invariance under a discrete gauge group $\mathfrak{G}$ one obtains the $\mathfrak{G}$ orbifold theory. As a simple example consider the seed CFT to be the theory of $\tilde{c}$ free bosons X^ζ with $\zeta = 1, \ldots, \tilde{c}$. The tensor product theory will contain simply the free bosons $X^\zeta_{(r)}$ with $r = 1, \ldots, N$. Orbifolding by the group $\mathfrak{G} = \mathbb{Z}_N$ gives a theory with a Hilbert space that is the product of "twisted sectors" labelled by the conjugacy classes of $\mathbb{Z}_N$, *i.e.* the kth sector contains fields invariant under a cyclic permutation of copies of the seed performed k times. These are "gauge invariant" states of the orbifold theory since the original fields on individual copies of the seed CFT are not invariant under a cyclic permutation of copies.

Given the above example we can now move on to describing the D1-D5 orbifold CFT$_2$. This theory uses a seed $\tilde{c} = 6$ sigma model with target space T^4, containing four bosonic and four chiral and anti-chiral fermionic fields and $\mathcal{N} = (4, 4)$ supersymmetry. We denote these basic fields as

$$X^i(z, \bar{z}) \quad , \quad \psi^{\alpha \dot{A}}(z) \quad , \quad \bar{\psi}^{\dot{\alpha} A}(\bar{z}) \,, \tag{2.56}$$

where α, $\dot{\alpha}$ are fundamental indices of $SU(2)_L$ and $SU(2)_R$ of the R-symmetry group $SO(4) \simeq SU(2)_L \times SU(2)_R$; A and $\dot{A}$ are fundamental indices of $SU(2)_C$ and $SU(2)_A$ factors of the "organisational" $SO(4)_I \simeq SU(2)_C \times SU(2)_A$ and i is a fundamental index of $SO(4)_I$. This $SO(4)_I$ originates from the T^4 whereas the R-symmetry $SO(4)$ comes from the S^3. The D1-D5 CFT is the S_N orbifold of $N \equiv n_1 n_5$ copies of this seed. The theory contains various twisted sectors, labelled by the conjugacy classes of the S_N – these consist of fields invariant under permutations of copies with a fixed cycle structure. The symmetry currents on each copy are the stress tensor, R-symmetry and supersymmetry generators (we omit the copy label here)

$$\left\{ T(z),\, J^a(z),\, G^{\alpha A}(z) \right\} \quad , \quad \left\{ \bar{T}(\bar{z}),\, \bar{J}^a(\bar{z}),\, \bar{G}^{\dot{\alpha} A}(\bar{z}) \right\} , \tag{2.57}$$

which can be constructed from the basic fields (2.56). Using (2.10) and its generalisations [120], these fields have the modes

$$\left\{ L_n ,\ J_n^a ,\ G_n^{\alpha A} \right\} \quad , \quad \left\{ \bar{L}_n ,\ \bar{J}_n^a ,\ \bar{G}_n^{\dot{\alpha} A} \right\} , \tag{2.58}$$

where $a = +, -, 3$ is a triplet representation index of $SU(2)$ and $n, m \in \mathbb{Z}$ or $\frac{1}{2} + \mathbb{Z}$ for bosonic and fermionic modes respectively. The algebra formed from these modes has a finite dimensional subgroup of the globally defined modes

$$\left\{ L_{\pm 1} ,\ L_0 ,\ J_0^a ,\ G_{\pm\frac{1}{2}}^{\alpha A} \right\} \quad , \quad \left\{ \bar{L}_{\pm 1} ,\ \bar{L}_0 ,\ \bar{J}_0^a ,\ \bar{G}_{\pm\frac{1}{2}}^{\dot{\alpha} A} \right\} . \tag{2.59}$$

Since the Cartan subalgebra of the holomorphic part of the mode algebra is formed from J_0^3 and L_0 we can label (holomorphic) states by their eigenvalues h and j. On top of the field content of each copy (2.56) there are also twist operators[26] σ_k that permute fields on k of the copies. If each copy is a CFT on a spatial circle of length $2\pi R_y$ then an order k twist operator can be thought of as linking together k copies into a single CFT[27] on a circle of length $2\pi k R_y$. As a point of nomenclature, a state on k linked copies is often referred to as a "strand" of length k. The states of interest for the CFT description of the superstrata of Section 2.2 are the 5 bosonic T^4-invariant Ramond-Ramond (RR) ground states per twist sector, all with dimensions $h = \bar{h} = \frac{c}{24}$ and labelled by their R-charges of $\pm\frac{1}{2}$ and 0

$$\left\{ |{\pm\pm}\rangle_k ,\ |00\rangle_k \right\} . \tag{2.60}$$

Under a spectral flow [168] transformation, these RR ground states are mapped in a 1-to-1 fashion to anti-chiral primaries in the Neveu–Schwarz (NS) sector[28]. Under such a spectral flow between the NS- and R-sectors, the conformal dimensions and R-charges are related via

$$h^{\mathrm{R}} = h^{\mathrm{NS}} + j^{\mathrm{NS}} + \frac{c}{24} \quad , \quad j^{\mathrm{R}} = j^{\mathrm{NS}} + \frac{c}{12} , \tag{2.61}$$

where in the k twisted sector the central charge is $c = 6k$. A holomorphic anti-chiral primary is defined by the condition

$$G_{-\frac{1}{2}}^{-A} |h, j\rangle = 0 , \tag{2.62}$$

---

[26]The notation σ_k refers to a twist operator representing the action of a permutation with one cycle of length k summed over all choices of k copies from N to get an S_N invariant object.

[27]In terms of fields on the plane, twist operators wind together their boundary conditions. A bosonic field on copy (r) has boundary conditions $X_{(r)}(e^{2\pi i}z) = X_{(r)}(z)$ whereas with a twist operator σ_k inserted at the origin, then $X_{(r)}(e^{2\pi i}z) = X_{(r+1)}(z)$. Circling $X_{(r)}(z)$ around the origin k times gives back $X_{(r)}(z)$.

[28]It is purely convention to map to anti-chiral primaries. If one spectral flows in the opposite direction then RR ground states map to chiral primaries, although (2.61) takes a slightly different form.

which is equivalent to having $h = -j$. These are lowest-weight states of a short multiplet which can be then filled out by the action of the symmetry mode operators

$$\left\{ L_{-1} \, , \; J_0^+ \, , \; G_{-\frac{1}{2}}^{+A} \right\} \quad , \quad \left\{ \bar{L}_{-1} \, , \; \bar{J}_0^+ \, , \; \bar{G}_{-\frac{1}{2}}^{\dot{+}A} \right\} . \tag{2.63}$$

In particular, two of the RR ground states in (2.60) (per twist sector) map under spectral flow as

$$|++\rangle_k \; \longleftrightarrow \; |0\rangle^{\text{NS}} \, , \tag{2.64a}$$

$$|00\rangle_k \; \longleftrightarrow \; |--\rangle_k^{\text{NS}} \, , \tag{2.64b}$$

where $|0\rangle^{\text{NS}}$ is the unique NS vacuum with $h = \bar{h} = j = \bar{j} = 0$ and $|--\rangle_k^{\text{NS}}$ is an anti-chiral primary with $h = \bar{h} = -j = -\bar{j} = \frac{1}{2}$. From the NS sector strand $|--\rangle_k^{\text{NS}}$, we build the excited strand[29]

$$|k, m, n\rangle^{\text{NS}} \equiv \left(J_0^+ \right)^m L_{-1}^n \, |--\rangle_k^{\text{NS}} \; . \tag{2.65}$$

The CFT state dual to a multi-mode (k, m, n) superstrata, when spectral flowed to the NS sector, is then a coherent sum of strands of the NS vacuum $|0\rangle^{\text{NS}}$ and excited strands of the type (2.65) with different choices of k, m and n. Of course, the total number of copies involved should equal N. In order to have a good description in supergravity, the number of each type of strand within this coherent sum should scale with N in the large N limit [169]. For a single-mode superstrata there will be only two types of strands, $|0\rangle^{\text{NS}}$ and one choice of $|k, m, n\rangle^{\text{NS}}$. Of particular interest for this thesis is the $(1, 0, n)$ family of superstrata, whose dual state (in the NS sector description) is given by

$$\left(|0\rangle^{\text{NS}} \right)^{N_{00}} \left(|1, 0, n\rangle^{\text{NS}} \right)^{N_{1,0,n}} , \tag{2.66}$$

with $N_{00}, N_{1,0,n} \sim N$ as $N \to \infty$ and subject to the constraint $N_{00} + N_{1,0,n} = N$. We emphasise that to be dual to a background geometry, the state must have dimensions $\Delta \sim N$ and so it is really the spectral flow of (2.66) to the RR sector that is dual to the $(1, 0, n)$ superstrata. In terms of the parameters a and b appearing in the bulk solution (2.47), the number of each strand type is given by

$$N_{00} = N \frac{a^2}{a_0^2} \quad , \quad N_{1,0,n} = N \frac{b^2}{2a_0^2} \; . \tag{2.67}$$

The precision holography of superstrata has been studied variously in [26, 49–51, 169–

---

[29]We note that a more general class of excited strand is used to construct the "supercharged superstrata" of [161]. These strands $|k, m, n, q\rangle$ are defined in a similar manner to (2.65) but with the additional action of the $G_{-\frac{1}{2}}^{+A}$ fermionic modes.

171] and lends a large amount of weight to the description of the dual states of super-strata being as described above.

2.2.3 Relation of expansion parameters

In this section we briefly give details on the relation between two expansion parameters $\frac{N_{1,0,n}}{N} = \frac{b^2}{2a_0^2}$ and μ used in Chapters 3 and 4. The definition of μ that we use matches that in [52, 53, 101, 172, 173]

$$\mu \equiv \frac{24 h_H^{[0]}}{c} = \frac{4 h_H^{[0]}}{N} \ , \tag{2.68}$$

where $h_H^{[0]}$ is the reduced dimension of a heavy operator $\mathcal{O}_H$. The mode algebra formed from (2.58) includes the commutator (see for instance appendix A.2 of [166])

$$\left[L_n, J_m^a \right] = -m J_{n+m}^a \ , \tag{2.69}$$

and so, in particular, the R-symmetry current modes mix with L_0 and thus contribute to the dimension of a state. In order to remove these contributions, the Sugawara construction [120] is used to define a stress tensor T^{Sug} with modes L_n^{Sug} describing the contribution of the current to the full stress tensor T. To decouple the algebra of Virasoro modes from those of the current it is possible to define the reduced Virasoro modes $L_n^{[0]} \equiv L_n - L_n^{\text{Sug}}$ with commutator

$$\left[L_n^{\text{Sug}}, J_m^a \right] = 0 \ . \tag{2.70}$$

The associated reduced conformal dimension is then the eigenvalue of $L_0^{[0]}$ given by

$$h^{[0]} \equiv h - \frac{J^2}{N} \ , \tag{2.71}$$

with J^2 being the eigenvalue of the quadratic Casimir of $SU(2)_L$. An analogous discussion holds for the anti-holomorphic sector.

We now compute this reduced dimension for the state dual to the $(1, 0, n)$ family of superstrata discussed in the previous two subsections. The dimension of the heavy operator is simpler to compute in the NS sector and then a spectral flow transformation will be used to relate the two. From the explicit form of the state in (2.66) the NS sector dimensions are

$$h_H^{\text{NS}} = N_{1,0,n} \left(n + \frac{1}{2} \right) \quad , \quad j_H^{\text{NS}} = -\frac{1}{2} N_{1,0,n} \ . \tag{2.72}$$

This then maps to the R-sector quantum numbers using the spectral flow transforma-

tion (2.61) with the full central charge $c = 6N$

$$h_H^{\mathrm{R}} = nN_{1,0,n} + \frac{N}{4} \quad , \quad j_H^{\mathrm{R}} = \frac{N}{2} - \frac{1}{2}N_{1,0,n} \ . \tag{2.73}$$

Using the values of N_{00} and $N_{1,0,n}$ in terms of the bulk parameters given in (2.67), the reduced conformal dimension is then given by

$$h_H^{[0]} = h_H^{\mathrm{R}} - \frac{\left(j_H^{\mathrm{R}}\right)^2}{N} = \frac{N}{4}\frac{b^2}{2a_0^2}\left[4n + 2 - \frac{b^2}{2a_0^2}\right] \ . \tag{2.74}$$

Using the relation between μ and h_H in (2.68) and inverting[30] gives

$$\frac{b^2}{2a_0^2} = 2n + 1 - \sqrt{(2n+1)^2 - \mu} \ . \tag{2.75}$$

2.3 AdS$_3$ HHLL holographic correlators

In this section we briefly outline the method of computation of 4-point holographic correlation functions involving two heavy and two light operators used in [70–72, 80]. In particular, we focus on the case of the heavy operator $\mathcal{O}_H$ dual to the $(1,0,0)$ two-charge microstate geometry obtained from the $(1,0,n)$ solution (2.47) by setting $n = 0$ and taking the decoupling limit (1.10). The light operator considered will be an untwisted sector $(k = 1)$ T^4-invariant chiral primary operator $\mathcal{O}_L$ of dimension $(h_L, \bar{h}_L) = (1/2, 1/2)$. For technical reasons, we will also need its superdescendent $\mathcal{O}_L^{\mathrm{B}}$ which has dimensions $(h_L^{\mathrm{B}}, \bar{h}_L^{\mathrm{B}}) = (1, 1)$ and $j = \bar{j} = 0$ (for this reason, the chiral primary is sometimes referred to as "fermionic" and the descendent as "bosonic", though the terminology may be misleading). The exact form of these light operators in terms of the basic fields (2.56) of the D1-D5 orbifold CFT is not crucial in this section, however, we give them for possible future reference as

$$\mathcal{O}_L = \sum_{r=1}^N \mathcal{O}_{(r)}^{++} = \frac{-i}{\sqrt{2N}} \sum_{r=1}^N \epsilon_{\dot{A}\dot{B}} \, \psi_{(r)}^{+\dot{A}} \bar{\psi}_{(r)}^{+\dot{B}} \ , \quad \mathcal{O}_L^{\mathrm{B}} = \frac{1}{\sqrt{2N}} \sum_{r=1}^N \epsilon_{\dot{A}\dot{B}} \, \partial X_{(r)}^{+\dot{A}} \bar{\partial} X_{(r)}^{+\dot{B}} \ , \tag{2.76}$$

where $r = 1, \ldots, N$ is a copy label and similar expressions hold for the "barred" operators. Correlators involving these two different light operators are related via the superconformal Ward identity

$$C^{\mathrm{B}}(z, \bar{z}) = \partial\bar{\partial}\big[|z|C(z, \bar{z})\big] \ , \tag{2.77}$$

---

[30]In inverting the expression, the root such that both sides vanish for $\mu = 0$ is chosen.

where we define the correlators (on the plane)

$$C^{\mathrm{B}}(z,\bar{z}) \equiv \langle \bar{\mathcal{O}}_H(0)\mathcal{O}_H(\infty)\mathcal{O}_L^{\mathrm{B}}(1)\bar{\mathcal{O}}_L^{\mathrm{B}}(z,\bar{z})\rangle \ , \tag{2.78a}$$

$$C(z,\bar{z}) \equiv \langle \bar{\mathcal{O}}_H(0)\mathcal{O}_H(\infty)\mathcal{O}_L(1)\bar{\mathcal{O}}_L(z,\bar{z})\rangle \ . \tag{2.78b}$$

Since C^{B} has a clearer bulk dual description than C, the idea is to compute (2.78a) by considering the bulk perturbation dual to $\mathcal{O}_L^{\mathrm{B}}$ on the background $(1,0,0)$ solution and then map the result to C using (2.77). This perturbation is described by a minimally coupled scalar Φ which satisfies the wave equation

$$\square_6 \Phi = \frac{1}{\sqrt{\widetilde{g}}}\partial_M\left(\sqrt{\widetilde{g}}\,\widetilde{g}^{MN}\partial_N\Phi\right) = 0 \ , \tag{2.79}$$

where $\square_6$ is the Laplace operator in the 6-dimensional $(1,0,0)$ metric $\widetilde{g}_{MN}$ with $\widetilde{g} \equiv |\det \widetilde{g}_{MN}|$. Since the light operator $\mathcal{O}_L^{\mathrm{B}}$ has zero R-charge, the scalar field Φ can be projected onto the singlet S^3 spherical harmonic. From the asymptotic expansion as $r \to \infty$ of the solution to (2.79) that is regular in the interior $(r \to 0)$, the 2-point function on the cylinder

$$b^{\mathrm{B}}(t,y) \equiv \langle \bar{\mathcal{O}}_H|\mathcal{O}_L^{\mathrm{B}}(0,0)\bar{\mathcal{O}}_L^{\mathrm{B}}(t,y)|\mathcal{O}_H\rangle = |z|^2 C^{\mathrm{B}}(z,\bar{z}) \ , \tag{2.80}$$

where $|\mathcal{O}_H\rangle = \mathcal{O}_H(t \to \infty)|0\rangle$ and similarly for $\langle\bar{\mathcal{O}}_H|$, can be extracted as

$$\Phi \approx D(t,y) + \frac{1}{r^2}b^{\mathrm{B}}(t,y) \ , \tag{2.81}$$

with $D(t,y)$ being the source on the boundary for $\mathcal{O}_L^{\mathrm{B}}$. In (2.80), the factor of $|z|^2$ is simply due to the transformation from the plane to the cylinder of the operator $\bar{\mathcal{O}}_L^{\mathrm{B}}(z,\bar{z})$. A dramatic simplification to this problem occurs for the $(1,0,n)$ family of superstrata (and thus also for the case of $(1,0,0)$ discussed here) in that the wave equation (2.79) is separable. As mentioned below equation (2.55), writing the 6D metric (2.47) in the form of a dimensional reduction on the S^3 as in (2.54) yields a 3-dimensional metric $g_{\mu\nu}$ that is *independent* of the S^3 coordinates (θ, ϕ_1, ϕ_2). In this special case, the problem of solving (2.79) reduces to the simpler problem of solving

$$\square_3 \Phi = \frac{1}{\sqrt{g}}\partial_\mu\left(\sqrt{g}\,g^{\mu\nu}\partial_\nu\Phi\right) = 0 \ , \tag{2.82}$$

with $g \equiv |\det g_{\mu\nu}|$. This separability is not a property shared generally with other superstrata and partly accounts for the use of the $(1,0,n)$ family as a workhorse for gaining insight into black hole microstates. As will be discussed in Section 4.4, the

$(1, 0, 0)$ reduced 3D metric takes the form

$$\frac{ds_3^2}{\sqrt{Q_1 Q_5}} = \frac{\rho^2 + \alpha^2}{(\rho^2 + 1)^2} \, d\rho^2 - \alpha^2 \left(\rho^2 + \alpha^2\right) d\tau^2 + \alpha^2 \rho^2 \, d\sigma^2 \,, \tag{2.83}$$

where the coordinate redefinitions used, relative to those in Section 2.2, are

$$\rho = \frac{r}{a} \quad, \quad \tau = \frac{t}{R_y} \quad, \quad \sigma = \frac{y}{R_y} \quad, \quad \alpha = \frac{a}{a_0} \,. \tag{2.84}$$

Decomposing $\Phi(\rho, \tau, \sigma)$ into Fourier modes of τ and σ labelled by $\omega \in \mathbb{R}$ and $\ell \in \mathbb{Z}$ respectively, the wave equation (2.82) reduces to a radial equation for $\Phi(\rho)$ given by

$$\frac{d^2 \Phi}{d\rho^2} + \frac{1 + 3\rho^2}{\rho(1 + \rho^2)} \frac{d\Phi}{d\rho} - \frac{\rho^2(\ell^2 - \omega^2) + \alpha^2 \ell^2}{\alpha^2 \rho^2 (1 + \rho^2)^2} \Phi = 0 \,. \tag{2.85}$$

Using the substitutions

$$w(x) = x^{\frac{\ell}{2}} \Phi(\rho) \quad \text{with} \quad x \equiv \frac{\rho^2}{1 + \rho^2} \,, \tag{2.86}$$

the equation (2.85) becomes the hypergeometric equation [174]

$$w'' + \left(\frac{c}{x(1 - x)} - \frac{a + b + 1}{1 - x}\right) w' - \frac{ab}{x(1 - x)} w = 0 \,, \tag{2.87}$$

with

$$a = \frac{\ell - \gamma}{2} \quad, \quad b = \frac{\ell + \gamma}{2} \quad, \quad c = 1 + \ell \quad, \quad \gamma \equiv \frac{1}{\alpha} \sqrt{\omega^2 - \ell^2 (1 - \alpha^2)} \,. \tag{2.88}$$

The hypergeometric equation has two independent solutions w_+ and w_- with a general solution being the linear combination

$$w(x) = c_+ w_+ + c_- w_- = c_+ \, {}_2F_1(a, b; c; x) + c_- \, x^{1-c} \, {}_2F_1(1 + a - c, 1 + b - c; 2 - c; x) \,. \tag{2.89}$$

The desired solution required for $b^{\mathrm{B}}(t, y)$ in (2.81) is the order $(1 - x)$ term as $x \to 1$ (corresponding to $\rho \to \infty$) which is regular as $x \to 0$ ($\rho \to 0$). The regularity condition in the interior fixes the constants in (2.89) to be $c_+ = 1$ and $c_- = 0$ and expanding the result around $x = 1$ gives

$$w(x) \approx \frac{\Gamma(1 + |\ell|)}{\Gamma\left(1 + \frac{|\ell| + \gamma}{2}\right) \Gamma\left(1 + \frac{|\ell| - \gamma}{2}\right)} \left[1 + \frac{\ell^2 - \gamma^2}{4} \left(H_{\frac{|\ell| + \gamma}{2}} + H_{\frac{|\ell| - \gamma}{2}} - 1\right)(1 - x)\right] \,, \tag{2.90}$$

where H_n is a Harmonic number. Using (2.86) to obtain the required solution to the original radial equation (2.85), $b^{\mathrm{B}}(t, y)$ can be found to be proportional to

$$b^{\mathrm{B}}(t, y) \sim \sum_{\ell=-\infty}^{\infty} \int \frac{d\omega}{4\pi^2} \, e^{i(\omega\tau + \ell\sigma)} \left[\frac{\ell^2 - \gamma^2}{4} \left(H_{\frac{|\ell|+\gamma}{2}} + H_{\frac{|\ell|-\gamma}{2}} - 1 \right) - \frac{|\ell|}{2} \right]. \qquad (2.91)$$

Using the Ward identity (2.77) to map $b^{\mathrm{B}}(t, y) \rightarrow b(t, y)$, with $b(t, y) = |z| C(z, \bar{z})$ involving the chiral primary light operator $\mathcal{O}_L$ and evaluating the Fourier integral over ω yields the correlator (2.78b)

$$C(\tau, \sigma) = \frac{a}{a_0} \sum_{k=1}^{\infty} \sum_{\ell \in \mathbb{Z}} e^{i\ell\sigma} \frac{\exp\left[-i\tau \frac{a}{a_0} \sqrt{(|\ell| + 2k)^2 + \frac{b^2 \ell^2}{2a^2}} \right]}{\sqrt{1 + \frac{b^2}{2a^2} \frac{\ell^2}{(|\ell|+2k)^2}}}. \qquad (2.92)$$

In terms of the coordinates on the plane $(z, \bar{z})$, related to $\tau = \frac{t}{R_y}$, $\sigma = \frac{y}{R_y}$ by $z = e^{i(\tau+\sigma)}$, $\bar{z} = e^{i(\tau-\sigma)}$, the correlator (2.92) becomes

$$C^{\mathrm{fer}}(z, \bar{z}) = \frac{a}{a_0} \sum_{k=1}^{\infty} \sum_{\ell \in \mathbb{Z}} \frac{1}{\sqrt{1 + \frac{b^2}{2a^2} \frac{\ell^2}{(|\ell|+2k)^2}}} \left(\frac{z}{\bar{z}} \right)^{\frac{\ell}{2}} (z\bar{z})^{-\frac{a}{2a_0} \sqrt{(|\ell|+2k)^2 + \frac{b^2}{2a^2}\ell^2}}. \qquad (2.93)$$

The details of this calculation can be found in [72]. While (2.92) is not able to be resummed directly, a closed form expression at first order in $\frac{b^2}{2a_0^2}$ was found in [133]. Despite this, the HHLL correlator (2.92) will be the starting point for Chapter 3. Equivalent correlators for other, more complicated, heavy operators have been considered only at first order in $\frac{b^2}{2a_0^2}$ (see for instance [80]).

2.4 The bulk phase shift

In this section we summarise the calculation of the eikonal phase in the AdS/CFT duality context. While the approach is general, we are particularly interested in the case relevant to the decoupling limit of a D1-D5 brane system, and so our equations will be specialised to the $\mathrm{AdS}_3/\mathrm{CFT}_2$ duality. We here provide a short discussion of the geodesic problem relevant to the semiclassical bulk calculation and then later in Section 4.2 summarise the technology that can be used to derive the eikonal from CFT four-point correlators.

In the gravitational picture of the analysis of Chapter 4, we will focus on three-dimensional geometries that arise from the dimensional reduction (2.54) of asymptotically $\mathrm{AdS}_3 \times S^3$ supergravity solutions that are holographically dual to known CFT_2 heavy operators. We will need to consider the time delay and angular shift accrued by

a null geodesic – approximating the high energy light probe[31] – that begins and ends on the AdS boundary.

The action describing a massive particle (with mass m) travelling in a curved background geometry with metric $g_{\mu\nu}$, along a path $x^\mu(\tau)$ with affine parameter τ, is given by

$$S_m = -m \int d\tau \sqrt{-\frac{dx^\mu}{d\tau}\frac{dx^\nu}{d\tau}g_{\mu\nu}} \ , \qquad (2.94)$$

where the negative sign inside the square root is to ensure the quantity in the square root is positive for a timelike worldline in the mostly plus signature. This action does not allow for the generalisation to the massless case and so an auxiliary variable $e(\tau)$ is introduced, acting as an einbein on the worldline, yielding the action

$$S = \int d\tau \left[(2e)^{-1} \frac{dx^\mu}{d\tau}\frac{dx^\nu}{d\tau}g_{\mu\nu} - \frac{em^2}{2} \right] \ , \qquad (2.95)$$

which does have a good massless limit, giving

$$S = \int d\tau \, (2e)^{-1} \frac{dx^\mu}{d\tau}\frac{dx^\nu}{d\tau}g_{\mu\nu} \ . \qquad (2.96)$$

This action is invariant under reparametrisations $\tau \to \tilde{\tau}(\tau)$ if $e(\tau)$ transforms as

$$e(\tau) \to e(\tilde{\tau}) = e(\tau)\frac{d\tau}{d\tilde{\tau}} \ . \qquad (2.97)$$

Here $e(\tau)$ is not dynamical since its equation of motion is purely algebraic; simply substituting its equation of motion back into (2.95) gives (2.94). In fixing the reparametrisation invariance (2.97), it is possible to set $e = 1$ simply giving the action

$$S = \int d\tau \, \frac{1}{2} \frac{dx^\mu}{d\tau}\frac{dx^\nu}{d\tau}g_{\mu\nu} \ . \qquad (2.98)$$

The momenta conjugate to the positions x^μ are given by

$$p_\nu \equiv \frac{\delta S}{\delta \dot{x}^\nu} = \dot{x}^\mu g_{\mu\nu} \quad , \quad p^\lambda = g^{\lambda\nu} p_\nu = \dot{x}^\lambda \ , \qquad (2.99)$$

which are conserved along the worldline if the spacetime has suitable Killing vectors (as is usual, a dot signifies a derivative with respect to τ). All of the three-dimensional reduced metrics that we will focus on have two Killing vectors; these are associated to the coordinates that, at the boundary, are identified with the temporal (t) and spatial (y) directions of the CFT. Thus, the momenta p_t and p_y will be conserved along the

---

[31]This approximation to the propagation of a probe emerges from the stationary phase approximation as discussed in [175].

a)

b)

c)

Pure AdS

Deformed Geometry
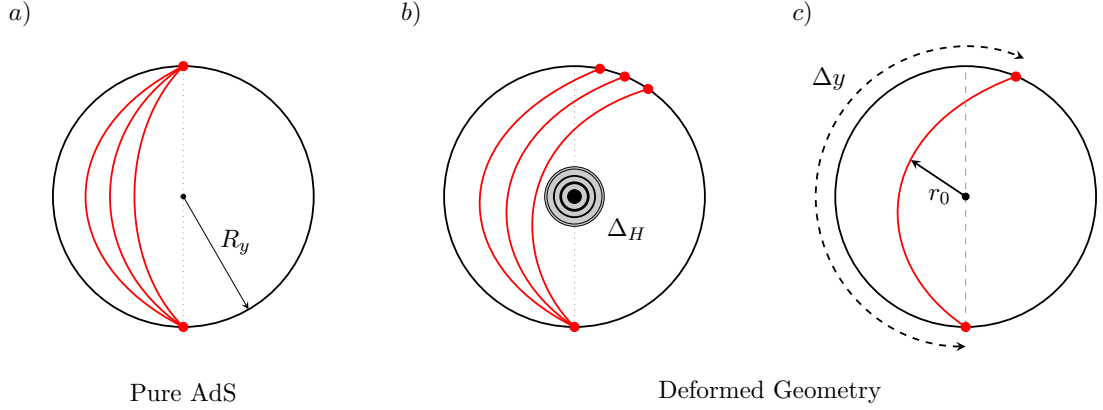
Figure 2.2: The projection of null geodesics in asymptotically AdS$_3$ spaces with time increasing out of the page and the asymptotic AdS boundary being the outer solid black circle. In *a)* we depict null geodesics in pure AdS which all converge to one point (with $\Delta y = \pi R_y$) given fixed initial boundary data. In *b)* we show an asymptotically AdS spacetime with a schematic representation of the deformation of spacetime away from empty AdS. This causes the geodesics to be deflected and they re-emerge from the bulk at different points. Figure *c)* indicates the spatial shift Δy acquired by a null geodesic as it crosses the bulk and the radial turning point r_0 as the point of closest approach to the origin $r = 0$.

worldline. From these, the phase shift is defined as [52, 175]

$$\delta(\mathbf{p}) \equiv -\mathbf{p} \cdot \Delta \mathbf{x} = -p_t \, \Delta t - p_y \, \Delta y \,, \tag{2.100}$$

where $\Delta \mathbf{x}$ denotes the variation of the boundary coordinate $\mathbf{x}$ between the two ends of the geodesic. The geometries we consider can be written in a coordinate system where the metric is block-diagonal, i.e. the mixed components involving the radial direction and t, y vanish. Then, the condition for a null geodesic $\dot{x}^\mu g_{\mu\nu} \dot{x}^\nu = 0$ can be rewritten in terms of the conserved quantities as follows

$$g_{rr}\dot{r}^2 = p_t^2 \, \frac{g_{yy} - 2\beta g_{ty} + \beta^2 g_{tt}}{g_{ty}^2 - g_{tt}g_{yy}} \,, \tag{2.101}$$

where β is related to the impact parameter of the geodesic and defined as

$$\beta \equiv \frac{p_y}{p_t} \,. \tag{2.102}$$

Other commonly used parameters are s and L, defined by[32]

$$|p_t| = \frac{s}{R_y} \, \cosh L \quad , \quad p_y = \frac{s}{R_y} \, \sinh L \quad \Rightarrow \quad \tanh L = \beta \,, \tag{2.103}$$

where R_y is the radius of the CFT spatial direction y. The radial turning point r_0 is

---

[32]Note that for us, p_t is negative for future-pointing geodesics.

given by the largest real solution of the equation $\dot{r} = 0$ and so is derived by setting Eq. (2.101) to zero. The time-delay Δt and angular shift Δy are then given by

$$\Delta t = 2 \int_{r_0}^{\infty} dr \, \frac{\dot{t}}{\dot{r}} \quad , \quad \Delta y = 2 \int_{r_0}^{\infty} dr \, \frac{\dot{y}}{\dot{r}} \ . \tag{2.104}$$

By using (2.101) and the conserved quantities (2.99), the eikonal can be written in terms of the following integral

$$\delta = 2 \, |p_t| \int_{r_0}^{\infty} dr \, \frac{\dot{t} + \beta \dot{y}}{\dot{r}} = 2 \, |p_t| \int_{r_0}^{\infty} dr \, \sqrt{g_{rr}} \, \sqrt{\frac{g_{yy} - 2\beta g_{ty} + \beta^2 g_{tt}}{g_{ty}^2 - g_{tt} g_{yy}}} \ . \tag{2.105}$$

This formula will be used in the bulk side of the calculations for explicit examples in Chapter 4.

Chapter 3

LLLL Holographic Correlators

The contents of this chapter are based on the paper [2].

3.1 Introduction and conclusion

In this chapter we extend the analysis of the light limit of HHLL correlators beyond
the first non-trivial order in the number of constituents and show that the sublead-
ing corrections capture interesting information about 4-point correlators that involve
two light, but multi-trace operators, and two standard single-trace operators. As is
usual for holographic results obtained with the use of a supergravity approximation,
these correlators are valid in the large N, strong coupling regime of the CFT. To be
more precise, we provide evidence that the results obtained from the light limit of the
supergravity HHLL correlators capture the *tree-level connected Witten diagram con-
tributions* relevant for the correlators under study. It is interesting to see that the
explicit results involve a generalisation of the D-function usually appearing in the cor-
relators among single-particle operators. These D-functions arise naturally from the
integrals appearing in a Witten diagram describing the contact 4-point interaction be-
tween bulk fields and can be written in terms of the Bloch-Wigner dilogarithm [176].
The multi-trace correlators we obtain here are written in terms of the Bloch-Wigner-
Ramakrishnan polylogarithms [177] which are generalisations sharing several properties
of the standard Bloch-Wigner function, but involve higher order polylogarithms. These
polylogarithms have also appeared in other physics applications, such as the evaluation
of multi-loop Feynman integrals [178], the analysis of the free energies in $O(N)$ and
$U(N)$ models [179, 180] and, in the holographic context, the expression of integrated
four-point correlators [181].

    As already mentioned above, the multi-trace operators we consider are made from
identical constituents which are mutually BPS and so it is possible to relate the 4-point
correlators we discuss to a particular kinematic limit of a higher-point function involving

just single-particle states. This relation to higher-point functions involves two steps. The first is the kinematic limit taking two groups of n identical operators in a $(2n+2)$-point correlator to the same position and the second is to relate the resulting n-trace operators to those that are natural from the point of view of the heavy operators dual to the smooth bulk geometries which are used in deriving the HHLL correlators. Despite these two steps, we argue that the functions appearing in the multi-trace correlators we construct are present also in higher-point functions of single-trace operators. As will be discussed in more detail in the main text, this picture makes it evident that these correlators contain both classical (tree-level) and quantum (loop) contributions in the gravity picture at a given order in the $1/N$-expansion. However, as previously stressed, our results capture only the classical part and provide a window on the structure of tree-level Witten diagrams for correlators with six or more single particle external states, albeit in the simplifying kinematic limit where only two cross-ratios survive. We point out that, even in this simplified regime, these results are qualitatively different from those obtained in [182] where an explicit five-point correlator was calculated in $AdS_5 \times S^5$ and the result could still be written in terms of standard Bloch-Wigner functions.

Since the extrapolation of the HHLL correlator to small values of the heavy operator's conformal dimension – on which we base our derivation of the correlators with multi-particle states – is a priori unjustified, it is important to gather independent evidence on the correctness of our conjecture. We thus take various OPE limits of the multi-particle correlators and verify that we obtain consistent results. One can, for example, focus on the light-cone OPE limit – where to leading order, only the conserved currents are exchanged – and check that our correlators reproduce the expected behaviour of their conformal blocks. Alternatively, one can isolate the exchange of protected multi-trace operators – produced in the OPE of operators preserving the same supersymmetries – and match the corresponding three-point couplings with those computed in the weakly coupled (orbifold) CFT. New dynamical information is contained in the anomalous dimensions and couplings of the non-BPS multi-trace operators and despite, at present, not knowing all of the necessary correlators to extract this information completely, we verify some qualitative features of the OPE in the non-protected channels and derive constraints on these dynamical quantities. We note, however, that the OPE data of the double-trace non-BPS operators with minimal (bare) twist can be inferred from known amplitudes of four single-trace chiral primary operators with the lowest dimension $(1/2, 1/2)$ – these sit in one of the N_f tensor multiplets (where $N_f = 5$ or 21 for the theory compactified on T^4 or $K3$). Unlike in $AdS_5 \times S^5$ [183], this task already involves a non-trivial mixing problem[33] between the different multi-

---

[33]In a recent article [184] the nice observation was made that, for non-BPS multi-traces in non-trivial flavour representations, the same mixing problem can be solved for arbitrary twist using the available

plet flavours. This analysis provides a somewhat surprising result: we find a *positive* anomalous dimension for operators of spin 0 *and 2*. The question of the existence of a consistent large N CFT with a spin-two operator with a positive anomalous dimension was raised in [185] and this is, to the best of our knowledge, the first affirmative answer to this search.

3.2 Correlators with multi-trace operators: the setup

The main object of study in this chapter is a special class of holographic correlators in the CFT$_2$ dual to type IIB superstring theory on AdS$_3 \times S^3 \times \mathcal{M}$, where $\mathcal{M}$ can be either T^4 or $K3$. A first way to characterise this class of correlators is in terms of 4-point functions involving two BPS-conjugate multi-trace operators and two BPS-conjugate single-trace operators. Since all operators that we consider are scalars, conformal invariance implies that the correlators depend on a single function of two cross-ratios

$$\langle \bar{\mathcal{O}}_f^n(z_1, \bar{z}_1)\, \mathcal{O}_f^n(z_2, \bar{z}_2)\, \mathcal{O}_g(z_3, \bar{z}_3)\, \bar{\mathcal{O}}_g(z_4, \bar{z}_4) \rangle = \frac{\mathcal{G}_n(z, \bar{z})}{|z_{12}|^{2n\Delta_f}|z_{34}|^{2\Delta_g}}\ , \qquad (3.1)$$

where $z_{ij} = z_i - z_j$ and $\mathcal{O}_{f,g}$ ($\bar{\mathcal{O}}_{f,g}$) are (anti-)chiral Primaries Operators (CPO) in the D1-D5 CFT$_2$ with identical holomorphic and antiholomorphic dimensions $h = \bar{h} = \Delta/2$ and flavour indices[34] f, g. We define the cross-ratio z as in (2.19) and so it is often convenient to work in the gauge given in (2.26) where the correlator takes the form

$$\mathcal{C}_n(z, \bar{z}) \equiv \lim_{z_2 \to \infty} |z_2|^{2n\Delta_f} \langle \bar{\mathcal{O}}_f^n(0, 0)\, \mathcal{O}_f^n(z_2, \bar{z}_2)\, \mathcal{O}_g(1, 1)\, \bar{\mathcal{O}}_g(z, \bar{z}) \rangle = \frac{\mathcal{G}_n(z, \bar{z})}{|1 - z|^{2\Delta_g}}\ . \qquad (3.2)$$

The function $\mathcal{G}_n(z, \bar{z})$, which contains the dynamical information, at least in principle can be calculated in the holographic regime by summing Witten diagrams. As depicted in Fig. 3.1, there are different types of contributing diagrams and we will focus on the connected tree-level diagrams, such that in b), which are of order $1/N^n$. For the class of correlators in (3.1) there are also other contributions relevant at the same order in the $1/N$ expansion (see the disconnected 1-loop diagram c in Fig. 3.1) and so our results do not in general represent the full holographic correlators (3.1) at order $1/N^n$. We will discuss below how these disconnected loop contributions cancel in our approach.

As Fig. 3.1 suggests, it is possible to view the correlators in (3.1) as a particular kinematic limit of a $(2n+2)$-point function where the multi-trace operators are replaced by n identical CPOs at different positions, which are then taken to the same point, for instance as $\mathcal{O}_f^n(z_2, \bar{z}_2) = \lim_{w_a \to z_2} \prod_{a=1}^n \mathcal{O}_f(w_a, \bar{w}_a)$. Thus our results provide a first

---

correlator data.

[34]Since the 6D bulk theory has 16 supercharges, the fields organise into different multiplets; we focus on CPOs of the matter tensor multiplets of which there are 5 (21) different flavours in the $\mathcal{M} = T^4$ ($K3$) case.
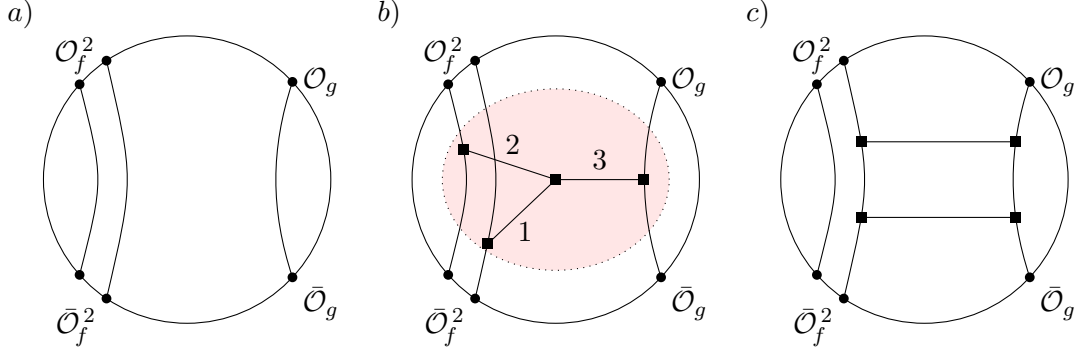
Figure 3.1: Three Witten diagrams contributing to (3.1) for the case of $n = 2$. Diagram $a)$ is disconnected and thus contributes at leading order in large N, while the remaining two involve four bulk vertices (denoted by a black square) and so are both suppressed by a factor of $1/N^2$ with respect to the first. Diagram $b)$ depicts a connected tree-level diagram, while $c)$ contains a disconnected 1-loop structure. The results derived in this chapter focus on the former class of contributions, where in the shaded region one considers all possible ways of obtaining a connected tree-level structure. Such diagrams contain up to three bulk-to-bulk propagators (labelled explicitly by $1, 2, 3$ in $b)$) and, as mentioned in the text, this makes a direct evaluation of such contributions challenging.

window on higher-point holographic correlators[35], making it possible to go beyond the explicit 5-point $AdS_5 \times S^5$ example discussed in [182], since the $n = 2$ case is already related to a correlator involving six single-trace operators. Correlators with six or more external points and their OPE limits discussed in this thesis are expected to be intrinsically more complicated than the lower point examples since the method introduced in [62] to deal with bulk-to-bulk propagators will not be sufficient to evaluate them. This can be seen by considering the connected tree-diagram given in Fig. 3.3a. By following [62] one can, for instance, write the part of the diagram involving one pair of the operators $\mathcal{O}_f$, $\bar{\mathcal{O}}_f$ and the bulk-to-bulk propagator 1 as a *finite* sum of boundary-to-bulk propagators directly linking the two positions of the boundary operators with the bulk interaction vertex (giving the diagram of Fig. 3.3b). This procedure can be repeated for the remaining pair of the operators $\mathcal{O}_f$, $\bar{\mathcal{O}}_f$ and the bulk-to-bulk propagator 3 to get a sum of diagrams of the form of Fig. 3.3c. However, after this second step it is not possible to eliminate the final bulk-to-bulk propagator (labelled 2) because each of its endpoints is connected to three external points. Thus, tree diagrams such as the one depicted in Fig. 3.3a cannot be recast as a sum of contact diagrams. This is in contrast to the connected tree-diagram given in Fig. 3.1b, which can be reduced to a finite sum

---

[35]In [186] a particular class of n-point functions in $\mathcal{N} = 4$ SYM was considered. These correlators violate maximally the $U(1)_Y$ bonus symmetry of the supergravity limit and are related to lower point correlators by a recursion relation. The multi-particle correlators relevant for our analysis preserve the corresponding bonus symmetry, which for the AdS_3 case is $SU(2)$, and do not obey any simple recursion relation.
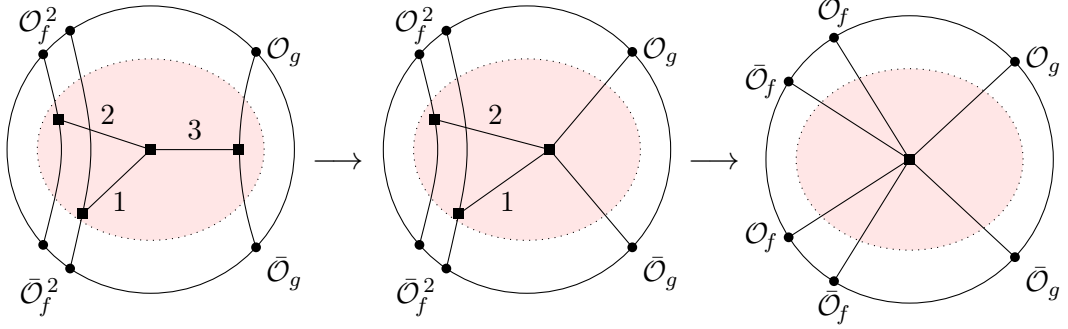
Figure 3.2: An example of the reduction of a Witten diagram contributing to the multi-trace correlator $\mathcal{C}_{n=2}$ that can be reduced to a contact diagram [62]. After each iteration, the result is a finite sum of such diagrams.

of contact diagrams following the method of [62]. Therefore, even after taking the kinematic limit reducing the higher-point correlators to the 4-point function (3.1), we do not expect that the contribution of all connected tree diagrams can be expressed in terms of the standard $D_{\Delta_1,\Delta_2,\Delta_3,\Delta_4}$ functions. Indeed as discussed in the next section, new objects (the Bloch-Wigner-Ramakrishnan polylogarithms) naturally appear in this case.

We conclude this introductory section by presenting an effective way to isolate the tree-level connected contributions to (3.1) which is suggested by the dual gravitational description for the "heavy states" (where $n \sim N$). To have a well-defined semiclassical description it is natural to consider particular coherent-state-like linear combinations of multi-particle states [26, 169, 187] that are dual to a class of asymptotically $\mathrm{AdS}_3 \times S^3$ supergravity solutions. Since these coherent states are classical supergravity objects, one can expect that they receive contributions only from the tree-level diagrams such as the ones in Fig. 3.1b and 3.3a and that loop diagrams cancel out. We will provide evidence that this is indeed the case. Then by following [26, 169, 187], we define the operator

$$\mathcal{O}_{H,f} = \sum_{p=0}^{N} \sqrt{\binom{N}{p}} \left(\frac{B}{\sqrt{N}} \right)^p \left(1 - \frac{B^2}{N} \right)^{\frac{N-p}{2}} \mathcal{O}_f^p \,, \tag{3.3}$$

where B is a parameter[36] that, for simplicity, we take real and $\mathcal{O}_f^p$ is defined such that the 2-point function with its conjugate operator is normalised to one. Then we can write an expansion linking the 4-point HHLL correlator involving the heavy operators $\mathcal{O}_{H,f}$ in (3.3) and the correlators $\mathcal{C}_p$ containing the multi-particle constituents $\mathcal{O}_f^p$, as

---

[36]In terms of the other expansion parameters used in this thesis, the B that is used in this chapter is related to the supergravity parameters of the $(1,0,n)$ superstrata via $B^2 = N\frac{b^2}{2a_0^2}$ which in turn can be related to the μ of Chapter 4 by equation (2.75).
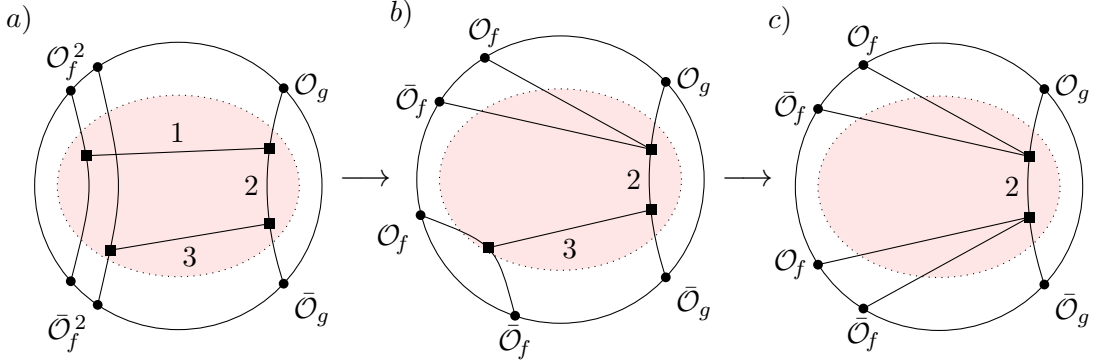
Figure 3.3: An example of a connected tree-level Witten diagram contributing to the multi-trace correlator $\mathcal{C}_{n=2}$ with three bulk-bulk propagators which cannot be reduced to a finite sum of contact diagrams using the results of [62]. After two applications of this technique, the remaining bulk-bulk propagator 2 in the rightmost diagram cannot be reduced further due to being connected to three boundary points at each vertex. After each step given, the result will be proportional to a finite sum of such diagrams.

follows:

$$
\begin{aligned}
\langle \bar{\mathcal{O}}_{H,f} \mathcal{O}_{H,f} \mathcal{O}_g \bar{\mathcal{O}}_g \rangle &= \sum_{p=0}^{N} \left(\frac{B^2}{N} \right)^p \left(1 - \frac{B^2}{N} \right)^{N-p} \binom{N}{p} \mathcal{C}_p \\
&= \sum_{p=0}^{N} \sum_{q=0}^{N-p} (-1)^q \left(\frac{B^2}{N} \right)^p \left(\frac{B^2}{N} \right)^q \binom{N-p}{q} \binom{N}{p} \mathcal{C}_p \\
&= \sum_{n=0}^{N} \left(\frac{B^2}{N} \right)^n \sum_{p=0}^{n} (-1)^{n-p} \binom{N-p}{n-p} \binom{N}{p} \mathcal{C}_p \\
&= \sum_{n=0}^{N} \left(\frac{B^2}{N} \right)^n \binom{N}{n} C_n \ ,
\end{aligned}
\tag{3.4}
$$

where

$$
C_n \equiv \sum_{p=0}^{n} (-1)^{n-p} \binom{n}{p} \mathcal{C}_p \ .
\tag{3.5}
$$

In the first step we simply expanded the $(N-p)$-th power and rearranged the sums so as to collect the factors of B^2 and in the final step we defined the combination C_n. This is the combination that is encoded in the HHLL correlator and, as mentioned above, it captures only the *connected tree-level* diagrams of $\mathcal{C}_n$ for each value of n. Let us see how this looks in the simplest examples. For $n = 1$ we have

$$
C_1 = \langle \bar{\mathcal{O}}_f \mathcal{O}_f \mathcal{O}_g \bar{\mathcal{O}}_g \rangle - \langle \mathcal{O}_g \bar{\mathcal{O}}_g \rangle \ ,
\tag{3.6}
$$

so the disconnected contribution to the first term is cancelled exactly by the 2-point

function appearing in the second term (note that we have chosen a normalisation such that $\langle \bar{\mathcal{O}}_f(0)\mathcal{O}_f(\infty)\rangle = 1$). The first example involving multi-trace operators requires $n = 2$ and from the definition (3.5) we have

$$C_2 = \langle \bar{\mathcal{O}}_f^2 \mathcal{O}_f^2 \mathcal{O}_g \bar{\mathcal{O}}_g \rangle - 2\langle \bar{\mathcal{O}}_f \mathcal{O}_f \mathcal{O}_g \bar{\mathcal{O}}_g \rangle + \langle \mathcal{O}_g \bar{\mathcal{O}}_g \rangle \ . \tag{3.7}$$

The fully disconnected contributions of order N^0 cancel as before, but now there is also a cancellation among the partially connected contributions – diagrams with a 2-point function factorised from the other four operators, which have a leading contribution of order N^{-1} and a 1-loop term of order N^{-2}. The remainder of the connected part of this correlator is thus the N^{-2} terms not containing loops.

3.3 Multi-trace correlators

One way of calculating a HHLL correlator of the type (3.4) requires solving a wave equation in the background of the geometry dual to the heavy state. In general this is a difficult problem that cannot be solved exactly and one usually resorts to approximation schemes to simplify the task. For example, one can use a WKB method [31,78] or alternatively work in the regime where the heavy state generates only small deformations of $AdS_3 \times S^3$ rather than a fully backreacted geometry. In the latter case, expressions can be obtained analytically using standard holographic techniques and correlators have been obtained employing this method for various heavy states [70,71,80]. However, such results are typically limited only to first order corrections around the $AdS_3 \times S^3$ vacuum and can be related to correlators of single-particle operator [73–75].

Nonetheless, for a specific choice of heavy state it was found that one can evaluate the heavy-heavy-light-light correlator exactly in terms of a double Fourier series [72]. In this section we study this particular correlator and use the expansion (3.4) to extract a closed form expression for connected tree-level correlation functions with double-trace operator insertions. We find that particular combinations of higher-order polylogarithms – the Bloch-Wigner-Ramakrishnan polylogarithm functions – appear in these multi-trace correlators and we dedicate a part of this section to a brief review of these functions.

Some of the more technical results, together with examples of correlators involving pairs of higher multi-trace operators can be found in Appendix B.1.

3.3.1 Explicit statement of higher-order correlators

To specify precisely which operators appear in the correlator that is to be the main focus of this section, we use the notation of the orbifold point of the D1-D5 CFT at which it is described by a sigma model with target space $(\mathcal{M})^N /S_N$ (most of our results

are valid for both $\mathcal{M} = T^4$ and $K3$). The theory contains a collection of N free bosonic and fermionic fields which naturally split into a holomorphic and an anti-holomorphic sector as

$$\left(\partial X_{(r)}^{A\dot{A}}(z) , \psi_{(r)}^{\alpha\dot{A}}(z)\right) , \qquad \left(\bar{\partial} X_{(r)}^{A\dot{A}}(\bar{z}) , \tilde{\psi}_{(r)}^{\dot{\alpha}\dot{A}}(\bar{z})\right) , \tag{3.8}$$

where the the indices $A, \dot{A} = 1, 2$ are related to the $SU(2)$ symmetries of the internal manifold $\mathcal{M}$; $\alpha, \dot{\alpha} = \pm$ are fundamental $SU(2)_L \times SU(2)_R$ R-symmetry indices; and $(r) = 1, 2, \ldots, N$ is an S_N index labelling the N copies of the target space. In this work we focus on operators in the untwisted sector of the orbifold theory and thus all fields are periodic under $(z, \bar{z}) \to (z\, e^{2\pi i}, \bar{z}\, e^{-2\pi i})$. For more details, see for example [41, 167] or appendix A of [169], whose conventions we follow.

The point in the moduli space of the D1-D5 CFT that admits a dual semiclassical supergravity description is an infinite distance away from the free orbifold point (see for example [188]). Despite this, the notation of the latter can be useful to describe protected supersymmetric operators such as those appearing in our correlators [189]. With that in mind, we consider light operators that are chiral primaries; since the $\mathrm{AdS}_3 \times S^3$ theory is not maximally supersymmetric, chiral primaries can originate from different 6D supergravity multiplets and in this chapter we restrict to those of the N_f tensor multiplets (where either $N_f = 5$ or 21 for $\mathcal{M} = T^4$ and $K3$ respectively). On top of this, we consider such operators with minimal conformal dimension, i.e. with $\Delta = 1$. For example, four of the five T^4 tensor multiplet CPOs are given in the free orbifold language by

$$\mathcal{O}_f(z, \bar{z}) = \frac{\sigma_{\dot{A}\dot{B}}^{(f)}}{\sqrt{2N}} \sum_{r=1}^{N} \psi_{(r)}^{+\dot{A}}(z)\, \tilde{\psi}_{(r)}^{+\dot{B}}(\bar{z}) = \frac{1}{\sqrt{N}} \sum_{r=1}^{N} \mathcal{O}_{f(r)} , \tag{3.9}$$

where $\sigma_{\dot{A}\dot{B}}^{(f)}$ form a basis of 2 by 2 matrices (the fifth CPO is given by the twist field of order 2). We use the same operator, but with a different flavour index, as the fundamental building block for the construction of the heavy states. As discussed in the previous section the most natural way to define the multi-particle operators in (3.3) is to take the OPE limit of the single particle states which is regular as all constituents are mutually BPS. It turns out that this is not the choice appropriate for defining the heavy states dual to the supergravity solutions used in [71, 72] to derive the HHLL correlators. It is easier to characterise these multi-particle states in terms of the free orbifold theory, where for instance the relevant double-trace operators are $: \mathcal{O}_f^2 : \sim \sum_{r<s} \mathcal{O}_{(r)}\mathcal{O}_{(s)}$. Notice that the contribution $r = s$ is absent, while a term of this type arises when taking the OPE limit $\mathcal{O}^2 \sim \lim_{w \to z} \mathcal{O}(w)\mathcal{O}(z)$. By following the dictionary [49, 51] for supersymmetric operators between the supergravity and the free

orbifold points, we have the following schematic form for the relation between the two types of double-trace operators discussed above

$$:O^2: = O^2 + \frac{1}{\sqrt{N}}\Big[\text{single-particle}\Big] + \frac{1}{N}\Big[\text{double-particle}\Big] \,, \qquad (3.10)$$

where the operators appearing on the right-hand side are the standard ones used in holographic calculations in the supergravity approximation[37]. A signal that the microstate geometries are constructed in terms of $:O^n:$ is that they induce a vev for dimension two operators [50,51] which would be absent when using the more standard definition because they involve extremal couplings. With a slight abuse of notation, from now on we will write between colons the (external) multi-trace operators relevant to the microstate geometries (3.10) and we will use the same notation also for the correlators involving this type of multi-trace operator. This notation will only be used for this chapter, in order to emphasise the difference between the two definitions of multi-trace operators. Thus we write the heavy-heavy-light-light correlation function on the plane[38] derived in[39] [72] as

$$:C:(z,\bar{z}) = \left(1 - \frac{B^2}{N}\right) \sum_{k=1}^{\infty} \sum_{\ell \in \mathbb{Z}} \frac{\left(z\,\bar{z}^{-1}\right)^{\frac{\ell}{2}}}{\sqrt{1 - \frac{B^2}{N}\left(1 - \frac{\ell^2}{(|\ell|+2k)^2}\right)}} \left(z\bar{z}\right)^{-\frac{|\ell|+2k}{2}\sqrt{1 - \frac{B^2}{N}\left(1 - \frac{\ell^2}{(|\ell|+2k)^2}\right)}} \,,$$

$$(3.11)$$

which describes a correlator involving the heavy states

$$:\mathcal{O}_{H,f}: = \sum_{p=0}^{N} \sqrt{\binom{N}{p}} \left(\frac{B}{\sqrt{N}}\right)^p \left(1 - \frac{B^2}{N}\right)^{\frac{N-p}{2}} :\mathcal{O}_f^p: \,, \qquad (3.12)$$

in the regime where the parameter B^2 in chosen to scale with N as $N \to \infty$. This scaling limit (the 'heavy scaling limit') is necessary in order to treat the heavy operator as a smooth deformation of $\text{AdS}_3 \times S^3$. However, following the discussion of Section 3.2 we are interested in the opposite regime, where the heavy operators are made light by keeping B^2 fixed and thus $B^2/N \to 0$ as $N \to \infty$. To describe this limit, it is convenient

---

[37]In particular the extremal correlators among them vanish and the single-particle states are orthogonal to the multi-particle states.

[38]To go from correlators on the plane to the cylinder with our choice of light operator involves simply a Jacobian factor of $|z|$.

[39]In [72] the result was given in terms of the continuous dimensionful parameters a, a_0, and b which appear naturally in the supergravity description of the smooth geometry dual to the heavy state. Here it is more convenient to use a dimensionless parameter B, which is related to the supergravity parameters via

$$\frac{a^2}{a_0^2} = 1 - \frac{B^2}{N} \,, \qquad \frac{b^2}{2a_0^2} = \frac{B^2}{N} \,,$$

where we used the smoothness constraint $a^2 + b^2/2 = a_0^2$.

to rewrite the correlator (3.11) as a series in B^2/N, as was done in (3.4). We note that when N is large and with n finite, the binomial appearing in the last line of (3.4) can be approximated as

$$\binom{N}{n} \xrightarrow[N\to\infty]{n\ll N} \frac{N^n}{n!},\tag{3.13}$$

so that the expansion of the correlator can also be written as

$$:C:(z,\bar{z}) \approx \sum_{n=0}^{\infty} \left(\frac{B^2}{N}\right)^n \frac{N^n}{n!} :C_n:(z,\bar{z}).\tag{3.14}$$

This expression, together with the fact that connected correlators $:C_n:$ scale as N^{-n}, makes it clear that the coefficients of each power of B^2/N are finite in the large N limit.

The main result of our analysis is that at each order in B^2/N the double Fourier series in (3.11) can be evaluated in a closed form using the procedure outlined in Appendix B.1 and one can rewrite the coefficients $:C_n:(z,\bar{z})$ in terms of elementary functions and polylogarithms. In Appendix B.1 we present terms up to $n=4$, however, in the main text we limit ourselves to the first new result which occurs for $n=2$. For the first three values of n, the correlators are given by

$$C_0 = \frac{1}{|1-z|^2},\tag{3.15a}$$

$$C_1 = -\frac{|z|^2}{N}\left[\frac{4i(z+\bar{z})}{(z-\bar{z})^3}P_2(z,\bar{z}) + \frac{4}{(z-\bar{z})^2}\log|1-z| + \frac{2(z+\bar{z}-2z\bar{z})}{(z-\bar{z})^2|1-z|^2}\log|z|\right]$$
$$-\frac{1}{N}\frac{1}{|1-z|^2},\tag{3.15b}$$

$$:C_2:= \frac{4|z|^2}{N^2}\left[\frac{6i(z+\bar{z})(z^2+10z\bar{z}+\bar{z}^2)}{(z-\bar{z})^5}P_4(z,\bar{z}) - \frac{12(z^2+4z\bar{z}+\bar{z}^2)}{(z-\bar{z})^4}P_3(z,\bar{z})\right.$$
$$+ \frac{8i(z+\bar{z})}{(z-\bar{z})^3}P_2(z,\bar{z}) + \frac{2}{(z-\bar{z})^2}\log|1-z| + \frac{z+\bar{z}-2z\bar{z}}{(z-\bar{z})^2|1-z|^2}\log|z|$$
$$\left.+ \frac{z+\bar{z}}{|1-z|^2(z-\bar{z})^2}\left(\log|z|\right)^2\right],\tag{3.15c}$$

where the functions P_n are the Bloch-Wigner dilogarithm and its generalisations (see for example [176]) discussed in section 3.3.2, see in particular (3.23) and (3.26).

The result for C_0 is simply the identity contribution to the 4-point correlator and C_1 reproduces the results of [71, 72]. The first new expression is $:C_2:$ which contains, in addition to the standard functions already appearing in known holographic correlators, the so-called Bloch-Wigner-Ramakrishnan (BWR) polylogarithm functions

$P_m(z, \bar{z})$ [177,190], which for $m > 2$ are higher order generalisations of the Bloch-Wigner dilogarithm. The same is true for the correlator C_2 involving the more standard double-particle operators defined as the OPE limit of mutually BPS single-particle operators. From the general structure shown in (3.10), one can see that the difference between C_2 and $:C_2:$ can be written in terms of connected k-point correlators with $k \leq 4$ and so these contributions do not affect the terms proportional to P_4 and P_3 in (3.15c). A similar structure can be found in the correlators $:C_n:$ for larger values of n, with the highest order BWR polylogarithm function appearing being P_{2n}, as we show for some additional cases in Appendix B.1. This contribution is not sensitive to the differences between $:C_n:$ and C_n showing that the presence of the higher order BWR polylogarithm functions is a generic feature of the OPE limit of supergravity holographic correlators with many single-particle external states.

3.3.2 Generalised Bloch-Wigner functions

The expression for $:C_2:$ in (3.15c) (and similarly for the higher order counterparts, see (B.12)) involves Bloch-Wigner-Ramakrishnan polylogarithms – analogues of the standard Bloch-Wigner functions containing higher-order polylogarithms – and since these generalised functions are not widely used in the literature, we use this subsection to briefly review their definition and some of their properties. In doing this we closely follow the works of Lewin [191], and Zagier [190] who first presented the generalisation of the Bloch-Wigner function in [176, 177] following the work of Ramakrishnan [192].

The starting point of our analysis are the polylogarithm functions: an infinite family of special functions generalising the logarithm function. One series representation for these functions is [193] [194]

$$\mathrm{Li}_s(x) = \sum_{k=1}^{\infty} \frac{x^k}{k^s} \quad \text{for } x \in \mathbb{R}, \, |x| < 1 \;, \tag{3.16}$$

where $s \in \mathbb{N}^0$ and from which it can be seen that

$$\mathrm{Li}_1(x) = -\log(1-x) \;. \tag{3.17}$$

A complex logarithm can be defined on its principle branch $z \in \mathbb{C} \setminus (-\infty, 0)$ as

$$\log(z) \equiv \log|z| + i \, \mathrm{Arg}(z) \;, \tag{3.18}$$

on which it is single-valued, with $(-\infty, 0)$ being a branch cut. Here the function $\mathrm{Arg}(z)$ is the principle branch of the argument function $\mathrm{Arg}(z)$ and $\log(x)$ is the real logarithm. Likewise, the above series definition of $\mathrm{Li}_s(x)$ can be extended to the complex plane,

where in the region $|z| < 1$ it is analytic and admits the series representation

$$\mathrm{Li}_n(z) = \sum_{k=1}^{\infty} \frac{z^k}{k^n}\,, \qquad |z| < 1\,, \tag{3.19}$$

where we take n to be an integer. For non-positive integer n this defines a rational function, while for $n = 1$ it gives simply

$$\mathrm{Li}_1(z) = -\log(1 - z)\,. \tag{3.20}$$

Polylogarithm functions associated with higher integer values do not admit a representation in terms of elementary functions but can be obtained by recursion relations that follow from their definition

$$z\,\partial_z \mathrm{Li}_n(z) = \mathrm{Li}_{n-1}(z)\,, \qquad \mathrm{Li}_{n+1}(z) = \int_0^z \frac{\mathrm{Li}_n(w)}{w}\,dw\,, \tag{3.21}$$

which can also be used to analytically continue the polylogarithm functions to generic $z \in \mathbb{C}\backslash[1, \infty)$ by repeated integration starting from (3.20). Therefore, the polylogarithm functions inherit some of their properties from the logarithm such as a branch cut along the real axis starting at $z = 1$, except here the polylogarithms are continuous but not analytic at their branch point (with e.g. $\mathrm{Li}_2(1) = \zeta(2) = \frac{\pi^2}{6}$). The polylogarithms have non-trivial monodromy around the branch point at $z = 1$, with

$$\mathrm{Li}_m(x + i\epsilon) - \mathrm{Li}_m(x - i\epsilon) = \frac{2\pi i}{(m - 1)!}\big(\log z\big)^{m-1}\,, \tag{3.22}$$

for $x > 1$, $\epsilon \ll 1$ and $m \in \mathbb{N}$. Because of this monodromy, the polylogarithms also have a branch point at $z = 0$ on any sheet that is not the principle one.

The dilogarithm function $\mathrm{Li}_2(z)$ has played an important role in the CFT literature, as it appears in the expressions of holographic 4-point correlation functions of single-trace operators. In fact, is it not the "bare" dilogarithm function that appears in these correlators but a particular combination called the Bloch-Wigner dilogarithm function, defined as[40]

$$\begin{aligned} P_2(z, \bar{z}) &\equiv \mathrm{Im}\big[\mathrm{Li}_2(z)\big] + \log|z|\,\arg\big[1 - z\big] \\ &= \frac{1}{2i}\left[\mathrm{Li}_2(z) - \mathrm{Li}_2(\bar{z}) + \log|z|\,\log\left(\frac{1 - z}{1 - \bar{z}}\right)\right]\,, \end{aligned} \tag{3.23}$$

which has some advantageous properties compared with the ordinary dilogarithm function. For example, the dilogarithm function satisfies various identities relating the

---

[40]It is customary to denote the Bloch-Wigner dilogarithm function by $D(z, \bar{z})$. Here we denote it with $P_2(z, \bar{z})$ in order to facilitate an easier generalisation to higher order functions.

values of the function at different points in the complex plane, such as

$$\text{Li}_2\left(\frac{1}{z}\right) = -\text{Li}_2(z) - \frac{\pi^2}{6} - \frac{1}{2}\log^2(-z)\,, \tag{3.24a}$$

$$\text{Li}_2(1-z) = -\text{Li}_2(z) + \frac{\pi^2}{6} - \log(z)\log(1-z)\,. \tag{3.24b}$$

In fact, one can show that $\text{Li}_2(z)$, $\text{Li}_2\left(\frac{1}{1-z}\right)$, $\text{Li}_2\left(\frac{z-1}{z}\right)$, $-\text{Li}_2\left(\frac{1}{z}\right)$, $-\text{Li}_2\left(\frac{z}{1-z}\right)$, and $-\text{Li}_2(1-z)$ are all equal up the addition of elementary functions such as logarithms, as in (3.24). In contrast to this, the function defined in (3.23) satisfies similar identities but importantly without any additional elementary function terms

$$P_2(z,\bar{z}) = -P_2\left(\frac{1}{z},\frac{1}{\bar{z}}\right) = -P_2(1-z,1-\bar{z}) = P_2\left(\frac{z-1}{z},\frac{\bar{z}-1}{\bar{z}}\right)$$

$$= P_2\left(\frac{1}{1-z},\frac{1}{1-\bar{z}}\right) = -P_2\left(\frac{z}{z-1},\frac{\bar{z}}{\bar{z}-1}\right)\,. \tag{3.25}$$

Considering the many symmetries of 4-point correlation functions involving single-trace operators, such symmetry properties are not unexpected. Furthermore, if $\bar{z} = z^*$ the Bloch-Wigner function is real-analytic on the whole complex plane bar the points $z = 0$ and $z = 1$ where it is continuous but not differentiable. Thus one finds no branch cut, unlike in the case of the dilogarithm. In our analysis we often take the analytically continued function where z and $\bar{z}$ are independent, in which case a more complicated analytic structure emerges [195]. Contrary to the dilogarithm, a generic polylogarithm function satisfies fewer simple symmetry identities. In fact, the inversion identity relating $\text{Li}_n(z)$ and $(-1)^{n-1}\text{Li}_n\left(\frac{1}{z}\right)$ (up to several terms that include different powers of $\log z$) is in general the only functional identity that involves polylogarithm functions evaluated at two generic points in the complex plane, while other identities typically relate the values of polylogarithm functions evaluated at multiple points. Nonetheless, it is possible to define a higher-order generalisation of (3.23) as [177]

$$P_n(z,\bar{z}) = \mathfrak{R}_n\left(\sum_{k=0}^{n-1}\frac{2^k B_k}{k!}\left(\log|z|\right)^k \text{Li}_{n-k}(z)\right)\,, \tag{3.26}$$

where $\mathfrak{R}_n$ denotes the real or imaginary part of the expression when n is odd or even respectively and the coefficients B_j denote the Bernoulli numbers[41]. Once again, as a function of a single complex variable (when $\bar{z} = z^*$), $P_n(z,\bar{z})$ defines a real-analytic function on the complex plane, except at $z = 0$ and $z = 1$ where is it only continuous.

---

[41]The first few non-zero Bernoulli numbers are $B_0 = 1$, $B_1 = -\frac{1}{2}$, $B_2 = \frac{1}{6}$, $B_4 = -\frac{1}{30}$, $B_6 = \frac{1}{42}$, $B_8 = -\frac{1}{30}$. Apart from B_1 all Bernoulli numbers with an odd index vanish.

In addition, the functions obey the inversion relation

$$P_n(z, \bar{z}) = (-1)^{n-1} P_n\left(\frac{1}{z}, \frac{1}{\bar{z}}\right), \tag{3.27}$$

however, the higher order generalisations do not obey other simple symmetry identities found in the $n = 2$ case (3.25). For completeness, we give the explicit expressions of the first few generalised Bloch-Wigner-Ramakrishnan functions, which are explicitly used in the main text

$$P_2(z, \bar{z}) = \frac{1}{2i}\left[\mathrm{Li}_2(z) - \mathrm{Li}_2(\bar{z}) + \log|z| \, \log\left(\frac{1-z}{1-\bar{z}}\right)\right], \tag{3.28a}$$

$$P_3(z, \bar{z}) = \frac{1}{2}\left[\mathrm{Li}_3(z) + \mathrm{Li}_3(\bar{z}) - \log|z|\left(\mathrm{Li}_2(z) + \mathrm{Li}_2(\bar{z})\right) - \frac{2}{3}\left(\log|z|\right)^2 \log|1-z|\right], \tag{3.28b}$$

$$P_4(z, \bar{z}) = \frac{1}{2i}\left[\mathrm{Li}_4(z) - \mathrm{Li}_4(\bar{z}) - \log|z|\left(\mathrm{Li}_3(z) - \mathrm{Li}_3(\bar{z})\right)\right.$$
$$\left. + \frac{1}{3}\left(\log|z|\right)^2\left(\mathrm{Li}_2(z) - \mathrm{Li}_2(\bar{z})\right)\right]. \tag{3.28c}$$

Further examples can be found in Appendix B.1.

3.4 OPE limits

We proposed to identify the B^{2n} term in the expansion of the HHLL correlator (3.11) computed in [72] with the "connected" correlator $:C_n:$ containing two n-trace operators of the type $:\mathcal{O}_f^n:$ and two single-trace operators. In this section we provide evidence supporting this identification, concentrating on the first non-trivial example – that of $n = 2$. As a first check of this result we focus on protected terms in the OPE expansion of the correlator (3.15c) that appear in the $z \to 1$ and $z \to 0$ channels. We show that these terms match the results obtained from CFT calculations at the free orbifold point, as required by non-renormalisation theorems [189] and by the affine symmetry.

We then look at terms originating from the exchange of non-protected double-trace operators appearing in the $z \to 1$ OPE. By following [196], we find the anomalous dimensions and 3-point couplings of the non-protected double-trace operators from $n = 1$ correlators. With respect to the case of $\mathcal{N} = 4$ SYM [183], there is an extra complication [184] related to the flavour symmetry of the CPOs (in passing we point out that the theory we are studying provides a top-down example of the pattern highlighted in [185], where it was noted, in an effective field theory approach, that anomalous dimensions of double-trace operators with low spin can be positive). Due to the flavour mixing one would need results for other correlators, besides (3.11), in order to extend

this analysis to $n > 1$ and extract precise information about the multi-trace operators exchanged. Here we focus on general checks relating to the presence or absence of log and $\log^2$ terms in the $z \to 1$ OPE. The $z \to \infty$ OPE involves triple-trace operators even at the first non-trivial order of the $n = 2$ correlator and again one would need other correlators to disentangle the flavour dependence and extract CFT data at strong coupling. We leave a detailed study of the multi-trace anomalous dimensions and 3-point couplings in the $\text{AdS}_3/\text{CFT}_2$ case to a future analysis.

3.4.1 The protected sector

In the limit where $\bar{z} \to 1$ with z kept fixed, the leading term of the correlator is determined by the exchange of operators with right conformal dimension $\bar{h} = 0$ and generic left conformal dimension h. These are the chiral currents of the theory, whose modes are the Virasoro L_{-n} and the R-symmetry[42] J^3_{-n} generators. Since their 3-point couplings are determined by symmetries of the theory, they can be computed exactly at any point in the CFT moduli space and compared with the gravity result.

The $z, \bar{z} \to 0$ limit of the correlator $:\mathcal{C}_n:$ is controlled by the non-singular OPE of the operators $\mathcal{O}_g$ and $:\mathcal{O}_f^n:$ – chiral primary operators preserving the same supercharges. The lowest dimension operator exchanged in this channel is thus protected and we reproduce the vanishing of the term of order $z^0 \bar{z}^0$ in $:C_2:$ from a computation at the free orbifold point.

$\bar{z} \to 1$ light-cone OPE

This check of the protected current contributions to the tree-level connected correlators (3.15) can be simplified slightly by replacing the two single-trace operators $\mathcal{O}_g$, $\bar{\mathcal{O}}_g$ with their superdescendant $\mathcal{O}_g^B$ – obtained by acting on $\mathcal{O}_g$ with a right-moving and a left-moving supercharge. The corresponding correlator, which we will denote by $:\mathcal{C}_n^B:$, is related to $:\mathcal{C}_n:$ by the supersymmetry Ward identity [72]

$$:\mathcal{C}_n^B:(z, \bar{z}) = \partial \bar{\partial} \ :\mathcal{C}_n:(z, \bar{z}). \tag{3.29}$$

Starting from the correlator $:C_2:$ in (3.15c), applying the Ward identity (3.29) and taking the leading order term as $\bar{z} \to 1$ one obtains

$$:C_2^B:(z, \bar{z}) \xrightarrow{\bar{z} \to 1} \frac{:G_2^B:(z)}{|1-z|^4} \quad \text{with} \quad N^2 :G_2^B:(z) = 2 + 4\frac{1+z}{1-z} \log z + \frac{1 + 4z + z^2}{(1-z)^2} \left(\log z \right)^2. \tag{3.30}$$

The goal of this subsection is to reproduce $:G_2^B:$ from a CFT computation. Since $\mathcal{O}_g^B$ has vanishing R-charge, the states obtained by acting on the vacuum with the J^3_{-n}

---

[42]Only R-symmetry neutral operators contribute in the $z \to 1$ channel, and thus we can restrict to the $U(1)$ subgroup of the $SU(2)$ R-symmetry.

modes of the current do not contribute to $:\mathcal{C}_n^B:$. In order to decouple the Virasoro from the R-current algebras it is convenient to subtract from the L_{-n} modes the Sugawara contribution: the algebra satisfied by these "reduced" Virasoro generators, which for notational simplicity we will still denote by L_{-n}, is identical to the Virasoro algebra but the conformal dimension h of an operator of R-charge j should be replaced by a "reduced" conformal dimension $h^{[0]} \equiv h - \frac{j^2}{N}$.

States of the form $L_{-n_1} L_{-n_2} \ldots L_{-n_p} |0\rangle$, containing p modes, have a norm proportional to $c^p \sim N^p$ and thus contribute to a correlator at order N^{-p}. Since we focus on $:\mathcal{C}_2^B:$ whose tree-level contribution is of order N^{-2}, we can simply consider such states up to $p = 2$. Resumming the states with $p = 1$ gives the well-known global conformal block of the stress-tensor: for a correlator with two operators of dimension h_g and two operators of dimension h_f, the contribution of these states to $\mathcal{G} = |1 - z|^{4h_g} \mathcal{C}$ is

$$p = 1: \quad \frac{1}{N} h_f h_g \, \mathcal{V}_1(1 - z) \quad \text{with} \quad \mathcal{V}_1(z) = \frac{1}{3} z^2 \, _2F_1(2, 2, 4; z) \,. \tag{3.31}$$

Likewise, the contribution due to the exchange of states with $p = 2$ to this same correlator is a sum of terms of the form

$$p = 2: \quad \frac{1}{N^2} \left(h_f^2 h_g^2 \, \mathcal{V}_2^{(2,2)}(1 - z) + (h_f^2 h_g + h_f h_g^2) \, \mathcal{V}_2^{(2,1)}(1 - z) + h_f h_g \, \mathcal{V}_2^{(1,1)}(1 - z) \right) \,. \tag{3.32}$$

The functions $\mathcal{V}_2^{(2,2)}$ and $\mathcal{V}_2^{(2,1)}$ can be readily computed and are given in Appendix D of [126] as

$$\mathcal{V}_2^{(2,2)}(z) = \frac{1}{18} \left(z^2 \, _2F_1(2, 2, 4; z) \right)^2 ,$$
$$\mathcal{V}_2^{(2,1)}(z) = -\frac{1}{18} \left(\left(z^2 \, _2F_1(2, 2, 4; z) \right)^2 + \frac{6}{5} z^3 \log(1 - z) \, _2F_1(3, 3, 6; z) \right) , \tag{3.33}$$

while, as will be clear in a moment, we will not need $\mathcal{V}_2^{(1,1)}$. For the correlator $:\mathcal{C}_n^B:$ we should take $h_g = 1$, the dimension of the superdescendant $\mathcal{O}_g^B$, and $h_{f,n} = \frac{n}{2} - \frac{n^2}{4N}$, the reduced dimension of the n-trace operator $:\mathcal{O}_f^n:$, where we made the dependence on n explicit. Then combining the correlators $:\mathcal{C}_1^B:$ and $:\mathcal{C}_2^B:$ according to the definition of the connected combination $:C_2^B:$ (of the same form as (3.7)) we deduce that in the light-cone limit and up to terms of order $1/N^3$

$$:G_2^B:(z) = \frac{1}{N} \left(h_{f,2} - 2h_{f,1} \right) \mathcal{V}_1(1 - z) + \frac{1}{N^2} \left[\left(h_{f,2}^2 - 2h_{f,1}^2 \right) \mathcal{V}_2^{(2,2)}(1 - z) \right.$$

$$+ \left(\left(h_{f,2}^2 + h_{f,2} \right) - 2\left(h_{f,1}^2 + h_{f,1} \right) \right) \mathcal{V}_2^{(2,1)}(1 - z) + \left(h_{f,2} - 2h_{f,1} \right) \mathcal{V}_2^{(1,1)}(1 - z) \right]$$

$$= \frac{1}{N^2} \left[2 + 4 \frac{1 + z}{1 - z} \log z + \frac{1 + 4z + z^2}{(1 - z)^2} \left(\log z \right)^2 \right] + O\left(\frac{1}{N^3} \right) , \tag{3.34}$$

where in the first step we used $h_g = 1$ and in the second we used (3.33) along with the large N expansion of the $h_{f,n}$. The final result agrees with the expression (3.30) obtained from the gravity computation. We note that in taking the connected combination both the $1/N$ term and the term proportional to $\mathcal{V}_2^{(1,1)}$ cancel. This latter term is interpreted as a quantum contribution related to bulk diagrams of the type shown in c) of Fig. 3.1 which vanish in the limit that a pair of operators is made heavy (i.e. $h_f \sim N$) and N is taken to infinity. One can show that analogous cancellations happen with $:C_n^B:$ for generic n.

Euclidean $z, \bar{z} \to 0$ OPE

The exchanged operator with lowest dimension in this channel is the supersymmetric multi-trace $:\mathcal{O}_f^n \mathcal{O}_g:$ whose protected 3-point couplings can be computed in the orbifold sigma-model. One can thus verify the gravity prediction, which gives for the connected correlator $:C_2:$ a vanishing coefficient for the lowest order term $z^0 \bar{z}^0$:

$$:C_2: \overset{z,\bar{z}\to 0}{\longrightarrow} O(z\bar{z}) . \tag{3.35}$$

The explicit expressions of the relevant single- and multi-trace operators in the $\mathcal{M}^N/S_N$ orbifold theory are

$$\mathcal{O}_f = \frac{1}{\sqrt{N}} \sum_r \mathcal{O}_{f(r)} , \quad :\mathcal{O}_f^2: = \frac{1}{\sqrt{\binom{N}{2}}} \sum_{r<s} \mathcal{O}_{f(r)} \mathcal{O}_{f(s)} , \tag{3.36}$$

$$:\mathcal{O}_f \mathcal{O}_g: = \frac{1}{\sqrt{N(N-1)}} \sum_{r \neq s} \mathcal{O}_{f(r)} \mathcal{O}_{g(s)} , \quad :\mathcal{O}_f^2 \mathcal{O}_g: = \frac{1}{\sqrt{\binom{N}{2}(N-2)}} \sum_{\substack{r<s \\ t \neq r,s}} \mathcal{O}_{f(r)} \mathcal{O}_{f(s)} \mathcal{O}_{g(t)} ,$$

where the subscripts $(r), (s), \dots$ denote the N copies of $\mathcal{M}$. The operators $\mathcal{O}_{f(r)}$ on different copies are orthogonal

$$\langle \mathcal{O}_{f(r)} \mathcal{O}_{g(s)} \rangle = \delta_{f,g} \delta_{r,s} , \tag{3.37}$$

and the N-dependent prefactors in (3.36) have been chosen to normalise two-point functions to 1. The relevant 3-point functions can then be immediately computed as

$$\langle \bar{\mathcal{O}}_f \bar{\mathcal{O}}_g : \mathcal{O}_f \mathcal{O}_g: \rangle = \left(1 - \frac{1}{N}\right)^{\frac{1}{2}} , \quad \langle :\bar{\mathcal{O}}_f^2: \bar{\mathcal{O}}_g :\mathcal{O}_f^2 \mathcal{O}_g: \rangle = \left(1 - \frac{2}{N}\right)^{\frac{1}{2}} , \tag{3.38}$$

and the coefficient of the $z^0 \bar{z}^0$ term in $:C_2:$ is

$$:C_2:\big|_{z^0,\bar{z}^0} = \left| \langle :\bar{\mathcal{O}}_f^2: \bar{\mathcal{O}}_g :\mathcal{O}_f^2 \mathcal{O}_g: \rangle \right|^2 - 2 \left| \langle \bar{\mathcal{O}}_f \bar{\mathcal{O}}_g :\mathcal{O}_f \mathcal{O}_g: \rangle \right|^2 + 1 = \left(1 - \frac{2}{N}\right) - 2\left(1 - \frac{1}{N}\right) + 1 = 0 ; \tag{3.39}$$

the cancellation between the three terms, which come respectively from $:\mathcal{C}_2:$, $-2\mathcal{C}_1$ and $\mathcal{C}_0$, is thus in agreement with the gravity prediction (3.35).

3.4.2   The non-protected sector of the $z, \bar{z} \to 1$ OPE

In the $z, \bar{z} \to 1$ OPE channel the dynamical contribution is due to the exchange of non-supersymmetric double-trace operators made of equal-flavour and opposite R-symmetry constituents, of the type $:\mathcal{O}_f \bar{\mathcal{O}}_f:$. At leading order in N, these operators are degenerate with the more general class of double-traces $:\mathcal{O}_f^{(\alpha,\dot{\alpha})} \bar{\mathcal{O}}_g^{(\beta,\dot{\beta})}:$ and in order to see how this degeneracy is lifted by $1/N$ corrections one needs to introduce a proper basis in the R-symmetry and flavour space. As a first step, we separate the results into the irreducible R-symmetry representations of the operators exchanged, which we characterise by their R-charge $(j, \bar{j})$. In the $n = 1$ case enough information is available in the literature to perform a similar decomposition also in flavour space for all representations[43] and hence in the first subsection we derive the "unmixed" CFT data for the relevant anomalous dimensions. In the second subsection we focus on the $n = 2$ correlator (3.15c) but limit ourselves only to averaged CFT data, however, we point out that this is sufficient to obtain a further consistency check of our results.

Though the results in (3.15a) and (3.15b) refer to correlators containing operators of two different flavours and with the particular R-symmetry choice obtained by replacing $\mathcal{O}_f$ in (3.1) with the highest R-charge operator $\mathcal{O}_f \equiv \mathcal{O}_f^{++}$ defined in (3.9), the analysis of the following subsections would require a more general class of correlators[44]

$$:\mathcal{C}_{n,f_1 f_2 f_3 f_4}^{\alpha\dot{\alpha},\,\beta\dot{\beta}}: = \langle\, :(\mathcal{O}_{f_1}^{--})^n: :(\mathcal{O}_{f_2}^{++})^n:\ \mathcal{O}_{f_3}^{\alpha\dot{\alpha}}\ \mathcal{O}_{f_4}^{\beta\dot{\beta}}\,\rangle\,. \tag{3.40}$$

These are known for generic flavour and R-symmetry indices only for $n = 1$, whose expressions at order $1/N$ we summarise in Appendix B.2.

To carry out the program outlined above and separate the different irreducible representations in the flavour and R-symmetry space, we need to introduce the appropriate projectors. For the flavour part, the exchanged operator in the $z \to 1$ Euclidean OPE sits in the product of two fundamental $SO(N_f)$ representations and can be decomposed in the singlet, symmetric-traceless and anti-symmetric irreps, whose contributions to

---

[43]At present this is true for correlators where the external operators have dimension $h = \bar{h} = 1/2$ and, as discussed in [184], for generic dimensions in the case of non-singlet flavour representations.

[44]To avoid clutter, we suppress the z and $\bar{z}$ dependence of correlators such as (3.40) throughout this section. It should be understood that operators are always inserted as in (3.2).

(3.40) can be selected by using the projection operators

$$\mathcal{P}^{\text{sing}}_{f_3 f_4, g_3 g_4} = \frac{1}{N_f} \delta_{f_3 f_4} \delta_{g_3 g_4} \, , \tag{3.41a}$$

$$\mathcal{P}^{\text{sym}}_{f_3 f_4, g_3 g_4} = \frac{1}{2} \Big(\delta_{f_3 g_3} \delta_{f_4 g_4} + \delta_{f_3 g_4} \delta_{f_4 g_3} - \frac{2}{N_f} \delta_{f_3 f_4} \delta_{g_3 g_4} \Big) \, , \tag{3.41b}$$

$$\mathcal{P}^{\text{asym}}_{f_3 f_4, g_3 g_4} = \frac{1}{2} \Big(\delta_{f_3 g_3} \delta_{f_4 g_4} - \delta_{f_3 g_4} \delta_{f_4 g_3} \Big) \, . \tag{3.41c}$$

Similarly, for the R-symmetry we can separate the singlet ($j = 0$) and the triplet ($j = 1$) in the product of the two $SU(2)_L$ doublets (α, β) using the projectors

$$\mathcal{R}^{\alpha\beta, \gamma\delta}_{(j)} = \frac{1}{2} \sigma^{\alpha\beta}_{(j)} \sigma^{\gamma\delta}_{(j)} \quad \text{where} \quad \sigma^{\alpha\beta}_{(0)} = \begin{pmatrix} 0 & -i \\ i & 0 \end{pmatrix} \quad \text{and} \quad \sigma^{\alpha\beta}_{(1)} = \begin{pmatrix} 0 & 1 \\ 1 & 0 \end{pmatrix} . \tag{3.42}$$

Identical projectors $\mathcal{R}^{(\bar{j})}_{\alpha\beta, \gamma\delta}$ with $\bar{j} = 0, 1$ act on the $SU(2)_R$ indices ($\dot\alpha, \dot\beta$). The correlator (3.40) can then be decomposed into its irreducible R-symmetry and flavour components $:\mathcal{C}^{\text{flav}}_{n\,(j,\bar{j})}:$ as

$$:\mathcal{C}^{\alpha\dot\alpha, \beta\dot\beta}_{n, f_1 f_2 f_3 f_4}: = \sum_{j, \bar{j} = 0, 1} \sum_{\text{flav}} \sigma^{\alpha\beta}_{(j)} \sigma^{\dot\alpha\dot\beta}_{(\bar{j})} \mathcal{P}^{\text{flav}}_{f_1 f_2 f_3 f_4} :\mathcal{C}^{\text{flav}}_{n\,(j,\bar{j})}: \, , \tag{3.43}$$

where flav $=$ sing, sym, asym. We discuss the R-symmetry projectors in Appendix B.3 and the $n = 1$ projected correlators given explicitly. Given the linear relation (3.5) between the correlators $: \mathcal{C}_n :$ and their connected combinations $: C_n :$, an identical decomposition defines the irreducible components $:C^{\text{flav}}_{n\,(j,\bar{j})}:$ of the connected correlators.

The $n = 1$ case and the double-trace CFT data

In this subsection we focus on the $n = 1$ correlators, which we give for arbitrary values of the flavour and the R-symmetry indices in Appendix B.2, extracting the OPE data for the lowest twist double-trace operators exchanged in the $z, \bar{z} \to 1$ channel. As standard in the Euclidean OPE, we can expand each function $\mathcal{C}^{\text{flav}}_{1\,(j,\bar{j})}$ defined in (3.43) as $z, \bar{z} \to 1$ and rewrite the result in terms of *global* conformal blocks. The coefficients of this block decomposition admit a large N expansion of the form

$$\Big| c^{\text{flav},k}_{(0)(j,\bar{j})} \Big|^2 + \frac{1}{N} \Big| c^{\text{flav},k}_{(1)(j,\bar{j})} \Big|^2 + \frac{1}{N^2} \Big| c^{\text{flav},k}_{(2)(j,\bar{j})} \Big|^2 + O\big(N^{-3}\big) . \tag{3.44}$$

The leading order coefficients $\left|c^{\text{flav},k}_{(0)(j,\bar{j})}\right|^2$ are explained by the exchange of non-BPS double-trace operators of the form[45] $(\mathcal{O}\bar{\mathcal{O}})_k \sim \mathcal{O}_{f_3}\partial^k\bar{\mathcal{O}}_{f_4}$ with conformal dimensions

$$
\begin{aligned}
h^{\text{flav},k}_{(j,\bar{j})} &= 1 + k + \gamma^{\text{flav},k}_{(j,\bar{j})} \approx 1 + k + \frac{1}{N}\gamma^{\text{flav},k}_{(1)(j,\bar{j})} + \frac{1}{N^2}\gamma^{\text{flav},k}_{(2)(j,\bar{j})} \,, \\
\bar{h}^{\text{flav},k}_{(j,\bar{j})} &= 1 + \gamma^{\text{flav},k}_{(j,\bar{j})} \approx 1 + \frac{1}{N}\gamma^{\text{flav},k}_{(1)(j,\bar{j})} + \frac{1}{N^2}\gamma^{\text{flav},k}_{(2)(j,\bar{j})} \,.
\end{aligned}
\tag{3.45}
$$

Then one has the identification

$$
\langle\bar{\mathcal{O}}_{f_1}\mathcal{O}_{f_2}(\mathcal{O}\bar{\mathcal{O}})_k\rangle\langle(\mathcal{O}\bar{\mathcal{O}})_k\mathcal{O}^{(\alpha,\dot{\alpha})}_{f_3}\mathcal{O}^{(\beta,\dot{\beta})}_{f_4}\rangle\mathcal{P}^{\text{flav}}_{f_1f_2,\,f_3f_4} = \left|c^{\text{flav},k}_{(0)(j,\bar{j})}\right|^2\sigma^{\alpha\beta}_{(j)}\sigma^{\dot{\alpha}\dot{\beta}}_{(\bar{j})} + O(N^{-1})\,.
\tag{3.46}
$$

The subleading terms $\left|c^{\text{flav},k}_{(1)(j,\bar{j})}\right|^2$, $\left|c^{\text{flav},k}_{(2)(j,\bar{j})}\right|^2$ receive contributions both from the $1/N$ and $1/N^2$ corrections to the 3-point couplings in (3.46) and from the couplings with triple-trace and quadruple-trace operators, which start at order $1/N$ and $1/N^2$ respectively. We will not try to disentangle these different contributions, but simply extract the total $1/N$ coefficients $\left|c^{\text{flav},k}_{(1)(j,\bar{j})}\right|^2$, which are also the data computable from the inversion formula (as done in Appendix C).

However, the $n = 1$ correlators summarised in Appendix B.2 are sufficient to derive the anomalous dimensions of the true conformal primaries at order $O(1/N)$ for each value of k. Let us start from the contribution related to double-trace operators in the R-symmetry singlet irrep $(j,\bar{j}) = (0,0)$ and flavour singlet: we expand $C^{\text{sing}}_{1\,(0,0)}$ up to order $(1-\bar{z})^0$ and keep the order of $(1-z)^t$ arbitrary and obtain

$$
\begin{aligned}
C^{\text{sing}}_{1\,(0,0)} \approx \sum_{t=0}^{\infty} (1-z)^t &\Bigg[\frac{1}{2N}\left(\frac{(t^2+t+2)N_f}{(t+1)(t+2)(t+3)} - (1+\delta_{t,0})\right)\log|1-z|^2 + \frac{1+\delta_{t,0}}{4} \\
&+ \frac{1}{N}\Big(A_t N_f + B_t\Big)\Bigg] + \sum_{t=0}^{\infty}\frac{(-1)^t(1-z)^{t+2}}{N|1-z|^2}\frac{(t+1)N_f}{2(t+2)(t+3)}\,,
\end{aligned}
\tag{3.47}
$$

where the first values of A_t and B_t are

$$
\begin{aligned}
A_t &= \left\{-\frac{7}{36},\,-\frac{1}{72},\,-\frac{1}{225},\,-\frac{1}{900},\,\frac{61}{44100},\,\frac{23}{7056},\,\frac{293}{63504},\,\dots\right\}\,, \\
B_t &= \left\{\frac{1}{2},\,-\frac{1}{4},\,-\frac{1}{6},\,-\frac{1}{6},\,-\frac{7}{40},\,-\frac{11}{60},\,-\frac{4}{21},\,\dots\right\}\,.
\end{aligned}
\tag{3.48}
$$

By focusing on the leading term in N, we can extract [145] a closed expression for the OPE coefficients with a double-trace operator of dimension $(h,\bar{h}) = (k+1,1) + O(1/N)$

$$
\left|c^{\text{sing},k}_{(0)(0,0)}\right|^2 = \left(1 + (-1)^k\right)\frac{(k!)^2}{4(2k)!}\,.
\tag{3.49}
$$

---

[45] We use this notation for double-trace operators exchanged only in this chapter, in order to distinguish them from those coming from the light limit of heavy external operators.

As expected, only states with even spin are non-trivial. In Appendix B.4 we outline a simple method used to extract Euclidean OPE data from a correlator. Likewise, by projecting along the conformal blocks, from the term proportional to $\log|1-z|^2$ we obtain the anomalous dimensions

$$\left|c^{\text{sing},k}_{(0)(0,0)}\right|^2 \gamma^{\text{sing},k}_{(1)(0,0)} = \frac{(k!)^2}{2(2k)!}\left[\frac{(-1)^k(k^2+k-2)^2}{\Gamma(k+4)\Gamma(3-k)}N_f - \left(1+(-1)^k\right)\right]. \tag{3.50}$$

We note that for $k > 2$ the first term in the square parenthesis vanishes (due to the $\Gamma(3-k)$ in the denominator) and the result for $\gamma_{(1)}$ agrees with that obtained from the Lorentzian inversion relation [68], as seen for instance in [197] and in (C.40a) with $\bar{n} = 0$. Then the pattern of these anomalous dimensions is

$$\gamma^{\text{sing},k}_{(1)(0,0)} = \left\{\frac{N_f}{3} - 2, 0, \frac{2N_f}{15} - 2, 0, -2, 0, -2, 0, \dots\right\}. \tag{3.51}$$

In the case of $\text{AdS}_3 \times S^3 \times T^4$, we have $N_f = 5$ and all $\gamma^{\text{sing},k}_{(1)(0,0)}$ are negative down to $k = 0$: this is also the case in $\mathcal{N} = 4$ SYM [69]. However, for $\text{AdS}_3 \times S^3 \times K3$, one has $N_f = 21$ and so the first two non-trivial values in (3.51), i.e. $k = 0, 2$, are positive. This realises the possibility discussed in [185] where it was pointed out that the gravitational interaction can counter-intuitively induce *positive* contributions to anomalous dimensions for values of spin up to 2. Notice that double-trace operators whose leading coupling is given by (3.49) can be viewed also as affine primaries. Since in each affine block there is an infinite number of quasi-primaries, in the $K3$ theory we have quasi-primaries with the same positive anomalous dimensions as the $k = 0, 2$ cases in (3.51) and arbitrarily high spin. This is due to the peculiar fact that for 2D CFTs the currents, such as the stress tensor, have twist zero.

It is possible to use the Lorentzian inversion relation [68] to extract a closed form for the $1/N$ terms in the expansion (3.44) of coefficients of global blocks with $k > 2$ and then we use the explicit data (3.48) to fix the low k values:

$$\left|c^{\text{sing},0}_{(1)(0,0)}\right|^2 = \frac{1}{2} - \frac{7N_f}{36}, \quad \left|c^{\text{sing},1}_{(1)(0,0)}\right|^2 = 0, \quad \left|c^{\text{sing},2}_{(1)(0,0)}\right|^2 = \frac{1}{9} - \frac{37N_f}{2700},$$
$$\left|c^{\text{sing},k}_{(1)(0,0)}\right|^2 = \frac{1+(-1)^k}{4}\frac{(k!)^2}{(2k)!}\left(4H_{2k} - 4H_k - 1\right) \quad \text{for} \quad k > 2, \tag{3.52}$$

where the $H_k = \sum_{n=1}^{k} n^{-1}$ are harmonic numbers. It is straightforward to select the other irreducible flavour representations and here we quote some key results, focusing always on double-trace operators of the class $\mathcal{O}_{f_3}\partial^k\bar{\mathcal{O}}_{f_4}$. We note that for $(j, \bar{j}) = (0,0)$ there are no contributions of this type for the antisymmetric representation in the flavour indices. By expanding the R-symmetry singlet and flavour symmetric traceless

projection $C^{\text{sym}}_{1(0,0)}$, we find the following CFT data

$$\left|c^{\text{sym},k}_{(0)(0,0)}\right|^2 = \left(1+(-1)^k\right)\frac{(k!)^2}{4(2k)!} \quad , \qquad \gamma^{\text{sym},k}_{(1)(0,0)} = -2 \quad \forall\, k \text{ even} , \tag{3.53}$$

and

$$\left|c^{\text{sym},k}_{(1)(0,0)}\right|^2 = \frac{1+(-1)^k}{4}\frac{(k!)^2}{(2k)!}\left(4H_{2k}-4H_k-1\right)+\delta_{k,0} . \tag{3.54}$$

As a final example, we provide the anomalous dimensions for another R-symmetry representation, that with $(j,\bar{j})=(1,0)$. In this case only double-trace operators with odd values of k contribute and in the flavour-singlet sector we have the data

$$\left|c^{\text{sing},k}_{(0)(1,0)}\right|^2 = \left(1+(-1)^{k+1}\right)\frac{(k!)^2}{4(2k)!} \quad , \qquad \gamma^{\text{sing},k}_{(1)(1,0)} = \left\{0,\frac{N_f}{3}-2,0,-2,0,-2,\dots\right\} , \tag{3.55}$$

and

$$\left|c^{\text{sing},k}_{(1)(1,0)}\right|^2 = \frac{1+(-1)^{k+1}}{4}\frac{(k!)^2}{(2k)!}\left(4H_{2k}-4H_k-1\right)-\frac{7N_f}{72}\delta_{k,1} . \tag{3.56}$$

Once again these anomalous dimensions are all negative for $N_f = 5$, while in the $K3$ case $\gamma^{\text{sing},1}_{(1)(1,0)}\big|_{N_f=21} = 5$, a shifted spectrum compared with (3.51). Finally, in the flavour-symmetric sector we have the data

$$\left|c^{\text{sym},k}_{(0)(1,0)}\right|^2 = \left(1+(-1)^{k+1}\right)\frac{(k!)^2}{4(2k)!} \quad , \qquad \gamma^{\text{sym},k}_{(1)(1,0)} = -2 \quad \forall\, k \text{ odd} , \tag{3.57}$$

and

$$\left|c^{\text{sym},k}_{(1)(1,0)}\right|^2 = \frac{1+(-1)^{k+1}}{4}\frac{(k!)^2}{(2k)!}\left(4H_{2k}-4H_k-1\right) . \tag{3.58}$$

One final comment is that the $c_{(1)}$ data matches that computed from the inversion formula in Appendix C since in both cases what is being extracted is simply the coefficient of global blocks, which as we have noted, does not necessarily give just the OPE coefficients of the double-trace operators $\bar{\mathcal{O}}\partial^k\mathcal{O}$ due to the mixing with triple-traces.

The $n=2$ case

While we will not attempt a systematic analysis of the $z,\bar{z}\to 1$ limit for the correlator containing double-traces, we will show in an explicit example how to extract from the correlator (3.15c) the OPE coefficients involving three double-trace operators.

A first general feature of the result (3.15c) is that there are no terms proportional to $\log^2|1-z|^2$ as $z,\bar{z}\to 1$. From the CFT point of view this is the result of cancellation between different terms entering in (3.7). In order to see this let us define, in analogy with the $n=1$ case (3.44), the couplings appearing in the OPE expansion: for instance

for the flavour singlet exchange we have

$$\langle :\bar{\mathcal{O}}_f^2::\mathcal{O}_f^2:(\bar{\mathcal{O}}\mathcal{O})_k\rangle\langle((\bar{\mathcal{O}}\mathcal{O})_k\mathcal{O}_g^{(\alpha,\dot\alpha)}\mathcal{O}_g^{(\beta,\dot\beta)}\rangle\mathcal{P}_{ff,gg}^{\text{sing}} = M_{(0)(j,\dot j)}^{\text{sing},k}\,\sigma_{(j)}^{\alpha\beta}\sigma_{(\dot j)}^{\dot\alpha\dot\beta} + O(N^{-1})\;,\quad (3.59)$$

where $M_{(0)}$ mixes information about the $c_{(0)}$ discussed in the previous section and new CFT data $\langle :\bar{\mathcal{O}}_f^2::\mathcal{O}_f^2:(\bar{\mathcal{O}}\mathcal{O})_k\rangle$ capturing the couplings between three double-trace operators. As explained above, the subleading coefficients $M_{(1)}$ and $M_{(2)}$ mix the $1/N$ and $1/N^2$ corrections to the couplings in (3.59) with new couplings of triple- or quadruple-trace primaries. The leading order $M_{(0)}$ can be easily derived by using the generalised free theory at infinite N which is described by the correlators

$$\begin{aligned}
\langle :(\mathcal{O}_{f_1}^{--})^2::(\mathcal{O}_{f_2}^{++})^2:\mathcal{O}_{f_3}^{++}\mathcal{O}_{f_4}^{--}\rangle &\approx \frac{1}{|1-z|^2}\left[\delta_{f_1f_2}\delta_{f_3f_4} + 2|1-z|^2\delta_{f_1f_3}\delta_{f_2f_4}\right],\\
\langle :(\mathcal{O}_{f_1}^{--})^2::(\mathcal{O}_{f_2}^{++})^2:\mathcal{O}_{f_3}^{--}\mathcal{O}_{f_4}^{++}\rangle &\approx \frac{1}{|1-z|^2}\left[\delta_{f_1f_2}\delta_{f_3f_4} + \frac{2|1-z|^2}{|z|^2}\delta_{f_1f_4}\delta_{f_2f_3}\right],\\
\langle :(\mathcal{O}_{f_1}^{--})^2::(\mathcal{O}_{f_2}^{++})^2:\mathcal{O}_{f_3}^{+-}\mathcal{O}_{f_4}^{-+}\rangle &\approx -\frac{1}{|1-z|^2}\delta_{f_1f_2}\delta_{f_3f_4}\,,\\
\langle :(\mathcal{O}_{f_1}^{--})^2::(\mathcal{O}_{f_2}^{++})^2:\mathcal{O}_{f_3}^{-+}\mathcal{O}_{f_4}^{+-}\rangle &\approx -\frac{1}{|1-z|^2}\delta_{f_1f_2}\delta_{f_3f_4}\,,
\end{aligned}$$

$$(3.60)$$

where, as usual, we assumed that the double-trace operators are normalised to one. Then it is straightforward to project these results onto the R-symmetry and flavour irreducible representations, as done before, and obtain

$$\begin{aligned}
M_{(0)(0,0)}^{\text{sing},k} &= 2\left|c_{(0)(0,0)}^{\text{sing},k}\right|^2\,, \quad M_{(0)(1,0)}^{\text{sing},k} = 2\left|c_{(0)(1,0)}^{\text{sing},k}\right|^2\,,\\
M_{(0)(0,0)}^{\text{sym},k} &= 2\left|c_{(0)(0,0)}^{\text{sym},k}\right|^2\,, \quad M_{(0)(1,0)}^{\text{sym},k} = 2\left|c_{(0)(1,0)}^{\text{sym},k}\right|^2\,,
\end{aligned}$$

$$(3.61)$$

where the extra factor of 2 simply follows from the fact that there are twice as many generalised free field diagrams connecting the single- and double-trace operators.

The next contribution to $:C_2:$, beyond the one captured by the generalised free theory, is given in (3.15c). Notice that each term in that result is multiplied by a factor of $|z|^2$ as is the case for the terms with D-functions in (B.19a). This reflects a particular choice of R-symmetry quantum numbers. We can perform the projection on

the R-symmetry singlet exactly as for the $n = 1$ correlators and obtain

$$
:C_{2,(0,0)}: = \frac{1}{N^2}\left(1 + z + \bar{z} + |z|^2\right)\left[\frac{6i(z+\bar{z})(z^2+10z\bar{z}+\bar{z}^2)}{(z-\bar{z})^5}P_4(z,\bar{z})\right.
$$
$$
- \frac{12(z^2+4z\bar{z}+\bar{z}^2)}{(z-\bar{z})^4}P_3(z,\bar{z}) + \frac{8i(z+\bar{z})}{(z-\bar{z})^3}P_2(z,\bar{z}) + \frac{2}{(z-\bar{z})^2}\log|1-z|
$$
$$
\left. + \frac{(z+\bar{z}-2z\bar{z})}{(z-\bar{z})^2|1-z|^2}\log|z| + \frac{(z+\bar{z})}{|1-z|^2(z-\bar{z})^2}\left(\log|z|\right)^2\right]. \tag{3.62}
$$

We don't have enough data to perform also the decomposition on the flavour irreducible representations since this would require a generalisation of Eq. (3.11) to the equal flavour case. Thus from now on we focus on the correlator (3.62) with a pair of fixed (and different) flavours. On general grounds, by focusing on the $(1-z)^0(1-\bar{z})^0$ terms in the $z, \bar{z} \to 1$ expansion of the connected combination $: C_2 :$, we have up to order $O(1/N)$

$$
:C_{2,(0,0)}: \approx \sum_{\text{flav}} \mathcal{P}_{ff,gg}^{\text{flav}}\left\{M_{(0),(0,0)}^{\text{flav},0} - 2\left|c_{(0),(0,0)}^{\text{flav},0}\right|^2 + \frac{1}{N}\left[M_{(1),(0,0)}^{\text{flav},0} - 2\left|c_{(1),(0,0)}^{\text{flav},0}\right|^2\right.\right.
$$
$$
\left.\left. + \left(M_{(0),(0,0)}^{\text{flav},0} - 2\left|c_{(0),(0,0)}^{\text{flav},0}\right|^2\right)\gamma_{(1),(0,0)}^{\text{flav},0}\log|1-z|^2\right]\right\}, \tag{3.63}
$$

where the sum is over the flavour representations 'flav' of the double-trace operator exchanged. Since the correlator under investigation has two pairs of external states with different flavours we have to take $f \neq g$ in the projectors (3.41). We know that the $n = 2$ connected correlators start at order $O(1/N^2)$, so the contributions in (3.63) must cancel. The first line vanishes thanks to the constraints (3.61), following from the generalised free theory and the same is true for the term proportional to $\log|1-z|^2$ in the second line. The absence of a rational term of order $1/N$ yields a relation between the couplings at $O(1/N)$

$$
\left(M_{(1),(0,0)}^{\text{sing},0} - 2\left|c_{(1),(0,0)}^{\text{sing},0}\right|^2\right) - \left(M_{(1),(0,0)}^{\text{sym},0} - 2\left|c_{(1),(0,0)}^{\text{sym},0}\right|^2\right) = 0. \tag{3.64}
$$

We then consider the order $O(1/N^2)$ terms in the OPE expansion (3.63)

$$
:C_{2,(0,0)}: \approx \frac{1}{N^2}\sum_{\text{flav}} \mathcal{P}_{ff,gg}^{\text{flav}}\left\{M_{(2),(0,0)}^{\text{flav},0} - 2\left|c_{(2),(0,0)}^{\text{flav},0}\right|^2 + \left[\left(M_{(0),(0,0)}^{\text{flav},0}\right.\right.\right.
$$
$$
\left.\left. - 2\left|c_{(0),(0,0)}^{\text{flav},0}\right|^2\right)\gamma_{(2),(0,0)}^{\text{flav},0} + \left(M_{(1),(0,0)}^{\text{flav},0} - 2\left|c_{(1),(0,0)}^{\text{flav},0}\right|^2\right)\gamma_{(1),(0,0)}^{\text{flav},0}\right]\log|1-z|^2
$$
$$
\left. + \frac{1}{2}\left(M_{(0),(0,0)}^{\text{flav},0} - 2\left|c_{(0),(0,0)}^{\text{flav},0}\right|^2\right)\left(\gamma_{(1),(0,0)}^{\text{flav},0}\right)^2\log^2|1-z|^2\right\}. \tag{3.65}
$$

Again, thanks to (3.61) the last line vanishes, thus explaining the absence of terms proportional to $\log^2 |1-z|^2$ in the OPE expansion of the holographic results. The same pattern holds for the term proportional to $\gamma_{(2)}$ in the first line. Thus the term with $\log |1-z|^2$ is determined by data at order $O(1/N)$. By using (3.64), the anomalous dimensions at order $1/c$, $\gamma^{\text{flav},0}_{(1),(0,0)}$, derived in the previous section and the OPE limit of (3.62) one can find an explicit expression for $M^{\text{sing}}_{(1),(0,0)}$ and $M^{\text{sym}}_{(1),(0,0)}$ separately. This new data is

$$
\begin{aligned}
M^{\text{sing},0}_{(1),(0,0)} &= 2\left|c^{\text{sing},0}_{(1),(0,0)}\right|^2 - 1 = -\frac{7}{18}N_f \ , \\
M^{\text{sym},0}_{(1),(0,0)} &= 2\left|c^{\text{sym},0}_{(1),(0,0)}\right|^2 - 1 = 0 \ ,
\end{aligned}
\tag{3.66}
$$

using the fact that $\left|c^{\text{sing},0}_{(1),(0,0)}\right|^2 = \frac{1}{2} - \frac{7}{36}N_f$ and $\left|c^{\text{sym},0}_{(1),(0,0)}\right|^2 = \frac{1}{2}$. The extension of the analysis to exchanged operators of the form $(\mathcal{O}\bar{\mathcal{O}})_{k>0} \sim \mathcal{O}_{f_3}\partial^{k>0}\bar{\mathcal{O}}_{f_4}$ is complicated by the fact that they can mix, at order in $1/N$, with triple-trace primaries. We leave this analysis for the future.

Chapter 4

The Regge Limit of Holographic Correlators

The contents of this chapter is based on the papers [1,3]. The Sections 4.5.3 and 4.4.4 are based on unpublished work.

4.1   Introduction and conclusion

In this chapter we consider the physical process of the scattering of a highly energetic light particle from a heavy object in asymptotically AdS$_3$ spacetimes. In the bulk, one can study such an experiment by approximating the path of the probe with a null geodesic in the spacetime obtained from the backreaction of the heavy object. A discussion of the geodesic problem relevant to the semiclassical bulk calculation was presented in Section 2.4, where the form of the bulk phase shift for three-dimensional metrics with suitable Killing vectors was derived. On the other hand, this scattering can be equivalently described in the dual two-dimensional CFT: there we study the OPE decomposition of HHLL correlators in the channel describing the fusion of a heavy and light state, producing an intermediate excited heavy state – this we call the "cross channel". The heavy operators in our correlators have conformal dimensions $\Delta \sim c$ in the large central charge limit due to the fact that they are formed from a large number $N_b \sim N$ of light constituents. Similarly to the case of standard LLLL correlators [90], the anomalous dimensions of these heavy excited states are directly related to the eikonal operator [52]. Likewise, the analytic bootstrap approach to the Regge regime can be adapted from the light [97] to the heavy case, and a systematic perturbative approach in N_b/N set up [53].

   This chapter focuses initially on the first order in N_b/N for each example – AdS$_3$ conical defects, 2-charge and 3-charge microstate geometries – at which the eikonal in the HHLL regime is derived for atypical heavy states. For the conical defect and

2-charge examples, this is then followed by an analysis at higher order, whereas for the 3-charge case only the bulk phase shift is considered beyond perturbation theory. Despite similarities between the conical defect and the effective 3D geometries describing the heavy pure states, the resulting eikonals are *different* already at this first order. We show that results obtained from CFT correlators are in perfect agreement with the eikonal derived by studying geodesics in the dual microstate geometry – the properties of geodesics in microstate geometries have been studied from various perspectives also in [30,31,33,198–200]. By following [53,97] we study the relevant bootstrap relation and show that it is satisfied by a different set of CFT data than in the conical defect case [52]. In both situations the "direct channel" – in which the two light operators are fused together – contains the contribution of the Virasoro block of the identity, but dressed by a different set of double-trace operators. In fact, generic conical defect geometries are not dual to pure states and it would be interesting to understand whether the CFT data extracted from them are fully consistent solutions of the bootstrap relation. As an aside, let us highlight that setting $N_b = 1$ in the HHLL correlators described above, as done in [66, 73, 74] and Chapter 3, reproduces the correlators of all light states in $\text{AdS}_3 \times S^3$ [66,75], despite the two regimes being not obviously connected. We analyse the Regge conformal bootstrap also in this regime in Section 4.4.3, providing an explicit $\text{AdS}_3/\text{CFT}_2$ example of the analysis in [96,97] and showing that the information obtained in the Regge regime can be used to fix some CFT data for spin-2 operators that was left undetermined in [73]. These LLLL correlators are also used to briefly consider the connection with the chaos regime of thermal correlators discussed in [115].

For comparison, in Section 4.3 we review the analogous calculation for the case of the AdS spacetime with a conical defect of order k in three bulk dimensions [52,53]. When this k is a positive integer, the geometry has a known dual pure heavy state [24,201,202]. However, if k is analytically continued to be real-valued this is no longer the case and the resulting geometry is instead thought to be dual to a mixed state in the CFT.

4.2 The Regge limit of 4-point CFT correlation functions

The gravitational picture described in Section 2.4 of a light highly energetic probe in a background geometry corresponds to a particular class of 4-point functions, dubbed heavy-heavy-light-light (HHLL), where two of the operators – dual to the geometry – are taken to be 'heavy' in the sense that in the large N limit their dimensions scale with the central charge ($\Delta_H \sim O(c)$). In contrast, the scaling dimensions of the remaining two operators – dual to the light probe – are kept fixed in this limit ($\Delta_L \sim O(1)$) and thus we refer to them as 'light'. We denote such HHLL correlators of the conformally-

fixed form (2.28) as

$$C(z, \bar{z}) \equiv \langle \mathcal{O}_H(\infty) \mathcal{O}_L(1) \bar{\mathcal{O}}_L(z, \bar{z}) \bar{\mathcal{O}}_H(0) \rangle = (1 - z)^{-2h_L} (1 - \bar{z})^{-2\bar{h}_L} G(z, \bar{z}) \ . \qquad (4.1)$$

The external heavy operators that we consider are a class of multi-trace operators made from a large number $N_b \sim N$ of identical single-particle states, $\mathcal{O}_H \sim \mathcal{O}_L^{N_b}$. These operators are "heavy", since their dimensions are of order c, and are dual to known asymptotically $\text{AdS}_3 \times S^3$ microstate geometries, as described in Section 2.2.2. From the CFT point of view they behave as standard local operators with h_H and j_H indicating their conformal weight and $U(1) \subset SU(2)_L$ R-charge (for notational simplicity we focus on the holomorphic part, but of course the discussion equally holds for the anti-holomorphic sector). In order to disentangle the Virasoro and $U(1)$ parts, it is convenient to introduce the "reduced" dimension of a heavy[46] operator $\mathcal{O}_H$, in which the Sugawara $U(1)$ contribution is subtracted (as discussed in Section 2.2.3) to give

$$h_H^{[0]} \equiv h_H - \frac{j_H^2}{N} \ . \qquad (4.2)$$

The class of heavy operators that we will consider are dual to the $(1, 0, n)$ family of superstrata discussed in Sections 2.2 and 2.2.2. Their dimensions and $U(1)$ quantum numbers are given in (2.72) and (2.73) and so have a reduced dimension of (the N_b of this chapter is equal to the $N_{1,0,n}$ of Section 2.2.3)

$$h_H^{[0]} = N_b \left(n + \frac{1}{2} - \frac{N_b}{4\,N} \right) \ . \qquad (4.3)$$

These heavy CFT states can be seen as part of an ensemble describing a black hole – or more generally, a singular geometry such as a conical defect. The reduced conformal dimension is related to the mass μ of the underlying black hole by the relation

$$\sqrt{1 - \mu} \equiv \alpha = \sqrt{1 - \frac{24\,h_H^{[0]}}{c}} = \sqrt{1 - \frac{4\,N_b}{N} \left(n + \frac{1}{2} - \frac{N_b}{4\,N} \right)} \ , \qquad (4.4)$$

where the central charge $c = 6N$ of the D1-D5 CFT was used. In this work we focus on the limit of small N_b/N where one has

$$\mu \equiv \frac{24 h_H^{[0]}}{c} = 4 \left(n + \frac{1}{2} \right) \frac{N_b}{N} + O\!\left(\frac{N_b}{N} \right)^2 \ . \qquad (4.5)$$

To facilitate comparison with the literature, we will use μ as our expansion parameter in everything that follows. A more complete discussion on the relation between μ and

---

[46]Under this procedure, the reduced dimensions of light operators and the value of the central charge are unchanged at leading order in the large N limit so we do not use these here.
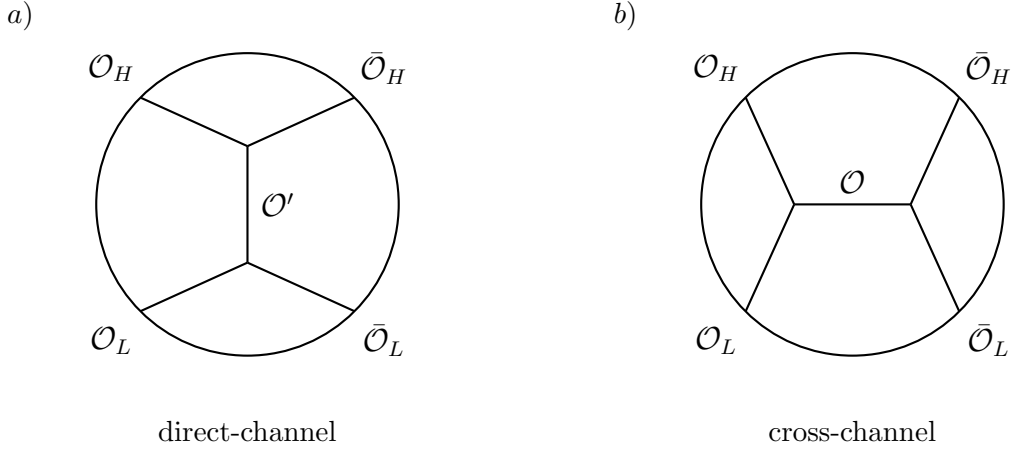
a)

$\mathcal{O}_H$ $\bar{\mathcal{O}}_H$

$\mathcal{O}'$

$\mathcal{O}_L$ $\bar{\mathcal{O}}_L$

b)

$\mathcal{O}_H$ $\bar{\mathcal{O}}_H$

$\mathcal{O}$

$\mathcal{O}_L$ $\bar{\mathcal{O}}_L$

direct-channel   cross-channel

Figure 4.1: A schematic expansion of the 4-point correlator into different channels. In figure a) we show the direct-channel ($z_1 \to z_2$ or equivalently $z \to 1$) where the two light operators in a HHLL correlator are brought together. In figure b) we depict the cross-channel expansion ($z_1 \to z_4$ or $z \to 0$) where the heavy and light operators are contracted. While one can equivalently expand in either channel, the set of operators exchanged (denoted by $\mathcal{O}'$ in the direct-channel and $\mathcal{O}$ in the cross-channel) are generically different.

the natural expansion parameters of the gravity solutions are given in Section 2.2.3.

The correlator (4.1) can be decomposed into different channels as discussed in Section 2.1.1, for instance by summing over the exchanges of quasi-primary operators (see figure 4.1)

$$C(z, \bar{z}) = (1 - z)^{-2h_L} (1 - \bar{z})^{-2\bar{h}_L} \sum_{\mathcal{O}'} C_{HH\mathcal{O}'} C_{\bar{\mathcal{O}}'LL}\, g_{h,\bar{h}}^{0,0}(1 - z, 1 - \bar{z}) \,, \qquad (4.6a)$$

$$= z^{-h_H^{[0]} - h_L}\, \bar{z}^{-\bar{h}_H^{[0]} - \bar{h}_L} \sum_{\mathcal{O}} C_{HL\mathcal{O}} C_{\bar{\mathcal{O}}LH}\, g_{h,\bar{h}}^{h_{HL}, \bar{h}_{HL}}(z, \bar{z}) \,, \qquad (4.6b)$$

where we define $h_{HL} \equiv h_H^{[0]} - h_L$ and use the global conformal blocks given in (2.33). The sets of operators $\{\mathcal{O}\}$ and $\{\mathcal{O}'\}$ exchanged in the intermediate channels in the bootstrap relations above are qualitatively different, as we now explain.

In line with Section 2.1.1, we refer to the OPE decomposition (4.6a) where the two light operators are brought together by taking $z_1 \to z_2$ (or equivalently $z \to 1$) as the 'direct channel'. The direct-channel expansion includes the contribution of the "universal" sector consisting of: the identity, stress tensor and R-symmetry currents. These operators and their descendants contribute a universal part to the correlator, in the sense that it is completely determined by the symmetry algebra of the CFT – depending only on the dimensions h_H, h_L, and $U(1)$ charges j_H, j_L of $\mathcal{O}_H(\infty)$ and $\bar{\mathcal{O}}_L(z)$. This universal contribution is given (for N large and fixed N_b/N) by the product

$\mathcal{V} = \mathcal{V}_V \mathcal{V}_A$ of the "reduced" Virasoro block of the identity [99, 100]

$$\mathcal{V}_V(z) = z^{h_L(\alpha-1)} \left(\frac{\alpha}{1-z^\alpha} \right)^{2h_L} \tag{4.7}$$

and the affine $U(1)$ block

$$\mathcal{V}_A(z) = z^{\frac{2j_H j_L}{N}} \tag{4.8}$$

(times the corresponding anti-holomorphic counterparts). On top of this "universal" sector, the direct channel contains a family of light-light double-trace operators $\{\mathcal{O}_{LL}\}$ given schematically[47] by

$$\mathcal{O}_{LL} \equiv \, :\bar{\mathcal{O}}_L \partial^m \bar{\partial}^{\bar{m}} \mathcal{O}_L: \, . \tag{4.9}$$

The associated CFT data can then be naturally expanded in $1/N$ as

$$\gamma_{m,\bar{m}} = \frac{1}{N} \, \gamma_{m,\bar{m}}^{(1)} + \frac{1}{N^2} \, \gamma_{m,\bar{m}}^{(2)} + \cdots$$

$$c_{m,\bar{m}}^2 \equiv c_{ij\mathcal{O}_{ij}} c_{\mathcal{O}_{ij}ij} = c_{(0)}^2(m,\bar{m}) \left(1 + \frac{1}{N} \, c_{(1)}^2(m,\bar{m}) + \frac{1}{N^2} \, c_{(2)}^2(m,\bar{m}) + \cdots \right) \, . \tag{4.10}$$

The leading-order OPE coefficients $c_{(0)}^2$ of the double-trace operators in the direct channel are proportional to N_b, while the expansion parameter of the CFT data is N^{-1} (see (4.10)), so at the first subleading order one reconstructs $N_b/N \sim \mu$ necessary to match the scaling of the cross channel (4.24). The analysis in the direct channel is then essentially the same for either HHLL or LLLL correlators: in both cases only single-trace or double-trace operators composed of two light constituents are exchanged, while all other multi-trace operators are suppressed in the large N limit. The perturbative expansion of the direct channel decomposition in (2.32) then reads

$$C(z,\bar{z}) = \mathcal{V}(z)\mathcal{V}(\bar{z}) + \sum_{m,\bar{m}} c_{(0)}^2(m,\bar{m}) \, (1-z)^m (1-\bar{z})^{\bar{m}} F_m(z) F_{\bar{m}}(\bar{z}) \tag{4.11}$$

$$+ \frac{\mu}{2} \sum_{m,\bar{m}} (1-z)^m (1-\bar{z})^{\bar{m}} \Big[\bar{\delta}(m,\bar{m}) \Big(\widehat{F}_m(z) F_{\bar{m}}(\bar{z}) + F_m(z) \widehat{F}_{\bar{m}}(\bar{z}) \Big)$$

$$+ \Big(c_{(1)}^2(m,\bar{m}) + \bar{\delta}(m,\bar{m}) \log|1-z|^2 \Big) F_m(z) F_{\bar{m}}(\bar{z}) \Big] + \dots \, ,$$

where the F's indicate the conformal block with $h = m + 2h_L$, $\bar{h} = \bar{m} + 2\bar{h}_L$ and its derivatives

$$F_m(z) = {}_2F_1(m + 2h_L, m + 2h_L; 2m + 4h_L; 1-z) \, , \quad \widehat{F}_m(z) = \partial_m F_m(z) \, . \tag{4.12}$$

Since in the direct channel it is possible to have a vanishing average of the leading order

---

[47]This form of writing the double-trace operators is schematic, since at each level the derivatives are understood to act in such a way as to define a primary operator.

OPE coefficients $c_{(0)}^2$, we have introduced the quantity

$$\bar{\delta} \equiv \langle c_{(0)}^2 \gamma^{(1)} \rangle \ , \tag{4.13}$$

which is generically not equal to the product of the averages of $c_{(0)}^2$ and $\gamma^{(1)}$.

Likewise, we call the OPE limit where a heavy and a light operator are brought together (4.6b) by taking $z_1 \rightarrow z_4$ ($z \rightarrow 0$) the 'cross channel'. In this channel, no single-trace operators are exchanged and the leading contribution in $1/N$ comes from the exchange of a family of heavy-light multi-trace[48] operators which we denote by

$$\mathcal{O}_{HL} \equiv \, :\!\mathcal{O}_H \partial^m \bar{\partial}^{\bar{m}} \mathcal{O}_L\!: \ \ . \tag{4.14}$$

The conformal dimensions of these operators are given by

$$H = h_H^{[0]} + h_L + m + \frac{1}{2}\Gamma_{m,\bar{m}} \ , \qquad \bar{H} = \bar{h}_H^{[0]} + \bar{h}_L + \bar{m} + \frac{1}{2}\Gamma_{m,\bar{m}} \ , \tag{4.15}$$

with $\Gamma_{m,\bar{m}}$ denoting the anomalous dimensions. Here the $\Gamma_{m,\bar{m}}$ are enhanced by a factor of N_b with respect to the anomalous dimensions $\gamma_{m,\bar{m}}$ of double-trace operators with two light constituents. Hence, the perturbative expansion of such heavy quantities will be in terms of $\mu \sim N_b/N$ (4.5), taking the form[49] (note that our conventions for the μ expansion of OPE coefficients differs from that of the $1/N$ expansion used in Chapter 3. Here we have factored out the zeroth order GFT OPE coefficients from each order.)

$$\Gamma_{m,\bar{m}} = \sum_{n=1}^{\infty} \Gamma_{(n)} \, \mu^n \ , \tag{4.16a}$$

$$C_{m,\bar{m}}^2 \equiv C_{HL\mathcal{O}_{HL}} C_{\bar{\mathcal{O}}_{HL}HL} = C_{(0)}^2 \left(1 + \sum_{n=1}^{\infty} C_{(n)}^2 \, \mu^n \right) \ , \tag{4.16b}$$

where we have suppressed the m and $\bar{m}$ dependence of the various series coefficients. Intuitively one can think of $\gamma_{m,\bar{m}}$ as the binding energy between the two single particle constituents and $\Gamma_{m,\bar{m}}$ accounting for the interaction of $\mathcal{O}_L$ with all constituents of the heavy operator $\mathcal{O}_H$. This picture holds only at first order in the ratio N_b/N, since in general the binding energies for the heavy/light bound states depend non-linearly on this ratio – see for instance (4.119). With the conformal dimensions of the external operators being fixed, at leading order in $1/N$ the sum over operators exchanged in the cross-channel expansion (4.6b) can thus be rewritten as sums over $m, \bar{m} = 0, 1, 2, \ldots$ for the family (4.14).

---

[48] We use the terminology of 'multi-trace' for these heavy-light composite operators since in general the heavy operator itself can – and for us will – be a multi-trace operator.

[49] These anomalous dimensions should be thought of as 'averages' over all operators in the spectrum that are degenerate at leading order in $1/N$. No lifting of this degeneracy [183] is studied here.

Our goal is to study how the information about bulk high-energy scattering processes at fixed impact parameter is encoded in the CFT. In the boundary theory this corresponds to studying 4-point correlators in the Lorentzian kinematical regime of the *Regge limit* [89–92], defined by an analytic continuation in one of the conformal cross-ratios (here chosen to be z) around the origin, followed by taking both z and $\bar{z}$ to 1:

$$z \to z\, e^{-2\pi i} \, , \qquad z, \bar{z} \to 1 \, . \tag{4.17}$$

Due to the branch cut along $(-\infty, 0]$ of the hypergeometric function ${}_2F_1(h, h\, ; 2h\, ; 1 - z)$, present in the blocks $g_{h,\bar{h}}^{0,0}(1 - z, 1 - \bar{z})$ in (A.15), the direct channel correlator will transform non-trivially upon moving to the second sheet relevant for the Regge limit. It is useful to parametrise the cross-ratios on the second sheet as [97]

$$z = 1 - \sigma \, , \qquad \bar{z} = 1 - \sigma\eta \, , \tag{4.18}$$

in which case the Regge limit is obtained by taking $\sigma \to 0$ with η held fixed. Using the analytic continuation across the branch cut of the hypergeometric function yields

$${}_2F_1(h, h; 2h; 1 - z) \xrightarrow{\circlearrowleft} {}_2F_1(h, h; 2h; 1 - z) + 2\pi i\, \frac{\Gamma(2h)}{\Gamma^2(h)}\, {}_2F_1(h, h; 1; z) \, . \tag{4.19}$$

Focusing on the imaginary part, the leading behaviour of a single direct channel global block in the $\sigma \to 0$ limit is then

$$g_{h,\bar{h}}^{0,0}(1 - z, 1 - \bar{z})\Big|_{\circlearrowleft} \approx 2\pi i\, \frac{\Gamma(2h)\, \Gamma(2h - 1)}{\Gamma^4(h)}\, \eta^{\bar{h}} \sigma^{1 - h + \bar{h}} \, , \tag{4.20}$$

showing that operators with $h - \bar{h}$ large (*i.e.* large spin states) dominate. In particular, the spin-1 R-charge contribution, i.e. the $U(1)$ affine block in (4.8), is subdominant with respect to the Virasoro block (4.7), which originates from the exchange of the stress-tensor. In our explicit examples we will see two different patterns. A first possibility is that operators with at most spin two are exchanged in the direct channel, such as the stress-tensor and the double-trace operators with $m = \bar{m} + 2$. In this case, the analytic continuation to the Regge regime can be performed block by block, using (4.20) at leading order. Another possibility is to have contributions in the direct channel with unbounded spin: it is then necessary to first resum the terms with $m > \bar{m} + 2$ and to perform the Regge analytic continuation on the result. We will later show how this is done in an explicit example (see section 4.4.3 from (4.130) onwards). In both cases, this direct channel analysis reproduces the Regge behaviour, *i.e.* the imaginary part of the correlator scales as $\sigma^{-2h_L - 1}$ in the $\sigma \to 0$ limit – the extra factor of -1 in the exponent is typical of the exchange of a spin-2 state, identified holographically with the

graviton.

In particular, we focus on the cross-channel expansion (4.6b) where the relevant data is contained in the anomalous dimensions $\Gamma_{m,\bar{m}}$ and the OPE coefficients $C_{HL\mathcal{O}}$. The exact comparison between the bulk and boundary is currently beyond our reach for the microstate geometries that we are interested in due to the fact that the relevant 4-point correlators are known only in terms of series (for instance the correlator discussed in Section 2.3). Since an analytic continuation is needed to go to the Regge regime of a correlator, we have to work perturbatively by expanding in the parameter μ (as defined in (4.5)) [1, 52, 53]. Such an expansion can be naturally interpreted in the bulk as an expansion in the mass of an AdS-Schwarzschild black hole, while on the CFT side it counts the number of copies of the stress tensor appearing in the Virasoro vacuum block [52].

The strategy for analysing the HHLL correlators will be to expand the supergravity result (initially at leading order, and later more generally) in $\mu \sim N_b/N$ and to read off the CFT data relevant for Eq. (4.6). At zeroth order in μ, only the identity contributes to the direct channel and the bootstrap relation (4.6) constrains the zeroth order OPE coefficients in exactly the same manner as Section 2.1.1 via[50]

$$(1-z)^{-2h_L}(1-\bar{z})^{-2\bar{h}_L} = z^{-(h_H+h_L)}\bar{z}^{-(\bar{h}_H+\bar{h}_L)}\sum_{\{\mathcal{O}_{HL}\}} C_{(0)}^2(m,\bar{m})\, g_{H,\bar{H}}^{h_{HL},\bar{h}_{HL}}(z,\bar{z})\Big|_{\mu^0}\,, \quad (4.21)$$

where $h_{HL} = h_H - h_L$, $\bar{h}_{HL} = \bar{h}_H - \bar{h}_L$, yielding $C_{(0)}^2(m,\bar{m})$ (with the same functional form as (2.42)) as

$$
\begin{aligned}
C_{(0)}^2(m,\bar{m}) &= \frac{\Gamma(2h_H+m)\,\Gamma(2h_L+m)\,\Gamma(2h_H+2h_L+m-1)}{m!\,\Gamma(2h_H)\,\Gamma(2h_L)\,\Gamma(2h_H+2h_L+2m-1)}\\
&\times \frac{\Gamma(2\bar{h}_H+\bar{m})\,\Gamma(2\bar{h}_L+\bar{m})\,\Gamma(2\bar{h}_H+2\bar{h}_L+\bar{m}-1)}{\bar{m}!\,\Gamma(2\bar{h}_H)\,\Gamma(2\bar{h}_L)\,\Gamma(2\bar{h}_H+2\bar{h}_L+2\bar{m}-1)}\,.
\end{aligned}
\quad (4.22)
$$

Looking now to the cross channel decomposition in (2.32) for the HHLL correlator at order μ, we have

$$C(z,\bar{z})\big|_\mu = z^{-(h_H^{[0]}+h_L)}\,\bar{z}^{-(\bar{h}_H^{[0]}+\bar{h}_L)}\sum_{\{\mathcal{O}_{HL}\}} C_{m,\bar{m}}^2\, g_{H,\bar{H}}^{h_{HL},\bar{h}_{HL}}(z,\bar{z})\Big|_\mu\,. \quad (4.23)$$

On the right-hand side, the μ dependence is in both the OPE coefficients and the blocks (due to the anomalous dimensions). One difficulty in solving this constraint is that the first order corrections to both the OPE coefficients and the conformal dimensions appear as unknowns. In order to decouple their contributions and to make a connection to the classical bulk scattering of Section 2.4, we consider (4.23) in the Regge limit. The

---

[50]Note that at the order μ^0 we have $h_H^{[0]} \approx h_H$, and likewise for the anti-holomorphic dimension.

order μ crossing equations (4.23) in the Regge limit then read

$$C_{\circlearrowleft}|_{\mu} = z^{-(h_H^{[0]}+h_L)}\,\bar{z}^{-(\bar{h}_H^{[0]}+\bar{h}_L)} \sum_{\{\mathcal{O}_{HL}\}} C_{m,\bar{m}}^2\, e^{-2\pi i(H-h_H^{[0]}-h_L)} g_{H,\bar{H}}^{h_{HL},\bar{H}_{HL}}(z,\bar{z})\Big|_{\mu} \qquad (4.24)$$

$$= z^{-(h_H^{[0]}+h_L)}\,\bar{z}^{-(\bar{h}_H^{[0]}+\bar{h}_L)} \sum_{m,\bar{m}=0}^{\infty} C_{(0)}^2 \bigg[C_{(1)}^2$$

$$+ \frac{1}{2}\Gamma_{m,\bar{m}}^{(1)}\Big(-2\pi i + (\partial_m + \partial_{\bar{m}})\Big)\bigg] g_{H,\bar{H}}^{h_{HL},\bar{h}_{HL}}(z,\bar{z})\Big|_{\mu=0}\,, \quad (4.25)$$

where the origin of the imaginary contribution follows from the factor of z^H in the global blocks (2.33). Selecting then the imaginary part of the above equation extracts a term proportional to the anomalous dimension and with no dependence on $C_{(1)}^2$:

$$\text{Im}\, C_{\circlearrowleft}|_{\mu} = -\pi z^{-(h_H^{[0]}+h_L)}\,\bar{z}^{-(\bar{h}_H^{[0]}+\bar{h}_L)} \sum_{m,\bar{m}=0}^{\infty} C_{(0)}^2(m,\bar{m})\,\Gamma_{m,\bar{m}}^{(1)}\, g_{H,\bar{H}}^{h_{HL},\bar{h}_{HL}}(z,\bar{z})\Big|_{\mu=0}\,.$$
$$(4.26)$$

By matching the $O(\mu)$ cross-channel expansion on the r.h.s. of (4.26) with the imaginary part of the correlator after having taken the Regge limit, one can extract the anomalous dimensions $\Gamma_{m,\bar{m}}^{(1)}$ for operators with $m, \bar{m} \gg 1$ – those dominating in the Regge regime.

The same strategy described above can be used to analyse correlators of the form (2.28) in which all external operators are light [97]: here $\Delta_1, \Delta_2 \sim 1$ as $c \to \infty$. In this case the expansion parameter is simply the inverse of the central charge, parametrised by N^{-1} and so it is then sufficient in the LLLL case to simply set $N_b = 1$. We analyse a particular LLLL correlator in the Regge limit in Section 4.4.3 as an example. At this stage, a number of simplifying approximations can be made for both the GFT OPE coefficients and the conformal blocks; these approximations are different for the HHLL and LLLL cases.

For HHLL correlators there is the hierarchy $h_H^{[0]} \gg h_L, m, \bar{m}$: in this limit the zeroth order OPE coefficients (4.22) simplify to

$$C_{(0)}^2(m,\bar{m}) \approx \frac{\Gamma(2h_L + m)\,\Gamma(2\bar{h}_L + \bar{m})}{m!\,\bar{m}!\,\Gamma(2h_L)\,\Gamma(2\bar{h}_L)}\,, \qquad (4.27)$$

and for the additional scaling $m, \bar{m} \gg 1$, relevant in the Regge limit, this further reduces to

$$C_{(0)}^2(m,\bar{m}) \approx \frac{m^{2h_L-1}\bar{m}^{2\bar{h}_L-1}}{\Gamma(2h_L)\,\Gamma(2\bar{h}_L)}\,. \qquad (4.28)$$

The hypergeometric functions in the cross-channel conformal blocks (2.33) can also be

approximated in the heavy scaling limit $h_H^{[0]} \gg h_L, m, \bar{m}$ by

$$
{}_2F_1(H - h_{HL}, H - h_{HL}; 2H; z) = \sum_{k=0}^{\infty} \frac{(H - h_{HL})_k^2}{k!(2H)_k} z^k \approx 1 + O(1/h_H) \ , \qquad (4.29)
$$

where we used the series representation of the hypergeometric function and the approximations $H \approx h_H^{[0]}$, which follows from (4.15), and $h_{HL} = h_H^{[0]} - h_L \approx h_H^{[0]}$. Implementing these approximations in the Regge crossing equation (4.26) gives

$$
\text{Im}\, C_{\circlearrowleft}|_{\mu^1} \approx -\pi \sum_{m,\bar{m}=0}^{\infty} C_{(0)}^2(m, \bar{m})\, \Gamma_{m,\bar{m}}^{(1)}\, z^m \bar{z}^{\bar{m}} \ . \qquad (4.30)
$$

For LLLL correlators, the cross-channel decomposition in the Regge limit at order μ^1 is identical to (4.26) with the replacements $C_{(0)}^2 \to c_{(0)}^2$, $\Gamma_{m,\bar{m}}^{(1)} \to \gamma_{m,\bar{m}}^{(1)}$, $g_{H,\bar{H}}^{h_{HL},\bar{h}_{HL}} \to g_{h,\bar{h}}^{h_{12},\bar{h}_{12}}$ and $h_H^{[0]} \to h_1$, where the conformal dimensions h_1, h_2 are of order 1 in the large c limit. In this regime, the Regge limit allows for an approximation to the conformal blocks in terms of modified Bessel functions of the second kind – since again, double-trace operators with large $m, \bar{m}$ dominate in the cross channel. This approximation is derived in Appendix D. Thus, considering $h, \bar{h} \gg 1$ with $\hat{z} \equiv h\sqrt{1-z}$ finite, the holomorphic part of the conformal blocks (2.33) approximates to [97]

$$
z^h\, {}_2F_1\big(h - h_{12}, h - h_{12}; 2h; z\big) \approx 2^{2h} \sqrt{\frac{h}{\pi}}\, (1-z)^{h_{12}}\, K_{-2h_{12}}\big(2h\sqrt{1-z}\big) \equiv \mathcal{K}_h^{h_{12}} \ ,
$$
$$
(4.31)
$$

giving the approximation to the full global block as

$$
g_{h,\bar{h}}^{h_{12},\bar{h}_{12}} \approx \mathcal{K}_h^{h_{12}}(z)\mathcal{K}_{\bar{h}}^{\bar{h}_{12}}(\bar{z}) \ . \qquad (4.32)
$$

The derivation of this approximation to the LLLL blocks can be found in Appendix D. We recall that the HHLL correlator at first order in N_b/N and the LLLL correlator (which has $N_b = 1$) at first order in $1/N$ are identical – see for instance the $n = 1$ term in the final line of equation (3.4). Despite this fact, the approximations to the conformal blocks and the OPE coefficients that are appropriate in the two regimes are different: for the conformal blocks one should use (4.29) in the HHLL regime and (4.31) in the LLLL one. For this reason the anomalous dimensions $\Gamma_{m,\bar{m}}^{(1)}$ and $\gamma_{m,\bar{m}}^{(1)}$ that one derives in the two cases are different. This fact will be illustrated in a specific example in Section 4.4.3.

Both anomalous dimensions $\Gamma_{m,\bar{m}}^{(1)}$ and $\gamma_{m,\bar{m}}^{(1)}$ for large values of $m, \bar{m}$ are linked to

the $O(\mu)$ phase shift $\delta^{(1)}$ computed on the gravity side by identical relations [52, 90, 96]

$$\Gamma^{(1)}_{m,\bar{m}} \approx -\frac{\delta^{(1)}}{\pi} \quad , \quad \gamma^{(1)}_{m,\bar{m}} \approx -\frac{\delta^{(1)}}{\pi} \quad \text{for} \quad m, \bar{m} \gg 1 \,, \qquad (4.33)$$

where the CFT variables $m, \bar{m}$ are mapped to the bulk momenta of Section 2.4, p_t, p_y – of which $\delta^{(1)}$ is a function – by

$$R_y |p_t| = m + \bar{m} \quad , \quad R_y \, p_y = m - \bar{m} \quad \Rightarrow \quad \beta = -\frac{m - \bar{m}}{m + \bar{m}} \,. \qquad (4.34)$$

These various relations and their extensions to arbitrary orders in μ will now be derived.

A generalisation to arbitrary orders in μ

The discussion thus far in this section has been essentially tailored towards an analysis of correlators – both HHLL and LLLL – at first order in the parameter μ. In the remainder of this section we generalise the comparison of the bulk phase shift and the Regge limit of CFT correlators in the HHLL case to arbitrary orders in μ.

By expanding the cross-channel data of the double-trace operators (4.14) as shown in (4.16), inserting these series into the cross-channel decomposition (4.6b) and expanding in μ, one finds that in general the expansion coefficients $\Gamma_{(n)}$ and $C^2_{(n)}$ are encoded in the correlator in a complicated manner. However, the analysis can be somewhat simplified by taking the Regge limit (4.17). The cross-channel decomposition of an analytically continued correlator can be written to leading order in large N as

$$C(z, \bar{z}) \xrightarrow{\circlearrowleft} z^{-h^{[0]}_H - h_L} \, \bar{z}^{-\bar{h}^{[0]}_H - \bar{h}_L} \sum_{m,\bar{m}=0}^{\infty} C^2_{m,\bar{m}} \, e^{-\pi i \, \Gamma_{m,\bar{m}}} g^{h_{HL}, \bar{h}_{HL}}_{H, \bar{H}}(z, \bar{z}) \,, \qquad (4.35)$$

where we sum over all members of the family of exchanged HL multi-trace operators (4.14). In the above sum, the global conformal blocks implicitly depend on μ via the conformal dimensions H and $\bar{H}$ given in (4.15). After taking $z, \bar{z} \to 1$ a large number of terms contribute in the cross-channel, however, the dominant multi-trace operators are those with $m, \bar{m} \gg 1$. Correspondingly, we can treat m and $\bar{m}$ as continuous variables and approximate the sums by integrals. Then using (4.16), one can write the explicit

expansion of the correlator in the Regge limit, which we denote by C_R, as

$$
C_{\mathrm{R}} \approx \frac{1}{z^{h_H^{[0]}+h_L}\,\bar{z}^{\bar{h}_H^{[0]}+\bar{h}_L}} \int_0^\infty dm \int_0^\infty d\bar{m}\, C_{(0)}^2 \left[1 + \mu\left(C_{(1)}^2 + \Gamma_{(1)}\widetilde{D}\right) + \mu^2\left(C_{(2)}^2 + \frac{1}{2}\Gamma_{(1)}^2\widetilde{D}^2\right.\right.
$$
$$
+ \left(C_{(1)}^2\Gamma_{(1)} + \Gamma_{(2)}\right)\widetilde{D}\Big) + \mu^3\left(C_{(3)}^2 + \frac{1}{6}\Gamma_{(1)}^3\widetilde{D}^3 + \frac{1}{2}\Gamma_{(1)}\left(C_{(1)}^2\Gamma_{(1)} + 2\Gamma_{(2)}\right)\widetilde{D}^2\right.
$$
$$
\left.\left. + \left(C_{(2)}^2\Gamma_{(1)} + C_{(1)}^2\Gamma_{(2)} + \Gamma_{(3)}\right)\widetilde{D}\right)\right] g_{H,\bar{H}}^{h_{HL},\bar{h}_{HL}}(z,\bar{z})\Bigg|_{\mu=0} , \tag{4.36}
$$

where $\widetilde{D} \equiv \frac{1}{2}(\partial_m + \partial_{\bar{m}}) - \pi i$ and the the conformal block functions should be evaluated at $\mu = 0$ only after the action of the derivatives in $\widetilde{D}$. Finally, when explicitly evaluating such integrals one can use the scaling limit $h_H^{[0]} \gg m, \bar{m} \gg 1$ in which the GFT OPE coefficients simplify to (4.28) and, since the hypergeometric functions are unity up to order $O(h_H^{-1})$ corrections as in (4.29), the global conformal blocks (2.33) in the cross channel can be approximated by

$$
g_{H,\bar{H}}^{h_{HL},\bar{h}_{HL}}(z,\bar{z}) \approx z^H \bar{z}^{\bar{H}} , \tag{4.37}
$$

with H and $\bar{H}$ being given by (4.15).

The link between the bulk phase shift (2.100) and the CFT data (4.15) is made by using the impact parameter representation of 4-point correlation functions in the Regge limit [52, 53, 90]. In what follows we limit our analysis to correlators involving only operators for which $h_L = \bar{h}_L$ and $h_H^{[0]} = \bar{h}_H^{[0]}$, as is the case for the explicit examples considered in section 4.3 and section 4.4. Starting from the cross-channel decomposition (4.6b), we want to write the correlator in the Regge limit as an expansion over impact parameter partial waves $\mathcal{I}_{m,\bar{m}}$ as

$$
C_{\mathrm{R}}(z,\bar{z}) \approx \sum_{m=0}^{\infty} \sum_{\bar{m}=0}^{m} \mathcal{I}_{m,\bar{m}}\, A(m,\bar{m}) , \tag{4.38}
$$

where $A(m,\bar{m})$ is an arbitrary symmetric function of m and $\bar{m}$ such that $A|_{\mu=0} = 1$. In $d = 2$, we define

$$
\mathcal{I}_{m,\bar{m}} \equiv \frac{C_{(0)}^2(m,\bar{m})}{|z|^{2(h_H^{[0]}+h_L)}}\, g_{H,\bar{H}}^{h_{HL},h_{HL}}(z,\bar{z})\Big|_{\mu=0} + (z \leftrightarrow \bar{z}) \approx \frac{(m\bar{m})^{2h_L-1}}{\Gamma^2(2h_L)}\left(z^m \bar{z}^{\bar{m}} + z^{\bar{m}} \bar{z}^m\right) ,
$$
$$
\tag{4.39}
$$

where we have used (4.28) and (4.37) in the final right-hand side. The impact parameter partial waves are defined to be the GFT ($\mu = 0$) cross-channel partial waves of the operators (4.14). Hence by setting $\mu = 0$ in (4.38) we recover the disconnected part of

the correlator in the Regge limit using

$$\sum_{m=0}^{\infty}\sum_{\bar{m}=0}^{m}\mathcal{I}_{m,\bar{m}} \approx |1-z|^{-4h_L} \, , \tag{4.40}$$

as was explained in Section 2.1.1. In [90] it was shown that $\mathcal{I}_{m,\bar{m}}$ admits an impact parameter representation, which in $d=2$ and in the HHLL regime takes the form[51]

$$\mathcal{I}_{m,\bar{m}} = \frac{2^{5-4h_L}\pi^2}{\Gamma^2(2h_L)} \int_{M^-} \frac{d^2p}{(2\pi)^2} (-p^2)^{2h_L-1} e^{-ip\cdot x} |m-\bar{m}| \, \delta^2 \, , \tag{4.41}$$

where the integral is over the lower Milne wedge $M^- \equiv \{\, \mathbf{p} \in \mathbb{R}^{1,1} \,|\, p^2 \leq 0, p_t \leq 0 \,\}$ and δ^2 is defined as the combination of delta functions

$$\delta^2 \equiv \delta(p\cdot\bar{e} + m + \bar{m})\,\delta\!\left(\frac{p^2}{4} + m\bar{m}\right) \, , \tag{4.42}$$

with $\bar{e}_\mu \equiv -\delta_\mu^0$. To show that the impact parameter representation (4.41) is equivalent to (4.39), we first evaluate the p integrals using lightcone coordinates $p_\pm = p_t \pm p_y$ and $x^\pm = t \pm y$ yielding

$$\mathcal{I}_{m,\bar{m}} = \frac{2^{2-4h_L}}{\Gamma^2(2h_L)} \int_0^\infty\!\!\int_0^\infty dp_+ dp_- \,(p_+ p_-)^{2h_L-1}\, e^{-\frac{1}{2}i(p_+ x^- + p_- x^+)} |m-\bar{m}| \, \delta^2 \, , \tag{4.43}$$

where the delta functions can be put into the form

$$\delta^2 = |m-\bar{m}|^{-1}\Big(\delta\big(\tfrac{1}{2}p^+ + m\big)\delta\big(\tfrac{1}{2}p^- + \bar{m}\big) + \delta\big(\tfrac{1}{2}p^+ + \bar{m}\big)\delta\big(\tfrac{1}{2}p^- + m\big)\Big) \, . \tag{4.44}$$

By defining the coordinates on the plane as

$$z \equiv e^{ix^+} \, , \qquad \bar{z} \equiv e^{ix^-} \, , \tag{4.45}$$

it is simple to evaluate the integrals in (4.43) to give exactly (4.39).

Equally, we can insert the impact parameter representation of $\mathcal{I}_{m,\bar{m}}$ into (4.38) and approximate the sums over m and $\bar{m}$ with integrals. By performing first the integrals over m and $\bar{m}$, one obtains

$$\begin{aligned} C_{\mathrm{R}}(z,\bar{z}) &\approx \int_0^\infty dm \int_0^m d\bar{m} \, \mathcal{I}_{m,\bar{m}} \, A(m,\bar{m}) \\ &= \frac{2^{5-4h_L}\pi^2}{\Gamma(2h_L)^2} \int_{M^-} \frac{d^2p}{(2\pi)^2} \,(-p^2)^{2h_L-1}\, e^{-ip\cdot x} \, A(-\tfrac{1}{2}\mathbf{p}) \, , \end{aligned} \tag{4.46}$$

with the identifications (4.45) implied. We have used the notation $\mathbf{p} \equiv (p_-, p_+)$ and

---

[51]Note that our conventions differ from those of [90] and [53].

the relations

$$\frac{p^+}{2} = -\bar{m} \quad , \quad \frac{p^-}{2} = -m \, , \tag{4.47}$$

which originate from the delta functions in (4.44). The final line of (4.46) can be inverted and if we set $A(m, \bar{m}) = e^{i\delta(m, \bar{m})}$ then the phase can be determined in terms of the Fourier transform of a 4-point function in the Regge limit

$$\int d^2x \, C_{\mathrm{R}}(z, \bar{z}) \, e^{ip \cdot x} = B_0(\mathbf{p}) \, e^{i\delta(\mathbf{p})} \, , \tag{4.48}$$

with

$$B_0(\mathbf{p}) = \frac{2^{3-4h_L} \, \pi^2}{\Gamma^2(2h_L)} \Theta(-p_t)\Theta(-p^2) \left(-p^2\right)^{2h_L-1} \, , \tag{4.49}$$

denoting the Fourier transform of the disconnected part of the correlator. Following the proposal of [52], we identify $\delta(\mathbf{p})$ as the bulk phase shift of (2.100) and interpret $\mathbf{p}$ as the conserved momentum along the null geodesics. In particular, from (4.47) it follows that

$$|p_t| = m + \bar{m} \, , \qquad p_y = m - \bar{m} \, , \tag{4.50}$$

and thus $\beta = -(m - \bar{m})/(m + \bar{m})$. This identification, valid in the Regge limit, directly links well-defined bulk quantities and the operators exchanged in 4-point correlators and will allow us to obtain concrete relations between the phase shift and CFT data (4.16). To obtain expressions linking the two sides, we insert (4.39) and $A(m, \bar{m}) = e^{i\delta(m, \bar{m})}$ into (4.38), approximate the sums over m and $\bar{m}$ with integrals and use the assumed symmetry of the phase shift to get

$$C_{\mathrm{R}}(z, \bar{z}) \approx \int_0^\infty \int_0^\infty dm d\bar{m} \, \frac{(m\bar{m})^{2h_L-1}}{\Gamma^2(2h_L)} \, z^m \bar{z}^{\bar{m}} \, e^{i\delta(m, \bar{m})} \, . \tag{4.51}$$

This relation incorporates the key idea of the eikonal regime; namely that by comparing with the GFT results (4.28) and (4.37) (valid in the Regge limit), one notes that the details of the interaction between the light probe and the heavy object are resummed into the phase. In the context of the proposal of [52], (4.51) directly relates the bulk phase shift $\delta(m, \bar{m})$ (with the relations (4.50) understood) to the CFT data (4.16). Therefore, this relation allows us to reproduce the Regge limit of particular HHLL correlators and to extract cross-channel CFT data, all purely from the bulk phase shift of the probe propagating in the geometry dual to the heavy operator.

To see this explicitly, we assume that the phase shift admits the perturbative ex-

pansion[52]

$$\delta(m, \bar{m}) = \sum_{n=1}^{\infty} \delta_{(n)} \mu^n \,, \tag{4.52}$$

where from now on we suppress the m and $\bar{m}$ dependence of both the expansion coefficients $\delta_{(k)}$ and the exact phase shift δ, and expand the right-hand side of (4.51) using

$$e^{i\delta} \approx 1 + i\delta_{(1)}\,\mu + \left(i\delta_{(2)} - \frac{1}{2}\delta_{(1)}^2 \right)\mu^2 + \left(i\delta_{(3)} - \delta_{(1)}\delta_{(2)} - \frac{i}{6}\delta_{(1)}^3 \right)\mu^3 \,. \tag{4.53}$$

Comparing the result term by term with the Regge limit cross-channel conformal block decomposition (4.36) one gets a series of differential relations between CFT data and the bulk phase shift. Since only elastic scattering is considered here, we take δ and all of its expansion coefficients to be real-valued. We similarly assume that the anomalous dimension $\Gamma_{m,\bar{m}}$ and the square of the OPE coefficients $C_{m,\bar{m}}^2$ take real values. Then the set of differential equations can be split by considering the real and imaginary parts separately, the first few of which yield previously known relations [52, 53, 90][53]

$$\Gamma_{(1)} = -\frac{\delta_{(1)}}{\pi} \,, \qquad\qquad C_{(0)}^2 C_{(1)}^2 = \partial_+\left(C_{(0)}^2 \Gamma_{(1)} \right) \,, \tag{4.54a}$$

$$\Gamma_{(2)} = -\frac{\delta_{(2)}}{\pi} + \Gamma_{(1)}\,\partial_+\Gamma_{(1)} \,, \quad C_{(0)}^2 C_{(2)}^2 = \partial_+\left(C_{(0)}^2 C_{(1)}^2 \Gamma_{(1)} + C_{(0)}^2 \Gamma_{(2)} \right) - \frac{1}{2}\partial_+^2\left(\Gamma_{(1)}^2 C_{(0)}^2 \right) \,, \tag{4.54b}$$

where we have defined the differential operator $\partial_+ \equiv \partial_{(m+\bar{m})} = \frac{1}{2}\left(\partial_m + \partial_{\bar{m}} \right)$. These relations quickly become cumbersome, particularly since they express CFT information in terms of both the phase shift expansion coefficients and lower order CFT data. However, as might be expected from the point of view of holography, the bulk and boundary information can be separated and so it is possible to express the anomalous dimensions and OPE coefficients purely in terms of the bulk phase shift. The first few

---

[52]To be precise, the bulk phase shift that is related to the CFT data is the difference in the phase shift relative to the pure AdS result. Therefore, the expansion of δ starts at linear order in μ, since the contribution from the pure AdS is first subtracted.

[53]There are additional total derivative terms which we omit in these expressions. Their contributions vanish in all examples we have considered and furthermore, the equations (4.54) have been checked in the example of AdS-Schwarzschild and agree with the results obtained by independent lightcone limit methods [52, 53].

such relations read

$$\Gamma_{(1)} = -\frac{\delta_{(1)}}{\pi} \,, \tag{4.55a}$$

$$\Gamma_{(2)} = -\frac{\delta_{(2)}}{\pi} + \frac{1}{2!}\partial_+\left(\frac{\delta_{(1)}^2}{\pi^2}\right) \,, \tag{4.55b}$$

$$\Gamma_{(3)} = -\frac{\delta_{(3)}}{\pi} + \partial_+\left(\frac{\delta_{(1)}\,\delta_{(2)}}{\pi^2}\right) - \frac{1}{3!}\partial_+^2\left(\frac{\delta_{(1)}^3}{\pi^3}\right) \,, \tag{4.55c}$$

and

$$C_{(1)}^2 = -\frac{1}{C_{(0)}^2}\partial_+\left(C_{(0)}^2\frac{\delta_{(1)}}{\pi}\right) \,, \tag{4.56a}$$

$$C_{(2)}^2 = -\frac{1}{C_{(0)}^2}\partial_+\left[C_{(0)}^2\frac{\delta_{(2)}}{\pi} - \frac{1}{2!}\partial_+\left(C_{(0)}^2\frac{\delta_{(1)}^2}{\pi^2}\right)\right] \,, \tag{4.56b}$$

$$C_{(3)}^2 = -\frac{1}{C_{(0)}^2}\partial_+\left[C_{(0)}^2\frac{\delta_{(3)}}{\pi} - \partial_+\left(C_{(0)}^2\frac{\delta_{(1)}\,\delta_{(2)}}{\pi^2}\right) + \frac{1}{3!}\partial_+^2\left(C_{(0)}^2\frac{\delta_{(1)}^3}{\pi^3}\right)\right] \,. \tag{4.56c}$$

A pattern soon emerges and so we conjecture that at an arbitrary order in μ these relations read

$$\Gamma_{(n)} = \sum_{\{k_t\}}\partial_+^{K-1}\left[\prod_{t=1}^{\infty}\frac{1}{k_t!}\left(-\frac{\delta_{(t)}}{\pi}\right)^{k_t}\right] \,, \tag{4.57a}$$

$$C_{(n)}^2 = \frac{1}{C_{(0)}^2}\sum_{\{k_t\}}\partial_+^{K}\left[C_{(0)}^2\prod_{t=1}^{\infty}\frac{1}{k_t!}\left(-\frac{\delta_{(t)}}{\pi}\right)^{k_t}\right] \,, \tag{4.57b}$$

where the sums run over all configurations of $k_t \in \mathbb{N}^0$ such that

$$n = \sum_{t=1}^{\infty}tk_t \quad \text{and} \quad K = \sum_{t=1}^{\infty}k_t \,. \tag{4.58}$$

What this means is that in (4.57), for each value of $n \in \mathbb{N}$ one sums over all integer partitions of n with each term being divided by the degeneracy of the parts appearing in the partition.

These equations were derived using expressions that are valid only in $d = 2$, however, it was argued in [53] that the relations (4.54) hold in any dimension and thus we can conjecture that the same should be true for (4.57). Interestingly, we observe that for light operators with $h_L = \bar{h}_L = \frac{1}{2}$, the zeroth order OPE coefficient (4.28) are $C_{(0)}^2 \approx 1$ in the Regge limit and as a consequence, the CFT data associated with such probes

satisfies a simple relationship at each order in μ

$$C^2_{(n)} = \partial_+ \Gamma_{(n)}. \tag{4.59}$$

Finally, let us note that one can resum the series coefficients appearing in (4.57) to obtain relations that are exact in μ

$$\Gamma_{m,\bar{m}} = \sum_{n=1}^{\infty} \frac{1}{n!} \partial_+^{n-1} \left(-\frac{\delta}{\pi} \right)^n \quad , \quad C^2_{m,\bar{m}} = \frac{1}{C^2_{(0)}} \sum_{n=1}^{\infty} \frac{1}{n!} \partial_+^n \left[C^2_{(0)} \left(-\frac{\delta}{\pi} \right)^n \right]. \tag{4.60}$$

While we do not use these exact expressions in this thesis, they have been checked in explicit examples and we will discuss their potential in Chapter 5.

4.3 Conical defect geometry

In this section we apply the methods of Sections 2.4 and 4.2 to the case of heavy operators dual to conical defect geometries. We begin by reviewing the bulk computation of the phase shift for this example, first computed in [52], followed by an analysis of the relevant 4-point correlation functions [70] for two types of light probes and find perfect agreement between the CFT data and bulk phase shift. Finally, we briefly comment on the possibility of the Regge limit distinguishing between pure and mixed states.

4.3.1 Bulk description

In order to make a connection with the AdS$_3$ conical defect geometry analysed in [52], we consider a particularly simple microstate geometry, first introduced in [201, 202]. This 6D geometry locally factorises into AdS$_3 \times$ S^3 and for our purposes only the reduced 3D metric is relevant, given by

$$(Q_1 Q_5)^{-\frac{1}{2}} ds^2_{\text{AdS}_3} = \frac{dr^2}{r^2 + \frac{a^2}{k^2}} - \frac{r^2 + \frac{a^2}{k^2}}{Q_1 Q_5} dt^2 + \frac{r^2}{Q_1 Q_5} dy^2, \tag{4.61}$$

where $k \in \mathbb{N}$. The radius R_y of the y coordinate is related to the D1 and D5 charges Q_1, Q_5 and the parameter a by $R_y = \frac{\sqrt{Q_1 Q_5}}{a}$. With the periodic identification $y \sim y + 2\pi R_y$, the above geometry has a conical singularity of order k at $r = 0$. One could formally eliminate the conical singularity and map the metric (4.61) to global AdS$_3$ by the local diffeomorphism $r \to r\, k^{-1}$, $t \to t\, k$, $y \to y\, k$. However, since this diffeomorphism is non-vanishing at the AdS boundary and is not globally defined due to the change in y periodicity it induces, the geometry (4.61) and global AdS$_3$ are physically inequivalent.

The conical singularity has a natural description at the free orbifold point of the dual D1-D5 CFT: the heavy operator dual to the geometry (4.61), after spectral flow

to the NS sector, is made up of N/k copies of the twist operator of order k [24]. This description makes it evident that only the geometries with integer k can be associated to states of the CFT. Nevertheless, in order to connect with [52], in which geometries with real-valued defect angles were considered, one can analytically continue k to take generic values in $[1, \infty)$ and parametrise it as

$$\frac{1}{k} = \sqrt{1 - \mu} \equiv \alpha \, , \tag{4.62}$$

where $\mu = 0$ describes pure AdS. The bulk phase shift computed in the reduced 3D metric (4.61) follows from the general formula (2.105):

$$\delta_k = 2aR_y \, |p_t| \int_{r_0}^{\infty} dr \left(r^2 + \frac{a^2}{k^2} \right)^{-1} \sqrt{1 - \frac{\beta^2}{r^2} \left(r^2 + \frac{a^2}{k^2} \right)} = \pi R_y \, k \, |p_t| (1 - |\beta|) \, , \tag{4.63}$$

with the radial turning point $r_0 = \frac{a}{k}(\beta^{-2} - 1)^{-1/2}$ obtained by setting Eq. (2.101) to zero. It is noted that setting $k \to 1$ here reproduces the phase shift in pure AdS$_3$ as expected. Subtracting the AdS result from (4.63) gives the deviation due to the presence of the defect as

$$\delta = \delta_k - \delta_{k=1} = \pi R_y \, |p_t| (1 - |\beta|) \, (k - 1) \, . \tag{4.64}$$

Using the analytic continuation (4.62), the phase shift can be expanded in small μ allowing for a CFT interpretation of the bulk result and comparison with [52]:

$$\delta = \pi R_y \, |p_t| (1 - |\beta|) \left[(1 - \mu)^{-\frac{1}{2}} - 1 \right] = \pi R_y \, |p_t| (1 - |\beta|) \left(\frac{1}{2}\mu + \frac{3}{8}\mu^2 + \cdots \right) \, . \tag{4.65}$$

4.3.2   CFT analysis at first order in μ

We would like to understand if the bulk phase shift (4.65) captures the Regge limit of some CFT correlator. For integer k this would be the four-point correlator between the heavy state dual to the conical defect (4.61) and two light operators of fixed conformal dimension $(h_L, \bar{h}_L)$. These relevant heavy operators belong to the set of Ramond-Ramond ground states of the D1-D5 CFT, each having conformal dimensions $h_H = \bar{h}_H = \frac{N}{4}$ and $SU(2)$ charges $j_H = \bar{j}_H = \frac{N}{2k}$, and hence the corresponding reduced conformal dimension (4.2) is given by

$$h_H^{[0]} = \frac{N}{4} \left(1 - \frac{1}{k^2} \right) \, . \tag{4.66}$$

This four-point correlator has been computed in [70] by solving the linearised wave equation describing small fluctuations of the light operator in the background (4.61)

of the heavy operator, in a similar manner to Section 2.3. When the light operator is taken to be the chiral primary operator $\mathcal{O}^{\text{fer}}$ of dimension $(h_L, \bar{h}_L) = (1/2, 1/2)$, the correlator in the NSNS sector is

$$C_k^{\text{fer}} = \frac{1/k}{|1-z|^2} \frac{1-|z|^2}{1-|z|^{2/k}} \ . \tag{4.67}$$

Another natural candidate for the light operator is $\mathcal{O}^{\text{bos}}$, with dimension $(h_L, \bar{h}_L) = (1,1)$. This superdescendant of $\mathcal{O}^{\text{fer}}$ is obtained by acting on the chiral primary with one left-moving and one right-moving supercharge. The explicit forms of the operators $\mathcal{O}^{\text{fer}}$ and $\mathcal{O}^{\text{bos}}$ in terms of the basic fields of the free orbifold point of the D1-D5 CFT can be found in (2.76). In the bulk, $\mathcal{O}^{\text{bos}}$ has a simpler description than $\mathcal{O}^{\text{fer}}$, being dual to a minimally coupled scalar in the background described by the 6D Einstein metric. The correlators C^{fer} and C^{bos} of the light operators $\mathcal{O}^{\text{fer}}$ and $\mathcal{O}^{\text{bos}}$ in a 1/2-BPS heavy state (such as the one dual to (4.61)) are related by a simple supersymmetric Ward identity, which gives

$$C_k^{\text{bos}} = \partial\bar{\partial} \left[C_k^{\text{fer}} \right] = \partial\bar{\partial} \left(\frac{1/k}{|1-z|^2} \frac{1-|z|^2}{1-|z|^{2/k}} \right) \ . \tag{4.68}$$

To compare with the bulk phase shift computed in a conical defect geometry with real-valued deficit angle, one can analytically continue the above correlators using the parametrisation (4.62) to get

$$C_\alpha^{\text{fer}} = \frac{\alpha}{|1-z|^2} \frac{1-|z|^2}{1-|z|^{2\alpha}} \ , \quad C_\alpha^{\text{bos}} = \partial\bar{\partial} \left(\frac{\alpha}{|1-z|^2} \frac{1-|z|^2}{1-|z|^{2\alpha}} \right) \ . \tag{4.69}$$

After analytic continuation, C_α^{fer} and C_α^{bos} can no longer be interpreted as correlators of a pure heavy state of the CFT. One possibility is that they represent correlators in an ensemble of 1/2-BPS states with an average conformal dimension set by the parameter α (4.4). This identification is consistent with the lightcone OPE limit $\bar{z} \to 1$ of the correlators. As an example, C^{bos} in this limit is given by [72]

$$C_\alpha^{\text{bos}} \xrightarrow{\bar{z}\to 1} \frac{z^{\alpha-1}}{(1-\bar{z})^2} \left(\frac{\alpha}{1-z^\alpha} \right)^2 \ , \tag{4.70}$$

which by comparison with (4.7), is the HHLL Virasoro identity block with light operators of dimension $h_L = 1$ (multiplied by the prefactor from (4.1)).

We now study the Regge limit of this correlator and, to help the CFT interpretation, we also take the small μ expansion. Focusing on the first order in μ, the imaginary part of the Regge limit of C^{bos} obtained after performing the analytic continuation (4.17)

reads

$$\text{Im}\, C_{\alpha\,\circlearrowleft}^{\text{bos}}\Big|_{\mu^1} \approx \frac{2\pi}{\sigma^4\eta^2}\left(\frac{1+3\eta+\eta^2}{\sigma(1+\eta)^3}\right) = \frac{2\pi}{\sigma^4\eta^2}\left(\frac{1-2\eta+5\eta^2-9\eta^4+\dots}{\sigma}\right),\qquad (4.71)$$

where we used the parametrisation in (4.18) and kept only the leading term in σ. The overall factor of $\sigma^{-4}\eta^{-2}$ comes from the prefactor $(1-z)^{-2h_2}(1-\bar{z})^{-2\bar{h}_2} = \sigma^{-2(h_2+\bar{h}_2)}\eta^{-2\bar{h}_2}$ in (4.1) with $h_2 = \bar{h}_2 = 1$. By expanding the remaining part of the result in small η (as done in the second equality of (4.71)) one can gain some insight on the CFT meaning of the correlator C_α^{bos}. Comparing each term of the small η expansion with the behaviour of the blocks in the Regge limit (4.20), it is natural to interpret a contribution scaling like $\sigma^{-1}\eta^n$ for $n \geq 0$ as being due to the exchange of primaries of weight $(h, \bar{h}) = (2+n, n)$. In particular, taking the Regge limit of the Virasoro block of the identity produces only the first term in the small η expansion. As a consistency check of this interpretation, we can compare the first few coefficients of the η expansion in (4.71) with those obtained in the Euclidean OPE decomposition as $z \to 1$ (given by (4.11) before the analytic continuation needed for the Regge limit). From the first few terms in the Euclidean decomposition one can see the following pattern emerging: both the leading order couplings $c_{(0)}^2$ and the anomalous dimensions $\bar{\delta}$ are trivial, while for the couplings at order μ there are no contributions of spin higher than two. For instance, one can easily obtain the following data

$$\begin{aligned}
&c_{(1)}^2(0,0) = \frac{1}{30}, \quad c_{(1)}^2(1,1) = -\frac{1}{210}, \quad c_{(1)}^2(2,2) = \frac{1}{275}, \; \dots \\
&c_{(1)}^2(2,0) = -\frac{1}{700}, \quad c_{(1)}^2(3,1) = \frac{1}{4410}, \quad c_{(1)}^2(4,2) = -\frac{1}{38808}, \; \dots,
\end{aligned} \qquad (4.72)$$

and of course $c_{(1)}^2(m, m+2) = c_{(1)}^2(m+2, m)$. The couplings of the states with spin 2 agree with the expansion of the round parenthesis in (4.71) once the normalisation in (4.20) is taken into account. This can be checked by multiplying the results in (4.72) by the factor present in (4.20): for $m = 2, 3, 4 \dots$

$$\frac{\Gamma(2m+4)\,\Gamma(2m+3)}{\Gamma^4(m+2)}\,\frac{\mu}{2}\,c_{(1)}^2(m, m-2) \to \mu\,(-2, 5, -9, \dots). \qquad (4.73)$$

We now analyse the cross channel interpretation of (4.71) using (4.30), which is dominated by the double-trace operators of the form $\mathcal{O}_H \partial^m \bar{\partial}^{\bar{m}} \mathcal{O}_L$, with large values of m and $\bar{m}$. The anomalous dimensions $\Gamma_{m,\bar{m}}^{(1)}$ are encoded in the phase shift (4.65), computed from the analytically continued conical defect geometry. From (4.33) and the identifications (4.34), one finds that

$$\Gamma_{m,\bar{m}}^{(1)} \approx -\min(m, \bar{m}), \qquad (4.74)$$

in agreement with [52] (see also Eq. (6.4) of [102] which captures the large $h_H^{[0]}$, $\bar{h}_H^{[0]}$ limit of Eq. (4.32) of [197]). We can then resum the contributions of these double-trace operators with (4.30) by approximating the sums with integrals and using (4.28) with $h_2 = \bar{h}_2 = 1$

$$
\begin{aligned}
\operatorname{Im} C_{\alpha\circlearrowleft}^{\text{bos}}\Big|_{\mu^1} &= \pi \left[\int_0^\infty dm \int_0^m d\bar{m}\, m\, \bar{m}^2\, z^m \bar{z}^{\bar{m}} + \int_0^\infty d\bar{m} \int_0^{\bar{m}} dm\, m^2 \bar{m}\, z^m \bar{z}^{\bar{m}} \right] \\
&= \pi \Big(I_{1,2,0}(z,\bar{z}) + I_{1,2,0}(\bar{z},z) \Big) = 2\pi \left(\frac{1 + 3\eta + \eta^2}{\sigma^5 \eta^2 (1+\eta)^3} \right) ,
\end{aligned}
\tag{4.75}
$$

where in the second line we used the result (E.10) and reproduced the Regge behaviour (4.71), including all terms of order $\sigma^{-1}\eta^n$ for $n \geq 0$. Thus, while the Virasoro block of the identity alone does not provide a consistent solution to the bootstrap problem, the "correlator" C_α^{bos} does. The terms $\sigma^{-1}\eta^n$ with $n \geq 0$ originate from the double-trace primaries $\bar{\mathcal{O}}_L \partial^{2+n} \bar{\partial}^n \mathcal{O}_L$ exchanged in the direct channel ($z, \bar{z} \to 1$).

The same analysis can be performed for the analytically-continued correlator with light operator $\mathcal{O}^{\text{fer}}$ given in (4.69). After the analytic continuation to the Regge region and the small μ expansion, the order μ contribution is

$$
\operatorname{Im} C_{\alpha\circlearrowleft}^{\text{fer}}\Big|_{\mu^1} \approx \frac{\pi}{\sigma^3 \eta (1+\eta)} .
\tag{4.76}
$$

Of course, one can relate (4.76) and (4.71) directly by writing the Ward identity (4.68) in the variables (σ, η) adapted to the Regge limit

$$
\partial = -\partial_\sigma + \frac{\eta}{\sigma}\partial_\eta , \quad \bar{\partial} = -\frac{1}{\sigma}\partial_\eta \quad \Rightarrow \quad \left(\partial_\sigma - \frac{\eta}{\sigma}\partial_\eta \right) \left(\frac{1}{\sigma}\partial_\eta \right) \operatorname{Im} C_{\alpha\circlearrowleft}^{\text{fer}}\Big|_{\mu^1} = \operatorname{Im} C_{\alpha\circlearrowleft}^{\text{bos}}\Big|_{\mu^1} .
\tag{4.77}
$$

For large values of m and $\bar{m}$, the anomalous dimensions $\Gamma_{m,\bar{m}}^{(1)}$ of the double-trace operators contributing to the cross channel of C_α^{fer} are equal to the ones extracted from C_α^{bos}. This agrees with the idea that the two light operators $\mathcal{O}^{\text{fer}}$ and $\mathcal{O}^{\text{bos}}$ are indistinguishable in the Regge limit, both being represented by null geodesics in the 3D spacetime. The couplings $C_{(0)}^2$ change simply due to the dimension of the light external operator now being $h_2 = 1/2$: using this value in (4.27), one obtains from the cross channel decomposition an integral with the same structure as in (4.75) but involving $I_{0,1,0}$ instead of $I_{1,2,0}$, which reproduces (4.76).

Let us conclude this section with some comments. The analysis of [52] starts from the HHLL Virasoro vacuum block in the direct channel, then from this input the CFT data in the cross channel are derived. The contributions from double-trace operators $\mathcal{O}_L \partial^m \bar{\partial}^{\bar{m}} \mathcal{O}_L$ in the direct channel are added as a final step in order to satisfy crossing. Here we start from C_α^{fer} or C_α^{bos} which already contain the exchanges of the operators $\mathcal{O}_L \partial^m \bar{\partial}^{\bar{m}} \mathcal{O}_L$ and provide directly a solution to the crossing constraint as discussed in

this section. In spite of this difference in starting point, the results for the anomalous dimensions in the Regge limit – given in Eq. (4.74) – of the double-trace operators $\mathcal{O}_H \partial^m \bar{\partial}^{\bar{m}} \mathcal{O}_L$ agree, implying that we are finding the same solution to the crossing constraint as in [52]. We emphasise that although C_α^{bos} and C_α^{fer} satisfy the bootstrap relation, we know from the argument given at the beginning of this section that they cannot represent correlators in pure states for generic real values of α. This argument is based on the observation that the conical defect geometry (4.61) has an allowed conical singularity only for integer k. It would be interesting to understand if there are consistency requirements, detectable purely within the CFT, that are violated by C_α^{bos} and C_α^{fer} for generic values of α.

4.3.3   Higher orders in μ

Now we turn to the study of the 4-point functions (4.69) involving heavy operators dual to the geometry in (4.61), at higher orders in the parameter μ.

We begin by analysing the Regge limit of the analytically continued correlator (4.69) with the chiral primary light operator. We use the prescription (4.17): first analytically continuing z around the origin (where the branch cut of z^α is crossed) and then using the parametrisation in (4.18) to take $\sigma \to 0$ with η fixed. This gives

$$
\begin{aligned}
C_{\text{R}}^{\text{fer}} &= \frac{\alpha}{|1-z|^2} \frac{1-|z|^2}{1-|z|^{2\alpha}e^{-2\pi i \alpha}} \bigg|_{z,\bar{z}\to 1} \\
&\approx \frac{1}{\eta \sigma^2} + \frac{\pi i}{\eta(1+\eta)\sigma^3}\,\mu - \frac{\pi^2}{\eta(1+\eta)^2\sigma^4}\,\mu^2 - \frac{\pi^3 i}{\eta(1+\eta)^3\sigma^5}\,\mu^3 \,,
\end{aligned}
\tag{4.78}
$$

where we have kept only the leading term in the small σ expansion at each order in μ, which at order μ^k behaves as σ^{-k-2}.

As discussed in section 4.2, it should be possible to reconstruct the Regge limit of this CFT correlator from the bulk phase shift, at arbitrary orders in μ, using (4.51). Using the phase shift computed for the conical defect (4.65), expanding the exponential function of (4.51) in μ and taking the Regge limit gives the following expression[54]

$$
\begin{aligned}
C_{\text{AdS}}^{\text{fer}} &\approx I_{0,0} + \pi i \mu\, I_{0,1} + \left(\pi i\, I_{0,1} - \frac{\pi^2}{2} I_{0,2}\right)\mu^2 + \left(\frac{5\pi i}{8} I_{0,1} - \frac{3\pi^2}{4} I_{0,2} - \frac{\pi^3 i}{6} I_{0,3}\right)\mu^3 \\
&\approx \frac{1}{\eta\sigma^2} + \frac{\pi i}{\eta(1+\eta)\sigma^3}\,\mu - \frac{\pi^2}{\eta(1+\eta)^2\sigma^4}\,\mu^2 - \frac{\pi^3 i}{\eta(1+\eta)^3\sigma^5}\,\mu^3 \,,
\end{aligned}
\tag{4.79}
$$

---

[54]In order to reduce clutter in our expressions, we use the notation $C_{\text{AdS}}^{\text{fer}}$ to mean the correlator predicted by the bulk phase shift using (4.51), which is only valid in the Regge limit.

where in the first line we have used the integral

$$I_{a,b}(z,\bar{z}) \equiv \int_0^\infty \int_0^\infty dm d\bar{m} \, m^a \bar{m}^b \big(z^m \bar{z}^{\bar{m}} + z^{\bar{m}} \bar{z}^m\big) = \frac{\Gamma(a+b+2)}{(b+1)} \big[F(z,\bar{z}) + F(\bar{z},z) \big],$$

(4.80)

with $F(z,\bar{z}) \equiv \big(-\log z\big)^{-a-b-2} {}_2F_1\big(b+1, a+b+2; b+2; -\frac{\log \bar{z}}{\log z}\big)$ and in the second line of (4.79) we have gone to the Regge limit by using the parametrisation (4.18), taking the leading contribution in the small σ expansion at each order in μ separately.

Comparing the two methods, we see that the phase shift calculation (4.79) precisely reproduces the Regge limit of the exact correlator (4.78). The matching of the two results can be checked to higher orders in μ and we do not expect the agreement to cease at an arbitrary order in the expansion. Note that taking the $\sigma \to 0$ limit is crucial here since the key relation (4.51) is valid only in the Regge limit. However, in the case of this conical defect correlator with chiral primary light operator, the matching extends beyond the first order terms in small σ as one finds additional agreement between the subleading terms at each order in μ. Neglecting the disconnected part of the correlator,[55] the two methods begin to differ at subsubleading order in σ with the leading differences being

$$\Delta C_{\mathrm{R}}^{\mathrm{fer}} \approx -\frac{3(1+\eta)^2 + \pi i(1+\eta+\eta^2)}{12\eta(1+\eta)\sigma} \mu - \frac{\pi^2}{12(1+\eta)^2\sigma^2} \mu^2 - \frac{\pi^3 i}{12(1+\eta)^3\sigma^3} \mu^3, \quad (4.81)$$

where we have used the notation $\Delta C_{\mathrm{R}}^{\mathrm{fer}} = C_{\mathrm{R}}^{\mathrm{fer}} - C_{\mathrm{AdS}}^{\mathrm{fer}}$.

One can repeat the above procedure for the conical defect correlator with the light operator $\mathcal{O}^{\mathrm{bos}}$, given in (4.69). Analytically continuing this correlator to the Regge regime and taking the small σ limit yields

$$C_{\mathrm{R}}^{\mathrm{bos}} \approx \frac{1}{\eta^2 \sigma^4} + \frac{2\pi i(1+3\eta+\eta^2)}{\eta^2(1+\eta)^3\sigma^5} \mu - \frac{3\pi^2(1+4\eta+\eta^2)}{\eta^2(1+\eta)^4\sigma^6} \mu^2 - \frac{4\pi^3 i(1+5\eta+\eta^2)}{\eta^2(1+\eta)^5\sigma^7} \mu^3,$$

(4.82)

where at each order in μ we have again kept only the leading contribution as $\sigma \to 0$, which now scales as σ^{-k-4} at order μ^k. Obtaining the Regge limit from the bulk phase shift follows in the same way as in the case of the chiral primary light operator, however, since in this case $h_L = \bar{h}_L = 1$ the GFT OPE coefficients appearing in (4.51) need to be modified appropriately. This simply has the effect of replacing each integral in (4.79) by $\mathcal{I}_{a,b} \to \mathcal{I}_{a+1,b+1}$. After taking the relevant limit, we find that the leading order again precisely matches the CFT result (4.82). However, unlike in the case of $\mathcal{O}_L = \mathcal{O}^{\mathrm{fer}}$, the

---

[55]We note that the order μ^0 term is the disconnected part of the correlators and as such does not contain any information about the interaction between the operators. This term is exact in σ: for four-point functions with light operators with $h_L = \bar{h}_L$, it is given by $\eta^{-2h_L}\sigma^{-4h_L}$.

discrepancy between the two approaches already sets in at the subleading term in σ at each order in μ, giving

$$\Delta C_{\mathrm{R}}^{\mathrm{bos}} \approx \frac{2\pi i (1 + 3\eta + \eta^2)}{\eta^2 (1+\eta)^2 \sigma^4}\, \mu - \frac{3\pi^2 (1 + 4\eta + \eta^2)}{\eta^2 (1+\eta)^3 \sigma^5}\, \mu^2 - \frac{4\pi^3 i (1 + 5\eta + \eta^2)}{\eta^2 (1+\eta)^4 \sigma^6}\, \mu^3 \; . \quad (4.83)$$

Let us note here that one can check that at each order in μ, the small η limit of the expansions of the correlator expressions (4.78) and (4.82) agree with the results of the Virasoro vacuum block with $h_L = \bar{h}_L = \frac{1}{2}$ and $h_L = \bar{h}_L = 1$ respectively.

As shown in section 4.2, the bulk phase shift can also be used to extract CFT data in the Regge limit. Using the expansion of the bulk phase shift (4.65) in the relations (4.55) and (4.56) gives the data

$$\begin{aligned}
&\Gamma_{(1)} \approx -\min(m, \bar{m})\,, &&\Gamma_{(2)} \approx -\frac{\min(m, \bar{m})}{4}\,, &&\Gamma_{(3)} \approx -\frac{\min(m, \bar{m})}{8}\,, \\
&C_{(1)}^2 \approx -\frac{1}{2}\,, &&C_{(2)}^2 \approx -\frac{1}{8}\,, &&C_{(3)}^2 \approx -\frac{1}{16}\,,
\end{aligned} \quad (4.84)$$

where the OPE coefficients are calculated for the chiral primary light operator. The exact anomalous dimensions are known from considerations of the bulk energy levels of the light probe in the conical defect geometry [52], which agree with our extracted data.

One of the current aims is to investigate whether it is possible use the Regge limit to distinguish between pure and mixed states. Previous results [1, 52, 53] suggest that the analysis at first order in μ cannot separate mixed from pure states and what we find at higher orders in μ agrees with this. On the flip side, this indicates the robustness of the proposal (4.51) in the sense that the bulk phase shift can reliably reconstruct the Regge limit of boundary correlators, even if the heavy operators are not pure states.

4.4   Two-charge black hole microstate

In this section, we now consider the phase shift in the context of the D1-D5 system. Firstly, we focus on the simplest subset of heavy states; the 1/2-BPS heavy operators that are in correspondence (via spectral flow of the CFT) with the Ramond-Ramond ground states of the theory. Though the ensemble of these states does not give rise to a classical black hole with finite horizon, it still represents a non-trivial ensemble with a macroscopically large entropy. The simplest states in this ensemble are the duals of the conical defect geometries with integer k, given in (4.61). On the CFT side those states are highly symmetric, being formed from many identical copies of one elementary constituent (a twist operator of the orbifold CFT) and this is reflected on the gravity side by the fact that the geometries are locally isomorphic to $\mathrm{AdS}_3 \times S^3$. It is interesting to extend the analysis to more generic states that still allow for an analytic treatment.

For instance, the $(k, 0, 0)$ family of solutions has tended to be a useful playground; these were first constructed in [26] and later provided the seed for the construction of [27]. Some 4-point correlation functions – discussed in Section 2.3 – involving these heavy states are known exactly in terms of a double Fourier series [72] and we use this result to analyse the Regge limit beyond the leading order in the deformation parameter μ. Finally, we compare and contrast our results to the expressions obtained in the conical defect geometry.

4.4.1 Bulk description

The $(k, 0, 0)$ spacetimes cannot be factorised, even locally, into asymptotically AdS$_3$ and asymptotically S^3 parts and thus have to be described in 6D. The full geometry is given, for example, in Eq. (3.11) of [54]. It is useful, for our purposes at least, to rewrite the 6D Einstein metric in the "dimensionally reduced" form given in Eq. (2.54). While a reduction of this form can always be written down, in general the 3D reduced metric $g_{\mu\nu}$ will depend on both the x^μ and x^α coordinates at finite r. A simplification occurs for $k = 1$; in this case $g_{\mu\nu}$ turns out to be x^α independent and thus can be thought of the Einstein metric of a 3D spacetime that is asymptotically, but not locally, AdS$_3$. For $k = 1$ one can thus reduce the 6D problem to a simpler 3D one and in the following we will restrict to the $(1, 0, 0)$ state to take advantage of this simplification.

Before giving the full form of the $(1, 0, 0)$ geometry, we review the set of parameters on which it depends: these are the D1, D5 charges Q_1, Q_5; the radius of the CFT spatial circle R_y; and two parameters a and b constrained by the relation

$$a^2 + \frac{b^2}{2} = \frac{Q_1 Q_5}{R_y^2} \equiv a_0^2 \ . \tag{4.85}$$

Therefore, the parameter b can be varied whilst keeping the CFT quantities Q_1, Q_5 and R_y fixed. In this way we get a continuous family of heavy states, all of which are collectively described by the $(1, 0, 0)$ solution. Specifically, b is related to the number N_b of single-particle constituents of the heavy state (given in the NS sector by (2.66) with $n = 0$) that are not the spectral flow of the NSNS vacuum via

$$\frac{N_b}{N} = \frac{b^2}{2a_0^2} \ . \tag{4.86}$$

In particular, when $b = 0$ we have $N_b = 0$ and the state is just the spectral flow of the NSNS vacuum, whose dual geometry is global AdS$_3 \times S^3$.

The explicit form of the $(1, 0, 0)$ solution in the fibred form (2.54) is given by the

asymptotically S^3 metric

$$G_{\theta\theta} = \sqrt{\mathcal{P}}\,\Sigma\,, \ G_{\phi\phi} = \frac{Q_1 Q_5}{\sqrt{\mathcal{P}}\,\Sigma}\,\sin^2\theta\,, \ G_{\psi\psi} = \frac{Q_1 Q_5}{\sqrt{\mathcal{P}}\,\Sigma}\frac{r^2 + \frac{a^4}{a_0^2}}{r^2 + a^2}\cos^2\theta\,; \tag{4.87}$$

the gauge fields

$$A^\theta = 0\,, \ A^\phi = -\frac{a^2}{a_0^2}\frac{dt}{R_y}\,, \ A^\psi = -\frac{a^2}{a_0^2}\frac{r^2 + a^2}{r^2 + \frac{a^4}{a_0^2}}\frac{dy}{R_y}\,; \tag{4.88}$$

and the 3D Einstein metric

$$ds_3^2 = g_{\mu\nu}dx^\mu dx^\nu = \sqrt{Q_1 Q_5}\,\frac{r^2 + \frac{a^4}{a_0^2}}{(r^2 + a^2)^2}\,dr^2 - \frac{r^2 + \frac{a^4}{a_0^2}}{\sqrt{Q_1 Q_5}}\,dt^2 + \frac{r^2}{\sqrt{Q_1 Q_5}}\,dy^2\,, \tag{4.89}$$

where
$$\Sigma \equiv r^2 + a^2\cos^2\theta\,, \quad \mathcal{P} \equiv \frac{Q_1 Q_5}{\Sigma^2}\left[1 - \frac{a^2 b^2}{2\,a_0^2}\frac{\sin^2\theta}{r^2 + a^2}\right]. \tag{4.90}$$

The regime in which the CFT state is described by a classical geometry is the one for which both N and N_b are very large numbers. We do, however, have the freedom to choose the ratio N_b/N. In the simplest limit, this ratio is small and hence the 3D geometry (4.89) is a small deformation of global AdS$_3$ (this can be seen from (4.89): when N_b/N and thus b vanish, $a_0 = a$ and ds_3^2 becomes AdS$_3$). To take advantage of this simplification, we can use the small expansion parameter μ defined by (4.4) with $n = 0$ and (4.86):

$$\sqrt{1 - \mu} = 1 - \frac{N}{N_b} = 1 - \frac{b^2}{2a_0^2} = \frac{a^2}{a_0^2}\,, \tag{4.91}$$

and perform a perturbative expansion in μ at fixed Q_1, Q_5, R_y, and hence fixed a_0. Keeping only the corrections of order μ, the 3D Einstein metric becomes

$$ds_3^2 \approx \frac{\sqrt{Q_1 Q_5}}{r^2 + a_0^2(1 - \mu)}\left[1 - \frac{a_0^2}{a_0^2 + r^2}\mu\right]dr^2 - \frac{r^2 + a_0^2(1 - \mu)}{\sqrt{Q_1 Q_5}}\,dt^2 + \frac{r^2}{\sqrt{Q_1 Q_5}}\,dy^2\,. \tag{4.92}$$

The g_{tt} and g_{yy} components of this metric match exactly those of the conical defect metric (4.61) with $\frac{a}{k}$ replaced with $a_0(1 - \mu)^{1/2}$, whereas g_{rr} receives corrections in μ already at first order. To make certain that this difference is not simply a coordinate artefact, one can compute the Ricci and Kretschmann scalars for the metric (4.89) to first order in μ

$$\sqrt{Q_1 Q_5}\,\mathcal{R} \approx -6 - \frac{2a_0^2(2a_0^2 + r^2)}{(a_0^2 + r^2)^2}\mu\,, \quad Q_1 Q_5\,\mathcal{K} \approx 12 + \frac{8a_0^2(2a_0^2 + r^2)}{(a_0^2 + r^2)^2}\mu\,, \tag{4.93}$$

and note that they differ by order μ terms from the (normalised) conical defect values $\mathcal{R} = -6$ and $\mathcal{K} = 12$. Therefore, the conical defect geometry (4.61) and the microstate geometry (4.89) are physically distinct already at first order in μ and only the latter is dual to a state of the CFT for generic values of μ.

Exploiting the separability of the $(1, 0, 0)$ family of microstates, one can compute the bulk phase shift in the reduced 3D metric (4.89) by applying the general formula (2.105). This yields

$$\delta_b = 2a_0 R_y \,|p_t| \int_{r_0}^{\infty} dr \,(r^2 + a^2)^{-1} \sqrt{1 - \frac{\beta^2}{r^2}\left(r^2 + \frac{a^4}{a_0^2}\right)}$$
$$= \pi R_y \,|p_t| \,|\beta| \left(-1 + \sqrt{1 + \frac{a_0^2}{a^2}(\beta^{-2} - 1)}\right), \qquad (4.94)$$

where the radial turning point, obtained by setting to zero (2.101), is

$$r_0 = \frac{a^2}{a_0}(\beta^{-2} - 1)^{-\frac{1}{2}}. \qquad (4.95)$$

Subtracting the phase shift for pure AdS (corresponding to $b = 0$) gives

$$\delta = \delta_b - \delta\,|_{b=0} = \pi R_y \,|p_t| \left(\sqrt{\frac{2a_0^2 - b^2\beta^2}{2a_0^2 - b^2}} - 1\right), \qquad (4.96)$$

where we used (4.85) to express the result in terms of a_0 and b. Though the phase shift in (4.96) is exact in b, we will only attempt a CFT interpretation perturbatively in the small b (small μ) limit, describing small deviations from the AdS$_3$ vacuum. The first two terms in the perturbative expansion of the phase shift for small μ are

$$\delta \approx \pi R_y \,|p_t| \left[\frac{\mu}{4}(1 - \beta^2) + \frac{\mu^2}{32}(1 - \beta^2)(5 + \beta^2) + \cdots\right]. \qquad (4.97)$$

It is noted that the above expansion is in small μ but fixed impact parameter β and hence it also applies to the regime of β small, in which the geodesic explores the region deep inside the bulk. In the next section we will give a CFT derivation of firstly the order μ term in (4.97), and then also a higher order analysis. For future reference, the bulk phase shift (4.97) can be written in terms of CFT parameters via the relations (4.34) giving

$$\frac{\delta}{\pi} \approx \frac{m\bar{m}}{m + \bar{m}}\mu + \left(\frac{3m\bar{m}}{4(m + \bar{m})} - \frac{m^2\bar{m}^2}{2(m + \bar{m})^3}\right)\mu^2 + \left(\frac{5m\bar{m}}{8(m + \bar{m})} - \frac{3m^2\bar{m}^2}{4(m + \bar{m})^3} + \frac{m^3\bar{m}^3}{2(m + \bar{m})^5}\right)\mu^3.$$
$$(4.98)$$

We conclude the bulk analysis with a comment: the phase shift is expected to be dominated by the graviton exchange which, in the limit of large s and L (2.103), implies a behaviour of the form $\delta \sim s\,e^{-L}$ for a 3D bulk (see for example [96]). Taking

the large L (or equivalently the $\beta \to 1$) expansion of the phase shift (4.96) gives

$$\delta \approx \pi R_y \, s \, e^{-L} \frac{b^2}{2a_0^2} \left(1 - \frac{b^2}{2a_0^2}\right)^{-1} , \qquad (4.99)$$

consistent with the expected generic behaviour mentioned above. This regime describes geodesics with large impact parameter, probing only a shallow region inside the bulk, though we will later check explicitly that the full phase shift is determined by the graviton exchange.

4.4.2 CFT analysis at first order in μ

With the aim of reproducing the phase shift (4.97) from a purely CFT computation, we consider the four-point correlation function $C = \langle \mathcal{O}_H \mathcal{O}_L \bar{\mathcal{O}}_L \bar{\mathcal{O}}_H \rangle$ in the supergravity regime. Again both $\mathcal{O}_L = \mathcal{O}^{\mathrm{bos}}$ and $\mathcal{O}^{\mathrm{fer}}$ are considered for the light operator, while the heavy operator is schematically $\mathcal{O}_H = (\mathcal{O}^{\mathrm{fer}})^{N_b}$, dual to the $(1,0,0)$ geometry with reduced metric (4.89). This pure heavy state of the D1-D5 CFT is an RR sector ground state with conformal dimensions $h_H = \bar{h}_H = \frac{N}{4}$ and R-symmetry charges $j_H = \bar{j}_H = \frac{1}{2}(N - N_b)$, with the corresponding reduced conformal dimension thus being

$$h_H^{[0]} = \frac{N_b}{2} \left(1 - \frac{N_b}{2N}\right) . \qquad (4.100)$$

The additional free parameter N_b appearing in the expression of the charges is related to the free parameters of the bulk description through [55]

$$\frac{N_b}{N} = \frac{b^2}{2a_0^2} \qquad \Longrightarrow \qquad 1 - \frac{N_b}{N} = \frac{a^2}{a_0^2} , \qquad (4.101)$$

which, when inserted into (4.100) and using the definition (4.5), justifies the relation (4.86) on the gravity side.[56] We note that in order for the operator to be dual to a semiclassical background representing a fully backreacted geometry and not just a small perturbation on top of global AdS, we require the 'heavy' scaling

$$N_b \sim O(N) \quad \text{as} \quad N \to \infty , \qquad (4.102)$$

where the ratio N_b/N is fixed and left undetermined. Our perturbative analysis in μ is in essence an expansion in this free parameter.

---

[56]The heavy states dual to the geometry (4.89) are related by a spectral flow transformation to a state in the NS-NS sector, composed of $N - N_b$ copies of the vacuum state and a coherent superposition of N_b (with scaling (4.102)) copies of an anti-chiral primary of dimension $h_{\mathrm{NS}} = \bar{h}_{\mathrm{NS}} = \frac{1}{2}$. This heuristically justifies the relation (4.101), since from this CFT point of view N_b can be considered a measure of the deviation from the vacuum state, which is holographically dual to global $\mathrm{AdS}_3 \times S^3$.

In the case that the CPO's $\mathcal{O}^{\text{fer}}$ appearing in the light and the heavy operators belong to different 6D multiplets[57], the correlator C^{fer} – containing the light operator $\mathcal{O}^{\text{fer}}$ – was computed in the supergravity limit at first order in $\frac{b^2}{a_0^2}$ in [71] and its completion to all orders in $\frac{b^2}{a_0^2}$ was found in the form of a double sum in [72]. Here we need only the $O(\frac{b^2}{a_0^2})$ result, which in the NSNS sector reads

$$C^{\text{fer}} \approx \frac{1}{|1-z|^2} + \frac{b^2}{2a_0^2}\left[\frac{N}{2} - \frac{1}{|1-z|^2} + \frac{2}{\pi}|z|^2\hat{D}_{1122}\right], \qquad (4.103)$$

where

$$\frac{2}{\pi}|z|^2\hat{D}_{1122} = -\frac{4i\,|z|^2}{(z-\bar{z})^2}\left(\frac{z+\bar{z}}{z-\bar{z}}\,D_2(z,\bar{z}) + \frac{\log|1-z|^2}{2i} + \frac{z+\bar{z}-2|z|^2}{4i\,|1-z|^2}\log|z|^2\right), \qquad (4.104)$$

with D_2 being the Bloch-Wigner function given by

$$D_2(z,\bar{z}) = \frac{1}{2i}\left[\text{Li}_2(z) - \text{Li}_2(\bar{z}) + \log|z|\log\left(\frac{1-z}{1-\bar{z}}\right)\right]. \qquad (4.105)$$

Due to the same supersymmetric Ward identity (4.68) used in the previous section, one can easily obtain the correlator C^{bos} involving the bosonic light operator from $C^{\text{bos}} = \partial\bar{\partial}\left[C^{\text{fer}}\right]$. Performing the analytic continuation (4.17) and extracting the imaginary part of the correlator C^{bos} at first order in $\frac{b^2}{a_0^2} \approx \mu$ we obtain

$$\text{Im}\,C^{\text{bos}}_{\circlearrowleft}\Big|_{\mu^1} \approx \frac{2\pi}{\sigma^4\eta^2}\left(\frac{1 - 8\eta + 8\eta^3 - \eta^4 - 12\,\eta^2\log\eta}{\sigma(1-\eta)^5} + O(\sigma^0)\right), \qquad (4.106)$$

where the parametrisation (4.18) is used to go to the Regge limit. It is noted that the power of σ in (4.106) again contains the contribution of the $|1-z|^{-4h_2}$ prefactor in (4.1) as well as of the leading Regge term of the exchanged operator. Further taking the limit $\eta \to 0$ of (4.106) selects the exchanged operator of minimal $\bar{h}$, i.e. the stress tensor: its contribution is captured by the global block with $h = 2$, $\bar{h} = 0$ and is given by $\text{Im}\,C^{\text{bos}}_{\circlearrowleft} \approx \frac{2\pi}{\eta^2\sigma^5}\,\mu$.

As was done for the case of the conical defect, one can try to match the higher order terms in the η expansion of (4.106) with the spin-2 operator blocks corresponding to the exchange of spin-2 double-trace operators $\mathcal{O}_{LL} \equiv \bar{\mathcal{O}}_L\partial^m\bar{\partial}^{\bar{m}}\mathcal{O}_L$. A new feature of (4.106) is the appearance of a term proportional to $\log\eta$ related to the anomalous dimensions[58] of the non-BPS double-trace operators $\mathcal{O}_{LL}$. This can also be seen from

---

[57]When all operators in the correlator descend from the same 6D multiplet, the HHLL correlator contains extra contributions that were not computed in [71, 72]. The LLLL version of this correlator was derived in [73] and it will be analysed in Section 4.4.3.

[58]In this discussion we use the $\bar{\delta}$ quantities introduced just below (4.12) rather than the more common γ's. The $\bar{\delta}$'s include the couplings $c_{(0)}^2$ which bring a dependence on N_b – see the comments before (4.11).

the direct channel Euclidean decomposition where terms containing $\log |1 - z|^2$ appear, from which we can extract the CFT data of (4.11):

$$
\begin{aligned}
\bar{\delta}(0,0) &= \frac{1}{30} \,, \quad \bar{\delta}(1,1) = \frac{1}{42} \,, \quad \bar{\delta}(2,2) = \frac{6930}{1102500} \,, \\
\bar{\delta}(2,0) &= -\frac{3}{350} \,, \quad \bar{\delta}(3,1) = -\frac{2}{735} \,, \quad \bar{\delta}(4,2) = -\frac{462000}{896464800} \quad \cdots \,,
\end{aligned}
\tag{4.107}
$$

while all contributions from operators with odd spin and operators with spin higher than two vanish. These Euclidean results can again be checked by comparing with the expansion of the $\log \eta$ term in (4.106)

$$
\frac{-12\eta^2}{(1-\eta)^5} \approx -12\eta^2 - 60\eta^3 - 180\eta^4 \,,
\tag{4.108}
$$

which agrees with the spin-2 contributions in (4.107) after multiplication by the factor present in (4.20). As an example, for $m = 2, 3, 4 \ldots$ we have

$$
\frac{\Gamma(2m+4)\,\Gamma(2m+3)}{\Gamma^4(m+2)} \frac{\mu}{2} \bar{\delta}(m, m-2) \rightarrow \mu \left(-12, -60, -180, \ldots \right) \,.
\tag{4.109}
$$

A similar check can also be performed for the terms in (4.106) that are not proportional to $\log \eta$: as for the conical defect case in (4.72), these contributions should be compared with couplings $c^2_{(1)}(m, \bar{m})$ in (4.11). In Section 4.4.3 we will discuss in more detail a similar comparison for the LLLL correlator with all operators in the same 6D multiplet – the interest in this case is due to its Euclidean decomposition involving also operators of spin larger than two.

We now consider the order μ Regge crossing equations (4.30). On the gravity side, we can read off the anomalous dimensions $\Gamma^{(1)}_{m,\bar{m}}$ from the leading eikonal (4.97) by using (4.33) and the identifications (4.34)

$$
\delta^{(1)}_{\text{bulk}} = \frac{\pi}{4} R_y \, |p_t| \, (1 - \beta^2) = \pi \frac{m \, \bar{m}}{m + \bar{m}} \,,
\tag{4.110}
$$

obtaining

$$
\Gamma^{(1)}_{m,\bar{m}} \approx -\frac{m \, \bar{m}}{(m + \bar{m})} \,.
\tag{4.111}
$$

As discussed in [53, 97], it is also possible to use the leading small η behaviour of (4.106) along with the OPE coefficients (4.28) (with $h_2 = 1$) to fix the anomalous dimensions $\Gamma^{(1)}_{m,\bar{m}}$. As an example of how this approach works, we start from an ansatz for $\Gamma^{(1)}_{m,\bar{m}}$ in the limit of large m and $\bar{m}$ (that is inspired by, but more general than, the one in (4.111))

$$
\Gamma^{(1)}_{m,\bar{m}} \approx \frac{A \, m^a \bar{m}^a}{(m + \bar{m})^c} \,,
\tag{4.112}
$$

and show that the bootstrap constraints require $a = c = -A = 1$, as predicted by the gravity computation. As a first step we approximate the sums in (4.30) by integrals

$$\text{Im}\, C_{\circlearrowleft}^{\text{bos}}\Big|_{\mu^1} \approx -\pi A \int_0^\infty \int_0^\infty d\bar{m}\, dm\, \frac{m^{a+1}\bar{m}^{a+1}}{(m+\bar{m})^c}\, z^m \bar{z}^{\bar{m}} \equiv -\pi A\, I_{a,c}(z,\bar{z})\ . \tag{4.113}$$

This integral is discussed in Appendix E.1: by using (E.4) and then focusing on the leading contribution for small σ we obtain

$$\text{Im}\, C_{\circlearrowleft}^{\text{bos}}\Big|_{\mu^1} \approx -\pi A\, \frac{\Gamma^2(a+2)\,\Gamma(2a+4-c)}{\Gamma(2a+4)}\, \eta^{c-a-2}\sigma^{c-2a-4}\, {}_2F_1(a+2,c;2a+4;1-\eta)\ . \tag{4.114}$$

Demanding that the leading small η contribution reproduces that of (4.106) fixes the ansatz parameters to $a = c = -A = 1$. Substituting these values back into the full Regge result for the cross channel (4.114) reproduces exactly the direct channel expression (4.106) for any η. This implies that the anomalous dimensions of the $\mathcal{O}_{HL}$ operators in the Regge limit are given by the expression in (4.111). In the lightcone OPE limit $m \gg \bar{m} \gg 1$ these anomalous dimensions reduce to $\Gamma^{(1)}_{m,\bar{m}} \approx -\bar{m}$, the result obtained from the conical defect geometry of section 4.3 and in [52] from considering the above CFT analysis for the Virasoro vacuum block. This match is unsurprising since it was shown in [72] that the correlator (4.103) at order b^2 reduces to the Virasoro block of the identity in the lightcone OPE limit. Finally, the anomalous dimensions (4.111) can be confirmed by a Euclidean block decomposition of the correlator C^{bos} in the cross channel, from which one can extract the anomalous dimensions at first order in μ but for finite values of m and $\bar{m}$. With the approximation (4.29) for the blocks, the anomalous dimensions $\Gamma^{(1)}_{m,\bar{m}}$ are the coefficients of the $z^m \bar{z}^{\bar{m}} \log|z|^2$ terms in the $z, \bar{z} \to 0$ expansion of the correlator $C^{\text{bos}}|_{\mu^1}$ divided by $C^2_{(0)}(m,\bar{m})$. By looking at the first few terms, it is simple to infer that

$$\Gamma^{(1)}_{m,\bar{m}} = -\frac{(m+1)\,(\bar{m}+1)}{(m+\bar{m}+2)}\ , \tag{4.115}$$

which agrees with (4.111) in the large $(m,\bar{m})$ limit. We have checked that (4.115) correctly reproduces the anomalous dimensions up to order 10 in the Euclidean expansion.

Of course, a similar analysis can also be carried out in much the same fashion for the four-point function with light operator $\mathcal{O}_L = \mathcal{O}^{\text{fer}}$, given in (4.103). Performing the analytic continuation to the Regge limit gives the leading term in small σ as

$$\text{Im}\, C_{\circlearrowleft}^{\text{fer}}\Big|_{\mu} \approx \frac{\pi}{\eta\sigma^2}\left(\frac{1-\eta^2+2\eta\log\eta}{(1-\eta)^3\,\sigma} + O(\sigma^0)\right)\ , \tag{4.116}$$

where the factor of $\eta^{-1}\sigma^{-2}$ comes from the usual prefactor $(1-z)^{-2h_2}(1-\bar{z})^{-2\bar{h}_2}$ in the

correlator. We note that, as was the case for the conical defect correlators, the Regge limit results in (4.116) and (4.106) are directly related by (4.77). Another explicit check we can perform in this case is that the Regge limit is dominated by the highest spin field exchanged between the light and heavy operators. In the supergravity approximation being used, this is just the graviton. For the case of (4.116), we can use the results of [66] where the contribution of the Witten diagram describing graviton exchange was calculated for the correlator involving four light operators of dimension $(h_L, \bar{h}_L) = (1/2, 1/2)$. Since the small $\frac{b^2}{2a_0^2}$ limit of the HHLL correlator smoothly reproduces the light one [74], we can obtain the first order contribution from the graviton exchange simply by multiplying the result of [66] by $\frac{b^2}{2a_0^2}$ to get

$$C_{\text{grav}}^{\text{fer}} = \frac{b^2}{2a_0^2} \left[\frac{2}{\pi}(z + \bar{z})\hat{D}_{1122} - \frac{1}{|1 - z|^2} \right] \, , \qquad (4.117)$$

where $\hat{D}_{1122}$ was defined in (4.104). By performing the usual analytic continuation relevant for the Regge limit on (4.117) one obtains, as expected, the result (4.116) derived from the full amplitude.

The cross channel calculation follows that of the bosonic case closely: using the same Regge limit ansatz (4.112) and the order μ^0 OPE coefficients (4.28), now with $h_2 = \bar{h}_2 = 1/2$, (4.30) gives

$$\text{Im}\, C_{\circlearrowleft}^{\text{fer}}\Big|_{\mu} \approx -\pi A \int_0^\infty \int_0^\infty dm d\bar{m} \, \frac{m^a \bar{m}^a}{(m + \bar{m})^c} \, z^m \bar{z}^{\bar{m}} = -\pi I_{a-1,c}(z, \bar{z}) \, . \qquad (4.118)$$

Again by using (E.4) in the leading small σ approximation, the choice $a = c = -A = 1$ is necessary to reproduce (4.116) exactly. Therefore, the anomalous dimensions at order μ from the fermionic correlator appear to be the same as from the bosonic one – thus from (4.33), the first order bulk phase shifts will also match. This is an explicit check of the universality of the Regge limit since the bulk analysis is independent of the nature of the probe used.

We conclude this analysis by re-deriving the anomalous dimensions (4.112) in yet one further way. As mentioned after (4.15), these anomalous dimensions describe the binding energy of a non-BPS bound state between the original heavy operator and the probe. From the bulk point of view, these binding energies can be derived by studying the equation of motion of the supergravity state dual to the light probe when propagating in the background dual to the heavy operator. In [52], the case of a bulk scalar propagating in the asymptotically AdS$_{d+1}$ Schwarzschild geometry was studied up to second order. In the case discussed here, we can still focus on a minimally coupled scalar – dual to the operator $\mathcal{O}^{\text{bos}}$ – but in the geometry relevant for the heavy state discussed at the beginning of this section. The energies of the bound states in this geometry were derived exactly in b^2 in [72]; see[59] Eq. (3.43) of that reference, which in

---

[59] The parameters l and n appearing in that equation are the spin $l = m - \bar{m}$ and twist $n =$

our notation reads

$$\Gamma_{m,\bar{m}} = \omega_{m,\bar{m}} - \omega_{m,\bar{m}}\big|_{b\to 0} = \frac{a}{a_0}\sqrt{(m+\bar{m}+2)^2 + (m-\bar{m})^2\frac{b^2}{2a^2}} - (m+\bar{m}+2)$$
$$\approx -\frac{m\bar{m}}{m+\bar{m}}\mu - \frac{m\bar{m}(m^2 + 4m\bar{m} + \bar{m}^2)}{4(m+\bar{m})^3}\mu^2 - \frac{m\bar{m}(m^4 + 6m^3\bar{m} + 14m^2\bar{m}^2 + 6m\bar{m}^3 + \bar{m}^4)}{8(m+\bar{m})^5}\mu^3 ,$$

$$(4.119)$$

where in the second line we performed both the small μ and the large $m, \bar{m}$ expansions. At first order in μ this matches precisely (4.111). It is also noted that, by keeping m and $\bar{m}$ exact while expanding the first line of (4.119) in μ, the finite shifts of (4.115) are reproduced. By using the result above, it is straightforward also to check the relation between anomalous dimensions and the phase shift at second order from [53]. The second-order version of (4.33) reads

$$\Gamma_{m,\bar{m}}^{(2)} \approx -\frac{\delta^{(2)}}{\pi} + \frac{1}{2}\frac{\delta^{(1)}}{\pi}(\partial_m + \partial_{\bar{m}})\frac{\delta^{(1)}}{\pi} \quad \text{for} \quad m, \bar{m} \gg 1 . \qquad (4.120)$$

It is straightforward to check that this identity is satisfied if the $O(\mu^2)$ term of (4.119) is used for the left-hand side, while the right hand side is calculated using (4.97) and the identifications (4.34).

4.4.3 Light case

In the preceding section, correlators involving the heavy operator $\mathcal{O}_H = (\mathcal{O}^{\text{fer}})^{N_b}$ were considered in the scaling limit $N_b \sim N \to \infty$. This amounts to taking the number of non-trivial single-particle constituents in the heavy state to be of order N (to have a backreaction on the dual geometry) but small enough for $\frac{N_b}{N} = \frac{b^2}{2a_0^2}$ to be a meaningful expansion parameter. Alternatively, it is possible to consider these correlators in the scaling limit $N \to \infty$ with N_b fixed. This implies that the dimension of the 'heavy' operator, which scales as $h_H^{[0]} \sim N_b \sim N\frac{b^2}{a_0^2}$, is no longer of order N. In the bulk it is therefore no longer dual to a semi-classical geometry that differs from pure AdS$_3 \times$ S^3 and in the CFT analysis the approximation (4.29) is no longer valid. However, the $N_b \to 1$ limit of the HHLL correlator reproduces the LLLL correlator [74]. Then for instance, C^{bos} at order b^2 in the light scaling limit is equal to the following LLLL four-point function

$$C_L^{\text{bos}}\big|_{b^2} = \langle \mathcal{O}^{\text{fer}}(\infty)\mathcal{O}^{\text{bos}}(1)\bar{\mathcal{O}}^{\text{bos}}(z,\bar{z})\bar{\mathcal{O}}^{\text{fer}}(0)\rangle . \qquad (4.121)$$

However, even if the analytic form of the LLLL correlator is identical to that of the HHLL correlator at order μ, the CFT data obtained in the Regge limit are different. Here we briefly discuss the LLLL analysis following [97]: the key difference with the

---

$\min(m, \bar{m}) + 1$.

HHLL case is that we now need to use the approximation for the conformal blocks in terms of Bessel functions (4.31). As before, the Regge limit crossing equations (4.26) can be used to solve for the anomalous dimensions of the double-trace operators

$$\mathcal{O}_{LL'} \equiv \, : \mathcal{O}^{\text{fer}} \partial^m \bar{\partial}^{\bar{m}} \mathcal{O}^{\text{bos}} : \, , \tag{4.122}$$

exchanged in the cross channel. In the Regge limit, in which operators with large $m, \bar{m}$ dominate, the OPE coefficients (2.42) with external operator dimensions $2h_1 = h_2 = 1$ reduce to

$$C_{(0)}^2 = \frac{\Gamma^2(2+m)\,\Gamma^2(2+\bar{m})}{\Gamma(2+2m)\,\Gamma(2+2\bar{m})} \approx \frac{\pi}{4}\, 2^{-2(m+\bar{m})}(m\bar{m})^{\frac{3}{2}} \, . \tag{4.123}$$

Using (4.31) and (4.123) in the first order Regge crossing equations (4.26) (for the LLLL case, *i.e.* with $\gamma^{(1)}$ instead of $\Gamma^{(1)}$) gives

$$\text{Im}\, C_2^{\text{bos}}\Big|_{\circlearrowleft} \approx -16\pi\, |1-z|^{-1} \int_0^\infty dm \int_0^m d\bar{m}\,(m\bar{m})^2 \gamma_{m,\bar{m}}^{(1)} \Big[K_1\Big(2m\sqrt{1-z}\Big) K_1\Big(2\bar{m}\sqrt{1-\bar{z}}\Big)$$
$$+ K_1\Big(2\bar{m}\sqrt{1-z}\Big) K_1\Big(2m\sqrt{1-\bar{z}}\Big) \Big] \, , \tag{4.124}$$

where we took the large $m, \bar{m}$ limit so that the sums can be substituted by integrals and the Bessel functions approximated using

$$K_1\Big(2\hat{z} + 3\sqrt{1-z}\Big) \approx K_1\big(2\hat{z}\big) + O\big(\sqrt{1-z}\,\big) \, , \tag{4.125}$$

where $\hat{z} \approx m\sqrt{1-z}$ is kept fixed as $m \to \infty$. For future convenience, we split the integral into two separate regions and exploited the fact that the anomalous dimensions are invariant under the exchange $m \leftrightarrow \bar{m}$, since all external states are left/right symmetric. Using an ansatz for the leading large $m, \bar{m}$ anomalous dimensions of the form

$$\gamma_{m,\bar{m}}^{(1)} = A\,(\max(m,\bar{m}))^{a_1}(\min(m,\bar{m}))^{a_2} \, , \tag{4.126}$$

the two types of integrals in (4.124) are

$$I_1(a_1, a_2, b) \equiv \int_0^\infty dm \int_0^m d\bar{m}\, m^{2+a_1} \bar{m}^{2+a_2} K_b\Big(2\bar{m}\sqrt{1-z}\Big) K_b\Big(2m\sqrt{1-\bar{z}}\Big) \, ,$$
$$I_2(a_1, a_2, b) \equiv \int_0^\infty dm \int_0^m d\bar{m}\, m^{2+a_1} \bar{m}^{2+a_2} K_b\Big(2m\sqrt{1-z}\Big) K_b\Big(2\bar{m}\sqrt{1-\bar{z}}\Big) \, . \tag{4.127}$$

Solving these integrals as shown in appendix E.2, the leading order part of (4.124) in small σ is given by

$$
\left. \mathrm{Im}\, C_L^{\mathrm{bos}} \right|_{\circlearrowleft} \approx -A\,\pi\, \sigma^{-4-\frac{1}{2}(a_1+a_2)} \eta^{-1} \left[G_{3,3}^{2,3} \left(\eta \left| \begin{matrix} -\frac{1}{2}(a_1+a_2)-2, -\frac{1}{2}(a_1+a_2)-1, -\frac{a_2}{2} \\ 1, 0, -\frac{a_2}{2}-1 \end{matrix} \right. \right) \right.
$$
$$
\left. + \eta^{-\frac{a_1}{2}-1}\, G_{3,3}^{2,3} \left(\frac{1}{\eta} \left| \begin{matrix} -\frac{1}{2}(a_1+a_2)-2, -\frac{1}{2}(a_1+a_2)-1, -\frac{a_2}{2} \\ 1, 0, -\frac{a_2}{2}-1 \end{matrix} \right. \right) \right] ,
$$
$$
(4.128)
$$

where $G_{p,q}^{m,n}$ is the Meijer G-function (defined in Eq. (E.17)). Expanding in small η and matching the powers of σ and η of the leading order term to the contribution of the stress tensor fixes $A = -1$, $a_1 = 0$ and $a_2 = 2$. Inserting these values of the ansatz parameters in (4.128) gives precisely (4.106) and so the anomalous dimensions solving the crossing equations in the Regge limit are

$$
\gamma_{m,\bar{m}}^{(1)} \approx -(\min(m,\bar{m}))^2 \ . \tag{4.129}
$$

Therefore, the anomalous dimensions of the $\mathcal{O}_{LL'}$ operators (4.122) in the Regge limit take a qualitatively different form from their HL counterpart (4.111) and agree with the structure expected from the analysis of [73] (see Eq. (5.3) of that reference).

We conclude this section by discussing the Regge limit of another LLLL correlator

$$
\langle \mathcal{O}^{\mathrm{fer}}(\infty) \mathcal{O}^{\mathrm{fer}}(1) \bar{\mathcal{O}}^{\mathrm{fer}}(z,\bar{z}) \bar{\mathcal{O}}^{\mathrm{fer}}(0) \rangle \ , \tag{4.130}
$$

given in Eq. (3.10) of [73]. This example is different from those considered earlier because the CPO's $\mathcal{O}^{\mathrm{fer}}$ in the correlator descend from the same 6D multiplet and, hence, single-trace operators are exchanged also in the cross channel. This implies that in the direct channel, double-trace operators of arbitrarily high spin are exchanged, as can be checked explicitly from the $z, \bar{z} \to 1$ Euclidean OPE (4.11). For the correlator (4.130), the leading direct channel OPE coefficients $c_{(0)}^2$ are

$$
c_{(0)}^2(m,\bar{m}) = (-1)^{m+\bar{m}} C_{(0)}^2(m,\bar{m}) , \tag{4.131}
$$

with $C_{(0)}^2(m,\bar{m})$ given in (2.42). For the anomalous dimensions of the double-trace operators exchanged in the direct channel one finds

$$
\bar{\delta}(0,0) = -\frac{5}{6} \ , \quad \bar{\delta}(1,0) = -\frac{5}{6}\, c_{(0)}^2(1,0) \ , \quad \bar{\delta}(2,0) = -\frac{14}{15}\, c_{(0)}^2(2,0) \ ,
$$
$$
\bar{\delta}(m,0) = -c_{(0)}^2(m,0) \qquad \text{for} \ \ m > 2 \ , \tag{4.132}
$$

when focusing on the case $\bar{m} = 0$ and

$$\bar{\delta}(1,1) = -\frac{61}{30}\, c_{(0)}^2(1,1)\,, \ \ \bar{\delta}(2,1) = -\frac{41}{15}\, c_{(0)}^2(2,1)\,, \ \ \bar{\delta}(3,1) = -\frac{102}{35} c_{(0)}^2(3,1)\,,$$

$$\bar{\delta}(m,1) = -3\, c_{(0)}^2(m,1) \quad \text{for} \ \ m > 3\,, \tag{4.133}$$

for $\bar{m} = 1$. As expected, the data for operators of spin larger than two takes the form

$$\bar{\delta}(m,\bar{m}) = -(n^2 + n + 1)\, c_{(0)}^2(m,\bar{m}) \quad \text{with} \quad n = \min(m,\bar{m}) \ \text{and} \ |m - \bar{m}| > 2\,, \tag{4.134}$$

in agreement with [73]. Clearly in this case one cannot follow the previous approach, of performing the Regge limit on the contribution of each block separately, since this would lead to poles σ^{-a} with $a > 1$. Such contributions are absent in the Regge limit of the correlator, which is again given by (4.116). We instead first need to resum all contributions with $m > \bar{m} + 2$ and then perform the analytic continuation (4.17). The result of this resummation, made possible by exploiting (4.134), is an *analytic* term around $z = 0$ (which does not contribute to the Regge limit) and a contribution equal to the naive extension of (4.134) to $m = \bar{m} + 2$. Then as before, the contribution to the $\log \eta$ term of (4.116) comes entirely from the operators of spin 2 and one can use (4.11) to relate the Regge limit and anomalous dimensions for these operators, obtaining

$$\bar{\delta}(\bar{m}+2,\,\bar{m}) = \frac{(\bar{m}+1)(\bar{m}+2)\,\Gamma^4(\bar{m}+3)}{\Gamma(2\bar{m}+6)\,\Gamma(2\bar{m}+5)} - (\bar{m}^2 + \bar{m} + 1)\frac{\Gamma^2(\bar{m}+3)}{\Gamma(2\bar{m}+5)}\frac{\Gamma^2(\bar{m}+1)}{\Gamma(2\bar{m}+1)}\,. \tag{4.135}$$

The first term in this expression encodes the input from the Regge limit and comes from the small η expansion of the $\log \eta$ term in (4.116). For example, the results of (4.132) and (4.133) are reproduced for $\bar{m} = 0, 1$.

A similar argument can be used to also derive the couplings $c_{(1)}^2(\bar{m}+2,\bar{m})$. Again one can use the asymptotic result [69, 145, 185] $c_{(1)}^2(m,\bar{m}) = (\partial_m + \partial_{\bar{m}})\bar{\delta}(m,\bar{m})$, valid for $|m - \bar{m}| > 2$, and the terms without $\log \eta$ in (4.116) to find the following explicit expression for the couplings

$$c_{(1)}^2(\bar{m}+2,\bar{m}) = \frac{(2\bar{m}+3)}{\Gamma} - \partial_{\bar{m}}\Big((\bar{m}^2 + \bar{m} + 1)\, C_{(0)}^2(\bar{m}+2,\bar{m})\Big) - \frac{(\bar{m}+1)(\bar{m}+2)}{\Gamma^2}\, \partial_{\bar{m}}\Gamma\,, \tag{4.136}$$

where we defined

$$\Gamma \equiv \frac{\Gamma(2\bar{m}+6)\,\Gamma(2\bar{m}+5)}{\Gamma^4(\bar{m}+3)}\,. \tag{4.137}$$

The first term in (4.136) comes from the expansion of the explicit correlator in the Regge limit and the other terms are obtained by rearranging the right-hand side of (4.11), thanks to (4.135) and the relation for $C_{(1)}^2$ for operators of spin $|m - \bar{m}| > 2$. We note that (4.136) agrees with the couplings obtained for the first few values of $\bar{m}$ from the

direct channel Euclidean OPE

$$c_{(1)}^2(2,0) = \frac{19}{1350} \quad , \quad c_{(1)}^2(3,1) = \frac{4331}{49000} \quad , \quad c_{(1)}^2(4,2) = \frac{520433}{18522000} \; . \tag{4.138}$$

4.4.4 Signs of chaos from LLLL correlators

In this section we make a brief detour to consider the question of what information about chaos can be extracted from the holographic correlators considered above in the context of the Regge limit. As discussed in the introduction, a measure of chaos in a thermal quantum system is the behaviour of the commutator squared correlator

$$\big\langle - \big[V, W(t)\big]^2 \big\rangle_\beta = \big\langle \, V \, W(t) W(t) V + W(t) V \, V W(t) - 2 \, V \, W(t) V \, W(t) \, \big\rangle_\beta \; , \tag{4.139}$$

with $V = V(0)$ and $W(t)$ being Hermitian operators and $\langle \cdots \rangle_\beta$ a thermal expectation value in the state $|\beta\rangle$. The first term in the correlator (4.139) is an expectation value of the operator $W(t)^2$ in the perturbed thermal state $V|\beta\rangle$ and the second term can be thought of similarly but for the operator V^2. As will become clear below, these two contributions to (4.139) for late times are dominated by the disconnected contribution and tend to $\langle VV \rangle_\beta \langle W(t)W(t) \rangle_\beta$. The third term in (4.139) is an out-of-time-ordered correlator (OTOC) built from the overlap of the states $W(t)V|\beta\rangle$ and $V \, W(t)|\beta\rangle$ that become approximately orthogonal for late times if the system is chaotic. Due to the OTOC term having non-trivial late-time behaviour in caparison with the first two terms of (4.139), we can study this out-of-time-ordered correlator in place of the full commutator squared correlator to observe signs of chaos. We define the "normalised OTOC" for convenience

$$F \equiv \frac{\big\langle \, V \, W(t) V \, W(t) \, \big\rangle_\beta}{\langle VV \rangle_\beta \langle W(t)W(t) \rangle_\beta} \; , \tag{4.140}$$

in terms of which, for large enough t, the "normalised commutator squared correlator" is related to (4.140) via

$$\frac{\big\langle - \big[V, W(t)\big]^2 \big\rangle_\beta}{2\langle VV \rangle_\beta \langle W(t)W(t) \rangle_\beta} \approx 1 - F \; . \tag{4.141}$$

The generically expected behaviour of this OTOC is shown in Figure 4.2, where the period of exponential decay around the scrambling time $t_* \sim \log c$ corresponds to an associated period of exponential growth in the commutator squared correlator. This universal signal of chaos is called transient Lyaponov decay (growth) and was observed [115] in the HHLL Virasoro vacuum block (4.7) approximation to a 4-point correlator. In this section we check for the same transient Lyapunov behaviour in a full supergravity correlator. To understand the late-time behaviour of the various correlators in (4.139), it is important to see how they are derived from the appropriate
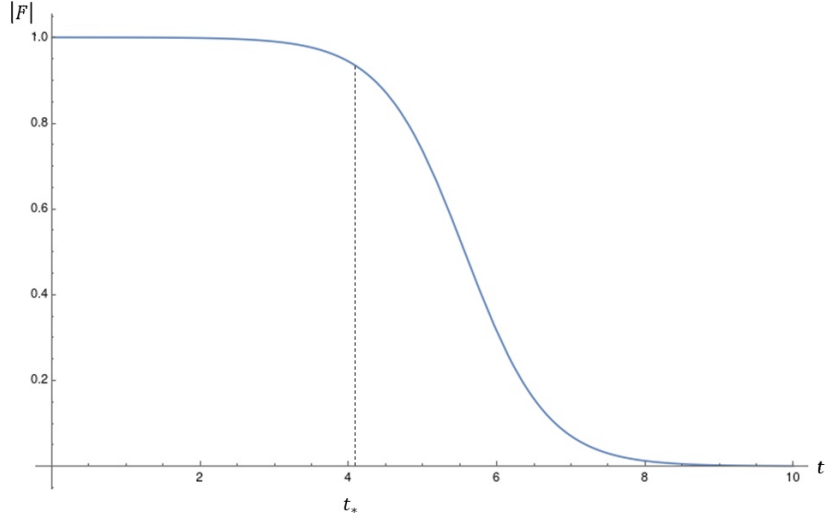
Figure 4.2: A plot showing the general behaviour of the absolute value of the normalised out-of-time-order correlators (F) of the type (4.140) with time t. The time scale at which chaos begins to affect the system is the scrambling time $t_* \sim \log c$, signalled by a period of exponential decay. This plot assumes that the operators V and W have vanishing two-point functions, otherwise there is a small period of growth at a thermal time scale $t \sim \beta$ before the decay shown ($\beta = 2\pi$ in the plot). A property of holographic systems appears to be that the hierarchy $t_* \gg \beta$ exists [118]. The behaviour shown here is just the "average" trend; in explicit examples there is a period of oscillatory behaviour that sets in after the scrambling time (see [203] for more discussion). This then dies off with time, eventually leading to the final decay seen in the figure.

Euclidean correlator. From a CFT$_2$ on the thermal cylinder $S^1_\tau \times \mathbb{R}_\xi$ we perform a double Wick rotation to the cylinder of a CFT$_2$ on a spatial circle, $\mathbb{R}_T \times S^1_y$. The radii of the S^1_τ and S^1_y are $\beta \sim R_y$. The "vacuum cylinder" can then be mapped to the plane with complex coordinates $(z, \bar{z})$, making the overall map from the thermal cylinder to this plane for each operator $\mathcal{O}_j$

$$z_j = e^{\frac{2\pi}{\beta}(\xi_j + \tau_j)} \quad , \quad \bar{z}_j = e^{\frac{2\pi}{\beta}(\xi_j - \tau_j)} \ . \tag{4.142}$$

Following the standard prescription, τ is analytically continued to be complex, with Lorentzian times being real and Euclidean times being purely imaginary. We note that, by design, the Jacobian factors from the transformation of operators (2.16) in the normalised correlator (4.140) cancel out. To obtain a particular operator ordering for a Lorentzian correlator, one first adds a small imaginary time $i\epsilon_j$ to each operator in order to regularise the problem (this avoids OPE singularities from operators being brought close to each other) and then the real part of τ can be increased. We also choose to separate the two pairs of operators in the spatial direction by an amount $\xi = x$. The resulting Lorentzian correlator is dictated by the hierarchy of the ϵ_j: the operators

112

will be ordered in the Lorentzian correlator from right to left with decreasing assigned values of imaginary time. During this process it is important to track the values of the conformal cross-ratios in the complex plane. In fact, the non-trivial behaviour of the OTOC at large times (as compared with the other correlators in (4.139)) is due to the crossing of a branch cut in the Euclidean correlator by the cross-ratio z.

Let us consider the LLLL correlator involving two different-flavour pairs of dimension $(h, \bar{h}) = (1/2, 1/2)$ CPOs and their conjugates, given in (B.19a) with $f_1 = f_2 = f$ and $f_3 = f_4 = g$ (with $f \neq g$). For ease of reference we give the correlator here

$$C_E(z, \bar{z}) \equiv \langle \bar{\mathcal{O}}_f(0) \mathcal{O}_f(\infty) \mathcal{O}_g(1) \bar{\mathcal{O}}_g(z, \bar{z}) \rangle$$
$$= \frac{1}{|1 - z|^2} \left[\left(1 - \frac{1}{N} \right) + \frac{2|z|^2 |1 - z|^2}{\pi N} \hat{D}_{1122} \right] , \tag{4.143}$$

with the standard D-function given in (4.104). To obtain the OTOC we use the operator insertion points (where the operators in (4.143) are labelled $1, \ldots, 4$ from left to right)

$$z_1 = e^{\frac{2\pi}{\beta}(\tau + i\epsilon_1)} \ , \ z_2 = e^{\frac{2\pi}{\beta}(\tau + i\epsilon_2)} \ , \ z_3 = e^{\frac{2\pi}{\beta}(x + i\epsilon_3)} \ , \ z_4 = e^{\frac{2\pi}{\beta}(x + i\epsilon_4)} \ , \tag{4.144}$$

and likewise for the anti-holomorphic positions. We will choose to have a real time $\tau = t > x$ in order to have the different pairs of operators in each other's lightcone. The hierarchy $\epsilon_4 > \epsilon_2 > \epsilon_3 > \epsilon_1$ will then give an OTOC of the form (4.140). For simplicity we take $\epsilon_1 = \epsilon$, $\epsilon_3 = 2\epsilon$, $\epsilon_2 = 3\epsilon$ and $\epsilon_4 = 4\epsilon$. With the operator insertions (4.144), the conformal cross-ratios (2.19) take the form

$$z(\tau, x) = 1 + \frac{\sin^2\left(\frac{2\pi}{\beta}\epsilon\right)}{\sinh^2\left(\frac{\pi}{\beta}(\tau - x - i\epsilon)\right)} \quad , \quad \bar{z}(\tau, x) = z(\tau, -x) \ . \tag{4.145}$$

Considering the cross-ratios (4.145) purely as functions of τ, increasing τ from 0 to $t > x$ yields Figure 4.3 in which we see that once τ is large enough, z will cross the negative real axis clockwise. For late times both cross-ratios should be taken to 1, however, due to the branch cut in (4.143), originating from $\log |z|^2$ terms of the D-function, this limit should be taken on the second sheet. In fact, this is exactly the prescription to go the the Regge limit of a vacuum correlator, given in (4.17) (this only occurs in the case of 2-dimensional CFTs [195, 204]). Repeating this process for the hierarchies of the ϵ_j relevant for the operator orderings of the first two terms on the right-hand side of (4.139) yields a path that tends simply to 1 without crossing any branch cuts for both z and $\bar{z}$ – hence their simpler behaviours in the chaos regime since this is the Euclidean OPE limit of the vacuum correlator, dominated by the identity
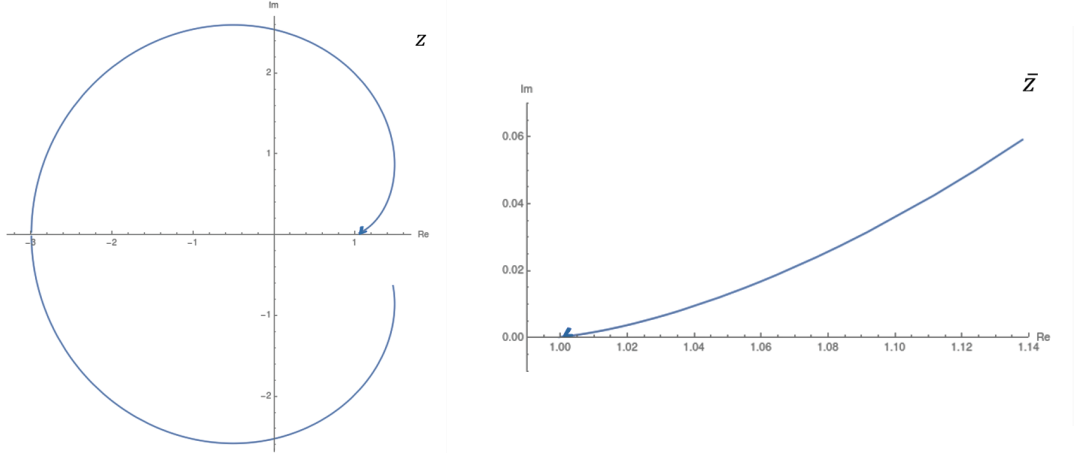
Figure 4.3: Plots showing the path in the complex plane that the cross-ratios z and $\bar{z}$ take when analytically continued to the "chaos regime". The path of z crosses branch cuts of the Euclidean correlator whereas the path of $\bar{z}$ is trivial. For $\epsilon \to 0$ in the plot of z, τ starts at 0, crosses the negative real axis at $\tau = x$ and for late times tends towards $z = 1$.

operator. Thus, we obtain the OTOC $F(t, x)$ from the Euclidean correlator (4.143) as

$$
\begin{aligned}
F(t, x) &= C_E\left(e^{-2\pi i}z, \bar{z}\right) \\
&= C_E(z, \bar{z}) + \frac{2\pi i |z|^2}{N(z - \bar{z})^2}\left(\frac{z + \bar{z}}{z - \bar{z}}\log\left(\frac{1 - z}{1 - \bar{z}}\right) + \frac{z + \bar{z} - 2|z|^2}{|1 - z|^2}\right),
\end{aligned}
\tag{4.146}
$$

where $z = z(t, x)$ and $\bar{z} = \bar{z}(t, x)$ take the form (4.145). Expanding (4.146) in the regime $t_* \gg t \gg x, \beta$ one obtains

$$
F(t, x) \approx \frac{\beta^2}{32\pi i \epsilon^2 N} e^{\frac{2\pi}{\beta}t} \sinh^{-3}\left(\frac{2\pi}{\beta}x\right)\left[\sinh\left(\frac{4\pi}{\beta}x\right) - \frac{4\pi x}{\beta}\right].
\tag{4.147}
$$

If also the hierarchy $x \gg \beta$ is chosen then (4.147) has the behaviour

$$
F(t, x) \approx \frac{\beta^2}{8\pi i N \epsilon^2} e^{\frac{2\pi}{\beta}(t-x)},
\tag{4.148}
$$

which has the same functional form as the Virasoro vacuum block approximation to the OTOC [115]. As was already mentioned, it is expected that for sufficiently late times (though still less than t_*) the absolute value of the OTOC should experience a period of exponential decay. In the case of the vacuum block approximation to the OTOC of [115], the full result is of the form

$$
F_{\text{vac}}(t, x) = \left(1 + \frac{fi}{c}e^{\frac{2\pi}{\beta}(t-x)}\right)^{-g},
\tag{4.149}
$$

for positive real coefficients f and g, with the absolute value having the correct expo-

nential decay of Figure 4.2. In the $1/c$ expansion of this one obtains

$$F_{\text{vac}}(t,x) \approx 1 - \frac{fg\,i}{c} e^{\frac{2\pi}{\beta}(t-x)} \ , \qquad (4.150)$$

which is exactly the exponential growth with imaginary coefficient seen in (4.148). Thus, we interpret (4.148) as the first term in an expansion of an analogous quantity to (4.149) which has the behaviour of Figure 4.2. In both cases, the Lyapunov exponent of this exponential is $\lambda_L = \frac{2\pi}{\beta}$ which is the saturation of the "bound on chaos" of [118] for holographic systems.

The exponential growth with t of (4.148) has a $\frac{1}{N}$ suppression due to the prefactor. The scrambling time is when this prefactor competes with the exponential growth, *i.e.*

$$t_* \approx \frac{2\pi}{\beta} \log \frac{8\pi N \epsilon^2}{\beta^2} \ . \qquad (4.151)$$

At this time our approximation breaks down since we can no longer trust simply the order $1/c$ supergravity correlator and new stringy modes should dominate [115, 117].

4.4.5   Higher orders in μ

This section builds upon the first order analysis of HHLL correlators in the Regge limit discussed in Section 4.4.2.

The 4-point HHLL correlation functions where the heavy operators are dual to the geometry (4.89) were studied in [71] to first order in the ratio $\frac{b^2}{2a_0^2}$ while in [72] an exact expression in terms of a double Fourier series was found. In the case of the light operator being the chiral primary $\mathcal{O}_L = \mathcal{O}^{\text{fer}}$ with $h_L = \bar{h}_L = \frac{1}{2}$, the correlator on the plane is given in (2.93). We can use (4.86) and expand this result as a series in μ

$$C^{\text{fer}}(z,\bar{z}) = \sum_{n=1}^{\infty} \mu^n \, C_n^{\text{fer}}(z,\bar{z}) \,, \qquad (4.152)$$

where now the expressions for $C_n^{\text{fer}}(z,\bar{z})$ can be written in a closed form in terms of Bloch-Wigner-Ramakrishnan polylogarithm functions [177]. The properties of these correlators were analysed in more detail in Chapter 3, with their derivation and explicit form given in Appendix B.1. Here we are interested purely in their behaviour in the Regge limit. Using the explicit forms of the correlators (B.17) one finds that in the

Regge limit the correlator with $\mathcal{O}_L = \mathcal{O}^{\text{fer}}$ is given to leading order in σ by

$$
\begin{aligned}
C_{\text{R}}^{\text{fer}} \approx &\; \frac{\pi i \left(1 - \eta^2 + 2\eta \log \eta\right)}{(1-\eta)^3 \eta \sigma^3} \, \mu - \frac{\pi^2 \left(1 + 9\eta - 9\eta^2 - \eta^3 + 6\eta(1+\eta)\log \eta\right)}{(1-\eta)^5 \eta \sigma^4} \, \mu^2 \\
&- \frac{\pi^3 i \left(1 + 28\eta - 28\eta^3 - \eta^4 + 12\eta(1 + 3\eta + \eta^2)\log \eta\right)}{(1-\eta)^7 \eta \sigma^5} \, \mu^3 \; .
\end{aligned}
\tag{4.153}
$$

On the other hand, using the bulk phase shift (4.96) in (4.51) and expanding in μ yields (in the Regge limit)

$$
\begin{aligned}
C_{\text{AdS}}^{\text{fer}} \approx &\; \Bigg[\pi i \, \tilde{I}_{1,1} \, \mu + \left(\frac{3\pi i}{4} \, \tilde{I}_{1,1} - \frac{2\pi i}{4} \, \tilde{I}_{2,3} - \frac{\pi^2}{2} \, \tilde{I}_{2,2} \right) \mu^2 \\
&+ \left(\frac{5\pi i}{8} \, \tilde{I}_{1,1} - \frac{3\pi i}{4} \, \tilde{I}_{2,3} + \frac{\pi i}{2} \, \tilde{I}_{3,5} - \frac{\pi^3 i}{6} \, \tilde{I}_{3,3} - \frac{3\pi^2}{4} \, \tilde{I}_{2,2} + \frac{\pi^2}{2} \, \tilde{I}_{3,4} \right) \mu^3 \Bigg] \Bigg|_{z,\bar{z} \to 1} ,
\end{aligned}
\tag{4.154}
$$

where we have made use of the integral (derived in Appendix E.1)

$$
\tilde{I}_{a,b} \equiv \int_0^\infty \int_0^\infty dm\, d\bar{m} \; z^m \bar{z}^{\bar{m}} \, \frac{(m\bar{m})^a}{(m+\bar{m})^b} = \frac{\Gamma^2(a+1)\,\Gamma(2a+2-b)}{\Gamma(2a+2)\,\left(-\log \bar{z}\right)^{a+1-b}} \, \widetilde{F}(z,\bar{z}) \, ,
\tag{4.155}
$$

with $\widetilde{F}(z,\bar{z}) = \left(-\log z\right)^{-a-1} {}_2F_1\left(a+1, b\,;\, 2a+2\,;\, 1 - \frac{\log \bar{z}}{\log z}\right)$. After using the parametrisation (4.18), the correlator predicted from the bulk phase shift agrees completely with (4.153) to leading order in σ, at each order in μ. In fact, the matching between these two results persists until order σ^{-1} for all terms in the μ expansion, with the leading difference being

$$
\Delta C_{\text{R}}^{\text{fer}} \approx -\frac{(3+i\pi)(1+\eta)}{12\eta\sigma} \, \mu - \frac{(3-i\pi)(1+\eta)}{48\eta\sigma} \, \mu^2 - \frac{(45 - 15\pi i + 2\pi^3 i)(1+\eta)}{1440\eta\sigma} \, \mu^3 \, ,
\tag{4.156}
$$

where we have again neglected the difference in the disconnected term. This breakdown of validity of the Regge limit approximation is very different in nature to that occurring in the conical defect correlator (4.81) case, especially as it seems that in this case the matching becomes increasingly better as we increase the order in μ. In principle the reconstruction of the correlator from the phase shift is expected to be valid only in the Regge limit, or in other words, at leading order in σ. It would be interesting to explain this enhancement of the reconstruction and see whether it might allow us to probe interactions beyond the Regge regime. However, we must note that this difference in matching between the $(1,0,0)$ fuzzball geometry and the conical defect cannot be seen if the light operator is $\mathcal{O}_L = \mathcal{O}^{\text{bos}}$ and the corresponding 4-point correlation function is related to (2.93) via the Ward identity $C^{\text{bos}} = \partial\bar{\partial}\left[C^{\text{fer}}\right]$. In that case – analysed in

more detail in Appendix B – the difference between the Regge limit of the correlator and the reconstruction from the bulk phase shift starts as expected at the subleading contribution in σ at each order in μ, just as in the example of the conical defect (4.83).

Finally, we perform a check on the validity of the relations (4.57a). In [72] the exact energy levels of the composite object formed of the light probe and the heavy operator dual to the geometry (4.89) were calculated. Since the anomalous dimensions can be thought of as the bulk binding energies of such bound states, we can compare with (4.119) at each order in μ to those obtained from the phase shift (4.98) and (4.57a) and find perfect agreement to arbitrary orders in μ. For the case of $\mathcal{O}_L = \mathcal{O}^{\text{fer}}$ we can then use the simple relation (4.59) to get the following OPE coefficients

$$C_{(1)}^2 \approx -\frac{m^2 + \bar{m}^2}{2(m + \bar{m})^2} \,, \qquad C_{(2)}^2 \approx -\frac{m^4 + 6m^3\bar{m} - 2m^2\bar{m}^2 + 6m\bar{m}^3 + \bar{m}^4}{8(m + \bar{m})^4} \,,$$
$$C_{(3)}^2 \approx -\frac{m^6 + 8m^5\bar{m} + 23m^4\bar{m}^2 - 8m^3\bar{m}^3 + 23m^2\bar{m}^4 + 8m\bar{m}^5 + \bar{m}^6}{16(m + \bar{m})^6} \,. \qquad (4.157)$$

4.5 A class of three-charge microstate geometries

4.5.1 Bulk description

As an extension to the case of the $(1,0,0)$ geometry considered in section 4.4, it is possible to add momentum charge yielding a class of 3-charge microstate geometries – these are the $(1,0,n)$ family of superstrata discussed in Sections 2.2 and 2.2.2. This can be done so as to preserve the separability of the 6D spacetimes into asymptotically S^3 and AdS$_3$ 3-manifolds – where the Einstein metric of the latter part is independent of the S^3 coordinates. From the CFT perspective, these are 1/4-BPS states obtained by acting n times on the single-particle constituents of the $(1,0,0)$ microstates with the Virasoro generator L_{-1}. Each of the new N_b single-particle constituents carries n units of momentum along the S^1 of the CFT and the quantised momentum charge of the full microstate is

$$n_{\text{P}} = n\, N_b \,. \qquad (4.158)$$

On the gravity side, the number of momentum-carrying strands N_b is controlled by the parameter b according to the same relation (4.86), though now with a more general dependence on the expansion parameter μ (derived in Section 2.2.3)

$$\frac{N_b}{N} = \frac{b^2}{2a_0^2} = 2n + 1 - \sqrt{(2n + 1)^2 - \mu} \,, \qquad (4.159)$$

where a_0 is defined in Eq. (4.85).

The full 10D geometry describing this $(1,0,n)$ family of microstates can be found for example in [27,55]. For the purposes of calculating the eikonal, it is again useful to write

the 6D part of this solution (given by the ansatz form in (2.47)) in the dimensionally-reduced form (2.54), with S^3 metric $G_{\alpha\beta}$, gauge fields A^α and 3D Einstein metric ds_3^2 here given by

$$G_{\theta\theta} = \Sigma\sqrt{\mathcal{P}}\,,\ G_{\phi\phi} = \frac{Q_1 Q_5}{\Sigma\sqrt{\mathcal{P}}}\sin^2\theta\,,\ G_{\psi\psi} = \frac{Q_1 Q_5}{\Sigma\sqrt{\mathcal{P}}}\left[1 - \frac{a^2 b^2}{2a_0^2(r^2+a^2)}\left(\frac{r^2}{r^2+a^2}\right)^n\right]\cos^2\theta\,, \tag{4.160}$$

$$A^\theta = 0\,,\ A^\phi = -\frac{a^2}{a_0^2}\frac{dt}{R_y}\,,\ A^\psi = -\frac{\frac{a^2}{a_0^2}F_n\frac{dt}{R_y} + \left(1 - \frac{b^2}{2a_0^2}\left(\frac{r^2}{r^2+a^2}\right)^n\right)\frac{dy}{R_y}}{1 - \frac{a^2 b^2}{2a_0^2(r^2+a^2)}\left(\frac{r^2}{r^2+a^2}\right)^n}\,, \tag{4.161}$$

$$\frac{ds_3^2}{\sqrt{Q_1 Q_5}} = \frac{r^2 + \frac{a^4}{a_0^2}(1 + F_n)}{(r^2+a^2)^2}\,dr^2 - \frac{r^2 + \frac{a^4}{a_0^2}}{Q_1 Q_5}\,dt^2 + \frac{r^2}{Q_1 Q_5}\,dy^2 + \frac{r^2 F_n}{Q_1 Q_5}\,(dt+dy)^2\,, \tag{4.162}$$

where Σ is as defined in (4.90) and

$$\mathcal{P} = \frac{Q_1 Q_5}{\Sigma^2}\left[1 - \frac{a^2 b^2}{2\,a_0^2}\frac{\sin^2\theta}{r^2+a^2}\left(\frac{r^2}{r^2+a^2}\right)^n\right]\,,\ F_n(r) \equiv \frac{b^2}{2a^2}\left[1 - \left(\frac{r^2}{r^2+a^2}\right)^n\right]\,. \tag{4.163}$$

The geometry (4.162) is in general difficult to work with and so for simplicity we focus on the particular case of the $(1,0,1)$ 3-charge microstate geometry. The analysis of the bulk eikonal now follows that outlined in Section 2.4 by considering null geodesics in the 3D geometry (4.162) (with $n = 1$) that begin and end on the boundary. For our current purposes, it is sufficient to evaluate the phase shift integral perturbatively in μ. Starting from (2.105), using the change of variables $x = \frac{r}{r_0}$ (removing all b dependence from the integral limits) and expanding in μ using (4.159) gives

$$\delta = \int_0^1 dx\,\delta_x = \sum_{j=0}^\infty \int_0^1 dx\,\delta_x^{(j)}\mu^j\,, \tag{4.164}$$

with the zeroth and first order integrands

$$\delta_x^{(0)} = 2|p_t|R_y\frac{|\beta|(1-\beta^2)\sqrt{1-x^2}}{x(1-\beta^2)+\beta^2}\,, \tag{4.165}$$

$$\delta_x^{(1)} = |p_t|R_y\frac{|\beta|^3(1-\beta^2)(3-2\beta+\beta^2)\sqrt{1-x^2}}{6\big(x(1-\beta^2)+\beta^2\big)^2}\,. \tag{4.166}$$

In deriving these integrands the expansion of the turning point in μ is used

$$r_0 \approx \frac{a_0|\beta|}{\sqrt{1-\beta^2}} - \frac{a_0|\beta|(3-2\beta+\beta^2)}{12\sqrt{1-\beta^2}}\mu\,. \tag{4.167}$$

The zeroth order phase shift obtained from the integral of (4.165) is just that of global AdS$_3$, $\delta^{(0)} = \pi R_y |p_t|(1 - |\beta|)$, whereas at first order one gets from (4.166)

$$\delta^{(1)} = \int_0^1 dx \, \delta_x^{(1)} = \frac{\pi}{24} R_y \, |p_t|(1 - \beta^2)(3 - 2\beta + \beta^2) \ . \tag{4.168}$$

The generalisation of this result to all orders in μ is given in Section 4.5.3.

4.5.2   CFT analysis at first order in μ

We would again like to compare this result for the phase shift with information contained in appropriate HHLL 4-point correlators of the dual CFT. In the heavy regime, the 1/4-BPS operators dual to the family of geometries in (4.162) have reduced dimensions (4.3), which scale with the central charge. These heavy operators will, for generic values of N_b and $n \neq 0$, be mixtures of quasi-primary and descendant parts; only in the light limit $N_b \to 1$ will they be pure descendants. In the latter case, and for $n = 1$, a Ward identity relates the correlator of primary operators with that containing two primaries and two descendants [80]. Exploiting the equivalence of the LLLL and HHLL correlators at order μ, the same Ward identity can be used to derive the $O(\mu)$ correlator in the $(1, 0, 1)$ heavy state from that in the $(1, 0, 0)$ heavy state:

$$G_{1,0,1}(z, \bar{z})\Big|_{\mu^1} = \Big[(1 - z)^2 \partial(z \, \partial) + 1\Big] G_{1,0,0}(z, \bar{z})\Big|_{\mu^1} \ . \tag{4.169}$$

The relation between the respective full correlators can then be obtained from (4.1) by including the appropriate prefactors. In this section we consider only HHLL correlators containing the light operator $\mathcal{O}^{\mathrm{bos}}$ with dimension $(h_2, \bar{h}_2) = (1, 1)$. The order μ^0 piece of this correlator is dependent solely on the dimension of the light operator used and so is equal to the $(1, 0, 0)$ case and given by $|1 - z|^{-4}$. At first order in μ, performing the analytic continuation to the Regge region and extracting the leading imaginary piece gives

$$\mathrm{Im} \, C_{1,0,1}^{\mathrm{bos}}\big|_{\circlearrowleft, \, \mu} \approx 2\pi \frac{3 - 42\eta - 199\eta^2 + 160\eta^3 + 69\eta^4 + 10\eta^5 - \eta^6 - 12\eta^2(13 + 14\eta + 3\eta^2) \log \eta}{3(1 - \eta)^7 \eta^2 \sigma^5} \ ,$$
$$\tag{4.170}$$

where the relation (4.159) with $n = 1$ and the parametrisation (4.18) have been used. One can also obtain (4.170) from (4.106) by rewriting the differential operator in (4.169) in terms of (σ, η) as done in (4.77).

We now move to analysing the cross channel interpretation of (4.170). From (4.30) the contributions from double-trace operators of the schematic form $\mathcal{O}_H \partial^m \bar{\partial}^{\bar{m}} \mathcal{O}_L$ can be resummed; again this is dominated by the operators with large m and $\bar{m}$. The anomalous dimensions $\Gamma_{m,\bar{m}}^{(1)}$ in the Regge limit can be extracted from the bulk phase

shift (4.168), once again using the relations (4.33) and (4.34), giving

$$\Gamma_{m,\bar{m}}^{(1)} \approx -\frac{\delta^{(1)}}{\pi} = -m\bar{m}\frac{m^2 + 2m\bar{m} + 3\bar{m}^2}{3(m+\bar{m})^3} \; . \tag{4.171}$$

We note that these anomalous dimensions are not symmetric under the exchange of m and $\bar{m}$, unlike those in the conical defect and $(1,0,0)$ cases. This is to be expected for the 1/4-BPS 3-charge microstates, in this case the $(1,0,n)$ family, as a consequence of having acted with only holomorphic Virasoro modes on the $(1,0,0)$ state – see Eq. (2.66) in the NS sector. Resumming these double-trace contributions, with the approximation to the OPE coefficients in (4.28), gives

$$\begin{aligned}
\mathrm{Im}\, C_{\circlearrowright}^{(1,0,1)}\Big|_{\mu} &\approx -\pi \int_0^\infty dm \int_0^\infty d\bar{m}\, C_{(0)}^2(m,\bar{m})\, \Gamma_{m,\bar{m}}^{(1)}\, z^m \bar{z}^{\bar{m}} \\
&= -\pi \int_0^\infty dm \int_0^m d\bar{m}\, C_{(0)}^2(m,\bar{m}) \left(\Gamma_{m,\bar{m}}^{(1)} z^m \bar{z}^{\bar{m}} + \Gamma_{\bar{m},m}^{(1)} z^{\bar{m}} \bar{z}^m\right) \\
&= \frac{\pi}{3}\left(I_{2,2,1}(z,\bar{z}) + I_{2,2,1}(\bar{z},z) + 2I_{2,4,3}(z,\bar{z}) + 2I_{4,2,3}(\bar{z},z)\right) \, , \tag{4.172}
\end{aligned}$$

which gives precisely (4.170) once expanded in σ. The final line of the above is written in terms of the integral defined in (E.5), whose solution is given in (E.10). This matching of (4.172) and (4.170) demonstrates that the anomalous dimensions (4.171) obtained from gravity are consistent with the crossing relations.

It is, however, curious that such a matching does occur in the 3-charge case using the above method. As mentioned above, in the heavy scaling regime the $(1,0,1)$ operator will not purely be a quasi-primary (N_b is small compared with N but still macroscopic) and so it appears that both the relation (4.33) and the decomposition of the correlator used in section 4.2 should not hold. Despite this, it seems that in the heavy limit at least, these differences in the key steps of the CFT analysis are subleading in $1/h_H$.

4.5.3 Towards the black hole regime

In order for the $(1,0,n)$ set of supergravity solutions described in Section 2.2 to be microstates of a (non-rotating) D1-D5-P black hole with a finite sized horizon, the set of parameters $\{b, a, n\}$ should satisfy the inequality [27]

$$1 \geq \frac{b^2}{2a_0^2} > 2n + 1 - 2\sqrt{n(n+1)} \, , \tag{4.173}$$

where as usual we have $a_0^2 = a^2 + \frac{b^2}{2}$. We note that in order to satisfy this inequality it is necessary to have $n \geq 1$: the 2-charge D1-D5 black hole has a horizon of vanishing area at the origin. Comparing this with the form of the parameter μ in (4.159) shows that in order to consider microstates above the black hole bound, we must go beyond

the perturbative approach in μ. Though we leave a systematic analysis of the black hole regime physics of these microstates to future work, some initial hints from the bulk phase shift are presented below.

Considering the $(1, 0, n)$ microstate geometries for generic n, using the 3-dimensional reduced metric (4.162), the integral in the phase shift (2.105) is likely not analytically tractable. However, we may try to attack the problem from various, simpler, angles. The bulk phase shift can be put into the form

$$\delta = -2R_y\, p_t\, \sqrt{1 - \beta^2} \int_{\rho_0}^{\infty} \frac{d\rho}{\rho} \sqrt{\rho^2 - \rho_0^2} \, \sqrt{\frac{\rho^2 + \bar{\rho}_0^2}{(\rho^2 + 1)^3}} \, , \tag{4.174}$$

where

$$\rho_0^2 \equiv \frac{r_0^2}{a^2} \, , \quad \bar{\rho}_0^2 \equiv -\frac{\bar{r}_0^2}{a^2} \, , \tag{4.175}$$

and r_0^2 and $\bar{r}_0^2$ are respectively the positive and negative roots of the turning point equation $\dot{r}^2 = 0$ which here reads

$$r_0^2 \beta^{-2} - \left(r_0^2 + \frac{a^4}{a_0^2}\right) + r_0^2 \frac{a_0^2 - a^2}{a^2}\left[1 - \left(\frac{r_0^2}{r_0^2 + a^2}\right)^n\right](\beta^{-1} - 1)^2 = 0 \, . \tag{4.176}$$

Note that $\bar{\rho}_0^2 \geq 1$ and $\bar{\rho}_0^2 = 1$ for $b = 0$ or $n = 0$. The integral in (4.174) could be computed with the residue method where it not for the branch cuts between $[i, i\bar{\rho}_0]$ and $[-i\bar{\rho}_0, -i]$.

Phase shift at $O(b^2)$ for generic n

One, possibly naïve, approach one could take is to first consider the phase shift at linear order in $\frac{b^2}{2a_0^2}$ with n general to see if anything can be gleaned from it. In the limit of small b one has for the turning point

$$r_0^2 \approx a_0^2\,(\beta^{-2} - 1)^{-1}\left[1 - \frac{b^2}{2a_0^2}(1 + \beta)^{-1}\left(3 + \beta - (1 - \beta)\beta^{2n}\right)\right]. \tag{4.177}$$

and the phase shift

$$\delta = \delta^{(0)} + \frac{b^2}{a_0^2}\,\delta^{(1)} + O(b^4)\,. \tag{4.178}$$

The zeroth order result is, as expected, the pure AdS result

$$\delta^{(0)} = p_t R_y \pi (1 - \beta) \, , \tag{4.179}$$

and at first order the result is

$$\delta^{(1)} = \frac{p_t R_y\, a_0}{4}(1-\beta^2)^{-1/2} \int_{s_0}^{\infty} \frac{ds}{\sqrt{s-s_0}} \frac{a_0^2(3-2\beta+\beta^2)+(1-\beta)^2\left(s-\frac{s^n}{(s+a_0^2)^{n-1}}\right)}{(s+a_0^2)^2}$$

$$= \frac{p_t R_y \pi}{8}\left[(1-\beta^2)(3-2\beta+\beta^2)+(1-\beta)^2\left(1+\beta^2-\frac{(2n-1)!!}{2^{n-1}\,n!}\,_2F_1\left(-n,\tfrac{1}{2};\tfrac{1}{2}-n;\beta^2\right)\right)\right],$$

(4.180)

where $s_0 \equiv a_0^2(\beta^{-2}-1)^{-1}$. Note that the hypergeometric function $_2F_1(-n,\tfrac{1}{2};\tfrac{1}{2}-n;\beta^2)$ is simply a polynomial in β^2 of degree n

$$_2F_1\left(-n,\tfrac{1}{2};\tfrac{1}{2}-n;\beta^2\right) = \sum_{m=0}^{n} c_n(m)\beta^{2m} \quad \text{with} \quad c_n(m) = \frac{(-1)^m}{\sqrt{\pi}}\binom{n}{m}\frac{\Gamma(m+\tfrac{1}{2})\Gamma(\tfrac{1}{2}-n)}{\Gamma(m-n+\tfrac{1}{2})}.$$

(4.181)

Considering now the limit

$$b^2 \to 0 \,, \quad n \to \infty \quad \text{with} \quad \frac{n\,b^2}{a_0^2} > \frac{1}{2} \,,$$

(4.182)

in such a way that the state is within the black hole limit (4.173). From (4.177), one has the turning point

$$r_0^2 \approx \frac{a_0^2}{\beta^{-2}-1}\left(1 - \frac{b^2}{2a_0^2}\frac{3+\beta}{1+\beta}\right) \,,$$

(4.183)

since $(1-\beta)\beta^{2n} \to 0$ for $\beta \le 1$ and $n \to \infty$. Thus r_0 remains *finite* in this limit, unlike in the case of the BTZ black hole (for which $r_0 \to 0$). The first order phase shift (4.180) is also finite in the limit . Using Stirling's approximation, one has

$$\frac{(2n-1)!!}{2^{n-1}\,n!} = \frac{(2n)!}{2^{2n-1}(n!)^2} \approx \frac{2}{\sqrt{\pi}\sqrt{n}} \,,$$

(4.184)

and using the fact that $c_n(m) \le 1$ (with $c_n(0) = c_n(n) = 1$) and that the hypergeometric $_2F_1(-n,\tfrac{1}{2};\tfrac{1}{2}-n;\beta^2)$ remains finite in the large n limit for any $\beta < 1$, from (4.180) one finds

$$\delta^{(1)} \approx \frac{p_t R_y \pi}{2}\,(1-\beta) \,.$$

(4.185)

If instead $\beta = 1$ then the hypergeometric function in (4.180) becomes

$$_2F_1\left(-n,\tfrac{1}{2};\tfrac{1}{2}-n;1\right) = \frac{\sqrt{\pi}\,n!}{\Gamma(n+\tfrac{1}{2})} \approx \sqrt{\pi}\sqrt{n} \,,$$

(4.186)

and thus $\delta^{(1)}\big|_{\beta=1} \approx 0$. In conclusion, from this first approach to considering the black hole regime of the $(1,0,n)$ microstates, the phase shift seems to remain finite in the limit (4.5.3), unlike for the BTZ black hole (for which $\delta \to \infty$, see Figure 4.4).

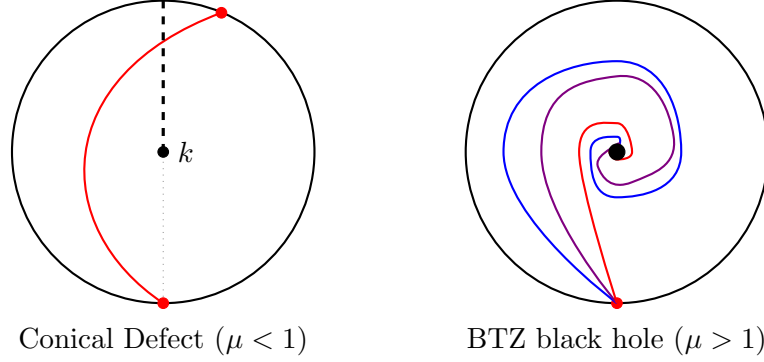Conical Defect $(\mu < 1)$ BTZ black hole $(\mu > 1)$

Figure 4.4: This figure schematically shows the difference in the bulk setup required for the computation of the phase shift, described in Section 2.4, for the cases of the conical defect and the BTZ black hole. In the latter case, the phase shift is not defined since all ingoing radial geodesics beginning at the asymptotic boundary reach the horizon. Viewed as a limit of the conical defect case, the phase shift obtained for the BTZ metric is $\delta \to \infty$.

Phase shift for $n = 1$ with generic b

A second approach to considering the black hole regime of the $(1, 0, n)$ family of microstate geometries is to take the simplest member – that of $n = 1$ – but for generic b. The bulk phase shift in the $(1, 0, 1)$ 3-dimensional reduced geometry (4.162) is given by the following integral

$$
\begin{aligned}
\delta &= 2p_t R_y \, a_0 \int_{r_0}^{\infty} \frac{dr}{r} \sqrt{\frac{r^4(1 - \beta^2) + r^2 a_0^2 \left(1 - 2\beta(1 - \alpha) + \beta^2(1 - 2\alpha - \alpha^2)\right) - a_0^4 \alpha^3 \beta^2}{(r^2 + a_0^2)^3}} \\
&\equiv 2p_t R_y \, \alpha^{-1/2} \sqrt{1 - \beta^2} \; \mathcal{I} \;,
\end{aligned}
\tag{4.187}
$$

where we have defined the parameter $\alpha \equiv \frac{a^2}{a_0^2}$ for future use. The integral $\mathcal{I}$ is computed in Appendix E.3 with the final result given in (E.45). The full phase shift obtained in the $(1, 0, 1)$ geometry is then

$$
\begin{aligned}
\delta = 2p_t R_y \, \alpha^{-1/2} \sqrt{1 - \beta^2} \Bigg[& \sqrt{\frac{x_0 + \bar{x}_0}{x_0 \bar{x}_0}} \, E\left(\sqrt{\frac{x_0(1 - \bar{x}_0)}{x_0 + \bar{x}_0}}\right) \\
& - \sqrt{\frac{\bar{x}_0}{x_0(x_0 + \bar{x}_0)}} \, \Pi\left(\frac{x_0}{x_0 + \bar{x}_0} \,\bigg|\, \frac{x_0(1 - \bar{x}_0)}{x_0 + \bar{x}_0}\right) \Bigg] \;,
\end{aligned}
\tag{4.188}
$$

where $E(k)$ and $\Pi(m|k)$ are the complete elliptic integrals of the second and third kind respectively, defined in (E.33b) and (E.33c). In (4.188), x_0 and $\bar{x}_0$ are the functions of α and β given explicitly in (E.26).

Now to test this phase shift against known results. Firstly, a zeroth order check is

that by setting $\alpha = 1$ (which is equivalent to setting $b = 0$) reduces (4.188) to the AdS$_3$ phase shift

$$\delta\big|_{\alpha=1} = \pi p_t R_y (1 - \beta) \ . \tag{4.189}$$

Since we can relate the parameters α and μ via $\alpha = -2 + \sqrt{9 - \mu}$ using (2.75) in the $n = 1$ case, we can expand (4.188) to first order in μ to get

$$\delta\big|_\mu = \pi p_t R_y \frac{\mu}{24} (1 - \beta^2)(3 - 2\beta + \beta^2) \ , \tag{4.190}$$

which is exactly what was found by doing the integral perturbatively in μ in Section 4.5.2. Since these checks give confidence in the result (4.188), we now consider the opposite scaling of $\alpha \to 0$ in which the leading terms in the phase shift are

$$\delta \approx 2 p_t R_y (1 - \beta)\, \alpha^{-1} - R_y \frac{p_t}{2} (1 + \beta) \log \alpha \ + \ \text{regular terms} \ . \tag{4.191}$$

Divergence in the strict $\alpha \to 0$ limit was expected since the $(1, 0, n)$ family of metrics tend to that of the BTZ black hole in this limit and the bulk phase shift is not defined directly for the BTZ metric (see Figure 4.4). The point $a = 0$ is not part of the ensemble of microstates of the D1-D5-P black hole, but by using the $(1, 0, n)$ family of microstate geometries – which can arbitrarily closely approximate the black hole – a finite value of the phase shift can be obtained all the way up to the point $\alpha = 0$.

A note on the regime of validity of this calculation is in order: the small a behaviour of the radial turning point of the probe geodesic for any n is given by

$$r_0 \approx a_0\, \alpha^{3/2} (\beta^{-1} - 1)^{-1} \left[1 + O\Big(a_0 \alpha^{3/2} (\beta^{-1} - 1)^{-1} \Big) \right] \ . \tag{4.192}$$

Note that the expansion parameter is $a_0\, \alpha^{3/2} (\beta^{-1} - 1)^{-1}$ and thus the small α expansion fails when $\beta \approx 1$; that is, when the geodesic probes the very centre of the bulk geometry. This is natural since near $r = 0$ the light probe will resolve the D-brane bound state that forms the black hole microstate and the supergravity approximation will break down.

Chapter 5

Conclusions and Outlook

This thesis has tried to build on two aspects of the study and construction of holographic correlators. Firstly, there is the use of HHLL holographic correlators computed from microstate geometries to obtain LLLL correlators, not just between single-trace operators but now also including multi-trace operators. Secondly, there is the study of HHLL correlators in the Regge limit – where the heavy operator is an explicit pure state of the theory – and the relation between the CFT data of non-protected heavy-light double-traces exchanged in the intermediate channel and a bulk phase shift computed in the geometry dual to the heavy state.

In Chapter 3 we have studied correlation functions involving two single-trace and two multi-trace light operators obtained from the light limit of HHLL holographic correlators. Since these HHLL correlators are computed from quadratic fluctuations around the classical supergravity background dual the heavy operator, it is the connected tree-level Witten diagram contributions to these n-trace correlators that are extracted. By way of a particular HHLL correlator, whose expression is known exactly in momentum space, we derived explicit expressions for correlation functions involving double-trace operators (3.15c) (for correlators involving higher multi-trace operators see (B.12)). The justification for our method of construction is that the behaviour of these multi-trace correlators in the various OPE channels is consistent in all of the checks we perform in Section 3.4, for example, we reproduce the behaviour of the $n = 2$ correlator in the $\bar{z} \to 1$ light-cone limit – dominated by the exchange of currents – from suitable conformal blocks and in the $z, \bar{z} \to 0$ Euclidean OPE from calculations at the free point involving protected multi-trace operators.

Since 4-point multi-trace correlators can be viewed as a particular kinematical limit of higher-point correlation functions of single-traces, we argued in Section 3.2 that, for 6-point functions and higher, there are Witten diagrams that cannot be reduced to a finite sum of contact diagrams. Hence, the usual D-functions are not a sufficient basis

of functions for this class of correlators. Indeed, from expressions such as (3.15c), we see that the new ingredient appearing in correlators with multi-traces are the Bloch-Wigner-Ramakrishnan polylogarithm functions. These are particular combinations of (higher-order) polylogarithm functions exhibiting simpler analytic properties than the "bare" polylogarithms.

It would be interesting to see whether other explicit computations of higher-point holographic correlators, in any kinematic limit, also have natural descriptions in terms of Bloch-Wigner-Ramakrishnan polylogarithms – in AdS$_3$ or otherwise. We believe that these functions appear generically in holographic correlators involving multi-trace operators. Furthermore, we have argued that despite such correlators derived from HHLL correlation functions not being exactly equal to those obtained from an OPE limit of higher-point functions, their functional structure is the same. Thus the conclusions made about the generic appearance of Bloch-Wigner-Ramakrishnan polylogarithm functions in multi-trace correlation functions apply to higher-order correlators as well. However, there might exist an even more appropriate basis of functions, possibly with a simple description in Mellin space. This new basis would contain higher-order analogues of the $D_{\Delta_1,\Delta_2,\Delta_3,\Delta_4}$ functions, commonly appearing in holographic correlators (see for example [58,59]) which are just constants when written in Mellin space [45]. It would also be interesting to find a Mellin description of our multi-trace connected correlators, however, the correlators with a simple Mellin form are likely to be those involving multi-trace operators formed from the OPE limit of single-trace operators, rather than those we have obtained from a HHLL correlator. If such Mellin transforms were to be found, it would be interesting to see whether they are related to the corresponding tree-level Feynman diagrams (see figures 3.1 and 3.3), with some of the Mellin-variables set to zero in order to implement the relevant OPE limit. A Mellin space formulation would also provide an explicit avenue towards the flat-space limit where checks with the relevant amplitudes in Minkowski space [205, 206] could be made. For a summary of the Mellin space description of a wide class of AdS$_3 \times S^3$ holographic correlators of single-trace operators see [76].

Since the part of the multi-trace correlators obtained from the light limit of HHLL correlators is the connected tree-level contribution, it is natural to ask about the remainder. As shown in Figure 3.1, these extra contributions come from disconnected one-loop Witten diagrams which contribute at the same order in $1/N$ as the associated connected tree-level part. That is, for a correlator involving n-trace operators these types of contributions will both be at order N^{-n}. While the direct calculation of loop-level Witten diagrams is technically extremely difficult, CFT techniques have been used to make progress in this direction, for instance, in the case of AdS$_5 \times S^5$ four-point correlators [207–210]. Finding similar results in AdS$_3 \times S^3$ would allow us to extend our $n = 2$ result from the connected part to the full $1/N^2$ double-trace correlator, however,

at present not all of the prerequisite tree-level correlators are known (see [75, 76] for the current standing of these correlators).

The known correlators of the $n = 1$ type are sufficient to extract dynamical data, such as the anomalous dimensions, of individual R-symmetry and flavour irreducible representations for the family of non-protected double-trace operators of the form $\bar{\mathcal{O}}_f \partial^k \mathcal{O}_g$ exchanged in the $z, \bar{z} \to 1$ OPE channel. This unmixed data of such operators (that are degenerate at leading order in large N) yields the result that, for the theory on $K3$, the anomalous dimensions for exchanged operators of spin $k \leq 2$ are positive. To the best of our knowledge, this gives the first known example of a theory with such behaviour – the possibility of which was first discussed in [185]. Using the $n = 2$ correlators it is possible to derive constraints on the 3-point coupling involving three double-trace operators, of the form $\langle : \bar{\mathcal{O}}_f^2 :: \mathcal{O}_f^2 : (\bar{\mathcal{O}}\mathcal{O})_{k=0} \rangle$. For $k > 0$, there is non-trivial mixing of these primaries with new triple-trace primaries. The full unmixing of these operators' data would require the input of a correlator involving two double-trace and two single-trace operators, all with identical flavour index. Such a correlator is not known currently.

Considering the very different qualitative behaviours of the order $1/N$ anomalous dimensions of the double-trace operators $\bar{\mathcal{O}}\partial^k \mathcal{O}$ in the cases of the theory compactified on T^4 and $K3$, it is possible that this suggests a fundamental difference between these theories. It would be interesting here to have access to similar LLLL correlators but containing different single-trace operators in order to see whether this pattern in anomalous dimensions is upheld by other families of double-trace operators in these theories.

The smoothness of the limit of correlators between our "heavy scaling regime" in which the dimension of the multi-trace operators $\mathcal{O}^n$ scales as $\Delta_n \sim c$ and the "light scaling regime" in which $\Delta_n \sim 1$ may be an unexpected feature, but there is now a mounting body of evidence that this is the case [73–75]. The fact that correlation functions of four light operators have been demonstrated to be obtainable from HHLL correlators begs the question of whether also correlators involving operators of intermediate dimensions are smoothly related. Two classes of such operators are the BMN [211, 212] and other semi-classical states with dimensions scaling as $\Delta \sim c^{1/4}$ and possibly giant graviton states [213] with $\Delta \sim c^{1/2}$.

In Chapter 4 we studied the Regge limit of four-point AdS$_3$ correlators in the supergravity approximation. For the most part we have concentrated on HHLL correlators in which one pair of operators corresponds to particular pure 1/2- or 1/4-BPS states with conformal dimensions Δ of order N, in the large N limit. These heavy operators ($\mathcal{O}_H$) are dual to non-trivial asymptotically AdS gravitational backgrounds, while the light operators ($\mathcal{O}_L$) are described in the Regge regime by null geodesics in these geometries

– from this set up, a phase shift can be computed. To relate this bulk phase shift with the CFT data, we have adopted a perturbative approach in $\mu \sim \Delta/N$, limiting ourselves initially to the first order. In this limit the HHLL correlators we consider take the same functional form as the single-trace LLLL correlators where the pair of heavy operators is replaced by two light CPO's. Despite this, different approximations are appropriate in the analyses for the two regimes $\Delta \sim N$ and $\Delta \sim 1$ (see for instance (4.29) and (4.31)). This explains why two different sets of CFT data are extracted from the HHLL and the LLLL correlators. For two of the example heavy operators discussed, the perturbative approach is then pushed to arbitrary orders in μ using, for instance, the correlators derived in Section 3.3 (and the higher order generalisations in Appendix B.1). We have verified that the first order relation (4.33) (first found in [90]) between the phase shift and the anomalous dimensions of double-trace operators (those exchanged between a heavy and a light operator) is satisfied in all the examples we have analysed. In the spirit of this first order relation and the second order considerations of [53], in Section 4.2 we derive all-order relations between the bulk phase shift and the anomalous dimensions and OPE coefficients of the HL double-traces (see Eq (4.60)). We have also looked at the bootstrap constraints relating the $\mathcal{O}_H \to \mathcal{O}_L$ and the $\mathcal{O}_L \to \mathcal{O}_L$ channels. This latter channel contains a "universal sector" that is completely determined by the Virasoro and R-symmetry algebras of the CFT – and is thus insensitive to the details of the states appearing in the correlator. Truncating a correlator to this universal contribution, as is often done in the literature, amounts to replacing the pure heavy states by a statistical ensemble characterised by Δ. The correlators in pure states, however, also contain a tower of double-trace operators that are needed for consistency with the bootstrap constraints. An intermediate example is represented by the correlator extracted from the conical defect geometry for generic values of the deficit angle: despite this geometry not being dual to a pure state, the correlator satisfies the bootstrap constraint mentioned above. Finally, as a technical by-product, we show that knowledge of the correlator in the Regge limit is enough to fix the anomalous dimensions and three-point couplings of double-trace operators with spin less than or equal to 2 – these are not captured by the Lorentzian inversion formula [68]. We work out explicitly an example with spin-2 operators. Our investigation leaves open a number of possible future developments. Firstly, at a more technical level, it would be useful to explain why the relation (4.33) between phase shift and anomalous dimensions (that is expected to apply only to correlators of quasi-primary operators) also works for the non-primary state considered in Section 4.5. This question becomes particularly relevant because non-primary operators are the microstates of the D1-D5-P black hole.

The most pressing physical question, however, is whether the Regge limit of pure-state correlators can be used as a tool to study the black hole regime of the CFT. Heavy

operators are dual to microstates of a black hole with a regular horizon of finite area only if the parameter μ, defined in (4.5), is greater than 1 ($\mu > 1$) and thus this requirement is incompatible with the perturbative approach of Chapter 4 – which is based on the small μ expansion. In this regime it was found that the phase shift of a light probe in the BTZ black hole geometry (which has $\mu > 1$) is ill-defined for all values of the impact parameter [52], owing to the fact that all in-falling null geodesics that begin on the asymptotic boundary fall into the black hole. In contrast, asymptotically AdS black holes in higher dimensions do not suffer from such issues [52] and one generically finds regions of both elastic and inelastic scattering [175]. For the $(1, 0, n)$ subfamily of microstates, the $\mu > 1$ condition translates into the "black hole bound"

$$1 \geq \frac{N_b}{N} > 2n + 1 - 2\sqrt{n(n + 1)} \ , \tag{5.1}$$

which, in particular, requires $n \geq 1$. While computing the full HHLL correlator requires solving the wave equation in the $(1, 0, n)$ geometry (4.162), and this is difficult[60] to do exactly (see [78, 79]), deriving the bulk phase shift is analytically doable, at least for $n = 1$ as shown in Section 4.5.3. One of the key observations is that, in contrast to the BTZ black hole, for horizonless fuzzball geometries considered thus far there seems to always exist a radial turning point for in-falling null geodesics and hence a well-defined phase shift. It would be interesting to see whether one could study classical black holes as a particular limit of microstate geometries and analyse the transition between the purely elastic scattering found in fuzzballs and purely inelastic capture seen for BTZ black holes. We expect that in order to fully analyse this black hole regime it will be necessary to work exactly in μ. Hence it would be important to understand precisely how the CFT information is encoded in the bulk phase shift for finite values of μ, the groundwork for which we lay in (4.60). We believe that this would provide a useful tool with which to study the gravitational description of black hole microstates and we hope to be able to make progress on this problem in the near future.

As a final word on this topic, we note that the derivation of (4.60) implicitly assumes that all quantities involved are real, or in other words that the scattering in the bulk is elastic. As discussed above, this is not always the case due to the inelastic part of the scattering process (such as capture of the light probe and radiative dissipation) typically being encoded in an imaginary component of the phase shift – seen for example in [175]. It would be interesting to extend (4.60) in this spirit and explore the implications.

The observation of transient Lyapunov behaviour in the AdS$_3$ holographic LLLL correlator considered in Section 4.4.4 allowed for a verification of the results of [115], in which the Virasoro vacuum block approximation was used, at least at leading order in

---

[60]It turns out that this problem can be reduced to a purely mathematical one based on the connection problem of confluent Heun equations. For recent progress on this connection problem see [214, 215]. We hope to have progress on this in the relatively near future.

large N. Since the correlator we used is only known at order $1/N$, it allows us to probe time scales only below the scrambling time $t_* \sim \log c$, beyond which higher orders and stringy contributions would be necessary. This behaviour appears quite robust since it has also been seen in higher derivative gravity [216] following the shockwave analysis of [113], and from non-Lorentzian CFTs [217]. One interesting avenue was initiated in [203] where an out-of-time-order 4-point function of light operators in the background of a heavy state dual to a black hole microstate was studied in the eikonal approximation. This is the analogue of the thermal OTOC, where the thermal state represents a classical black hole. This represents an avenue of understanding the similarities and differences of scrambling for black holes and for individual microstate geometries.

The study of Lyapunov growth in OTOCs is just one way of probing microstates of black holes – a particular initiative of the microstate program currently. Various current directions fall into the categories of (see [218] for a review of the phenomenology of fuzzballs): entanglement entropy [219–221], gravitational multipoles [222–226], geodesics and shadows [198–200, 227–231], tidal Love numbers [232], gravitational wave echos [19, 78, 233–236], quasi-normal modes [78, 214, 237] and tidal trapping [32, 34, 79, 238–241]. One might hope that, using these probes and more, in the future it might be possible to see evidence of black hole microstructure from experiments such as the future iterations of LIGO (see for instance [242, 243] for general discussions of fundamental physics from gravitational wave detections).

A second main line of development of the black hole microstate program is towards the construction of microstate geometries that are non-BPS; undoubtedly a key step towards understanding more realistic black holes. Some very recent progress has been made in this direction in [164, 244–247]. As well as looking for black hole microstates away from extremality, there is also the important question of microstates away from atypicality for which very limited progress has been made [36].

One curious result that has recently come out of the study of the D1-D5 CFT at the free orbifold point [248] is that, from the study of the lifting of states under deformation of this theory [166, 249–252], the key state (2.66) used in the construction of the $(1, 0, n)$ family of superstrata becomes non-BPS at second order in the deformation. Clearly this is in tension with evidence from the many holographic tests that have been performed using protected quantities based on this microstate geometry [51] at the supergravity point. Work on resolving this tension is ongoing.

Appendix A

Global Conformal Blocks

This appendix derives the form of the global conformal blocks in two different ways, firstly by explicit resummation of a quasi-primary's global descendants and secondly by use of the quadratic Casimir of the global conformal group.

Global conformal blocks from projectors

The conformally invariant function $G(z, \bar{z})$ from the 4-point function (2.20) can be expanded in a basis of global conformal blocks, labelled by global primaries $\mathcal{O}_{h,\bar{h}}$, as in (2.32) where a global primary is defined as

$$L_1 \, |h\rangle \equiv L_1 \, \mathcal{O}_h(0)|0\rangle = 0 \ , \tag{A.1}$$

with equivalent statements in the anti-holomorphic sector. A global block for a given quasi-primary resums the contribution of that quasi-primary and its tower of descendants generated by the action of L_{-1}. The space of global descendants of the quasi-primary state $|h\rangle$ is then spanned by $\left\{ L_{-1}^q \, |h\rangle \right\}$ for $q \in \mathbb{Z}^+$. For simplicity, we here calculate the form of the T-channel global conformal blocks. The T-channel decomposition of the 4-point function $\langle \bar{\mathcal{O}}_1 \mathcal{O}_2 \mathcal{O}_3 \bar{\mathcal{O}}_4 \rangle$ can equivalently be thought of as the S-channel of the correlator $\langle \mathcal{O}_2 \mathcal{O}_3 \bar{\mathcal{O}}_4 \bar{\mathcal{O}}_1 \rangle$. Projecting this latter 4-point function onto the contribution of a single quasi-primary's conformal family in the T-channel sum of (2.32) gives

$$\langle \mathcal{O}_2(\infty) \mathcal{O}_3(1) \, \mathcal{P}_h \, \bar{\mathcal{O}}_4(z, \bar{z}) \bar{\mathcal{O}}_1(0) \rangle = C_{23\mathcal{O}} C_{\mathcal{O}41} \, z^{-h_1 - h_4} \bar{z}^{-\bar{h}_1 - \bar{h}_4} \, \mathcal{V}_h(z) \bar{\mathcal{V}}_{\bar{h}}(\bar{z}) \ , \tag{A.2}$$

where the projection operator for the holomorphic sector is given by

$$\mathcal{P}_h \equiv \sum_{q=0}^{\infty} \frac{L_{-1}^q |h\rangle \langle h| L_1^q}{\langle h| L_1^q L_{-1}^q |h\rangle} \ , \tag{A.3}$$

and $\langle h| \equiv \lim_{z\to\infty} z^{2h}\langle 0|\mathcal{O}_h(z)$. From now on in this derivation, we suppress the anti-holomorphic part of any expression since it follows in precisely the same way. The computation of the 4-point function (A.2) is then reduced to finding three- and two-point functions since

$$\langle \mathcal{O}_2(\infty)\mathcal{O}_3(1)\,\mathcal{P}_{h,\bar{h}}\,\bar{\mathcal{O}}_4(z,\bar{z})\bar{\mathcal{O}}_1(0)\rangle = \sum_{q=0}^{\infty} \frac{\langle \mathcal{O}_1(\infty)\mathcal{O}_2(1)L_{-1}^q|h\rangle\,\langle h|L_1^q\,\mathcal{O}_3(z)\mathcal{O}_4(0)\rangle}{\langle h|L_1^q L_{-1}^q|h\rangle}\,.$$
(A.4)

The forms of two- and three-point functions are fixed by conformal symmetry and are given in (2.18). In order to calculate correlators containing descendants, we use the conformal Ward identity

$$\big\langle (L_{-k_1}\cdots L_{-k_n}\mathcal{O}_h)(z)\mathcal{O}_1(z_1)\cdots\mathcal{O}_n(z_n)\big\rangle = \mathcal{L}_{-k_1}\cdots\mathcal{L}_{-k_n}\langle \mathcal{O}_h(z)\mathcal{O}_1(z_1)\cdots\mathcal{O}_n(z_n)\rangle\,,$$
(A.5)

where $\mathcal{O}_h$ and $\mathcal{O}_i$ for $i = 1,\ldots,n$ are quasi-primary operators, and the operators $\mathcal{L}_{-k}$ are given by

$$\mathcal{L}_{-k} \equiv \sum_{i=1}^{n} \left[\frac{(k-1)h_i}{(z_i-z)^k} - (z_i-z)^{1-k}\,\partial_{z_i} \right]\,.$$
(A.6)

The two such operators that will be needed in the calculation below are

$$\mathcal{L}_1 = \sum_{i=1}^{n} \left[-2h_i(z_i-z) - (z_i-z)^2\,\partial_{z_i} \right]\,,$$
(A.7)

$$\mathcal{L}_{-1} = \sum_{i=1}^{n} -\partial_{z_i} = \partial_z\,,$$
(A.8)

with the final equality in $\mathcal{L}_{-1}$ being due to translation invariance [120]. Starting with the norm of the exchanged state, we find using (A.7) and (2.18)

$$\begin{aligned}
\langle h|L_1^q L_{-1}^q|h\rangle &= \lim_{\substack{z_1\to\infty\\z_2\to0}} z_1^{2h}\mathcal{L}_1^q\mathcal{L}_{-1}^q\langle \mathcal{O}_h(z_1)\mathcal{O}_h(z_2)\rangle\\
&= \lim_{\substack{z_1\to\infty\\z_2\to0}} z_1^{2h}\big[-2h\,z_{12} - z_{12}^2\partial_{z_1}\big]^q\big(\partial_{z_2}\big)^q z_{12}^{-2h}\\
&= \lim_{\substack{z_1\to\infty\\z_2\to0}} z_1^{2h}\big[-2h\,z_{12} - z_{12}^2\partial_{z_1}\big]^q(2h)_q\,z_{12}^{-2h+q}\\
&= q!\,(2h)_q\,,
\end{aligned}$$
(A.9)

where the rising Pochhammer symbol is defined as

$$(h)_q \equiv \frac{\Gamma(h+q)}{\Gamma(h)}\,.$$
(A.10)

Next, in (A.4) we require the three-point function

$$
\begin{aligned}
\frac{\langle \mathcal{O}_2(\infty)\mathcal{O}_3(1)L^q_{-1}|h\rangle}{C_{23\mathcal{O}}} &= \lim_{\substack{z_2\to\infty \\ z_3\to 1 \\ z_4\to 0}} z_2^{2h_2}\mathcal{L}^q_{-1}\frac{\langle \mathcal{O}_2(z_2)\mathcal{O}_3(z_3)\mathcal{O}_h(z_4)\rangle}{C_{23\mathcal{O}}} \\
&= \lim_{\substack{z_2\to\infty \\ z_3\to 1 \\ z_4\to 0}} z_2^{2h_2}\left(\partial_{z_4}\right)^q z_{23}^{h-h_2-h_3} z_{34}^{h_2-h_3-h} z_{24}^{h_3-h_2-h} \\
&= (h-h_2+h_3)_q \ . \tag{A.11}
\end{aligned}
$$

Lastly, the remaining three-point function in (A.4) we calculate, via its Hermitian conjugate, as

$$
\begin{aligned}
\frac{\langle h|L^q_1\,\bar{\mathcal{O}}_4(z)\bar{\mathcal{O}}_1(0)\rangle}{C_{\mathcal{O}41}} &= \frac{1}{C_{\mathcal{O}41}}\left[\langle (\bar{\mathcal{O}}_1(0))^\dagger(\bar{\mathcal{O}}_4(z))^\dagger L^q_{-1}\mathcal{O}_h(0)\rangle\right]^\dagger \\
&= \frac{1}{C_{\mathcal{O}41}}\left[\lim_{\substack{\bar{z}_1\to 0 \\ \bar{z}_4\to\bar{z} \\ w_2\to 0}} \bar{z}_1^{-2h_1}\bar{z}_4^{-2h_4}\mathcal{L}^q_{-1}\langle \bar{\mathcal{O}}_1(\bar{z}_1^{-1})\bar{\mathcal{O}}_4(\bar{z}_4^{-1})\mathcal{O}_h(w_2)\rangle\right]^\dagger \\
&= \left[\lim_{\substack{w_1\to\infty \\ w_4\to w \\ w_2\to 0}} w_1^{2h_1}w_4^{2h_4}\left(\partial_{w_2}\right)^q w_{14}^{h-h_1-h_4} w_{42}^{h_1-h-h_4} w_{12}^{h_4-h-h_1}\right]^* \\
&= \left[(h-h_1+h_4)_q\, w^{-h-q+h_1+h_4}\right]^* \\
&= (h-h_1+h_4)_q\, z^{h+q-h_1-h_4} \ , \tag{A.12}
\end{aligned}
$$

where we have used the renaming $w_i = \bar{z}^{-1}$ and

$$
\left(\mathcal{O}(z,\bar{z})\right)^\dagger = \bar{z}^{-2h_\mathcal{O}} z^{-2\bar{h}_\mathcal{O}} \mathcal{O}(\bar{z}^{-1},z^{-1}) \ . \tag{A.13}
$$

Putting these various pieces (A.9), (A.11) and (A.12) together in (A.4) gives

$$
\begin{aligned}
\frac{\langle \mathcal{O}_2(\infty)\mathcal{O}_3(1)\,\mathcal{P}_h\,\bar{\mathcal{O}}_4(z,\bar{z})\bar{\mathcal{O}}_1(0)\rangle}{C_{23\mathcal{O}}C_{\mathcal{O}41}} &= \sum_{q=0}^{\infty} \frac{(h-h_{23})_q\,(h-h_{14})_q}{q!\,(2h)_q}\, z^{h-h_1-h_4+q} \\
&= z^{h-h_1-h_4}\,{}_2F_1(h-h_2+h_3, h-h_1+h_4; 2h; z) \ , \tag{A.14}
\end{aligned}
$$

where once again $h_{ij} \equiv h_i - h_j$. Comparing this result with (A.2) gives for the T-channel global blocks

$$
\mathcal{V}_h(z) = z^h\,{}_2F_1(h-h_{23}, h-h_{14}; 2h; z) \ , \tag{A.15}
$$

and similarly for $\bar{\mathcal{V}}_{\bar{h}}(\bar{z})$. We note that in terms of the notation used in (2.32), these T-channel global conformal blocks for external operator dimensions $h_1 = h_2$ and $h_3 = h_4$

are

$$g_{h,\bar{h}}^{h_{14},\bar{h}_{14}}(z,\bar{z}) = \mathcal{V}_h(z)\bar{\mathcal{V}}_{\bar{h}}(\bar{z}) . \tag{A.16}$$

Global conformal blocks as eigenfunctions

A second method for calculating conformal blocks is by making use of the quadratic Casimir of $SL(2,\mathbb{R})$ (here focusing solely on the holomorphic sector) which is given in terms of the globally defined Virasoro modes (2.12) by

$$L^2 = \frac{1}{2}\Big(L_{-1}L_1 + L_1L_{-1}\Big) - L_0^2 . \tag{A.17}$$

By construction, the commutators of L^2 with the generators L_0, $L_{\pm 1}$ are vanishing and inserting the quadratic Casimir operator in the projected four-point function (A.4) and acting to the left and right yields the following equality

$$\langle \mathcal{O}_2(\infty)\mathcal{O}_3(1)\, \mathcal{P}_h\overleftarrow{L^2}\bar{\mathcal{O}}_4(z)\bar{\mathcal{O}}_1(0)\rangle = \langle \mathcal{O}_2(\infty)\mathcal{O}_3(1)\, \mathcal{P}_h\overrightarrow{L^2}\bar{\mathcal{O}}_4(z)\bar{\mathcal{O}}_1(0)\rangle . \tag{A.18}$$

We will evaluate the two sides of this equality separately and then equate them at the end. From the left-hand side of (A.18), using (A.3) the part that is of interest is thus

$$
\begin{aligned}
\langle h|L_1^q\overleftarrow{L^2} &= \langle h|\overleftarrow{L^2}L_1^q \\
&= -\lim_{z\to\infty} z^{2h} \langle 0| \left(\tfrac{1}{2}\big[L_1L_{-1},\mathcal{O}_h\big] + \tfrac{1}{2}\big[L_{-1}L_1,\mathcal{O}_h\big] - \big[L_0^2,\mathcal{O}_h\big] \right)L_1^q \\
&= -\lim_{z\to\infty} z^{2h} \langle 0| \left(\tfrac{1}{2}\partial\mathcal{O}_hL_1 + \tfrac{1}{2}(z^2\partial + 2hz)\mathcal{O}_hL_{-1} - (z\partial + h)\mathcal{O}_hL_0 \right)L_1^q \\
&= -h(h-1)\langle h|L_1^q ,
\end{aligned}
\tag{A.19}
$$

where in the third line we have used the commutator between a quasi-primary and the global Virasoro modes, given by

$$\big[L_n, \mathcal{O}_h(z)\big] = h(n+1)z^n\mathcal{O}(z) + z^{n+1}\partial_z\mathcal{O}_h , \tag{A.20}$$

which is valid for $n = \pm 1, 0$ if $\mathcal{O}_h$ is quasi-primary and for $n \in \mathbb{Z}$ if $\mathcal{O}_h$ is primary. The fact that $\langle 0|$ is the $SL(2,\mathbb{C})$ invariant vacuum has been used repeatedly. Therefore, using (A.2) the left-hand side of (A.18) reads

$$\langle \mathcal{O}_2(\infty)\mathcal{O}_3(1)\, \mathcal{P}_h\overleftarrow{L^2}\bar{\mathcal{O}}_4(z)\bar{\mathcal{O}}_1(0)\rangle = -h(h-1)C_{23\mathcal{O}}C_{\mathcal{O}41}\, z^{-h_1-h_4}\mathcal{V}_h(z) . \tag{A.21}$$

Turning now to the right-hand side of (A.18), we require the quantity

$$
\vec{L^2}\bar{\mathcal{O}}_4(z_4)\bar{\mathcal{O}}_1(z_1)|0\rangle = \left[\frac{1}{2}L_{-1}\left(z_4^2\partial_{z_4}\bar{\mathcal{O}}_4 + 2z_4h_4\bar{\mathcal{O}}_4 + \bar{\mathcal{O}}_4L_1\right) + \frac{1}{2}L_1\left(\partial_{z_4}\bar{\mathcal{O}}_4 + \bar{\mathcal{O}}_4L_{-1}\right)\right.
$$
$$
\left. - \left((z_4\partial_{z_4} + h_4)^2\bar{\mathcal{O}}_4 + 2(z_4\partial_{z_4} + h_4)\bar{\mathcal{O}}_4L_0 + \bar{\mathcal{O}}_4L_0^2\right)\right]\bar{\mathcal{O}}_1|0\rangle
$$
$$
= \left[z_{41}^2\partial_{z_4}\partial_{z_1} - 2h_1z_{41}\partial_{z_4} + 2h_4z_{41}\partial_{z_1}\right.
$$
$$
\left. - (h_4 + h_1)(h_4 + h_1 - 1)\right]\bar{\mathcal{O}}_4\bar{\mathcal{O}}_1|0\rangle
$$
$$
= \mathcal{D}_{41}\bar{\mathcal{O}}_4(z_4)\bar{\mathcal{O}}_1(z_1)|0\rangle , \tag{A.22}
$$

where we define the differential operator

$$
\mathcal{D}_{ij} = z_{ij}^2\partial_{z_i}\partial_{z_j} - 2h_jz_{ij}\partial_{z_i} + 2h_iz_{ij}\partial_{z_j} - (h_i + h_j)(h_i + h_j - 1) . \tag{A.23}
$$

Using (A.22), the right-hand side of (A.18) can be written as

$$
\langle\mathcal{O}_1(z_1)\mathcal{O}_2(z_2)\,\mathcal{P}_h\vec{L^2}\mathcal{O}_3(z_3)\mathcal{O}_4(z_4)\rangle = C_{23\mathcal{O}}C_{\mathcal{O}41}\,\mathcal{D}_{41}\left[K_t\mathcal{V}_h(z)\right]
$$
$$
= C_{23\mathcal{O}}C_{\mathcal{O}41}\frac{K_t\,z_{14}}{z_{24}z_{21}z_{13}}\left[z_{31}\left((h_4 - h_1)z_{24}^2\partial_{z_4} + (h_4 - h_1)z_{21}^2\partial_{z_1} + z_{24}z_{21}z_{41}\partial_{z_4}\partial_{z_1}\right)\right.
$$
$$
\left. - (h_2 - h_3)z_{23}\left((h_4 - h_1)z_{21} + z_{24}z_{41}\partial_{z_4}\right)\right]\mathcal{V}_h(z)
$$
$$
= -C_{23\mathcal{O}}C_{\mathcal{O}41}K_t\left[z^2(1 - z)\partial^2\mathcal{V}_h - (1 - h_{23} - h_{14})z^2\,\partial\mathcal{V}_h - h_{23}h_{14}z\,\mathcal{V}_h\right] , \tag{A.24}
$$

where the relations $\partial_i = \frac{\partial z}{\partial z_i}\partial$ were used in the third line. In the above we used the quantity $K_t \equiv K(z_2, z_3, z_4, z_1)$ which is the prefactor for the correlator $\langle\mathcal{O}_2\mathcal{O}_3\bar{\mathcal{O}}_4\bar{\mathcal{O}}_1\rangle$ and can be obtained from (2.21) by the permutation (1234) on both the positions z_i and the dimensions h_i. The equation (A.18) is then obtained by equating (A.21) and (A.22). We are interested in the gauge-fixed correlator, obtained by taking the appropriate limits (2.26) in order to fix the positions of the four operators z_i, giving (A.18) as

$$
h(h - 1)\mathcal{V}_h = z^2(1 - z)\partial^2\mathcal{V}_h - (1 - h_{23} - h_{14})z^2\partial\mathcal{V}_h - h_{23}h_{14}\,z\,\mathcal{V}_h \equiv \mathcal{D}_z\left[\mathcal{V}_h\right] , \tag{A.25}
$$

where we defined the gauge-fixed differential operator

$$
\mathcal{D}_z = z^2(1 - z)\partial^2 - (1 - h_{14} - h_{23})z^2\partial - h_{23}h_{14}z . \tag{A.26}
$$

Making the ansatz $\mathcal{V}_h = z^hF(z)$, the differential equation (A.25) becomes

$$
z(1 - z)\partial^2F(z) + \left[2h - (2h - h_{14} - h_{23} + 1)z\right]\partial F(z) - (h - h_{23})(h - h_{14})F(z) = 0 , \tag{A.27}
$$

which is simply the hypergeometric differential equation with the choices for the canonical parameters $a = h - h_{23}$, $b = h - h_{14}$ and $c = 2h$, and so a solution to this equation is then

$$F(z) = {}_2F_1(h - h_{23}, h - h_{14}; 2h; z) \ . \tag{A.28}$$

The equation (A.25) makes it explicit that global conformal blocks are eigenfunctions of the differential operator $\mathcal{D}_z$ with eigenvalue $h(h-1)$. Global conformal blocks for the anti-holomorphic sector take the same form with $z \to \bar{z}$, $h_i \to \bar{h}_i$ and $h \to \bar{h}$ as usual.

Appendix B

Details of LLLL Holographic Correlators

B.1 Derivation of connected multi-particle correlators

In this appendix we give details on the derivation of the closed form expressions for the correlators in (3.15). In addition, we present higher order connected correlation functions that are not discussed in the main text, together with explicit expressions of the Bloch-Wigner-Ramakrishnan polylogarithm functions appearing in them.

The starting point is the HHLL correlation function from Eq. (2.92), which for completeness we reproduce here using the parameter B defined in Section 3.2

$$:C:(\tau,\sigma) = \left(1 - \frac{B^2}{N}\right) \sum_{k=1}^{\infty} \sum_{\ell \in \mathbb{Z}} e^{i\ell\sigma} \frac{\exp\left[-i(|\ell|+2k)\sqrt{1-\frac{B^2}{N}\left(1-\frac{\ell^2}{(|\ell|+2k)^2}\right)}\,\tau\right]}{\sqrt{1-\frac{B^2}{N}\left(1-\frac{\ell^2}{(|\ell|+2k)^2}\right)}}\,.$$

(B.1)

The above expression is written in terms of the dimensionless coordinates (τ,σ), related to the coordinates (t,y) of the boundary of AdS$_3$ through

$$\tau = \frac{t}{R_y}\,, \quad \sigma = \frac{y}{R_y}\,,$$

(B.2)

with R_y being the radius of the spatial circle, so that $y \sim y + 2\pi R_y$. Despite being written in terms of the cylinder coordinates (τ,σ), the expression in (B.1) represents the correlator on the plane, whose complex coordinates z and $\bar{z}$ are defined by

$$z \equiv e^{i(\tau+\sigma)}\,, \quad \bar{z} \equiv e^{i(\tau-\sigma)}\,.$$

(B.3)

In the following we will always work on the Euclidean patch, obtained by the usual

137

Wick rotation $\tau \to -i\tau_e$, or on its analytically continued version with z and $\bar{z}$ being independent complex coordinates with $\bar{z} \neq z^*$. Our goal is to rewrite the correlator (B.1) in the form of (3.14) and so we expand in B^2/N

$$:C:(\tau, \sigma) = \sum_{n=0}^{\infty} \left(\frac{B^2}{N}\right)^n \sum_{\ell \in \mathbb{Z}} \sum_{k=1}^{\infty} f_n(\tau) \, e^{i\ell\sigma - i(|\ell|+2k)\tau} \,, \tag{B.4}$$

where we assumed that the sums are well behaved so that their order can be exchanged. By comparing (B.4) with (3.14), we can extract the connected tree-level correlation functions at each order in B^2/N to get

$$:C_n: = \frac{n!}{N^n} \sum_{\ell \in \mathbb{Z}} \sum_{k=1}^{\infty} f_n(\tau) \, e^{i\ell\sigma - i(|\ell|+2k)\tau} \,, \tag{B.5}$$

and in what follows we show how to systematically evaluate these double sums.

In (B.4) we denote by $f_n(\tau)$ polynomial functions of τ (generically of degree n), which are read off by performing the explicit expansion of (B.1). The first few are given by

$$f_0(\tau) = 1 \,, \tag{B.6a}$$

$$f_1(\tau) = -\frac{1}{2} - \frac{\ell^2}{2(|\ell|+2k)^2} - i\tau \left(\frac{\ell^2}{2(|\ell|+2k)} - \frac{(|\ell|+2k)}{2}\right) \,, \tag{B.6b}$$

$$f_2(\tau) = -\frac{1}{8} + \frac{3\ell^4}{8(|\ell|+2k)^4} - \frac{\ell^2}{4(|\ell|+2k)^2} - i\tau \left(-\frac{3\ell^4}{8(|\ell|+2k)^3} + \frac{\ell^2}{4(|\ell|+2k)} + \frac{(|\ell|+2k)}{8}\right)$$
$$+ (-i\tau)^2 \left(-\frac{\ell^2}{4} + \frac{\ell^4}{8(|\ell|+2k)^2} + \frac{(|\ell|+2k)^2}{8}\right) \,, \tag{B.6c}$$

$$f_3(\tau) = -\frac{1}{16} - \frac{5\ell^6}{16(|\ell|+2k)^6} + \frac{9\ell^4}{16(|\ell|+2k)^4} - \frac{3\ell^2}{16(|\ell|+2k)^2} - i\tau \left(\frac{5\ell^6}{16(|\ell|+2k)^5}\right.$$
$$\left. - \frac{9\ell^4}{16(|\ell|+2k)^3} + \frac{3\ell^2}{16(|\ell|+2k)} + \frac{(|\ell|+2k)}{16}\right) + (-i\tau)^2 \left(-\frac{\ell^2}{8} - \frac{\ell^6}{8(|\ell|+2k)^4}\right.$$
$$\left. + \frac{\ell^4}{4(|\ell|+2k)^2}\right) + (-i\tau)^3 \left(\frac{\ell^6}{48(|\ell|+2k)^3} - \frac{\ell^4}{16(|\ell|+2k)} + \frac{\ell^2(|\ell|+2k)}{16} - \frac{(|\ell|+2k)^3}{48}\right) \,. \tag{B.6d}$$

Since $f_0(\tau)$ is trivial, it follows simply that

$$C_0 = \sum_{\ell \in \mathbb{Z}} \sum_{k=1}^{\infty} e^{i\ell\sigma - i(|\ell|+2k)\tau} \tag{B.7a}$$

$$= \frac{1}{\left(1 - e^{i(\tau+\sigma)}\right)\left(1 - e^{i(\tau-\sigma)}\right)} = -\left[\frac{\mathrm{Li}_0\left(e^{-i(\tau+\sigma)}\right)}{1 - e^{-2i\sigma}} + \frac{\mathrm{Li}_0\left(e^{-i(\tau-\sigma)}\right)}{1 - e^{2i\sigma}}\right] \,, \tag{B.7b}$$

where in the last equality we have used that $\mathrm{Li}_0(x) = x/(1-x)$. Finally, by using the

complex coordinates given in (B.3) the correlator can be expressed in the simple form

$$C_0(z, \bar{z}) = \frac{1}{|1 - z|^2} \, . \tag{B.8}$$

To find closed form expressions for higher order correlators we observe that the polynomials $f_n(\tau)$ are generically of the form

$$f_n(\tau) = \sum_{p=0}^{n} \sum_{q=0}^{n} \frac{a_q}{(2n)!!} (-i\tau)^p \, \ell^{2q} \, (|\ell| + 2k)^{p-2q} \, , \tag{B.9}$$

where $a_q \in \mathbb{Z}$ are some integers. Since in (B.5), these functions are multiplied by $e^{i\ell\sigma - i(|\ell| + 2k)\tau}$, the appropriate powers of ℓ and $(|\ell| + 2k)$ can be obtained term-wise by differentiation or integration of (B.7a) using[61]

$$i\partial_\tau C_0 = \sum_{\ell \in \mathbb{Z}} \sum_{k=1}^{\infty} (|\ell| + 2k) \, e^{i\ell\sigma - i(|\ell| + 2k)\tau} \, , \tag{B.10a}$$

$$\frac{1}{i} \int^\tau d\tau_1 \, C_0 = \sum_{\ell \in \mathbb{Z}} \sum_{k=1}^{\infty} \frac{1}{|\ell| + 2k} \, e^{i\ell\sigma - i(|\ell| + 2k)\tau} \, , \tag{B.10b}$$

$$-i\partial_\sigma C_0 = \sum_{\ell \in \mathbb{Z}} \sum_{k=1}^{\infty} \ell \, e^{i\ell\sigma - i(|\ell| + 2k)\tau} \, , \tag{B.10c}$$

where we have chosen the constant of integration in (B.10b) to vanish. Importantly, we assume that the sums on the right-hand side of these expressions are convergent so that term-wise differentiation and integration is well defined.

In practice, the left-hand side of (B.10) is obtained by using (B.7b) written in terms of Li_0 functions, since in that form the τ variable appears only in the polylogarithm functions. Thus one can use the recursion relations (3.21) to show that

$$\mathcal{I}_n^\tau(\tau, \sigma) \equiv \begin{cases} (i)^n \, \partial_\tau^n \, C_0 & n \geq 0 \\ (i)^n \int^\tau d\tau_1 \int^{\tau_1} d\tau_2 \int \dots \int^{\tau_{|n|-1}} d\tau_{|n|} \, C_0 & n < 0 \end{cases}$$
$$= -\left[\frac{\mathrm{Li}_{-n}\big(e^{-i(\tau+\sigma)}\big)}{1 - e^{-2i\sigma}} + \frac{\mathrm{Li}_{-n}\big(e^{-i(\tau-\sigma)}\big)}{1 - e^{2i\sigma}} \right] \, , \tag{B.11}$$

which gives a closed form expression for any integer power of $(|\ell| + 2k)$ appearing in (B.9). Differentiating (B.11) with respect to σ is trivial, but cumbersome, and we are not aware of any closed form expression for such an action. However, since τ and σ are independent one can always perform any τ operation first, after which the remaining σ differentiation is easily performed. All in all, this allows us to algorithmically translate the expansion polynomials $f_n(\tau)$ into connected tree-level correlators at any order and

---

[61]Integration over σ is not needed since ℓ appears only with positive powers in (B.9).

after rewriting the results in terms of z and $\bar{z}$, we get

$$C_0(z,\bar{z}) = \frac{1}{|1-z|^2} \, , \tag{B.12a}$$

$$C_1(z,\bar{z}) = \frac{1}{N}\left[-\frac{i}{2}r_2\,P_2(z,\bar{z}) + \frac{1}{2}r_1\left(2\log|1-z| + \frac{z+\bar{z}-2z\bar{z}}{|1-z|^2}\log|z| \right) - \frac{1}{|1-z|^2} \right], \tag{B.12b}$$

$$:C_2:(z,\bar{z}) = \frac{2}{N^2}\left[\frac{3i}{8}r_4\,P_4(z,\bar{z}) + \frac{3}{2}r_3\,P_3(z,\bar{z}) + 2ir_2\left(P_2(z,\bar{z}) - \frac{i}{8}\frac{z-\bar{z}}{|1-z|^2}\big(\log|z|\big)^2 \right) \right.$$
$$\left. - \frac{1}{2}r_1\left(2\log|1-z| + \frac{z+\bar{z}-2z\bar{z}}{|1-z|^2}\log|z| \right) \right], \tag{B.12c}$$

$$:C_3:(z,\bar{z}) = \frac{6}{N^3}\left[-\frac{5i}{16}r_6\left(P_6(z,\bar{z}) + \frac{1}{15}\big(\log|z|\big)^2 P_4(z,\bar{z}) \right) - \frac{15}{8}r_5\bigg(P_5(z,\bar{z}) \right.$$
$$+ \frac{1}{15}\big(\log|z|\big)^2 P_3(z,\bar{z}) \bigg) - \frac{33i}{8}r_4\left(P_4(z,\bar{z}) + \frac{2}{33}\big(\log|z|\big)^2 P_2(z,\bar{z}) \right)$$
$$- 4r_3\left(P_3(z,\bar{z}) - \frac{1}{24}\big(\log|z|\big)^2\log|1-z| - \frac{1}{48}\frac{z+\bar{z}-2z\bar{z}}{|1-z|^2}\big(\log|z|\big)^3 \right)$$
$$\left. - \frac{3i}{2}r_2\left(P_2(z,\bar{z}) - \frac{i}{6}\frac{z-\bar{z}}{|1-z|^2}\big(\log|z|\big)^2 \right) \right], \tag{B.12d}$$

$$:C_4:(z,\bar{z}) = \frac{24}{N^4}\left[\frac{35i}{128}r_8\left(P_8(z,\bar{z}) + \frac{2}{21}\big(\log|z|\big)^2 P_6(z,\bar{z}) \right) + \frac{35}{16}r_7\bigg(P_7(z,\bar{z}) \right.$$
$$+ \frac{2}{21}\big(\log|z|\big)^2 P_5(z,\bar{z}) \bigg) + \frac{55i}{8}r_6\left(P_6(z,\bar{z}) + \frac{31}{330}\big(\log|z|\big)^2 P_4(z,\bar{z}) \right)$$
$$+ \frac{85}{8}r_5\left(P_5(z,\bar{z}) + \frac{23}{255}\big(\log|z|\big)^2 P_3(z,\bar{z}) \right) + \frac{65i}{8}r_4\bigg(P_4(z,\bar{z})$$
$$+ \frac{16}{195}\big(\log|z|\big)^2 P_2(z,\bar{z}) - \frac{i}{6240}\frac{z-\bar{z}}{|1-z|^2}\big(\log|z|\big)^4 \bigg) + \frac{5}{2}r_3\bigg(P_3(z,\bar{z})$$
$$\left. - \frac{1}{15}\big(\log|z|\big)^2\log|1-z| - \frac{1}{30}\frac{z+\bar{z}-2z\bar{z}}{|1-z|^2}\big(\log|z|\big)^3 \bigg) \right], \tag{B.12e}$$

where r_n denote rational functions of z and $\bar{z}$ defined as

$$r_n \equiv \big(z\partial_z - \bar{z}\partial_{\bar{z}}\big)^n \left(\frac{z+\bar{z}}{z-\bar{z}} \right). \tag{B.13}$$

We see that higher-order correlation functions involve higher order generalised Bloch-Wigner-Ramakrishnan polylogarithm functions, as defined in Section 3.3. The explicit

forms of P_2, P_3 and P_4 are given in (3.28), while the next few read

$$P_5(z, \bar{z}) = \frac{1}{2} \Bigg[\mathrm{Li}_5(z) + \mathrm{Li}_5(\bar{z}) - \log|z| \big(\mathrm{Li}_4(z) + \mathrm{Li}_4(\bar{z}) \big) + \frac{1}{3} \big(\log|z| \big)^2 \big(\mathrm{Li}_3(z) + \mathrm{Li}_3(\bar{z}) \big)$$

$$+ \frac{2}{45} \big(\log|z| \big)^4 \log|1-z| \Bigg] , \tag{B.14a}$$

$$P_6(z, \bar{z}) = \frac{1}{2i} \Bigg[\mathrm{Li}_6(z) - \mathrm{Li}_6(\bar{z}) - \log|z| \big(\mathrm{Li}_5(z) - \mathrm{Li}_5(\bar{z}) \big) + \frac{1}{3} \big(\log|z| \big)^2 \big(\mathrm{Li}_4(z) - \mathrm{Li}_4(\bar{z}) \big)$$

$$- \frac{1}{45} \big(\log|z| \big)^4 \big(\mathrm{Li}_2(z) - \mathrm{Li}_2(\bar{z}) \big) \Bigg] , \tag{B.14b}$$

$$P_7(z, \bar{z}) = \frac{1}{2} \Bigg[\mathrm{Li}_7(z) + \mathrm{Li}_7(\bar{z}) - \log|z| \big(\mathrm{Li}_6(z) + \mathrm{Li}_6(\bar{z}) \big) + \frac{1}{3} \big(\log|z| \big)^2 \big(\mathrm{Li}_5(z) + \mathrm{Li}_5(\bar{z}) \big)$$

$$- \frac{1}{45} \big(\log|z| \big)^4 \big(\mathrm{Li}_3(z) + \mathrm{Li}_3(\bar{z}) \big) - \frac{4}{945} \big(\log|z| \big)^6 \log|1-z| \Bigg] , \tag{B.14c}$$

$$P_8(z, \bar{z}) = \frac{1}{2i} \Bigg[\mathrm{Li}_8(z) - \mathrm{Li}_8(\bar{z}) - \log|z| \big(\mathrm{Li}_7(z) - \mathrm{Li}_7(\bar{z}) \big) + \frac{1}{3} \big(\log|z| \big)^2 \big(\mathrm{Li}_6(z) - \mathrm{Li}_6(\bar{z}) \big)$$

$$- \frac{1}{45} \big(\log|z| \big)^4 \big(\mathrm{Li}_4(z) - \mathrm{Li}_4(\bar{z}) \big) + \frac{2}{945} \big(\log|z| \big)^6 \big(\mathrm{Li}_2(z) - \mathrm{Li}_2(\bar{z}) \big) \Bigg] . \tag{B.14d}$$

We note that when fully written out the expressions (B.12) match (3.15).

Lastly, in Chapter 4 we find it more useful to expand the correlator (B.1) in the parameter μ where (given in (2.75) with $n = 0$)

$$\frac{b^2}{2a_0^2} = 1 - \sqrt{1 - \mu} , \tag{B.15}$$

so that the correlator takes on the form

$$C^{\mathrm{fer}}(z, \bar{z}) = \sum_{n=1}^{\infty} \mu^n \, C_n^{\mathrm{fer}}(z, \bar{z}) . \tag{B.16}$$

We give the first few series coefficients here for completeness:

$$C_0^{\text{fer}} = \frac{1}{|1-z|^2}\,, \tag{B.17a}$$

$$C_1^{\text{fer}} = -\frac{1}{2|1-z|^2} - \frac{|z|^2(z+\bar{z}-2|z|^2)}{2(z-\bar{z})^2|1-z|^2}\log|z|^2 - \frac{|z|^2}{(z-\bar{z})^2}\log|1-z|^2 - \frac{2i|z|^2(z+\bar{z})}{(z-\bar{z})^3}P_2(z,\bar{z})\,, \tag{B.17b}$$

$$\begin{aligned}
C_2^{\text{fer}} = \frac{1}{8}\Bigg[&-\frac{1}{|1-z|^2} + \frac{|z|^2(z+\bar{z}-2|z|^2)}{(z-\bar{z})^2|1-z|^2}\log|z|^2 + \frac{|z|^2(z+\bar{z})}{(z-\bar{z})^2|1-z|^2}\left(\log|z|^2\right)^2 \\
&+ \frac{2|z|^2}{(z-\bar{z})^2}\log|1-z|^2 + \frac{28i|z|^2(z+\bar{z})}{(z-\bar{z})^3}P_2(z,\bar{z}) - \frac{48|z|^2(z^2+4|z|^2+\bar{z}^2)}{(z-\bar{z})^4}P_3(z,\bar{z}) \\
&+ \frac{24i|z|^2(z+\bar{z})(z^2+10|z|^2+\bar{z}^2)}{(z-\bar{z})^5}P_4(z,\bar{z})\Bigg]\,, \tag{B.17c}
\end{aligned}$$

$$\begin{aligned}
C_3^{\text{fer}} = \frac{1}{16}\Bigg[&-\frac{1}{|1-z|^2} + \frac{|z|^2(z+\bar{z}-2|z|^2)}{(z-\bar{z})^2|1-z|^2}\log|z|^2 - \frac{|z|^2(z+\bar{z})}{2(z-\bar{z})^2|1-z|^2}\left(\log|z|^2\right)^2 \\
&- \frac{2|z|^2(z^2+4|z|^2+\bar{z}^2)\left(\log|z|^2\right)^2}{3(z-\bar{z})^4}\left(\frac{z+\bar{z}-2|z|^2}{2|1-z|^2}\log|z|^2 + \log|1-z|^2\right) \\
&+ \frac{2|z|^2}{(z-\bar{z})^2}\log|1-z|^2 + \frac{4i|z|^2(z+\bar{z})}{(z-\bar{z})^3}P_2(z,\bar{z}) + \frac{80|z|^2(z^2+4|z|^2+\bar{z}^2)}{(z-\bar{z})^4}P_3(z,\bar{z}) \\
&- \frac{4i|z|^2(z+\bar{z})(z^2+10|z|^2+\bar{z}^2)}{(z-\bar{z})^5}\left(60P_4(z,\bar{z}) + \left(\log|z|^2\right)^2 P_2(z,\bar{z})\right) \\
&+ \frac{4|z|^2(z^4+26z^3\bar{z}+66z^2\bar{z}^2+26z\bar{z}^3+\bar{z}^4)}{(z-\bar{z})^6}\left(60P_5(z,\bar{z}) + \left(\log|z|^2\right)^2 P_3(z,\bar{z})\right) \\
&- \frac{4i|z|^2(z+\bar{z})(z^4+56z^3\bar{z}+246z^2\bar{z}^2+56z\bar{z}^3+\bar{z}^4)}{3(z-\bar{z})^7}\left(60P_6(z,\bar{z}) + \left(\log|z|^2\right)^2 P_4(z,\bar{z})\right)\Bigg]\,. \tag{B.17d}
\end{aligned}$$

The two sets of results, (B.12) and (B.17), are simply linear combinations of each other, determined by the relation (B.15).

B.2   Summary of the $n=1$ correlators

To order $1/N$ all 4-point correlations functions of matter fields s_1 in $\text{AdS}_3 \times S^3$ are known [66, 73]. Using the notation

$$\mathcal{C}_{1,f_1f_2f_3f_4}^{\alpha\dot{\alpha},\beta\dot{\beta}} \equiv \langle \mathcal{O}_{f_1}^{--}(0)\mathcal{O}_{f_2}^{++}(\infty)\mathcal{O}_{f_3}^{\alpha\dot{\alpha}}(1)\mathcal{O}_{f_4}^{\beta\dot{\beta}}(z,\bar{z})\rangle\,, \tag{B.18}$$

one finds the following expressions

$$
\mathcal{C}^{++--}_{1,\,f_1 f_2 f_3 f_4} = \frac{1}{|1-z|^2}\left[\left(1 - \frac{1}{N}\right)\left(\delta_{f_1 f_2}\delta_{f_3 f_4} + |1-z|^2 \delta_{f_1 f_3}\delta_{f_2 f_4}\right) + \frac{2}{N\pi}|1-z|^2 |z|^2 \times \right.
$$
$$
\left. \left(\delta_{f_1 f_2}\delta_{f_3 f_4}\hat{D}_{1122}(z,\bar{z}) + \delta_{f_1 f_4}\delta_{f_2 f_3}\hat{D}_{2112}(z,\bar{z}) + \delta_{f_1 f_3}\delta_{f_2 f_4}\hat{D}_{1212}(z,\bar{z})\right)\right],
$$
$$\tag{B.19a}$$

$$
\mathcal{C}^{--++}_{1,\,f_1 f_2 f_3 f_4} = \frac{1}{|1-z|^2}\left[\left(1 - \frac{1}{N}\right)\left(\delta_{f_1 f_2}\delta_{f_3 f_4} + \frac{|1-z|^2}{|z|^2}\delta_{f_1 f_4}\delta_{f_2 f_3}\right) + \frac{2}{N\pi}|1-z|^2 \times \right.
$$
$$
\left. \left(\delta_{f_1 f_2}\delta_{f_3 f_4}\hat{D}_{1122}(z,\bar{z}) + \delta_{f_1 f_4}\delta_{f_2 f_3}\hat{D}_{2112}(z,\bar{z}) + \delta_{f_1 f_3}\delta_{f_2 f_4}\hat{D}_{1212}(z,\bar{z})\right)\right],
$$
$$\tag{B.19b}$$

$$
\mathcal{C}^{+--+}_{1,\,f_1 f_2 f_3 f_4} = -\frac{1}{|1-z|^2}\left[\left(1 - \frac{1}{N}\right)\delta_{f_1 f_2}\delta_{f_3 f_4} + \frac{2}{N\pi}|1-z|^2 z\left(\delta_{f_1 f_2}\delta_{f_3 f_4}\hat{D}_{1122}(z,\bar{z}) \right.\right.
$$
$$
\left.\left. + \delta_{f_1 f_4}\delta_{f_2 f_3}\hat{D}_{2112}(z,\bar{z}) + \delta_{f_1 f_3}\delta_{f_2 f_4}\hat{D}_{1212}(z,\bar{z})\right)\right],
$$
$$\tag{B.19c}$$

$$
\mathcal{C}^{-++-}_{1,\,f_1 f_2 f_3 f_4} = -\frac{1}{|1-z|^2}\left[\left(1 - \frac{1}{N}\right)\delta_{f_1 f_2}\delta_{f_3 f_4} + \frac{2}{N\pi}|1-z|^2 \bar{z}\left(\delta_{f_1 f_2}\delta_{f_3 f_4}\hat{D}_{1122}(z,\bar{z}) \right.\right.
$$
$$
\left.\left. + \delta_{f_1 f_4}\delta_{f_2 f_3}\hat{D}_{2112}(z,\bar{z}) + \delta_{f_1 f_3}\delta_{f_2 f_4}\hat{D}_{1212}(z,\bar{z})\right)\right].
$$
$$\tag{B.19d}$$

In the above we use the compact notation $\hat{D}_{\Delta_1,\Delta_2,\Delta_3,\Delta_4}$, which are specific combinations of logarithms of z and $\bar{z}$, and $P_2(z,\bar{z})$ – the second order Bloch-Wigner-Ramakrisnan function[62]. These functions naturally arise in four-point correlation functions in the context of the AdS/CFT correspondence [40, 56, 253]. For example, contact Witten diagrams in AdS_{d+1} involving four operators with scaling dimensions Δ_i, dual to scalar fields in the bulk, can be written as an integral over four scalar bulk-to-boundary propagators [254, 255]

$$
D_{\Delta_1,\Delta_2,\Delta_3,\Delta_4}(\vec{z}_i) = \int d^{d+1}w\,\sqrt{g}\,\prod_{i=1}^{4} K_{\Delta_i}(w;\vec{z}_i)\,, \tag{B.20}
$$

where we work in the Poincaré patch of AdS_{d+1} in Euclidean signature

$$
ds^2 = \frac{1}{\omega_0^2}\left(dw_0^2 + d\vec{w}^2\right)\,, \tag{B.21}
$$

---

[62]Note that while in the present context it might have been more natural to denote $\hat{D}_{\Delta_1,\Delta_2,\Delta_3,\Delta_4}$ as $\hat{P}^{(2)}_{\Delta_1,\Delta_2,\Delta_3,\Delta_4}$, we retain the notation commonly used in the literature as generalisations involving higher order BWR functions P_n are not known.

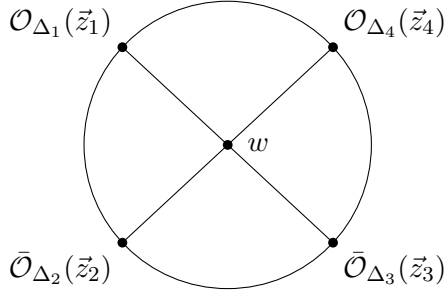**Figure B.1:** The contact Witten diagram corresponding to the integral (B.20). Four scalar operator insertions $\mathcal{O}_{\Delta_i}$ with scaling dimensions Δ_i interact via a quartic vertex in the bulk. In the expression for $D_{\Delta_1,\Delta_2,\Delta_3,\Delta_4}$ one has to integrate over all possible interaction points w.

with the flat d-dimensional boundary being located at $w_0 = 0$ and $\vec{z}_i$ with $i = 1, 2, 3, 4$ denoting four insertion points of the external operators on this boundary (see figure B.1). In this spacetime, bulk-to-boundary propagators take the form

$$K_{\Delta_i}(w; \vec{z}_i) = \left[\frac{w_0}{w_0^2 + (\vec{w} - \vec{z}_i)^2} \right]^{\Delta_i} , \tag{B.22}$$

which, after introducing four Schwinger parameters t_i, allows us to rewrite (B.20) as

$$D_{\Delta_1,\Delta_2,\Delta_3,\Delta_4}(\vec{z}_i) = \Gamma\left(\frac{\hat{\Delta} - d}{2} \right) \int_0^\infty \prod_{i=1}^4 \left[dt_i \frac{t_i^{\Delta_i - 1}}{\Gamma(\Delta_i)} \right] \frac{\pi^{d/2}}{2T^{\frac{\hat{\Delta}}{2}}} e^{- \sum_{i,j=1}^4 |\vec{z}_{ij}|^2 \frac{t_i t_j}{2T}} , \tag{B.23}$$

where

$$\vec{z}_{ij} = \vec{z}_i - \vec{z}_j , \qquad \hat{\Delta} = \sum_{i=1}^4 \Delta_i , \qquad T = \sum_{i=1}^4 t_i . \tag{B.24}$$

By rewriting the integral in this form, one notices that differentiating $D_{\Delta_1,\Delta_2,\Delta_3,\Delta_4}$ with respect to $|\vec{z}_{ij}|^2$ one obtains an expression which is proportional to the D-function related to contact diagrams with operator insertions that have higher scaling dimensions, for example

$$\frac{\partial}{\partial |\vec{z}_{12}|^2} D_{\Delta_1,\Delta_2,\Delta_3,\Delta_4}(\vec{z}_i) = -\frac{2\Delta_1 \Delta_2}{\hat{\Delta} - d} D_{\Delta_1+1,\Delta_2+1,\Delta_3,\Delta_4} . \tag{B.25}$$

Such relations become especially valuable, since in $d = 2$ one can evaluate

$$D_{1111}(\vec{z}_i) = \frac{2\pi i}{|\vec{z}_{13}|^2 |\vec{z}_{24}|^2 (z - \bar{z})} P_2(z, \bar{z}) , \tag{B.26}$$

where we used the conformal cross-ratios (B.3) and the second order Bloch-Wigner-Ramakrishnan polylogarithm function (3.23). Furthermore, recall that in our analysis we pick a specific gauge (2.26) and thus it is convenient to define a new set of functions

$$\hat{D}_{\Delta_1, \Delta_2, \Delta_3, \Delta_4}(z, \bar{z}) \equiv \lim_{z_2 \to \infty} |z_2|^{2\Delta_2} D_{\Delta_1, \Delta_2, \Delta_3, \Delta_4}(z_1 = 0, z_2, z_3 = 1, z_4 = z), \quad \text{(B.27)}$$

where z_i, which denote points on the two-dimensional boundary, are now complex variables[63]. Using this definition it follows that

$$\hat{D}_{1111}(z, \bar{z}) = \frac{2\pi i}{z - \bar{z}} P_2(z, \bar{z}), \quad \text{(B.29)}$$

while functions with higher values of the indices can be obtained from $\hat{D}_{1111}$ using the derivative relations (B.25) together with several identities that $\hat{D}$-functions satisfy, such as[64]

$$\hat{D}_{\Delta_2, \Delta_1, \Delta_3, \Delta_4}\left(\frac{1}{z}, \frac{1}{\bar{z}}\right) = |z|^{2\Delta_4} \hat{D}_{\Delta_1, \Delta_2, \Delta_3, \Delta_4}(z, \bar{z}). \quad \text{(B.30)}$$

Concretely, the functions appearing in (B.19) can be written explicitly as

$$\hat{D}_{1122}(z, \bar{z}) = \frac{-2\pi i}{(z - \bar{z})^2}\left[\frac{z + \bar{z}}{z - \bar{z}} P_2(z, \bar{z}) + \frac{\log|1 - z|^2}{2i} + \frac{z + \bar{z} - 2|z|^2}{4i|1 - z|^2} \log|z|^2\right], \quad \text{(B.31a)}$$

$$\hat{D}_{2112}(z, \bar{z}) = \frac{-2\pi i}{(z - \bar{z})^2}\left[\frac{2 - z - \bar{z}}{z - \bar{z}} P_2(z, \bar{z}) + \frac{z + \bar{z} - 2|z|^2}{4i|z|^2} \log|1 - z|^2 + \frac{\log|z|^2}{2i}\right], \quad \text{(B.31b)}$$

$$\hat{D}_{1212}(z, \bar{z}) = \frac{-2\pi i}{(z - \bar{z})^2}\left[\frac{2|z|^2 - z - \bar{z}}{z - \bar{z}} P_2(z, \bar{z}) + \frac{z + \bar{z} - 2}{4i} \log|1 - z|^2 - \frac{z + \bar{z}}{2i} \log|z|^2\right]. \quad \text{(B.31c)}$$

Let us conclude with the observation that the $\hat{D}$-functions written above can be written schematically as

$$\hat{D} \sim f_1(z, \bar{z}) P_2(z, \bar{z}) + f_2(z, \bar{z}) \log|1 - z|^2 + f_3(z, \bar{z}) \log|z|^2, \quad \text{(B.32)}$$

where $f_i(z, \bar{z})$ are some meromorphic functions of z and $\bar{z}$. The same structure can also

---

[63]Note that $\hat{D}$-functions are related to $\bar{D}$-functions, which are often used in the literature [45,254,255], by

$$\hat{D}_{\Delta_1, \Delta_2, \Delta_3, \Delta_4}(z, \bar{z}) = \frac{\pi \Gamma\left(\frac{\hat{\Delta} - 2}{2}\right)}{2 \prod_{i=1}^4 \Gamma(\Delta_i)} |z|^{\hat{\Delta} - 2\Delta_1 - 2\Delta_4} |1 - z|^{\hat{\Delta} - 2\Delta_3 - 2\Delta_4} \bar{D}_{\Delta_1, \Delta_2, \Delta_3, \Delta_4}(z, \bar{z}). \quad \text{(B.28)}$$

[64]Other identities can be found for example in [73, 80].

be seen in $\hat{D}$-functions with higher values for the indices and generalisations of (B.20) corresponding to higher n-point contact diagrams, discussed for example in [182]. Since $\hat{D}$-functions form the main building blocks of 4-point correlation functions in $\mathrm{AdS}_3 \times S^3$, it follows that correlators themselves should have the same structure.

B.3 R-symmetry projections

The R-symmetry group of the D1-D5 CFT is $SU(2)_L \times SU(2)_R$, as discussed in Section 2.2.2. The class of correlators considered in Section 3.4 are compactly given by

$$\mathcal{C}^{\alpha\dot{\alpha},\beta\dot{\beta}}_{n,f_1 f_2 f_3 f_4} = \langle (\mathcal{O}^{--}_{f_1})^n(0)(\mathcal{O}^{++}_{f_2})^n(\infty)\mathcal{O}^{\alpha\dot{\alpha}}_{f_3}(1)\mathcal{O}^{\beta\dot{\beta}}_{f_4}(z,\bar{z}) \rangle \ , \tag{B.33}$$

where α, β and $\dot{\alpha}, \dot{\beta}$ are $SU(2)_L$ and $SU(2)_R$ fundamental indices respectively. The single-trace operators transform in the $(\mathbf{2}, \mathbf{2})$ irreducible representation of the $SU(2)_L \times SU(2)_R$ R-symmetry. Note that the usual physics notation for the representations of $SU(2)$ are using the quantity j (and $\bar{j}$ for the right-hand sector) related to the dimension of the representation R by $\dim(R) = 2j + 1$. In this notation the operators $\mathcal{O}^{\alpha\dot{\alpha}}_{f_3}$ are in the $(j, \bar{j}) = (\frac{1}{2}, \frac{1}{2})$ representation of the R-symmetry group. The double-trace operators of the form $: \mathcal{O}^{\alpha\dot{\alpha}}_{f_3} \mathcal{O}^{\beta\dot{\beta}}_{f_4} : \sim \mathcal{O}^{\alpha\beta,\dot{\alpha}\dot{\beta}}_{f_3 f_4}$ exchanged in the $z \to 1$ OPE channel of these correlators can then be classified by representations of the tensor product group $SU(2) \times SU(2)$ in both the left and right sectors. In this section we detail the projectors onto the irreducible representations of the tensor product group.

We start by constructing the Euclidean signature gamma matrices in the Weyl basis for $I = 0, 1, 2, 3$ as

$$\gamma^I_E = \begin{pmatrix} 0 & \sigma^I \\ \bar{\sigma}^I & 0 \end{pmatrix} \quad \text{where} \quad \sigma^I_{\alpha\dot{\alpha}} = (\mathbb{I}_2 \,, -i\underline{\sigma})_{\alpha\dot{\alpha}} \quad , \quad \bar{\sigma}^{I\dot{\alpha}\alpha} = (\mathbb{I}_2 \,, i\underline{\sigma})^{\dot{\alpha}\alpha} \ , \tag{B.34}$$

where $\underline{\sigma}$ is a 3-vector of the usual $SU(2)$ generators – the Pauli matrices

$$\sigma_1 = \begin{pmatrix} 0 & 1 \\ 1 & 0 \end{pmatrix} \quad , \quad \sigma_2 = \begin{pmatrix} 0 & -i \\ i & 0 \end{pmatrix} \quad , \quad \sigma_3 = \begin{pmatrix} 1 & 0 \\ 0 & -1 \end{pmatrix} . \tag{B.35}$$

The gamma matrices (B.34) satisfy the $Cl_{4,0}(\mathbb{R}) = Cl_4(\mathbb{R})$ Clifford algebra

$$\{\gamma^I_E, \gamma^J_E\} = 2\delta^{IJ}\mathbb{I}_4 \ , \tag{B.36}$$

where δ_{IJ} is the usual metric on 4-dimensional Euclidean space. The choice of gamma

matrices in (B.34) yields the fifth gamma matrix in the diagonal form

$$\gamma_E^5 \equiv -\gamma^0\gamma^1\gamma^2\gamma^3 = \begin{pmatrix} \mathbb{I}_2 & 0 \\ 0 & -\mathbb{I}_2 \end{pmatrix} \, . \tag{B.37}$$

One can define the anti-symmetrised combinations of the σ and $\bar{\sigma}$ $SO(4)$ vectors

$$\sigma^{IJ}{}_\alpha{}^\beta \equiv \frac{i}{4}\big(\sigma^I\bar{\sigma}^J - \sigma^J\bar{\sigma}^I\big)_\alpha{}^\beta = \frac{i}{4}\big(\sigma^I_{\alpha\dot\alpha}\bar{\sigma}^{J\dot\alpha\beta} - \sigma^J_{\alpha\dot\alpha}\bar{\sigma}^{I\dot\alpha\beta}\big) \, ,$$

$$\bar{\sigma}^{IJ}{}_{\dot\alpha}{}^{\dot\beta} \equiv \frac{i}{4}\big(\bar{\sigma}^I\sigma^J - \bar{\sigma}^J\sigma^I\big)_{\dot\alpha}{}^{\dot\beta} = \frac{i}{4}\big(\bar{\sigma}^{I\dot\beta\beta}\sigma^J_{\beta\dot\alpha} - \bar{\sigma}^{J\dot\beta\beta}\sigma^I_{\beta\dot\alpha}\big) \, , \tag{B.38}$$

which satisfy the (anti-)self-duality conditions

$$\frac{1}{2}\epsilon^{IJKL}\sigma_{KL}{}_\alpha{}^\beta = \sigma^{IJ}{}_\alpha{}^\beta \, ,$$

$$\frac{1}{2}\epsilon^{IJKL}\bar{\sigma}_{KL}{}_{\dot\alpha}{}^{\dot\beta} = -\bar{\sigma}^{IJ}{}_{\dot\alpha}{}^{\dot\beta} \, , \tag{B.39}$$

and the commutation relations

$$\big[\sigma^{IJ}, \sigma^{KL}\big]_\alpha{}^\beta = \big(\delta^{IL}\sigma^{JK} + \delta^{JK}\sigma^{IL} - \delta^{IK}\sigma^{JL} - \delta^{JL}\sigma^{IK}\big)_\alpha{}^\beta \, , \tag{B.40}$$

and similarly for $\bar{\sigma}^{IJ}$. The $SU(2)_L$ and $SU(2)_R$ indices are raised with $\epsilon^{\alpha\beta}$ and $\epsilon^{\dot\alpha\dot\beta}$ respectively – such that $\epsilon^{12} = 1$ and $\chi^\alpha = \epsilon^{\alpha\beta}\chi_\beta$. The Fierz identity for the decomposition of irreps of $SU(2)$ for $\mathbf{2} \otimes \mathbf{2} = \mathbf{0} \oplus \mathbf{3}$ are

$$\chi^\alpha\psi^\beta = \frac{1}{2}\epsilon^{\alpha\beta}\big(\chi\psi\big) + \frac{1}{2}\sigma^{IJ\alpha\beta}\big(\chi\,\sigma_{IJ}\,\psi\big) \, . \tag{B.41}$$

The singlet projection of the object $\chi^\alpha\psi^\beta$ is then given by $\frac{1}{2}\epsilon^{\alpha\beta}$ since the scalar product is $\chi\psi \equiv \chi^\gamma\psi_\gamma = \chi^\gamma\epsilon_{\gamma\delta}\psi^\delta$. The projection onto the triplet of $SU(2)$ is then the bilinear $\frac{1}{2}\big(\chi\,\sigma_{IJ}\,\psi\big) = \frac{1}{2}\big(\chi^\gamma\sigma_{IJ\gamma\delta}\lambda^\delta\big)$ for which there are three independent choices of I and J due to σ^{IJ} being anti-symmetric and self-dual – one can choose

$$\sigma^{01}_{\alpha\beta} \sim \begin{pmatrix} 1 & 0 \\ 0 & -1 \end{pmatrix}_{\alpha\beta} \, , \quad \sigma^{02}_{\alpha\beta} \sim \begin{pmatrix} 1 & 0 \\ 0 & 1 \end{pmatrix}_{\alpha\beta} \, , \quad \sigma^{03}_{\alpha\beta} = \frac{1}{2}\begin{pmatrix} 0 & 1 \\ 1 & 0 \end{pmatrix}_{\alpha\beta} \, . \tag{B.42}$$

Including both the left and right sectors requires the equivalent expression for the decomposition $(\frac{1}{2}, \frac{1}{2}) \otimes (\frac{1}{2}, \frac{1}{2}) = (0,0) \oplus (1,0) \oplus (0,1) \oplus (1,1)$ which follows trivially from (B.41) with the triplet projection in the right sectors using instead $\bar{\sigma}^{IJ}$.

For our correlators we have that $\mathcal{C}^{\alpha\dot\alpha, \beta\dot\beta}_{n, f_1 f_2 f_3 f_4} = 0$ for $\alpha = \beta$ or $\dot\alpha = \dot\beta$ and so the only non-zero triplet projection out those in (B.42) is that of σ^{03}. We then arrive at the

four R-symmetry projections of the $n = 1$ correlators:

$$\mathcal{C}_{1(0,0)} \equiv \frac{1}{4} \, \epsilon_{\alpha\beta} \, \epsilon_{\dot\alpha\dot\beta} \, \mathcal{C}_{1,f_1f_2f_3f_4}^{\alpha\dot\alpha,\beta\dot\beta} = \frac{1}{4}\left(\mathcal{C}^{++--} - \mathcal{C}^{+--+} - \mathcal{C}^{-++-} + \mathcal{C}^{--++}\right)$$

$$= \left(1 - \frac{1}{N}\right)\left(\frac{1}{4|1-z|^2}\delta_{f_1f_2}\delta_{f_3f_4} + \frac{1}{4|z|^2}\delta_{f_1f_4}\delta_{f_2f_3} + \frac{1}{4}\delta_{f_1f_3}\delta_{f_2f_4}\right)$$

$$+ \frac{2}{N\pi}\frac{1 + |z|^2 + \bar{z} + z}{4}\left[\delta_{f_1f_2}\delta_{f_3f_4}\hat{D}_{1122} + \delta_{f_1f_4}\delta_{f_2f_3}\hat{D}_{2112} + \delta_{f_1f_3}\delta_{f_2f_4}\hat{D}_{1212}\right],$$
$$(\text{B.43a})$$

$$\mathcal{C}_{1(1,0)} \equiv \frac{1}{2} \, \sigma_{\alpha\beta}^{03} \, \epsilon_{\dot\alpha\dot\beta} \, \mathcal{C}_{1,f_1f_2f_3f_4}^{\alpha\dot\alpha,\beta\dot\beta} = \frac{1}{4}\left(\mathcal{C}^{+--+} - \mathcal{C}^{++--} - \mathcal{C}^{-++-} + \mathcal{C}^{--++}\right)$$

$$= \left(1 - \frac{1}{N}\right)\left(\frac{1}{4|z|^2}\delta_{f_1f_4}\delta_{f_2f_3} - \frac{1}{4}\delta_{f_1f_3}\delta_{f_2f_4}\right) + \frac{2}{N\pi}\frac{1 - |z|^2 + \bar{z} - z}{4}\Bigg[$$

$$\delta_{f_1f_2}\delta_{f_3f_4}\hat{D}_{1122} + \delta_{f_1f_4}\delta_{f_2f_3}\hat{D}_{2112} + \delta_{f_1f_3}\delta_{f_2f_4}\hat{D}_{1212}\Bigg],$$
$$(\text{B.43b})$$

$$\mathcal{C}_{1(0,1)} \equiv \frac{1}{2} \, \epsilon_{\alpha\beta} \, \bar\sigma_{\dot\alpha\dot\beta}^{03} \, \mathcal{C}_{1,f_1f_2f_3f_4}^{\alpha\dot\alpha,\beta\dot\beta} = \frac{1}{4}\left(\mathcal{C}^{+--+} + \mathcal{C}^{++--} - \mathcal{C}^{-++-} - \mathcal{C}^{--++}\right)$$

$$= \left(1 - \frac{1}{N}\right)\left(\frac{1}{4}\delta_{f_1f_3}\delta_{f_2f_4} - \frac{1}{4|z|^2}\delta_{f_1f_4}\delta_{f_2f_3}\right) + \frac{2}{N\pi}\frac{-1 + |z|^2 + \bar{z} - z}{4}\Bigg[$$

$$\delta_{f_1f_2}\delta_{f_3f_4}\hat{D}_{1122} + \delta_{f_1f_4}\delta_{f_2f_3}\hat{D}_{2112} + \delta_{f_1f_3}\delta_{f_2f_4}\hat{D}_{1212}\Bigg],$$
$$(\text{B.43c})$$

$$\mathcal{C}_{1(1,1)} \equiv \sigma_{\alpha\beta}^{03} \, \bar\sigma_{\dot\alpha\dot\beta}^{03} \, \mathcal{C}_{1,f_1f_2f_3f_4}^{\alpha\dot\alpha,\beta\dot\beta} = \frac{1}{4}\left(\mathcal{C}^{+--+} + \mathcal{C}^{++--} + \mathcal{C}^{-++-} + \mathcal{C}^{--++}\right)$$

$$= \left(1 - \frac{1}{N}\right)\left(\frac{1}{4|z|^2}\delta_{f_1f_4}\delta_{f_2f_3} + \frac{1}{4}\delta_{f_1f_3}\delta_{f_2f_4}\right) + \frac{2}{N\pi}\frac{1 + |z|^2 - \bar{z} - z}{4}\Bigg[$$

$$\delta_{f_1f_2}\delta_{f_3f_4}\hat{D}_{1122} + \delta_{f_1f_4}\delta_{f_2f_3}\hat{D}_{2112} + \delta_{f_1f_3}\delta_{f_2f_4}\hat{D}_{1212}\Bigg],$$
$$(\text{B.43d})$$

where the $n = 1$ correlators $\mathcal{C}^{++--}, \mathcal{C}^{+--+}, \mathcal{C}^{--++}, \mathcal{C}^{-++-}$ are given in (B.19).

B.4   Euclidean $z, \bar{z} \to 1$ OPE data of $C_{n=1}$

In this section we give details on the extraction of the Euclidean $z, \bar{z} \to 1$ analysis of the connected correlator C_1 containing double-trace operators from Section 3.4.2 to arbitrary orders in $(1 - z)$. We only consider the exchange of double-trace operators of minimal twist $(\bar{\mathcal{O}}\mathcal{O})_k \sim \bar{\mathcal{O}}\partial^k\mathcal{O}$ and use the case of the the $n = 1$ correlator projected onto the R-symmetry and flavour irreps. This is given by (B.43a) with the additional

projection (3.41a) applied, yielding

$$
C^{\text{sing}}_{(0,0)} = \frac{1}{|1-z|^2} \left[\left(1 - \frac{1}{N} \right) \left(N_f + \frac{|1-z|^2}{4} + \frac{|1-z|^2}{4|z|^2} \right) \right.
$$
$$
\left. + \frac{2|1-z|^2}{N\pi} \frac{1+|z|^2+z+\bar{z}}{4} \left(N_f \hat{D}_{1122} + \hat{D}_{2112} + \hat{D}_{1212} \right) \right] . \tag{B.44}
$$

where the relevant D-functions are given in (B.31). Expanding this in the $z, \bar{z} \to 1$ channel at order $(1-\bar{z})^0$ gives

$$
C^{\text{sing}}_{1\,(0,0)} \approx \sum_{t=0}^{\infty} (1-z)^t \left[\frac{1}{2N} \left(\frac{(t^2+t+2)N_f}{(t+1)(t+2)(t+3)} - \left(1+\delta_{t,0}\right) \right) \log|1-z|^2 + \frac{1+\delta_{t,0}}{4} \right.
$$
$$
\left. + \frac{1}{N} \left(A_t N_f + B_t \right) \right] + \sum_{t=0}^{\infty} \frac{(-1)^t(1-z)^{t+2}}{N|1-z|^2} \frac{(t+1)N_f}{2(t+2)(t+3)} , \tag{B.45}
$$

with the coefficients A_t and B_t given by

$$
A_t = \left\{ -\frac{7}{36}, -\frac{1}{72}, -\frac{1}{225}, -\frac{1}{900}, \frac{61}{44100}, \frac{23}{7056}, \frac{293}{63504}, \cdots \right\} ,
$$
$$
B_t = \left\{ \frac{1}{2}, -\frac{1}{4}, -\frac{1}{6}, -\frac{1}{6}, -\frac{7}{40}, -\frac{11}{60}, -\frac{4}{21}, \cdots \right\} . \tag{B.46}
$$

The goal is to write the conformal block decomposition of this correlator in the s-channel up to order $1/N$ and at order $(1-\bar{z})^0$ with generic $(1-z)$. As discussed in Section 3.4.2, there are triple-trace operators that mix with the R-symmetry and flavour singlet double-trace operators

$$
\mathcal{O}^{\text{sing}}_{k,\bar{k}} \equiv :\bar{\mathcal{O}}_f \partial^k \bar{\partial}^{\bar{k}} \mathcal{O}_f :^{\text{sing}}_{(0,0)} , \tag{B.47}
$$

even at order $1/N$, however, these contributions to the correlator (B.45) are only in the $1/N$ rational terms. As discussed in Section 2.1.1 the contribution of a given quasi-primary and its global descendants to a correlation function is packaged into global conformal blocks (2.33), up to the OPE coefficients (2.27). The general form of a quasi-primary's contribution to a correlator of the form $C = \langle \bar{\mathcal{O}}_1(0)\mathcal{O}_1(\infty)\mathcal{O}_2(1)\bar{\mathcal{O}}_2(z,\bar{z}) \rangle$ in the direct channel is thus

$$
C(z,\bar{z}) \sim (1-z)^{-2h_2+h}(1-\bar{z})^{-2\bar{h}_2+\bar{h}} C_{11h} C_{h22} \,_2F_1(h,h;2h;1-z) \,_2F_1(\bar{h},\bar{h};2\bar{h};1-\bar{z}) , \tag{B.48}
$$

where $h, \bar{h}$ are the dimensions of the exchanged primary. Conserved currents, having either h or $\bar{h}$ equal to zero, will be the only operators contributing with negative powers of either $(1-z)$ or $(1-\bar{z})$ and so their contributions in (B.45) can be easily identified.

The contribution of the operators (B.47), with dimensions

$$h_{k,\bar{k}} = 1 + k + \gamma_{(0,0)}^{\text{sing},k,\bar{k}} \quad , \quad \bar{h}_{k,\bar{k}} = 1 + \bar{k} + \gamma_{(0,0)}^{\text{sing},k,\bar{k}} \ , \tag{B.49}$$

to the correlator (B.44) (whose external operators have dimensions $(1/2, 1/2)$) will then be

$$C_{1\,(0,0)}^{\text{sing}} \sim |1 - z|^{-2} \sum_{k,\bar{k}=0}^{\infty} \left| c_{(0,0)}^{\text{sing},k,\bar{k}} \right|^2 (1-z)^{h_{k,\bar{k}}} (1-\bar{z})^{\bar{h}_{k,\bar{k}}} {}_2F_1\big(h_{k,\bar{k}}, h_{k,\bar{k}}; 2h_{k,\bar{k}}; 1-z\big)$$

$$\times {}_2F_1\big(\bar{h}_{k,\bar{k}}, \bar{h}_{k,\bar{k}}; 2\bar{h}_{k,\bar{k}}; 1-\bar{z}\big) \ . \tag{B.50}$$

The minimal twist double-trace operators have $\bar{k} = 0$ and so from now on, these are the contributions that we consider. For ease of notation we redefine $\left| c_{(0,0)}^{\text{sing},k,0} \right|^2 \equiv \left| c_{(0,0)}^{\text{sing},k} \right|^2$ and $\gamma_{(0,0)}^{\text{sing},k,0} \equiv \gamma_{(0,0)}^{\text{sing},k}$ as in the main text. We now expand these contributions in the large N limit up to order $1/N$

$$C_{1\,(0,0)}^{\text{sing}} \approx \sum_{k=0}^{\infty} (1-z)^k \left(\left| c_{(0)(0,0)}^{\text{sing},k} \right|^2 + \frac{1}{N} \left| c_{(1)(0,0)}^{\text{sing},k} \right|^2 \right) \left(1 + \frac{1}{N} \gamma_{(1)(0,0)}^{\text{sing},k} \log|1-z|^2 \right)$$

$$\times \left(1 + \frac{1}{N} \gamma_{(1)(0,0)}^{\text{sing},k} \partial_k \right) F_k$$

$$\approx \sum_{k=0}^{\infty} (1-z)^k \left[\left| c_{(0)(0,0)}^{\text{sing},k} \right|^2 + \frac{1}{N} \left(\left| c_{(1)(0,0)}^{\text{sing},k} \right|^2 + \left| c_{(0)(0,0)}^{\text{sing},k} \right|^2 \gamma_{(1)(0,0)}^{\text{sing},k} \big(\log|1-z|^2 + \partial_k \big) \right) \right] F_k \ , \tag{B.51}$$

where the expansion of the data

$$\left| c_{(0,0)}^{\text{sing},k} \right|^2 \approx \left| c_{(0)(0,0)}^{\text{sing},k} \right|^2 + \frac{1}{N} \left| c_{(1)(0,0)}^{\text{sing},k} \right|^2 + \dots \ ,$$

$$\gamma_{(0,0)}^{\text{sing},k} \approx \frac{1}{N} \gamma_{(1)(0,0)}^{\text{sing},k} + \dots \ , \tag{B.52}$$

has been used, along with

$$\partial_{\frac{1}{N}} {}_2F_1\big(h_{k,0}, h_{k,0}; 2h_{k,0}; 1-z\big)\Big|_{N \to \infty} = \gamma_{(0,0)}^{\text{sing},k} \partial_k F_k \ ,$$

$$F_k \equiv {}_2F_1(1+k, 1+k; 2+2k; 1-z) \tag{B.53}$$

As noted in Section 3.4.2 we have cheated here slightly, since only the leading term $\left| c_{(0)(0,0)}^{\text{sing},k} \right|^2$ can be interpreted as a three-point function involving the double-trace operators (B.47). The higher-order terms are a mixture of the subleading double-trace OPE coefficients and leading-order triple-trace OPE coefficients at a given level. As in Section 3.4.2, we content ourselves with finding the sum of these contributions which we call $\left| c_{(1)(0,0)}^{\text{sing},k} \right|^2$. In order to match (B.51) term by term in powers of $(1-z)$ with the

expansion of the explicit correlator (B.45) we need to use a series representation of the hypergeometric function F_k and its k derivative given by

$$F_k = \sum_{q=0}^{\infty} \frac{(1+k)_q^2 (1-z)^q}{q!(2+2k)_q} \, , \tag{B.54a}$$

$$\partial_k F_k = \sum_{q=0}^{\infty} \frac{(1+k)_q^2 (1-z)^q}{q!(2+2k)_q} \, \mathcal{H}_{q,k}^{(1)} \, , \tag{B.54b}$$

where

$$\mathcal{H}_{q,k}^{(1)} \equiv 2\big(H_{2k+1} - H_k + H_{k+q} - H_{2k+q+1}\big) \, . \tag{B.55}$$

Using these results, (B.51) can be rewritten as

$$
\begin{aligned}
C_{1\,(0,0)}^{\text{sing}} \approx \sum_{t=0}^{\infty} \sum_{k=0}^{t} \frac{(1+k)_{t-k}^2 (1-z)^t}{(t-k)!(2+2k)_{t-k}} \Bigg[\left| c_{(0)(0,0)}^{\text{sing},k} \right|^2 + \frac{1}{N} \left(\left| c_{(1)(0,0)}^{\text{sing},k} \right|^2 \right. \\
\left. + \left| c_{(0)(0,0)}^{\text{sing},k} \right|^2 \gamma_{(1)(0,0)}^{\text{sing},k} \left(\log |1-z|^2 + \mathcal{H}_{t-k,k}^{(1)} \right) \right) \Bigg] \, ,
\end{aligned}
\tag{B.56}
$$

where we relabelled the series as $\sum_{k=0}^{\infty} \sum_{q=0}^{\infty} \to \sum_{t=0}^{\infty} \sum_{k=0}^{t}$ where $t = k + q$. Thus, comparing (B.45) and (B.56) per order in $(1-z)$, $1/N$ and the number of logs we get the relations

$$\frac{1+\delta_{t,0}}{4} = \sum_{k=0}^{t} \frac{(1+k)_{t-k}^2}{(t-k)!(2+2k)_{t-k}} \left| c_{(0)(0,0)}^{\text{sing},k} \right|^2 \, , \tag{B.57a}$$

$$A_t N_f + B_t = \sum_{k=0}^{t} \frac{(1+k)_{t-k}^2}{(t-k)!(2+2k)_{t-k}} \left| c_{(1)(0,0)}^{\text{sing},k} \right|^2 \, , \tag{B.57b}$$

$$\frac{(t^2+t+2)N_f}{2(t+1)(t+2)(t+3)} - \frac{1+\delta_{t,0}}{2} = \sum_{k=0}^{t} \frac{(1+k)_{t-k}^2}{(t-k)!(2+2k)_{t-k}} \left| c_{(0)(0,0)}^{\text{sing},k} \right|^2 \gamma_{(1)(0,0)}^{\text{sing},k} \, , \tag{B.57c}$$

with the terms A_t and B_t given in (B.46). These equations can then be solved recursively per value of t to obtain the data quoted in the main text in (3.49), (3.51) and (3.52).

Appendix C

Double-trace Data from the Inversion Formula

In this section we derive the anomalous dimensions and OPE coefficients that were presented in section 3.4.2 using the Lorentzian inversion formula [68,256]. In particular, we are interested in the OPE data of double-trace operators exchanged in the $z, \bar{z} \to 1$ (or equivalently $z_1 \to z_2$) channel of the $n = 1$ correlator in (3.40), which can be extracted from the singularities of the remaining two channels.

Begin by writing the four-point correlation function as

$$
\mathcal{C}_{n=1,f_1f_2f_3f_4}^{\alpha\dot{\alpha},\beta\dot{\beta}} = \langle \mathcal{O}_{f_1}^{--}(0)\mathcal{O}_{f_2}^{++}(\infty)\mathcal{O}_{f_3}^{\alpha\dot{\alpha}}(1)\mathcal{O}_{f_4}^{\beta\dot{\beta}}(z,\bar{z})\rangle = \frac{1}{|1-z|^2}\mathcal{G}_{n=1,f_1f_2f_3f_4}^{\alpha\dot{\alpha},\beta\dot{\beta}}(z,\bar{z}) \ ,
\tag{C.1}
$$

where we used the conformal cross-ratios $z, \bar{z}$ defined in (2.19). Here we find it convenient instead to define

$$
Z = \frac{z_{12}z_{34}}{z_{13}z_{24}} \quad , \quad \bar{Z} = \frac{\bar{z}_{12}\bar{z}_{34}}{\bar{z}_{13}\bar{z}_{24}} \ ,
\tag{C.2}
$$

which are related to the $z, \bar{z}$ by

$$
z = 1 - Z \ , \quad \bar{z} = 1 - \bar{Z} \ ,
\tag{C.3}
$$

and as before $z_{ij} = z_i - z_j$. The use of these capitalised conformal cross-ratios allows us to make close contact with [68] (see also [69,197]). The s-channel OPE limit $z_1 \to z_2$, which corresponds to taking $Z, \bar{Z} \to 0$, can be written as a sum over the exchange of quasi-primary operators, with spin $k = |h - \bar{h}|$ and scaling dimension $\Delta = h + \bar{h}$. The Lorentzian inversion formula states that for large enough spin the CFT data in the

s-channel is completely encapsulated by a function[65]

$$c(h, \bar{h}) \equiv c^t(h, \bar{h}) + (-1)^k c^u(h, \bar{h}) \,, \tag{C.4}$$

which is analytic in spin and built from the information of the t-channel ($Z \to 1$) and u-channel ($Z \to \infty$) of the correlator, with the details of the function depending on the external operators and the dimension of the spacetime. Assuming $h \geq \bar{h}$, so that $k = h - \bar{h}$ and

$$h = \frac{\Delta + k}{2} \,, \qquad \bar{h} = \frac{\Delta - k}{2} \,, \tag{C.5}$$

in $d = 2$ and for the correlator (C.1), we use

$$c^t(h, \bar{h}) \equiv \frac{\kappa}{2} \int_0^1 \frac{dZ}{Z^2} \frac{d\bar{Z}}{\bar{Z}^2} \, g_h(Z) \, g_{1-\bar{h}}(\bar{Z}) \, \mathrm{dDisc}\big[\mathcal{G}(Z, \bar{Z})\big] \,, \tag{C.6}$$

where

$$\kappa = \frac{\Gamma^4(h)}{2\pi^2 \, \Gamma(2h - 1) \, \Gamma(2h)} \,, \tag{C.7a}$$

$$g_h(Z) = z^h \, {}_2F_1(h, h, 2h, Z) \,. \tag{C.7b}$$

The double discontinuity that picks out the relevant singularities we take to be

$$\mathrm{dDisc}\big[\mathcal{G}(Z, \bar{Z})\big] \equiv \mathcal{G}(Z, \bar{Z}) - \frac{1}{2}\Big(\mathcal{G}_\circlearrowright(Z, \bar{Z}) + \mathcal{G}_\circlearrowleft(Z, \bar{Z})\Big) \,, \tag{C.8}$$

where we analytically continue around $Z = 1$, while leaving $\bar{Z}$ fixed as[66]

$$\mathcal{G}_\circlearrowright(Z, \bar{Z}) : \qquad (1 - Z) \to e^{-2\pi i}(1 - Z) \,, \tag{C.9a}$$

$$\mathcal{G}_\circlearrowleft(Z, \bar{Z}) : \qquad (1 - Z) \to e^{2\pi i}(1 - Z) \,. \tag{C.9b}$$

The function $c^u(h, \bar{h})$ can be obtained in a similar manner, only that the analytic continuation is performed around $Z \to \infty$. In practice, this can be done by swapping $z_1 \leftrightarrow z_2$, so that $z \to z^{-1}$ and $\bar{z} \to \bar{z}^{-1}$ followed by using (C.3), in which case one can again analytically continue around $Z = 1$ as in (C.9).

The CFT data is contained in the analytic structure of the inversion function. The location of simple poles gives information about the twists of the exchanged quasi-primary operators, while the residue at that pole is related to the coefficients of *global* blocks in the s-channel. If only one quasi-primary for given conformal dimensions

---

[65]Here we suppress flavour and R-symmetry indices until we consider specific correlators.

[66]Note that in [68] the analytic continuation is performed around $\bar{Z} = 1$, however, there h and $\bar{h}$ are exchanged as compared to (C.5).

contributes to the correlator under question, these coefficients will simply be the square of the OPE coefficients of external operators with the quasi-primary. The precise form of (C.4) near a pole corresponding to the exchange of a quasi-primary with left- and right-moving conformal dimensions $(h_p, \bar{h}_p)$ is given by

$$c(h, \bar{h}) \sim -\frac{1}{2} \frac{C^2_{h_p, \bar{h}_p}}{\bar{h} - \bar{h}_p}, \tag{C.10}$$

where the factor of $1/2$ comes from replacing the twist $\Delta - k$ with $\bar{h}$.

We aim to reproduce the CFT data of double-trace operators exchanged in the s-channel of (C.1), having the schematic form $:\mathcal{O}\bar{\mathcal{O}}:_{\bar{n},k} \sim \mathcal{O}_{f_3} \partial^{\bar{n}+k} \bar{\partial}^{\bar{n}} \bar{\mathcal{O}}_{f_4}$, for which at large N

$$h_{\bar{n},k} = 1 + \bar{n} + k + \frac{\gamma^{\bar{n},k}_{(1)}}{N} + O(1/N^2), \tag{C.11a}$$

$$\bar{h}_{\bar{n},k} = 1 + \bar{n} + \frac{\gamma^{\bar{n},k}_{(1)}}{N} + O(1/N^2), \tag{C.11b}$$

with $\gamma^{\bar{n},k}_{(1)}$ denoting the anomalous dimensions. We also expand the residues in large N (see Section 3.4.2 for a more detailed discussion on the relation of these coefficients to the 3-point functions of the double-trace operators $:\mathcal{O}\bar{\mathcal{O}}:_{\bar{n},k}$)

$$C^2_{h_p \bar{h}_p} = \left| c^{\bar{n},k}_{(0)} \right|^2 + \frac{1}{N} \left| c^{\bar{n},k}_{(1)} \right|^2 + O(1/N^2). \tag{C.12}$$

Inserting these expressions into (C.10) and expanding in $1/N$ yields

$$c(h, \bar{h}) \approx -\frac{1}{2} \left[\frac{|c^{\bar{n},k}_{(0)}|^2}{\bar{h} - (1+\bar{n})} + \frac{1}{N} \left(\frac{|c^{\bar{n},k}_{(1)}|^2}{\bar{h} - (1+\bar{n})} + \frac{|c^{\bar{n},k}_{(0)}|^2 \gamma^{\bar{n},k}_{(1)}}{(\bar{h} - (1+\bar{n}))^2} \right) \right] + O(1/N^2), \tag{C.13}$$

and thus one is able to extract the unknown quantities by analysing poles of different degrees at $\bar{h} = 1 + \bar{n}$, order by order in the large N expansion. In particular, to make contact with the analysis of section 3.4.2, we focus on the minimal-twist operators[67] $:\mathcal{O}\bar{\mathcal{O}}:_k \sim \mathcal{O}_{f_3} \partial^k \bar{\mathcal{O}}_{f_4}$, with $\bar{n} = 0$, for which we can extract the CFT data by other independent methods as well.

Let us now consider the specific example of the $n = 1$ correlator (3.40) in the

---

[67]To avoid the cluttering of indices and to have notation consistent with section 3.4, the CFT data of double-traces with $\bar{n} = 0$ will only have a single index k denoting the spin of the exchanged operator, for example $\gamma^k_{(1)} \equiv \gamma^{\bar{n}=0,k}_{(1)}$.

R-symmetry singlet projection

$$
\mathcal{G}_{1,\,f_1f_2f_3f_4}^{(0,0)}(z,\bar{z}) = \left(1 - \frac{1}{N}\right)\left(\delta_{f_1f_2}\delta_{f_3f_4} + \frac{|1-z|^2}{4}\delta_{f_1f_3}\delta_{f_2f_4} + \frac{|1-z|^2}{4|z|^2}\delta_{f_1f_4}\delta_{f_2f_3}\right)
$$

$$
+ \frac{|1-z|^2}{N\pi}\frac{|1+z|^2}{2}\left(\delta_{f_1f_2}\delta_{f_3f_4}\hat{D}_{1122} + \delta_{f_1f_4}\delta_{f_2f_3}\hat{D}_{2112} + \delta_{f_1f_3}\delta_{f_2f_4}\hat{D}_{1212}\right),
$$

$$(C.14)$$

where the D-functions are given in (B.31). We first analyse the t-channel contribution $c^t(h,\bar{h})$ to the inversion formula. Begin by using (C.3) to rewrite $\mathcal{G}_{1,\,f_1f_2f_3f_4}^{(0,0)}$ in terms of Z and $\bar{Z}$, expand the expression in[68] $(1-Z)/Z$ to find

$$
\mathcal{G}_{1,\,f_1f_2f_3f_4}^{(0,0)}(1-Z,1-\bar{Z}) \sim \frac{\delta_{f_1f_4}\delta_{f_2f_3}}{4}\,\widetilde{\mathcal{G}}_1^{(0,0)}(\bar{Z})\,\frac{Z}{1-Z} + \dots,\qquad (C.15)
$$

where

$$
\widetilde{\mathcal{G}}_1^{(0,0)}(\bar{Z}) = \left[\frac{\bar{Z}}{1-\bar{Z}} - \frac{1}{N}\left(\frac{\bar{Z}}{1-\bar{Z}} + \left(2\frac{\bar{Z}}{1-\bar{Z}} + \frac{\bar{Z}^2}{(1-\bar{Z})^2}\right)\log\bar{Z}\right)\right].\qquad (C.16)
$$

In (C.15) we only show terms that are non-vanishing after taking the double discontinuity (C.8), which are poles and *double* logarithms at $Z=1$. After inserting (C.15) into (C.6) the integrals factorise to give

$$
c^t(h,\bar{h}) = \frac{\delta_{f_1f_4}\delta_{f_2f_3}}{4}\frac{\kappa}{2}\int_0^1\frac{dZ}{Z^2}\,g_h(Z)\,\mathrm{dDisc}\left[\frac{Z}{1-Z}\right]\int_0^1\frac{d\bar{Z}}{\bar{Z}^2}\,g_{1-\bar{h}}(\bar{Z})\,\widetilde{\mathcal{G}}_1^{(0,0)}(\bar{Z}).\quad (C.17)
$$

The integral involving the double discontinuity has to be evaluated with extra care. Begin by noting that for a generic exponent p [68, 69]

$$
\mathrm{dDisc}\left[\left(\frac{1-Z}{Z}\right)^p\right] = 2\sin^2(p\pi)\left(\frac{1-Z}{Z}\right)^p,\qquad (C.18)
$$

which would naïvely vanish for integer p, however, the resulting double root precisely cancels out a double pole arising from the integral over Z. Let us rewrite (C.17) as

$$
c^t(h,\bar{h}) = \frac{\delta_{f_1f_4}\delta_{f_2f_3}}{4}\frac{\kappa}{2}\lim_{p\to-1}\int_0^1\frac{dZ}{Z^2}\,g_h(Z)\,\mathrm{dDisc}\left[\left(\frac{1-Z}{Z}\right)^p\right]\int_0^1\frac{d\bar{Z}}{\bar{Z}^2}\,g_{1-\bar{h}}(\bar{Z})\,\widetilde{\mathcal{G}}_1^{(0,0)}(\bar{Z})
$$

$$
= \frac{\delta_{f_1f_4}\delta_{f_2f_3}}{4}\frac{\kappa}{2}\lim_{p\to-1}\left[2\sin^2(p\pi)\,\mathcal{I}^p(h)\right]\times\qquad\qquad (C.19)
$$

$$
\left[\mathcal{I}^{-1}(1-\bar{h}) - \frac{1}{N}\left(\mathcal{I}^{-1}(1-\bar{h}) + 2\mathcal{J}^{-1}(1-\bar{h}) + \mathcal{J}^{-2}(1-\bar{h})\right)\right],
$$

---

[68] The choice of this particular combination of Z is convenient as it allows us to evaluate the integrals that appear in the inversion function in a closed form [68, 69].

where we defined

$$\mathcal{I}^a(h) \equiv \int_0^1 \frac{dZ}{Z^2} \, g_h(Z) \left(\frac{1-Z}{Z}\right)^a = \frac{\Gamma(2h)\,\Gamma^2(a+1)\,\Gamma(h-a-1)}{\Gamma^2(h)\,\Gamma(h+a+1)}, \qquad (C.20a)$$

$$\mathcal{J}^a(h) \equiv \int_0^1 \frac{d\bar{Z}}{\bar{Z}^2} \, g_h(\bar{Z}) \left(\frac{1-\bar{Z}}{\bar{Z}}\right)^a \log \bar{Z}. \qquad (C.20b)$$

Integral (C.20a) is evaluated following [69] and using this closed from expression we get

$$2\sin^2(p\pi)\mathcal{I}^p(h) = 2\pi^2 \frac{\Gamma(2h)\,\Gamma(h-p-1)}{\Gamma^2(h)\,\Gamma(h+p+1)\,\Gamma^2(-p)}, \qquad (C.21)$$

which vanishes only for non-negative integer values of p. It also follows that

$$\kappa \lim_{p\to-1} \left[2\sin^2(p\pi)\,\mathcal{I}^p(h)\right] = \frac{\Gamma^2(h)}{\Gamma(2h-1)}. \qquad (C.22)$$

Next, we can repeat this procedure for the u-channel of (C.14). As already discussed, we swap $z_1 \leftrightarrow z_2$ causing $z \to z^{-1}$ and $\bar{z} \to \bar{z}^{-1}$, followed by the change to Z, $\bar{Z}$ variables using (C.3). Extracting the singular terms at $Z = 1$ yields

$$\mathcal{G}^{(0,0)}_{1,\,f_1f_2f_3f_4}\left(\frac{1}{1-Z}, \frac{1}{1-\bar{Z}}\right) \sim \frac{\delta_{f_1f_3}\delta_{f_2f_4}}{4} \, \widetilde{\mathcal{G}}^{(0,0)}_1(\bar{Z}) \frac{Z}{1-Z} + \dots, \qquad (C.23)$$

with the function of $\bar{Z}$ again being given by (C.16)[69]. Since this expansion is identical to (C.15) up to the exchange of flavour indices $\delta_{f_1f_4}\delta_{f_2f_3} \leftrightarrow \delta_{f_1f_3}\delta_{f_2f_4}$, one can simply repeat the procedure applied to the t-channel and obtain the full inversion function for (C.14)

$$c(h,\bar{h}) = \frac{\delta_{f_1f_4}\delta_{f_2f_3} + (-1)^k\delta_{f_1f_3}\delta_{f_2f_4}}{4} \frac{\Gamma^2(h)}{2\Gamma(2h-1)} \times$$
$$\left[\mathcal{I}^{-1}(1-\bar{h}) - \frac{1}{N}\left(\mathcal{I}^{-1}(1-\bar{h}) + 2\mathcal{J}^{-1}(1-\bar{h}) + \mathcal{J}^{-2}(1-\bar{h})\right)\right]. \qquad (C.24)$$

Functions of $\bar{h}$ in (C.24) contain poles that allow us to extract CFT data. Let us first consider

$$\mathcal{I}^a(1-\bar{h}) = \frac{\Gamma(2-2\bar{h})\,\Gamma^2(a+1)\,\Gamma(-\bar{h}-a)}{\Gamma^2(1-\bar{h})\,\Gamma(2+a-\bar{h})}, \qquad (C.25)$$

with generic a. The relevant poles[70] arise whenever the argument of $\Gamma(-\bar{h}-a)$ is a

---

[69]This can be understood from the fact that sending $z \to z^{-1}$ and $\bar{z} \to \bar{z}^{-1}$ has the effect of exchanging $\delta_{f_1f_4}\delta_{f_2f_3} \leftrightarrow \delta_{f_1f_3}\delta_{f_2f_4}$ in (C.14), if one uses the identity (B.30). As a consequence, the expansions (C.15) and (C.23) are identical up to this exchange of flavour indices.

[70]There are additional spurious poles due to $\Gamma(2-2\bar{h})$ which we ignore [68, 256].

non-positive integer, where the gamma function behaves as

$$\Gamma(-\bar{h} - a) \sim -\frac{(-1)^{\bar{n}}}{\bar{n}!} \frac{1}{\bar{h} - (\bar{n} - a)} , \qquad \bar{h} \to \bar{n} - a , \qquad \bar{n} = 0, 1, 2, \ldots . \qquad \text{(C.26)}$$

Expanding $\mathcal{I}^a(1 - \bar{h})$ around this value yields

$$\mathcal{I}^a(1 - \bar{h}) \sim -\frac{(-a)_{\bar{n}}^2}{\bar{n}! (\bar{n} - 2a - 1)_{\bar{n}}} \frac{1}{\bar{h} - (\bar{n} - a)} , \qquad \text{(C.27)}$$

where

$$(x)_n = \frac{\Gamma(x + n)}{\Gamma(x)} = (-1)^n \frac{\Gamma(1 - x)}{\Gamma(1 - x - n)} , \qquad \text{(C.28)}$$

denotes the rising Pochhammer symbol. Writing the behaviour of $\mathcal{I}^a(1 - \bar{h})$ near the pole in this form makes it manifest that the residue is a finite positive number if a is a negative integer. Using this result, we can analyse simple poles in (C.24) at order N^0 and find

$$c(h, \bar{h})\big|_{N^0} \sim -\frac{1}{2} \frac{\delta_{f_1 f_4} \delta_{f_2 f_3} + (-1)^k \delta_{f_1 f_3} \delta_{f_2 f_4}}{4} \frac{(\bar{n}!)^2}{(2\bar{n})!} \frac{[(\bar{n} + k)!]^2}{(2\bar{n} + 2k)!} \frac{1}{\bar{h} - (1 + \bar{n})} , \qquad \text{(C.29)}$$

where we have used that h and $\bar{h}$ are related by $h = \bar{h} + k$, from which it follows that as $\bar{h} \to 1 + \bar{n}$ so too $h \to 1 + \bar{n} + k$. After being inserted into (C.22), this results in the appearance k-dependent factorials. By comparing the above expression with (C.13), we can extract the squares of generalised free field OPE coefficients

$$\left| c_{(0)(0,0)}^{\bar{n},k} \right|^2 = \frac{\delta_{f_1 f_4} \delta_{f_2 f_3} + (-1)^k \delta_{f_1 f_3} \delta_{f_2 f_4}}{4} \frac{(\bar{n}!)^2}{(2\bar{n})!} \frac{[(\bar{n} + k)!]^2}{(2\bar{n} + 2k)!} . \qquad \text{(C.30)}$$

By setting $\bar{n} = 0$ one obtains

$$\left| c_{(0)(0,0)}^{k} \right|^2 = \frac{\delta_{f_1 f_4} \delta_{f_2 f_3} + (-1)^k \delta_{f_1 f_3} \delta_{f_2 f_4}}{4} \frac{(k!)^2}{(2k)!} , \qquad \text{(C.31)}$$

which are the leading OPE coefficients for the exchange of minimal-twist operators and after using appropriate flavour projections (3.41) we obtain (3.49) and (3.53).

At order $1/N$, we expect (C.24) to contain simple and double poles as $\bar{h} \to 1 + \bar{n}$. In general, the location and the degree of such divergences in the inversion formula is determined by the behaviour of integrands in (C.20) as $Z, \bar{Z} \to 0$, with double poles arising due to the presence of $\log \bar{Z}$ terms. To see this, we can manipulate the logarithm function in (C.20b) and obtain

$$\mathcal{J}^a(1 - \bar{h}) = -\frac{d}{da} \mathcal{I}^a(1 - \bar{h}) + \sum_{m=1}^{\infty} \frac{(-1)^m}{m} \mathcal{I}^{a-m}(1 - \bar{h}) . \qquad \text{(C.32)}$$

One finds that

$$-\frac{d}{da}\mathcal{I}^a(1-\bar{h}) = \mathcal{I}^a(1-\bar{h})\Big[\psi(-a-\bar{h})+\psi(2+a-\bar{h})-2\psi(a+1)\Big], \qquad \text{(C.33)}$$

where $\psi(z) \equiv \Gamma'(z)/\Gamma(z)$ is the digamma function, which diverges whenever its argument is a non-positive integer. As such, the relevant double poles arise due to the combination of simple poles in both $\psi(-\bar{h}-a)$ and $\Gamma(-\bar{h}-a)$ in $\mathcal{I}^a(1-\bar{h})$, with

$$\Gamma(-a-\bar{h})\psi(-a-\bar{h}) \sim -\frac{(-1)^{\bar{n}}}{\bar{n}!}\frac{1}{\big(\bar{h}-(\bar{n}-a)\big)^2} + \dots\,, \qquad \bar{n}=0,1,2,\dots \quad \text{(C.34)}$$

where the dots denote regular terms. In contrast, simple poles in $\mathcal{J}^a$ arise from three different places: from the series term in the second line of (C.32), from $\Gamma(-\bar{h}-a)$ in $\mathcal{I}^a(1-\bar{h})$ when it is multiplied by the remaining two digamma functions in (C.33), and from the first order terms in the $\bar{h}-(\bar{n}-a)$ expansion of the prefactors multiplying (C.34)

$$\frac{\Gamma(2-2\bar{h})\,\Gamma^2(1+a)}{\Gamma^2(1-\bar{h})\,\Gamma(2+a-\bar{h})} \xrightarrow{\bar{h}\to\bar{n}-a} \frac{(-1)^{\bar{n}}(-a)_{\bar{n}}^2}{(\bar{n}-2a-1)_{\bar{n}}}\Big[1 + \big(\bar{h}-(\bar{n}-a)\big)\times$$

$$\big(2\psi(1+a-\bar{n})-2\psi(2+2a-2\bar{n})+\psi(2+2a-\bar{n})\big)+O\Big(\big(\bar{h}-(\bar{n}-a)\big)^2\Big)\Big]. \quad \text{(C.35)}$$

After combining all these contributions, one finds that the pole structure of (C.20b) near $\bar{h}=\bar{n}-a$ is given by

$$\mathcal{J}^a(1-\bar{h}) \sim -\frac{(-a)_{\bar{n}}^2}{\bar{n}!\,(\bar{n}-2a-1)_{\bar{n}}}\left[\frac{1}{\big(\bar{h}-(\bar{n}-a)\big)^2} + \frac{2\psi(\bar{n}-2a-1)-2\psi(2\bar{n}-2a-1)}{\bar{h}-(\bar{n}-a)}\right].$$
$$\text{(C.36)}$$

There is also an additional, spin-dependent, contribution coming from the prefactor (C.22)

$$\frac{\Gamma^2(h)}{\Gamma(2h-1)} \sim \frac{\Gamma^2(k+\bar{n}-a)}{\Gamma(2k+2\bar{n}-2a-1)}\Big[1+2\big(\bar{h}-(\bar{n}-a)\big)\Big(\psi(\bar{n}+k-a)-\psi(2k+2\bar{n}-2a-1)\Big)\Big],$$
$$\text{(C.37)}$$

which is multiplying the $\mathcal{J}^a(1-\bar{h})$ in (C.24). Thus all in all

$$\frac{\Gamma^2(h)}{\Gamma(2h-1)}\mathcal{J}^a(1-\bar{h}) \sim -\frac{(-a)_{\bar{n}}^2}{\bar{n}!(\bar{n}-2a-1)_{\bar{n}}}\frac{\Gamma^2(k+\bar{n}-a)}{\Gamma(2k+2\bar{n}-2a-1)}\left[\frac{1}{\big(\bar{h}-(\bar{n}-a)\big)^2}\right.$$

$$\left. +2\frac{\psi(\bar{n}-2a-1)-\psi(2\bar{n}-2a-1)+\psi(\bar{n}+k-a)-\psi(2\bar{n}+2k-2a-1)}{\bar{h}-(\bar{n}-a)}\right]. \quad \text{(C.38)}$$

Applying this result to (C.24) at order $1/N$, one finds

$$
\begin{aligned}
c(h,\bar{h})\Big|_{1/N} &\sim \\
&-\frac{1}{2}\frac{\delta_{f_1 f_4}\delta_{f_2 f_3} + (-1)^k \delta_{f_1 f_3}\delta_{f_2 f_4}}{4}\frac{(\bar{n}!)^2}{(2\bar{n})!}\frac{[(\bar{n}+k)!]^2}{(2\bar{n}+2k)!}\left\{\frac{-(\bar{n}^2 + \bar{n} + 2)}{(\bar{h}-(\bar{n}+1))^2} - \frac{1}{\bar{h}-(\bar{n}+1)}\times\right. \\
&\left[1 + 4\Big(\psi(\bar{n}+1) - \psi(2\bar{n}+1) + \psi(\bar{n}+k+1) - \psi(2\bar{n}+2k+1)\Big)\right. \tag{C.39}\\
&\left.\left.+ 2\bar{n}(\bar{n}+1)\Big(\psi(\bar{n}+2) - \psi(2\bar{n}+1) + \psi(\bar{n}+k+1) - \psi(2\bar{n}+2k+1)\Big)\right]\right\} + \dots ,
\end{aligned}
$$

where the dots again denote regular terms. By comparing with (C.13), one can read off

$$
\gamma^{\bar{n},k}_{(1),(0,0)} = -(\bar{n}^2 + \bar{n} + 2)\ , \tag{C.40a}
$$

$$
\begin{aligned}
\left|c^{\bar{n},k}_{(1)(0,0)}\right|^2 = -\left|c^{\bar{n},k}_{(0)(0,0)}\right|^2 &\left[4\Big(\psi(\bar{n}+1) - \psi(2\bar{n}+1) + \psi(\bar{n}+k+1) - \psi(2\bar{n}+2k+1)\Big)\right. \\
&\left.+ 1 + 2\bar{n}(\bar{n}+1)\Big(\psi(\bar{n}+2) - \psi(2\bar{n}+1) + \psi(\bar{n}+k+1) - \psi(2\bar{n}+2k+1)\Big)\right],
\end{aligned}
$$
$$\tag{C.40b}$$

where we have used (C.30). For $\bar{n} = 0$ this CFT data simplifies greatly, in particular, the anomalous dimensions are equal for all spins and are given by $\gamma^{k}_{(1),(0,0)} = -2$, which for $k > 2$ agrees with (3.50) and (3.53). Similarly, the $1/N$ corrections to the coefficients in (C.12) can be written in terms of harmonic numbers as

$$
\left|c^{k}_{(1)(0,0)}\right|^2 = \left|c^{k}_{(0)(0,0)}\right|^2\left(4H_{2k} - 4H_k - 1\right), \tag{C.41}
$$

which, after suitable flavour projections, match (3.52) and (3.54) provided the spin is large enough.

One can also apply the above procedure to other R-symmetry projections of (C.1). For the $(1,0)$ projection, the anomalous dimensions and coefficients of global blocks to order $1/N$ in different flavour projections are given in equations (3.55)–(3.58). The most important difference with respect to the R-symmetry singlet is an additional relative minus factor between the t-channel and u-channel contributions to the inversion function, which correctly reproduces non-zero results only for exchanges of operators with odd spin. On the other hand, minimal twist operators exchanged in $(0,1)$ and $(1,1)$ R-symmetry projections of (C.1) are protected by supersymmetry and correspondingly the inversion formula shows that anomalous dimensions are non-zero only for $\bar{n} \geq 1$ and that for $\bar{n} = 0$ the OPE coefficients match free field results.

Appendix D

LLLL Global Blocks in the Regge Limit

In this appendix we review the derivation of the approximation to the $d = 2$ global conformal blocks when the external operators are all light – their dimensions scale as $\Delta \sim 1$ as $c \to \infty$ – in the Regge limit, used in Section 4.4.3. In this 'light scaling regime' the approximation in (4.29) – valid in the 'heavy scaling regime – no longer holds since now the dimensions of the exchanged double-trace operators $\mathcal{O}_{LL'} \equiv \mathcal{O}_L \partial^m \bar{\partial}^{\bar{m}} \mathcal{O}_{L'}$ do not scale with N. These dimensions are given by

$$h = h_L + h_{L'} + m + O(1/N) , \quad \bar{h} = \bar{h}_L + \bar{h}_{L'} + \bar{m} + O(1/N) , \tag{D.1}$$

with h_L, $h_{L'}$ and the anti-holomorphic versions are order 1 in the large c limit. In the Regge limit, the dominant exchanged operators are those of large $m, \bar{m}$ and so h and $\bar{h}$ are still large but not order N. In this regime, the form of the conformal blocks are approximated by modified Bessel functions of the second kind. To see this, the standard form of the (holomorphic) global blocks (A.15) can be rewritten using a linear transformation between hypergeometric functions to give (in this section we use $\alpha = -h_{23}$ and $\beta = -h_{14}$)

$$
\begin{aligned}
\mathcal{V}_h(z) &= z^h \, {}_2F_1(h + \alpha, h + \beta; 2h; z) \\
&= z^h \left[\Gamma_- \Gamma(-\alpha - \beta) \, {}_2F_1(h + \alpha, h + \beta; 1 + \alpha + \beta; 1 - z) \right. \\
&\qquad \left. + \Gamma_+ \Gamma(\alpha + \beta) \, (1 - z)^{-\alpha - \beta} {}_2F_1(h - \alpha, h - \beta; 1 - \alpha - \beta; 1 - z) \right] , \tag{D.2}
\end{aligned}
$$

where we have defined the combination of gamma functions

$$\Gamma_\pm \equiv \frac{\Gamma(2h)}{\Gamma(h \pm \alpha)\,\Gamma(h \pm \beta)} . \tag{D.3}$$

It is now possible to use Stirling's approximation for the gamma function

$$\log \Gamma(x) \approx x \log x - x + \frac{1}{2} \log \frac{2\pi}{x} + \sum_{n=1}^{N-1} \frac{B_{2n} \, x^{1-2n}}{2n(2n-1)}$$

$$\approx \log \left(x^x \sqrt{\frac{2\pi}{x}} \right) - x \; , \tag{D.4}$$

and so the ratios (D.3) can be approximated by

$$\Gamma_{\pm} \approx \frac{\sqrt{\frac{2\pi}{2h}} \, (2h)^{2h} \, e^{-2h}}{\sqrt{\frac{2\pi}{h \pm \alpha}} \, (h \pm \alpha)^{h \pm \alpha} \, e^{-h \mp \alpha} \sqrt{\frac{2\pi}{h \pm \beta}} \, (h \pm \beta)^{h \pm \beta} \, e^{-h \mp \beta}}$$

$$\approx \pi^{-\frac{1}{2}} 2^{2h-1} \sqrt{h} \, h^{\mp(\alpha+\beta)} \left(1 + O(h^{-1}) \right) \; , \tag{D.5}$$

where in the second line, $h \gg \alpha, \beta$ was used. Using this in (D.2) gives

$$\mathcal{V}_h(z) \approx \frac{z^h \, 2^{2h-1} \sqrt{h}}{\sqrt{\pi}} (1-z)^{-\frac{\gamma}{2}} \left[\Gamma(-\gamma) \, h^\gamma (1-z)^{\frac{\gamma}{2}} {}_2F_1(h+\alpha, h+\beta; 1+\alpha+\beta; 1-z) \right.$$

$$\left. + \Gamma(\gamma) \, h^{-\gamma} (1-z)^{-\frac{\gamma}{2}} {}_2F_1(h-\alpha, h-\beta; 1-\alpha-\beta; 1-z) \right] \; , \tag{D.6}$$

where $\gamma \equiv \alpha + \beta$. Taking the first term in the square brackets, this can be rewritten using the sum representation of the hypergeometric function to give

$$\Gamma(-\gamma) \, h^\gamma (1-z)^{\frac{\gamma}{2}} \sum_{k=0}^{\infty} \frac{(h+\alpha)_k (h+\beta)_k}{k! \, (1+\gamma)_k} (1-z)^k \approx \Gamma(-\gamma) \, h^\gamma (1-z)^{\frac{\gamma}{2}} \sum_{k=0}^{\infty} \frac{h^{2k}(1-z)^k}{k! \, (1+\gamma)_k}$$

$$= -\pi \csc(\pi\gamma) \sum_{k=0}^{\infty} \frac{\left(h\sqrt{1-z} \right)^{2k+\gamma}}{k! \, \Gamma(1+\gamma+k)}$$

$$= -\pi \csc(\pi\gamma) \, I_\gamma \left(2h\sqrt{1-z} \right) \; , \tag{D.7}$$

where we used $(h+\alpha)_k \approx h^k (1 + O(h^{-1}))$ and the gamma function inversion formula $\Gamma(x)\Gamma(1-x) = \pi \csc(\pi x)$ for $x \notin \mathbb{Z}$ was used, along with the series representation of the modified Bessel function of the first kind

$$I_\nu(x) = \sum_{k=0}^{\infty} \frac{1}{k! \, \Gamma(k+\nu+1)} \left(\frac{x}{2} \right)^{2k+\nu} \; . \tag{D.8}$$

Repeating similar steps for the second term in (D.6) leads to

$$
\begin{aligned}
\mathcal{V}_h(z) &\approx \frac{z^h \, 2^{2h-1} \sqrt{h}}{\sqrt{\pi}} (1-z)^{-\frac{\gamma}{2}} \left[-\pi \csc(\pi\gamma) \, I_\gamma\big(2h\sqrt{1-z}\big) + \pi \csc(\pi\gamma) \, I_{-\gamma}\big(2h\sqrt{1-z}\big) \right] \\
&= \frac{z^h \, 2^{2h} \sqrt{h}}{\sqrt{\pi}} (1-z)^{-\frac{\gamma}{2}} \, K_\gamma\big(2h\sqrt{1-z}\big) \, ,
\end{aligned}
\tag{D.9}
$$

using a relation between the modified Bessel functions of the first and second kinds

$$
K_\nu(x) = \frac{\pi}{2} \csc(\pi\nu)\Big(I_{-\nu}(x) - I_\nu(x)\Big) \, ,
\tag{D.10}
$$

for $\nu \notin \mathbb{Z}$. One check is whether (D.9) is an eigenfunction of the quadratic Casimir operator (A.26) in the large h limit. It turns out that (D.9) is valid in the regime $h, \bar{h} \gg 1$ with $\hat{z} \equiv h\sqrt{1-z}$ finite: since the behaviour of the Bessel function in purely the $h, \bar{h} \gg 1$ limit is exponentially suppressed, relative to the case of also keeping $\hat{z}$ fixed, since

$$
K_\gamma\big(2h\sqrt{1-z}\big) \approx \frac{1}{2}\sqrt{\frac{\pi}{h}} \, (1-z)^{-\frac{1}{4}} \, e^{-2h\sqrt{1-z}} \, .
\tag{D.11}
$$

Then to first order, the factor of z^h can be dropped in (D.9) giving

$$
\mathcal{V}_h(z) \approx 2^{2h} \sqrt{\frac{h}{\pi}} \, (1-z)^{-\frac{\gamma}{2}} \, K_\gamma\big(2h\sqrt{1-z}\big) \, .
\tag{D.12}
$$

Appendix E

Useful Integrals

E.1 Cross channel heavy integrals

Integral 1:

In the discussion of the HHLL bootstrap constraints of Section 4.4, we needed to evaluate

$$I_{a,c}(z,\bar{z}) \equiv \int_0^\infty\!\!\int_0^\infty d\bar{m}\, dm\, \frac{m^{a+1}\bar{m}^{a+1}}{(m+\bar{m})^c}\, z^m \bar{z}^{\bar{m}} \ . \tag{E.1}$$

In order to perform this integral, it is first helpful to decouple the two variables by using a Schwinger parameter t to rewrite the denominator of the integrand. This gives the simpler triple integral

$$
\begin{aligned}
I_{a,c}(z,\bar{z}) &= \int_0^\infty dt\, \frac{t^{c-1}}{\Gamma(c)} \int_0^\infty dm\, m^{a+1} e^{-m(t-\log z)} \int_0^\infty d\bar{m}\, \bar{m}^{a+1} e^{-\bar{m}(t-\log\bar{z})}\\
&= \frac{\Gamma^2(a+2)}{\Gamma(c)} \int_0^\infty dt\, t^{c-2a-5}\Big(1-\frac{\log z}{t}\Big)^{-a-2}\Big(1-\frac{\log\bar{z}}{t}\Big)^{-a-2} \ .
\end{aligned}
\tag{E.2}
$$

Making a change of variables to $x = \frac{\tau}{1+\tau}$ where $t = -\tau\log\bar{z}$ and using the integral form of the hypergeometric function

$$_2F_1(a,b\,;c\,;z) = \frac{\Gamma(c)}{\Gamma(b)\Gamma(c-b)} \int_0^1 ds\, s^{b-1}(1-s)^{c-b-1}(1-zs)^{-a} \ , \tag{E.3}$$

the final integral can be performed to give

$$I_{a,c}(z,\bar{z}) = \frac{\Gamma^2(a+2)\,\Gamma(2a+4-c)}{\Gamma(2a+4)\,\big(-\log\bar{z}\big)^{2a+4-c}}\left(\frac{\log\bar{z}}{\log z}\right)^{a+2}{}_2F_1\left(a+2,c;2a+4;1-\frac{\log\bar{z}}{\log z}\right) \ . \tag{E.4}$$

Integral 2:

In section 4.5 the resummation of contributions of the double-trace operators $\{\mathcal{O}_{HL}\}$ requires the computation of integrals of the following, more general, kind

$$I_{a,b,c}(z,\bar{z}) \equiv \int_0^\infty dm \int_0^m d\bar{m}\, \frac{m^a \bar{m}^b}{(m+\bar{m})^c}\, z^m \bar{z}^{\bar{m}}\ . \tag{E.5}$$

We now derive the result of this integral. Making a change of variables in the $\bar{m}$ integral to $x = \frac{\bar{m}}{m}$ gives

$$
\begin{aligned}
I_{a,b,c}(z,\bar{z}) &\equiv \int_0^\infty dm\, z^m\, m^{a+b-c+1} \int_0^1 dx\, \frac{x^b\, \bar{z}^{mx}}{(1+x)^c} \\
&= \int_0^1 dx\, \frac{x^b}{(1+x)^c} \int_0^\infty dm\, m^{a+b-c+1} e^{m(x\log\bar{z}+\log z)}\ .
\end{aligned}
\tag{E.6}
$$

Using the integral representation of the gamma function

$$\Gamma(c) = \int_0^\infty ds\, s^{c-1} e^{-s}\ , \tag{E.7}$$

with $s = -t\,(x\log\bar{z} + \log z)$ gives

$$I_{a,b,c}(z,\bar{z}) = \frac{\Gamma(a+b+2-c)}{(-\log z)^{a+b+2-c}} \int_0^1 dx\, x^b\,(1+x)^{-c} \left(1 + x\,\frac{\log\bar{z}}{\log z}\right)^{c-a-b-2}\ . \tag{E.8}$$

Now with the use of the integral

$$\int_0^1 dx\, x^{\lambda-1}\,(1-x)^{\mu-1}\,(1-ux)^{-\rho}\,(1-vx)^{-\sigma} = B(\mu,\lambda)\, F_1(\lambda\,;\rho,\sigma\,;\lambda+\mu\,;u,v)\ , \tag{E.9}$$

with $\mu = 1$ and $B(\mu,\lambda)$ the Euler beta function, (E.8) becomes

$$I_{a,b,c}(z,\bar{z}) = \frac{\Gamma(a+b+2-c)}{(1+b)\big(-\log z\big)^{a+b+2-c}}\, F_1\left(b+1\,;c,a+b+2-c\,;2+b\,;-1,-\frac{\log\bar{z}}{\log z}\right)\ . \tag{E.10}$$

Here F_1 is an Appell hypergeometric function with series representation

$$F_1(a;b_1,b_2;c\,;x,y) = \sum_{m,n=0}^\infty \frac{(a)_{m+n}(b_1)_m(b_2)_n}{m!\,n!\,(c)_{m+n}}\, x^m y^n\ . \tag{E.11}$$

As a check, one can verify that setting $b = a$ in (E.10) yields the previous result (E.4).

E.2 Cross channel light integrals

In solving the Regge limit crossing equations at first order in the $\frac{1}{N}$ expansion for the case of all operators being light in Section 4.4.3, the following equation is to be solved

$$\left. \mathrm{Im}\, C_2^{\mathrm{bos}} \right|_{\circlearrowleft} \approx -16\pi A \left|1-z\right|^{-1} \left[I_2(a_1, a_2, 1) + I_1(a_1, a_2, 1) \right] , \tag{E.12}$$

where the two integrals required are

$$I_1(a_1, a_2, b) \equiv \int_0^\infty dm \int_0^m d\bar{m}\, m^{2+a_1} \bar{m}^{2+a_2} K_b\Big(2\bar{m}\sqrt{1-z}\Big) K_b\Big(2m\sqrt{1-\bar{z}}\Big)$$

$$I_2(a_1, a_2, b) \equiv \int_0^\infty dm \int_0^m d\bar{m}\, m^{2+a_1} \bar{m}^{2+a_2} K_b\Big(2m\sqrt{1-z}\Big) K_b\Big(2\bar{m}\sqrt{1-\bar{z}}\Big) . \tag{E.13}$$

Focusing on I_2 first, with $b = 1$, performing a change of variables in the $\bar{m}$ integral using $\sqrt{x} = \frac{\bar{m}}{m}$ gives

$$I_2(a_1, a_2, 1) = \frac{1}{2} \int_0^\infty dm\, m^{5+a_1+a_2} K_1\Big(2m\sqrt{1-z}\Big) \int_0^1 dx\, x^{\frac{1}{2}(1+a_2)} K_1\Big(2m\sqrt{x}\,\sqrt{1-\bar{z}}\Big)$$

$$= \frac{1}{4}(1-\bar{z})^{-\frac{1}{2}} \int_0^\infty dm\, m^{4+a_1+a_2} K_1\Big(2m\sqrt{1-z}\Big) G_{1,3}^{2,1}\left(m^2(1-\bar{z}) \;\middle|\; \begin{matrix} -\frac{a_2}{2} \\ 1, 0, -\frac{a_2}{2}-1 \end{matrix} \right) , \tag{E.14}$$

where in the second line the following integral from Eq. (6.592.2) of [174] was used

$$\int_0^1 dx\, x^\lambda (1-x)^{\mu-1} K_\nu\big(a\sqrt{x}\big) = \frac{2^{\nu-1}}{a^\nu} \Gamma(\mu)\; G_{1,3}^{2,1}\left(\frac{a^2}{2} \;\middle|\; \begin{matrix} \frac{\nu}{2}-\lambda \\ \nu, 0, \frac{\nu}{2}-\lambda-\mu \end{matrix} \right) , \tag{E.15}$$

valid for $\mathrm{Re}(\lambda) > \frac{1}{2}|\mathrm{Re}(\nu)| - 1$ and $\mathrm{Re}(\mu) > 0$. The remaining integral in (E.14) after the change of variables $m = \sqrt{\frac{y}{1-z}}$ is then of the form (Eq. (7.821.3) of [174])

$$2\int_0^\infty dy\, y^{-\rho} K_\nu\big(2y^{\frac{1}{2}}\big) G_{p,q}^{m,n}\left(\alpha y \;\middle|\; \begin{matrix} a_1, \ldots, a_p \\ b_1, \ldots, b_q \end{matrix} \right) = G_{p+2,q}^{m,n+2}\left(\alpha \;\middle|\; \begin{matrix} \rho-\frac{\nu}{2}, \rho+\frac{\nu}{2}, a_1, \ldots, a_p \\ b_1, \ldots, b_q \end{matrix} \right) , \tag{E.16}$$

with $p+q < 2(m+n)$, $|\arg\alpha| < (m+n-\frac{1}{2}(p+q))\pi$ and $\mathrm{Re}(\rho) < 1-\frac{1}{2}\mathrm{Re}(\nu)+\min\mathrm{Re}(b_j)$. The Meijer G-function is a particularly general function, designed to include as special cases most other common special functions – such as the generalised hypergeometric function. The primary definition of this function is in terms of the Mellin-Barnes type

line integral

$$G_{p,q}^{m,n}\left(x\,\middle|\,\begin{matrix}a_1,\ldots,a_p\\b_1,\ldots,b_q\end{matrix}\right)=\frac{1}{2\pi i}\int_L ds\,x^s\,\frac{\prod_{j=1}^m \Gamma(b_j-s)\prod_{j=1}^n \Gamma(1-a_j+s)}{\prod_{j=m+1}^q \Gamma(1-b_j+s)\prod_{j=n+1}^p \Gamma(a_j-s)}\,,$$

$$(\text{E.}17)$$

where the choices of integration path L are given in section 9.302 of [174]. Using (E.16) in (E.14) gives

$$
\begin{aligned}
I_2 &= \frac{1}{8}\frac{(1-z)^{-2-\frac{1}{2}(a_1+a_2)}}{|1-z|}\int_0^\infty dy\, y^{\frac{1}{2}(a_1+a_2+3)}K_1\big(2\sqrt{y}\big)\,G_{1,3}^{2,1}\left(y\,\frac{1-\bar{z}}{1-z}\,\middle|\,\begin{matrix}-\frac{a_2}{2}\\1,0,-\frac{a_2}{2}-1\end{matrix}\right)\\
&= \frac{1}{16}\frac{(1-z)^{-2-\frac{1}{2}(a_1+a_2)}}{|1-z|}\,G_{3,3}^{2,3}\left(\frac{1-\bar{z}}{1-z}\,\middle|\,\begin{matrix}-\frac{1}{2}(a_1+a_2)-2,-\frac{1}{2}(a_1+a_2)-1,-\frac{a_2}{2}\\1,0,-\frac{a_2}{2}-1\end{matrix}\right)\\
&\approx \frac{1}{16}\eta^{-\frac{1}{2}}\sigma^{-3-\frac{1}{2}(a_1+a_2)}\,G_{3,3}^{2,3}\left(\eta\,\middle|\,\begin{matrix}-\frac{1}{2}(a_1+a_2)-2,-\frac{1}{2}(a_1+a_2)-1,-\frac{a_2}{2}\\1,0,-\frac{a_2}{2}-1\end{matrix}\right)\\
&\approx \frac{1}{16}\eta^{-\frac{1}{2}}\sigma^{-3-\frac{1}{2}(a_1+a_2)}\left(1+\frac{a_2}{2}\right)^{-1}\Gamma\big(2+\tfrac{1}{2}(a_1+a_2)\big)\,\Gamma\big(3+\tfrac{1}{2}(a_1+a_2)\big)\,,
\end{aligned}
$$

$$(\text{E.}18)$$

where in the third and fourth lines an expansion in small σ and then η is performed. Likewise, I_1 can be found by exchanging z and $\bar{z}$ in the second line of (E.18), giving

$$
\begin{aligned}
I_1 &= \frac{1}{16}\frac{(1-\bar{z})^{-2-\frac{1}{2}(a_1+a_2)}}{|1-z|}\,G_{3,3}^{2,3}\left(\frac{1-z}{1-\bar{z}}\,\middle|\,\begin{matrix}-\frac{1}{2}(a_1+a_2)-2,-\frac{1}{2}(a_1+a_2)-1,-\frac{a_2}{2}\\1,0,-\frac{a_2}{2}-1\end{matrix}\right)\\
&\approx \frac{1}{16}\sigma^{-3-\frac{1}{2}(a_1+a_2)}\eta^{-\frac{1}{2}(a_1+a_2+5)}\,G_{3,3}^{2,3}\left(\frac{1}{\eta}\,\middle|\,\begin{matrix}-\frac{1}{2}(a_1+a_2)-2,-\frac{1}{2}(a_1+a_2)-1,-\frac{a_2}{2}\\1,0,-\frac{a_2}{2}-1\end{matrix}\right)\\
&\approx \frac{1}{16}\sigma^{-3-\frac{1}{2}(a_1+a_2)}\eta^{-\frac{1}{2}(a_1+3)}\,\Gamma\big(1+\tfrac{a_1}{2}\big)\,\Gamma\big(2+\tfrac{a_1}{2}\big)\,\Gamma\big(1+\tfrac{a_2}{2}\big)\,\Gamma\big(2+\tfrac{a_2}{2}\big)\,.
\end{aligned}
$$

$$(\text{E.}19)$$

Using (E.18) and (E.19) in (E.12) gives

$$
\begin{aligned}
\mathrm{Im}\,C_2^{\mathrm{bos}}\Big|_{\circlearrowleft} &\approx -A\,\pi\sigma^{-4-\frac{1}{2}(a_1+a_2)}\eta^{-1}\bigg[\left(1+\frac{a_2}{2}\right)^{-1}\Gamma\big(2+\tfrac{1}{2}(a_1+a_2)\big)\,\Gamma\big(3+\tfrac{1}{2}(a_1+a_2)\big)\\
&\quad + \eta^{-\frac{a_1}{2}-1}\Gamma\big(1+\tfrac{a_1}{2}\big)\,\Gamma\big(2+\tfrac{a_1}{2}\big)\,\Gamma\big(1+\tfrac{a_2}{2}\big)\,\Gamma\big(2+\tfrac{a_2}{2}\big)\bigg]\,.
\end{aligned}
$$

$$(\text{E.}20)$$

In order to match the stress tensor's leading σ and η behaviour, it is necessary to have $a_1 = 0$, $a_2 = 2$ and $A = -1$. Plugging these values back into the leading σ term of (E.12) and using the following functional relations of the Meijer G-function (see section

9.31 of [174])

$$G_{p,q}^{m,n}\left(x\,\middle|\,\begin{matrix}a_1,a_2,\ldots,a_p\\b_1,\ldots,b_{q-1},a_1\end{matrix}\right) = G_{p-1,q-1}^{m,n-1}\left(x\,\middle|\,\begin{matrix}a_2,\ldots,a_p\\b_1,\ldots,b_{q-1}\end{matrix}\right) \tag{E.21}$$

$$G_{p,q}^{m,n}\left(x\,\middle|\,\begin{matrix}a_1,\ldots,a_p\\b_1,\ldots,b_q\end{matrix}\right) = x^k\,G_{p,q}^{m,n}\left(x\,\middle|\,\begin{matrix}a_1-k,\ldots,a_p-k\\b_1-k,\ldots,b_q-k\end{matrix}\right), \tag{E.22}$$

gives

$$\mathrm{Im}\,C_2^{\mathrm{bos}}\Big|_{\circlearrowleft} \approx \frac{\pi}{\eta^4\sigma^5}\left[G_{2,2}^{2,2}\left(\eta^{-1}\,\middle|\,\begin{matrix}-3,-1\\1,0\end{matrix}\right) + G_{2,2}^{2,2}\left(\eta\,\middle|\,\begin{matrix}0,2\\4,3\end{matrix}\right)\right] + O(\sigma^{-4})\,. \tag{E.23}$$

The relation

$$G_{2,2}^{2,2}\left(\eta\,\middle|\,\begin{matrix}a_1,a_2\\b_1,b_2\end{matrix}\right) = B(1-a_1+b_1,1-a_2+b_2)\,\Gamma(1-a_2+b_1)\,\Gamma(1-a_1+b_2)\,\eta^{b_1}$$

$$\times\ {}_2F_1\big(1-a_1+b_1,1-a_2+b_1;2-a_1-a_2+b_1+b_2;1-\eta\big)\,, \tag{E.24}$$

with $B(x,y)$ the Euler beta function, allows the Meijer G-functions in (E.23) to be evaluated, giving precisely the leading small σ term of the correlator in (4.106).

E.3 (1,0,1) bulk phase shift integrals

In this section we compute the integral $\mathcal{I}$ required in the bulk phase shift in the 3D reduced geometry obtained from the $(1,0,1)$ microstate geometry, as discussed in Section 4.5.3. With the change of variables $r^2 = a_0^2\,\alpha\rho^2$ from the integral in (4.187), we define the integral to be performed as

$$\mathcal{I} \equiv \int_{\rho_0}^{\infty}\frac{d\rho}{\rho}\sqrt{\frac{\rho^4 + \frac{\rho^2}{\alpha(1-\beta^2)}\left(1-2\beta(1-\alpha)+\beta^2(1-2\alpha-\alpha^2)\right) - \frac{\alpha\beta^2}{1-\beta^2}}{(\rho^2+1)^3}}$$

$$= \int_{\rho_0}^{\infty}\frac{d\rho}{\rho}\sqrt{\frac{(\rho^2-\rho_0^2)(\rho^2+\bar\rho_0^2)}{(\rho^2+1)^3}}\,, \tag{E.25}$$

where ρ_0 and $\bar\rho_0$ are solutions to the radial turning point equation $\dot r = 0$ (given explicitly in (4.176) with $n=1$) and we have $0 < \alpha, \beta < 1$. Changing variables to $x = \rho^{-2}$ and defining $x_0 = \rho_0^{-2}$ and $\bar x_0 = \bar\rho_0^{-2}$ with

$$\overset{(-)}{x_0} = \frac{\pm 2\alpha(1-\beta^2)}{-1+2\beta(1-\alpha)-\beta^2(1-2\alpha-\alpha^2)\pm\sqrt{4\alpha^3\beta^2(1-\beta^2)+\big(1-2\beta+\beta^2(1-2\alpha-\alpha^2)+2\alpha\beta\big)^2}}\,, \tag{E.26}$$

where $\bar{x}_0$ has the minus sign from each of the $\pm$ symbols, gives the form of the integral as

$$
\begin{aligned}
\mathcal{I} &= \frac{1}{2} \int_0^{x_0} dx \, \sqrt{\frac{\left(1 - \frac{x}{x_0}\right)\left(1 + \frac{x}{\bar{x}_0}\right)}{x(1+x)^3}} \\
&= \frac{1}{2} \int_0^{x_0} dx \, \frac{\left(1 - \frac{x}{x_0}\right)\left(1 + \frac{x}{\bar{x}_0}\right)(1+x)^{-1}}{\sqrt{x(1+x)\left(1 - \frac{x}{x_0}\right)\left(1 + \frac{x}{\bar{x}_0}\right)}} \\
&= \mathcal{I}_A + \mathcal{I}_B + \mathcal{I}_C \ .
\end{aligned}
\tag{E.27}
$$

The three integrals that then need to be computed we define as

$$
\mathcal{I}_A \equiv \frac{(x_0 + 1)(\bar{x}_0 - 1)}{2x_0 \bar{x}_0} \int_0^{x_0} \frac{dx \, (1+x)^{-1}}{\sqrt{x(1+x)\left(1 - \frac{x}{x_0}\right)\left(1 + \frac{x}{\bar{x}_0}\right)}} \ ,
\tag{E.28a}
$$

$$
\mathcal{I}_B \equiv \frac{x_0 + 1}{2x_0 \bar{x}_0} \int_0^{x_0} \frac{dx}{\sqrt{x(1+x)\left(1 - \frac{x}{x_0}\right)\left(1 + \frac{x}{\bar{x}_0}\right)}} \ ,
\tag{E.28b}
$$

$$
\mathcal{I}_C \equiv \frac{-1}{2x_0 \sqrt{\bar{x}_0}} \int_0^{x_0} dx \, \frac{\sqrt{\bar{x}_0 + x}}{\sqrt{x(1+x)\left(1 - \frac{x}{x_0}\right)}} \ .
\tag{E.28c}
$$

In decomposing the integral $\mathcal{I}$ into those in (E.28), the numerator in the second line of (E.27) can be written as

$$
\left(1 - \frac{x}{x_0}\right)\left(1 + \frac{x}{\bar{x}_0}\right)(1+x)^{-1} = \frac{(x_0 + 1)(\bar{x}_0 - 1)}{x_0 \bar{x}_0 (1+x)} + \frac{1 + x_0}{x_0 \bar{x}_0} - \frac{x + \bar{x}_0}{x_0 \bar{x}_0} \ .
\tag{E.29}
$$

We note that as defined above, $\bar{x}_0$ is a convex function of α going to zero as $\alpha \to 0$ and to one as $\alpha \to 1$ while increasing β causes $\bar{x}_0$ to increase faster with α, plateauing off sooner. By contrast x_0 tends to zero as $\alpha \to 1$ and increases sharply as $\alpha \to 0$, which is amplified for smaller β (becomes greater than 1). Thus we have $x_0 > 0$ and $1 > \bar{x}_0 > 0$.

In solving these integrals, we start by defining a one-parameter family of integrals from which we will derive those in (E.28):

$$
J(f) \equiv \frac{1}{2} \int_0^{x_0} \frac{dx}{\sqrt{x(f+x)\left(1 - \frac{x}{x_0}\right)\left(1 + \frac{x}{\bar{x}_0}\right)}} \ ,
\tag{E.30}
$$

the integrand of which has branch points at $x = 0, -f, x_0, -\bar{x}_0$. This is an elliptic integral and so is invariant under $\mathrm{SL}(2, \mathbb{R})$ transformations

$$
x \to \tilde{x} = \frac{ax + b}{cx + d} \quad \text{such that} \quad ad - bc = 1 \ .
\tag{E.31}
$$

The tactic is to use such a transformations to put $J(f)$ into one of the Legendre normal

forms, with our conventions for the incomplete elliptic integrals of the first, second and third kind being given by

$$F(x;k) = \int_0^x \frac{dt}{\sqrt{(1-t^2)(1-k^2t^2)}} \ , \tag{E.32a}$$

$$E(x;k) = \int_0^x dt \sqrt{\frac{(1-k^2t^2)}{1-t^2}} \ , \tag{E.32b}$$

$$\Pi(n;x|m) = \int_0^x \frac{dt}{1-nt^2} \frac{1}{\sqrt{(1-t^2)(1-mt^2)}} \ , \tag{E.32c}$$

with the complete versions being

$$K(k) \equiv F(1;k) = \frac{\pi}{2}\,{}_2F_1(1/2,1/2;1;k^2) \ , \tag{E.33a}$$

$$E(k) \equiv E(1;k) = \int_0^1 dt\, \frac{\sqrt{1-k^2t^2}}{\sqrt{1-t^2}} = \frac{\pi}{2}\,{}_2F_1(1/2,-1/2;1;k^2) \ , \tag{E.33b}$$

$$\Pi(n|m) \equiv \Pi(n;1|m) = \int_0^1 \frac{dt}{1-nt^2} \frac{1}{\sqrt{(1-t^2)(1-mt^2)}} \ . \tag{E.33c}$$

With this goal in mind we map the branch points $(0, -f, x_0, -\bar{x}_0) \to (-1, -k, 1, k)$ using an $SL(2, \mathbb{R})$ transformation (E.31) $x \to \tilde{x}$ with

$$\tilde{x} = \frac{f(\bar{x}_0 + x) + x(x_0 + \bar{x}_0) - \sqrt{f\bar{x}_0(f+x_0)(x_0+\bar{x}_0)}}{f\bar{x}_0\left(\frac{x}{x_0} - 1\right) + x(x_0+\bar{x}_0)\left(1 + \frac{f}{x_0}\right) + \left(1 - \frac{2x}{x_0}\right)\sqrt{f\bar{x}_0(f+x_0)(x_0+\bar{x}_0)}} \ , \tag{E.34}$$

yielding from (E.30)

$$J(f) = \frac{2\,\bar{x}_0^{\frac{1}{2}}}{\sqrt{-(f-\bar{x}_0)k(f)}} \int_0^1 \frac{d\tilde{x}}{\sqrt{(1-\tilde{x}^2)\left(1 - \frac{\tilde{x}^2}{k(f)^2}\right)}} = \frac{2\,\bar{x}_0^{\frac{1}{2}}}{\sqrt{-(f-\bar{x}_0)k(f)}} K\left(k(f)^{-1}\right) \ , \tag{E.35}$$

where we have defined the quantity

$$k(f) = \frac{x_0\bar{x}_0 + f(x_0 + 2\bar{x}_0) + 2\sqrt{f\bar{x}_0(f+x_0)(x_0+\bar{x}_0)}}{-x_0(f-\bar{x}_0)} \ . \tag{E.36}$$

Thus this solves one part of the integral, $\mathcal{I}_B$ given in (E.28b), to be

$$\mathcal{I}_B = \frac{1+x_0}{x_0\bar{x}_0} J(1) = \frac{2(1+x_0)}{x_0\sqrt{-k\bar{x}_0(1-\bar{x}_0)}} K\left(k^{-1}\right) \ , \tag{E.37}$$

where $k \equiv k(1)$. One can continue in a similar manner with the integrals in (E.28a) and (E.28c), mapping the branch points to canonical points and writing them as com-

binations of elliptic integrals, however, one can notice that the substitution

$$x \to t = \sqrt{\frac{x(x_0 + \bar{x}_0)}{x_0(x + \bar{x}_0)}} \ , \tag{E.38}$$

can be used to solve all three most efficiently. Performing this change of variables on the integral $J(f)$ in (E.30) gives

$$J(f) = \sqrt{\frac{x_0 \bar{x}_0}{f(x_0 + \bar{x}_0)}} \int_0^1 \frac{dt}{\sqrt{(1 - t^2)(1 - T^2 t^2)}} = \sqrt{\frac{x_0 \bar{x}_0}{f(x_0 + \bar{x}_0)}} K(T) \ , \tag{E.39}$$

where we define

$$T^2 = T(f)^2 \equiv \frac{x_0(f - \bar{x}_0)}{f(x_0 + \bar{x}_0)} \ . \tag{E.40}$$

This gives immediately

$$\mathcal{I}_B = \frac{(1 + x_0)}{\sqrt{x_0 \bar{x}_0 (x_0 + \bar{x}_0)}} K\left(\sqrt{\frac{x_0(1 - \bar{x}_0)}{x_0 + \bar{x}_0}}\right) \ . \tag{E.41}$$

Next one notices that

$$-2J'(f)\big|_{f=1} = \frac{1}{2} \int_0^{x_0} \frac{dx \, (1 + x)^{-1}}{\sqrt{x(1 + x)\left(1 - \frac{x}{x_0}\right)\left(1 + \frac{x}{\bar{x}_0}\right)}} \ , \tag{E.42}$$

where the prime denotes a derivative with respect to f, and so this gives the integral (E.28a) as

$$\mathcal{I}_A = -2 \frac{(1 + x_0)(\bar{x}_0 - 1)}{x_0 \bar{x}_0} J'(f)\big|_{f=1}$$
$$= \frac{\sqrt{x_0 + \bar{x}_0}}{\sqrt{x_0 \bar{x}_0}} E\left(\sqrt{\frac{x_0(1 - \bar{x}_0)}{x_0 + \bar{x}_0}}\right) - \frac{1 + x_0}{\sqrt{x_0 \bar{x}_0 (x_0 + \bar{x}_0)}} K\left(\sqrt{\frac{x_0(1 - \bar{x}_0)}{x_0 + \bar{x}_0}}\right) \ . \tag{E.43}$$

Finally, performing again the change of variables (E.38) on $\mathcal{I}_C$ gives

$$\mathcal{I}_C = -\sqrt{\frac{\bar{x}_0}{x_0(x_0 + \bar{x}_0)}} \, \Pi\left(\frac{x_0}{x_0 + \bar{x}_0} \middle| \frac{x_0(1 - \bar{x}_0)}{x_0 + \bar{x}_0}\right) \ . \tag{E.44}$$

The full integral $\mathcal{I}$ is then

$$\mathcal{I} = \sqrt{\frac{x_0 + \bar{x}_0}{x_0 \bar{x}_0}} \, E\left(\sqrt{\frac{x_0(1 - \bar{x}_0)}{x_0 + \bar{x}_0}}\right) - \sqrt{\frac{\bar{x}_0}{x_0(x_0 + \bar{x}_0)}} \, \Pi\left(\frac{x_0}{x_0 + \bar{x}_0} \middle| \frac{x_0(1 - \bar{x}_0)}{x_0 + \bar{x}_0}\right) \ , \tag{E.45}$$

where we note that the second term of $\mathcal{I}_A$ cancels with $\mathcal{I}_B$, implying that our method of computation of this integral was not optimal.

Appendix F

Regge Limit of the $(1, 0, 0)$ Correlator with $\mathcal{O}_L = \mathcal{O}^{\text{bos}}$

Here we analyse the Regge limit of the 4-point function of the correlator involving the heavy state dual to the $(1, 0, 0)$ geometry presented in section 4.4 and light operator $\mathcal{O}_L = \mathcal{O}^{\text{bos}}$ with $h_L = \bar{h}_L = 1$. This correlator is again related to the that involving the chiral primary light operator (2.93) through a superconformal Ward identity $C^{\text{bos}} = \partial \bar{\partial} \left[C^{\text{fer}} \right]$ [72]. However, if we expand this correlator in a series as

$$C^{\text{bos}}(z, \bar{z}) = \sum_{n=0}^{\infty} \mu^n\, C_n^{\text{bos}}(z, \bar{z})\,, \tag{F.1}$$

then we can apply the Ward identity at each order in the series expansion directly

$$C_n^{\text{bos}}(z, \bar{z}) = \partial \bar{\partial} \left[C_n^{\text{fer}}(z, \bar{z}) \right]\,, \tag{F.2}$$

and use the closed form expressions in (B.17).

We can now repeat the Regge analysis for this 4-point function. Using the above method of obtaining the C_n^{bos}, we find that analytically continuing the obtained results and taking $z, \bar{z} \to 1$ gives

$$
\begin{aligned}
C_{\text{R}}^{\text{bos}} \approx\ & \frac{1}{\eta^2 \sigma^4} + \frac{2\pi i}{\eta^2 (1-\eta)^5 \sigma^5}\, \left(1 - 8\eta + 8\eta^3 - \eta^4 - 12\eta^2 \log \eta \right) \mu \\
& - \frac{3\pi^2}{\eta^2 (1-\eta)^7 \sigma^6} (1 - 15\eta - 80\eta^2 + 80\eta^3 + 15\eta^4 - \eta^5 - 60\eta^2 (1+\eta) \log \eta)\, \mu^2 \\
& - \frac{4i\pi^3}{\eta^2 (1-\eta)^9 \sigma^7}\, \left(1 - 24\eta - 375\eta^2 + 375\eta^4 + 24\eta^5 - \eta^6 - 60\eta^2 (3 + 8\eta + 3\eta^3) \log \eta \right) \mu^3.
\end{aligned}
\tag{F.3}
$$

On the other hand we can use the bulk phase shift (4.96) and its expansion in μ to reconstruct the Regge limit of the CFT correlator using (4.51). We find that the analysis

is the same as before only that now, due to the conformal dimensions of $\mathcal{O}_L = \mathcal{O}^{\mathrm{bos}}$ being $h_L = \bar{h}_L = 1$, we need to replace $\tilde{I}_{a,b} \to \tilde{I}_{a+1,b+1}$ in (4.154) which explicitly yields

$$
\begin{aligned}
C^{\mathrm{bos}}_{\mathrm{AdS}} \approx \Bigg[& \pi i \, \tilde{I}_{2,2}\, \mu + \left(\frac{3\pi i}{4}\, \tilde{I}_{2,2} - \frac{2\pi i}{4}\, \tilde{I}_{3,4} - \frac{\pi^2}{2}\, \tilde{I}_{3,3} \right) \mu^2 \\
& + \left(\frac{5\pi i}{8}\, \tilde{I}_{2,2} - \frac{3\pi i}{4}\, \tilde{I}_{3,4} + \frac{\pi i}{2}\, \tilde{I}_{4,6} - \frac{\pi^3 i}{6}\, \tilde{I}_{4,4} - \frac{3\pi^2}{4}\, \tilde{I}_{3,3} + \frac{\pi^2}{2}\, \tilde{I}_{4,5} \right) \mu^3 \Bigg]\Bigg|_{z,\bar{z}\to 1}.
\end{aligned}
$$

$$(F.4)$$

Explicitly evaluating the integrals (4.155) and executing the limit completely reproduces the leading σ behaviour of (F.3) at each order in μ. However, for this correlator – unlike the case of the $\mathcal{O}_L = \mathcal{O}^{\mathrm{fer}}$ light operator and the $(1,0,0)$ heavy state – the matching between the bulk reconstruction and the CFT Regge limit analysis ceases already at the subleading order in σ at each order in μ. In fact for the first few orders that we have analysed, we find that

$$
C^{\mathrm{bos}}_{\mathrm{R}} \approx \left(1 + \sigma(1+\eta) \right) C^{\mathrm{bos}}_{\mathrm{AdS}} \,,
$$

$$(F.5)$$

where at each order in μ the difference starts at the subsubleading contribution in σ. The same behaviour can also be seen in the case where the heavy operator is dual to the conical defect (compare (4.82) and (4.83)).

Bibliography

[1] S. Giusto, M. R. R. Hughes and R. Russo, *The Regge limit of AdS$_3$ holographic correlators*, *JHEP* **11** (2020) 018 [2007.12118].

[2] N. Ceplak, S. Giusto, M. R. R. Hughes and R. Russo, *Holographic correlators with multi-particle states*, 2105.04670.

[3] N. Ceplak and M. R. R. Hughes, *The Regge limit of AdS$_3$ holographic correlators with heavy states: towards the black hole regime*, 2102.09549.

[4] S. M. Carroll, *Spacetime and Geometry*. Cambridge University Press, 7, 2019.

[5] S. W. Hawking and G. F. R. Ellis, *The Large Scale Structure of Space-Time*, Cambridge Monographs on Mathematical Physics. Cambridge University Press, 1973, 10.1017/CBO9780511524646.

[6] M. B. Green, J. H. Schwarz and E. Witten, *Superstring Theory Vol. 1: 25th Anniversary Edition*, Cambridge Monographs on Mathematical Physics. Cambridge University Press, 11, 2012, 10.1017/CBO9781139248563.

[7] M. B. Green, J. H. Schwarz and E. Witten, *Superstring Theory Vol. 2: 25th Anniversary Edition*, Cambridge Monographs on Mathematical Physics. Cambridge University Press, 11, 2012, 10.1017/CBO9781139248570.

[8] R. Blumenhagen, D. Lüst and S. Theisen, *Basic concepts of string theory*, Theoretical and Mathematical Physics. Springer, Heidelberg, Germany, 2013, 10.1007/978-3-642-29497-6.

[9] J. M. Bardeen, B. Carter and S. W. Hawking, *The Four laws of black hole mechanics*, *Commun. Math. Phys.* **31** (1973) 161.

[10] S. W. Hawking, *Gravitational radiation from colliding black holes*, *Phys. Rev. Lett.* **26** (1971) 1344.

[11] S. W. Hawking, *Particle Creation by Black Holes*, *Commun. Math. Phys.* **43** (1975) 199.

[12] S. W. Hawking, *Breakdown of Predictability in Gravitational Collapse*, *Phys. Rev.* **D14** (1976) 2460.

[13] S. D. Mathur, *The information paradox: A pedagogical introduction*, *Class. Quant. Grav.* **26** (2009) 224001 [`0909.1038`].

[14] S. Raju, *Lessons from the Information Paradox*, `2012.05770`.

[15] S. B. Giddings, *Nonviolent nonlocality*, *Phys. Rev. D* **88** (2013) 064023 [`1211.7070`].

[16] A. Almheiri, T. Hartman, J. Maldacena, E. Shaghoulian and A. Tajdini, *The entropy of Hawking radiation*, `2006.06872`.

[17] P. Chen, Y. C. Ong and D.-h. Yeom, *Black Hole Remnants and the Information Loss Paradox*, *Phys. Rept.* **603** (2015) 1 [`1412.8366`].

[18] S. D. Mathur, *Remnants, Fuzzballs or Wormholes?*, *Int. J. Mod. Phys. D* **23** (2014) 1442024 [`1406.0807`].

[19] S. Raju and P. Shrivastava, *Critique of the fuzzball program*, *Phys. Rev. D* **99** (2019) 066009 [`1804.10616`].

[20] S. D. Mathur, *The fuzzball proposal for black holes: An elementary review*, *Fortsch. Phys.* **53** (2005) 793 [`hep-th/0502050`].

[21] H. A. Buchdahl, *General Relativistic Fluid Spheres*, *Phys. Rev.* **116** (1959) 1027.

[22] V. Cardoso and P. Pani, *Testing the nature of dark compact objects: a status report*, *Living Rev. Rel.* **22** (2019) 4 [`1904.05363`].

[23] A. Strominger and C. Vafa, *Microscopic origin of the Bekenstein-Hawking entropy*, *Phys.Lett.* **B379** (1996) 99 [`hep-th/9601029`].

[24] O. Lunin and S. D. Mathur, *AdS/CFT duality and the black hole information paradox*, *Nucl. Phys.* **B623** (2002) 342 [`hep-th/0109154`].

[25] I. Bena, C.-W. Wang and N. P. Warner, *Mergers and Typical Black Hole Microstates*, *JHEP* **11** (2006) 042 [`hep-th/0608217`].

[26] I. Kanitscheider, K. Skenderis and M. Taylor, *Fuzzballs with internal excitations*, *JHEP* **06** (2007) 056 [`0704.0690`].

[27] I. Bena, S. Giusto, E. J. Martinec, R. Russo, M. Shigemori, D. Turton et al., *Smooth horizonless geometries deep inside the black-hole regime*, *Phys. Rev. Lett.* **117** (2016) 201601 [`1607.03908`].

[28] N. P. Warner, *Lectures on Microstate Geometries*, 1912.13108.

[29] A. Almheiri, D. Marolf, J. Polchinski and J. Sully, *Black Holes: Complementarity or Firewalls?*, *JHEP* **02** (2013) 062 [1207.3123].

[30] A. Tyukov, R. Walker and N. P. Warner, *Tidal Stresses and Energy Gaps in Microstate Geometries*, *JHEP* **02** (2018) 122 [1710.09006].

[31] I. Bena, A. Houppe and N. P. Warner, *Delaying the Inevitable: Tidal Disruption in Microstate Geometries*, 2006.13939.

[32] E. J. Martinec and N. P. Warner, *The Harder They Fall, the Bigger They Become: Tidal Trapping of Strings by Microstate Geometries*, *JHEP* **04** (2021) 259 [2009.07847].

[33] I. Bena, E. J. Martinec, R. Walker and N. P. Warner, *Early Scrambling and Capped BTZ Geometries*, *JHEP* **04** (2019) 126 [1812.05110].

[34] N. Ceplak, S. Hampton and Y. Li, *A Helix Down the Throat: Internal Tidal Effects*, 2106.03841.

[35] S. D. Mathur, *Fuzzballs and the information paradox: a summary and conjectures*, 0810.4525.

[36] V. Balasubramanian, P. Kraus and M. Shigemori, *Massless black holes and black rings as effective geometries of the D1-D5 system*, *Class. Quant. Grav.* **22** (2005) 4803 [hep-th/0508110].

[37] E. J. Martinec and S. Massai, *String Theory of Supertubes*, *JHEP* **07** (2018) 163 [1705.10844].

[38] E. J. Martinec, S. Massai and D. Turton, *Little Strings, Long Strings, and Fuzzballs*, *JHEP* **11** (2019) 019 [1906.11473].

[39] E. J. Martinec, S. Massai and D. Turton, *Stringy Structure at the BPS Bound*, *JHEP* **12** (2020) 135 [2005.12344].

[40] J. M. Maldacena, *The large N limit of superconformal field theories and supergravity*, *Adv. Theor. Math. Phys.* **2** (1998) 231 [hep-th/9711200].

[41] J. R. David, G. Mandal and S. R. Wadia, *Microscopic formulation of black holes in string theory*, *Phys. Rept.* **369** (2002) 549 [hep-th/0203048].

[42] S. B. Giddings, *Flat space scattering and bulk locality in the AdS / CFT correspondence*, *Phys. Rev. D* **61** (2000) 106008 [hep-th/9907129].

[43] S. B. Giddings, *The Boundary S matrix and the AdS to CFT dictionary*, *Phys. Rev. Lett.* **83** (1999) 2707 [`hep-th/9903048`].

[44] J. Polchinski, *S matrices from AdS space-time*, `hep-th/9901076`.

[45] J. Penedones, *Writing CFT correlation functions as AdS scattering amplitudes*, *JHEP* **03** (2011) 025 [`1011.1485`].

[46] M. Ammon and J. Erdmenger, *Gauge/gravity duality: Foundations and applications*. Cambridge University Press, Cambridge, 4, 2015.

[47] F. Aprile, J. Drummond, P. Heslop and H. Paul, *Double-trace spectrum of $N = 4$ supersymmetric Yang-Mills theory at strong coupling*, *Phys. Rev.* **D98** (2018) 126008 [`1802.06889`].

[48] F. Aprile, J. M. Drummond, P. Heslop, H. Paul, F. Sanfilippo, M. Santagata et al., *Single particle operators and their correlators in free $\mathcal{N} = 4$ SYM*, *JHEP* **11** (2020) 072 [`2007.09395`].

[49] M. Taylor, *Matching of correlators in AdS(3) / CFT(2)*, *JHEP* **0806** (2008) 010 [`0709.1838`].

[50] S. Giusto, S. Rawash and D. Turton, *Ads_3 holography at dimension two*, *JHEP* **07** (2019) 171 [`1904.12880`].

[51] S. Rawash and D. Turton, *Supercharged AdS_3 Holography*, `2105.13046`.

[52] M. Kulaxizi, G. S. Ng and A. Parnachev, *Black Holes, Heavy States, Phase Shift and Anomalous Dimensions*, *SciPost Phys.* **6** (2019) 065 [`1812.03120`].

[53] R. Karlsson, M. Kulaxizi, A. Parnachev and P. Tadić, *Black Holes and Conformal Regge Bootstrap*, *JHEP* **10** (2019) 046 [`1904.00060`].

[54] I. Bena, S. Giusto, R. Russo, M. Shigemori and N. P. Warner, *Habemus Superstratum! A constructive proof of the existence of superstrata*, *JHEP* **1505** (2015) 110 [`1503.01463`].

[55] I. Bena, S. Giusto, E. J. Martinec, R. Russo, M. Shigemori, D. Turton et al., *Asymptotically-flat supergravity solutions deep inside the black-hole regime*, *JHEP* **02** (2018) 014 [`1711.10474`].

[56] E. Witten, *Anti-de Sitter space and holography*, *Adv. Theor. Math. Phys.* **2** (1998) 253 [`hep-th/9802150`].

[57] H. Liu and A. A. Tseytlin, *On four point functions in the CFT / AdS correspondence*, *Phys. Rev. D* **59** (1999) 086002 [`hep-th/9807097`].

[58] E. D'Hoker, D. Z. Freedman, S. D. Mathur, A. Matusis and L. Rastelli, *Extremal correlators in the AdS/CFT correspondence*, `hep-th/9908160`.

[59] E. D'Hoker, D. Z. Freedman, S. D. Mathur, A. Matusis and L. Rastelli, *Graviton and gauge boson propagators in AdS(d+1)*, *Nucl. Phys.* **B562** (1999) 330 [`hep-th/9902042`].

[60] E. D'Hoker, S. D. Mathur, A. Matusis and L. Rastelli, *The operator product expansion of N = 4 SYM and the 4- point functions of supergravity*, *Nucl. Phys.* **B589** (2000) 38 [`hep-th/9911222`].

[61] E. D'Hoker, D. Z. Freedman, S. D. Mathur, A. Matusis and L. Rastelli, *Graviton exchange and complete 4-point functions in the AdS/CFT correspondence*, *Nucl. Phys.* **B562** (1999) 353 [`hep-th/9903196`].

[62] E. D'Hoker, D. Z. Freedman and L. Rastelli, *AdS / CFT four point functions: How to succeed at z integrals without really trying*, *Nucl. Phys.* **B562** (1999) 395 [`hep-th/9905049`].

[63] A. Fitzpatrick, J. Kaplan, J. Penedones, S. Raju and B. C. van Rees, *A Natural Language for AdS/CFT Correlators*, *JHEP* **11** (2011) 095 [`1107.1499`].

[64] L. Rastelli and X. Zhou, *Mellin amplitudes for $AdS_5 \times S^5$*, *Phys. Rev. Lett.* **118** (2017) 091602 [`1608.06624`].

[65] L. Rastelli and X. Zhou, *How to Succeed at Holographic Correlators Without Really Trying*, *JHEP* **04** (2018) 014 [`1710.05923`].

[66] L. Rastelli, K. Roumpedakis and X. Zhou, **$AdS_3 \times S^3$** *Tree-Level Correlators: Hidden Six-Dimensional Conformal Symmetry*, *JHEP* **10** (2019) 140 [`1905.11983`].

[67] L. F. Alday, *Large Spin Perturbation Theory for Conformal Field Theories*, *Phys. Rev. Lett.* **119** (2017) 111601 [`1611.01500`].

[68] S. Caron-Huot, *Analyticity in Spin in Conformal Theories*, *JHEP* **09** (2017) 078 [`1703.00278`].

[69] L. F. Alday and S. Caron-Huot, *Gravitational S-matrix from CFT dispersion relations*, *JHEP* **12** (2018) 017 [`1711.02031`].

[70] A. Galliani, S. Giusto, E. Moscato and R. Russo, *Correlators at large c without information loss*, *JHEP* **09** (2016) 065 [`1606.01119`].

[71] A. Galliani, S. Giusto and R. Russo, *Holographic 4-point correlators with heavy states*, *JHEP* **10** (2017) 040 [`1705.09250`].

[72] A. Bombini, A. Galliani, S. Giusto, E. Moscato and R. Russo, *Unitary 4-point correlators from classical geometries*, *Eur. Phys. J.* **C78** (2018) 8 [`1710.06820`].

[73] S. Giusto, R. Russo and C. Wen, *Holographic correlators in AdS₃*, *JHEP* **03** (2019) 096 [`1812.06479`].

[74] S. Giusto, R. Russo, A. Tyukov and C. Wen, *Holographic correlators in AdS₃ without Witten diagrams*, *JHEP* **09** (2019) 030 [`1905.12314`].

[75] S. Giusto, R. Russo, A. Tyukov and C. Wen, *The CFT₆ origin of all tree-level 4-point correlators in AdS₃ × S³*, *Eur. Phys. J. C* **80** (2020) 736 [`2005.08560`].

[76] C. Wen and S.-Q. Zhang, *Notes on gravity multiplet correlators in AdS₃ × S³*, `2106.03499`.

[77] O. Lunin and S. D. Mathur, *Metric of the multiply wound rotating string*, *Nucl. Phys.* **B610** (2001) 49 [`hep-th/0105136`].

[78] I. Bena, P. Heidmann, R. Monten and N. P. Warner, *Thermal Decay without Information Loss in Horizonless Microstate Geometries*, `1905.05194`.

[79] I. Bena, F. Eperon, P. Heidmann and N. P. Warner, *The Great Escape: Tunneling out of Microstate Geometries*, *JHEP* **04** (2021) 112 [`2005.11323`].

[80] A. Bombini and A. Galliani, *AdS₃ four-point functions from $\frac{1}{8}$ -BPS states*, *JHEP* **06** (2019) 044 [`1904.02656`].

[81] J. Tian, J. Hou and B. Chen, *Holographic Correlators on Integrable Superstrata*, `1904.04532`.

[82] S. B. Giddings and R. A. Porto, *The Gravitational S-matrix*, *Phys. Rev. D* **81** (2010) 025002 [`0908.0004`].

[83] M. Levy and J. Sucher, *Eikonal approximation in quantum field theory*, *Phys. Rev.* **186** (1969) 1656.

[84] I. Sachs and T. Tran, *On Non-Perturbative Unitarity in Gravitational Scattering*, *Eur. Phys. J. C* **79** (2019) 914 [`1902.08409`].

[85] D. Amati, M. Ciafaloni and G. Veneziano, *Superstring Collisions at Planckian Energies*, *Phys. Lett.* **B197** (1987) 81.

[86] D. Amati, M. Ciafaloni and G. Veneziano, *Classical and Quantum Gravity Effects from Planckian Energy Superstring Collisions*, *Int. J. Mod. Phys.* **A3** (1988) 1615.

[87] P. C. Aichelburg and R. U. Sexl, *On the Gravitational field of a massless particle*, *Gen. Rel. Grav.* **2** (1971) 303.

[88] G. 't Hooft, *Graviton Dominance in Ultrahigh-Energy Scattering*, *Phys. Lett. B* **198** (1987) 61.

[89] L. Cornalba, M. S. Costa, J. Penedones and R. Schiappa, *Eikonal Approximation in AdS/CFT: From Shock Waves to Four-Point Functions*, *JHEP* **08** (2007) 019 [`hep-th/0611122`].

[90] L. Cornalba, M. S. Costa, J. Penedones and R. Schiappa, *Eikonal Approximation in AdS/CFT: Conformal Partial Waves and Finite N Four-Point Functions*, *Nucl. Phys. B* **767** (2007) 327 [`hep-th/0611123`].

[91] L. Cornalba, M. S. Costa and J. Penedones, *Eikonal approximation in AdS/CFT: Resumming the gravitational loop expansion*, *JHEP* **09** (2007) 037 [`0707.0120`].

[92] L. Cornalba, *Eikonal methods in AdS/CFT: Regge theory and multi-reggeon exchange*, `0710.5480`.

[93] L. Cornalba, M. S. Costa and J. Penedones, *Deep Inelastic Scattering in Conformal QCD*, *JHEP* **03** (2010) 133 [`0911.0043`].

[94] M. S. Costa, V. Goncalves and J. Penedones, *Conformal Regge theory*, *JHEP* **12** (2012) 091 [`1209.4355`].

[95] M. S. Costa, T. Hansen and J. a. Penedones, *Bounds for OPE coefficients on the Regge trajectory*, *JHEP* **10** (2017) 197 [`1707.07689`].

[96] M. Kulaxizi, A. Parnachev and A. Zhiboedov, *Bulk Phase Shift, CFT Regge Limit and Einstein Gravity*, *JHEP* **06** (2018) 121 [`1705.02934`].

[97] D. Li, D. Meltzer and D. Poland, *Conformal Bootstrap in the Regge Limit*, *JHEP* **12** (2017) 013 [`1705.03453`].

[98] G. D'Appollonio, P. Di Vecchia, R. Russo and G. Veneziano, *High-energy string-brane scattering: leading eikonal and beyond*, *JHEP* **11** (2010) 100 [`1008.4773`].

[99] A. L. Fitzpatrick, J. Kaplan and M. T. Walters, *Universality of Long-Distance AdS Physics from the CFT Bootstrap*, *JHEP* **08** (2014) 145 [`1403.6829`].

[100] A. L. Fitzpatrick, J. Kaplan and M. T. Walters, *Virasoro Conformal Blocks and Thermality from Classical Background Fields*, *JHEP* **11** (2015) 200 [`1501.05315`].

[101] R. Karlsson, M. Kulaxizi, A. Parnachev and P. Tadić, *Leading Multi-Stress Tensors and Conformal Bootstrap*, *JHEP* **01** (2020) 076 [1909.05775].

[102] Y.-Z. Li and H.-Y. Zhang, *More on heavy-light bootstrap up to double-stress-tensor*, *JHEP* **10** (2020) 055 [2004.04758].

[103] L. Cornalba, M. S. Costa and J. Penedones, *Eikonal Methods in AdS/CFT: BFKL Pomeron at Weak Coupling*, *JHEP* **06** (2008) 048 [0801.3002].

[104] R. C. Brower, M. J. Strassler and C.-I. Tan, *On The Pomeron at Large 't Hooft Coupling*, *JHEP* **03** (2009) 092 [0710.4378].

[105] D. Meltzer, *AdS/CFT Unitarity at Higher Loops: High-Energy String Scattering*, *JHEP* **05** (2020) 133 [1912.05580].

[106] A. Antunes, M. S. Costa, T. Hansen, A. Salgarkar and S. Sarkar, *The perturbative CFT optical theorem and high-energy string scattering in AdS at one loop*, *JHEP* **04** (2021) 088 [2012.01515].

[107] S. H. Strogatz, *Nonlinear Dynamics and Chaos: With Applications to Physics, Biology, Chemistry and Engineering*. Westview Press, 2000.

[108] D. A. Roberts, D. Stanford and L. Susskind, *Localized shocks*, *JHEP* **03** (2015) 051 [1409.8180].

[109] J. Riddell and E. S. Sørensen, *Out-of-time ordered correlators and entanglement growth in the random-field XX spin chain*, *Phys. Rev. B* **99** (2019) 054205 [1810.00038].

[110] J.-H. Bao and C.-Y. Zhang, *Out-of-time-order correlators in the one-dimensional XY model*, *Commun. Theor. Phys.* **72** (2020) 085103 [1901.09327].

[111] B. Craps, M. De Clerck, D. Janssens, V. Luyten and C. Rabideau, *Lyapunov growth in quantum spin chains*, *Phys. Rev. B* **101** (2020) 174313 [1908.08059].

[112] J. Polchinski, *Chaos in the black hole S-matrix*, 1505.08108.

[113] S. H. Shenker and D. Stanford, *Black holes and the butterfly effect*, *JHEP* **03** (2014) 067 [1306.0622].

[114] S. H. Shenker and D. Stanford, *Multiple Shocks*, *JHEP* **12** (2014) 046 [1312.3296].

[115] D. A. Roberts and D. Stanford, *Two-dimensional conformal field theory and the butterfly effect*, *Phys. Rev. Lett.* **115** (2015) 131603 [1412.5123].

[116] S. Leichenauer, *Disrupting Entanglement of Black Holes*, *Phys. Rev. D* **90** (2014) 046009 [`1405.7365`].

[117] S. H. Shenker and D. Stanford, *Stringy effects in scrambling*, *JHEP* **05** (2015) 132 [`1412.6087`].

[118] J. Maldacena, S. H. Shenker and D. Stanford, *A bound on chaos*, *JHEP* **08** (2016) 106 [`1503.01409`].

[119] Y. Sekino and L. Susskind, *Fast Scramblers*, *JHEP* **10** (2008) 065 [`0808.2096`].

[120] P. Di Francesco, P. Mathieu and D. Senechal, *Conformal Field Theory*, Graduate Texts in Contemporary Physics. Springer-Verlag, New York, 1997, 10.1007/978-1-4612-2256-9.

[121] A. A. Belavin, A. M. Polyakov and A. B. Zamolodchikov, *Infinite Conformal Symmetry in Two-Dimensional Quantum Field Theory*, *Nucl. Phys. B* **241** (1984) 333.

[122] A. B. Zamolodchikov, *Two-dimensional conformal symmetry and critical four-spin correlation functions in the Ashkin-Teller model*, Sov. Phys. - JETP **63** (1986) 1061.

[123] I. Runkel and G. M. T. Watts, *A Nonrational CFT with c = 1 as a limit of minimal models*, *JHEP* **09** (2001) 006 [`hep-th/0107118`].

[124] O. Gamayun, N. Iorgov and O. Lisovyy, *Conformal field theory of Painlevé VI*, *JHEP* **10** (2012) 038 [`1207.0787`].

[125] A. B. Zamolodchikov, *CONFORMAL SYMMETRY IN TWO-DIMENSIONS: AN EXPLICIT RECURRENCE FORMULA FOR THE CONFORMAL PARTIAL WAVE AMPLITUDE*, *Commun. Math. Phys.* **96** (1984) 419.

[126] A. L. Fitzpatrick, J. Kaplan, M. T. Walters and J. Wang, *Eikonalization of Conformal Blocks*, *JHEP* **09** (2015) 019 [`1504.01737`].

[127] A. L. Fitzpatrick, J. Kaplan, D. Li and J. Wang, *Exact Virasoro Blocks from Wilson Lines and Background-Independent Operators*, *JHEP* **07** (2017) 092 [`1612.06385`].

[128] E. Hijano, P. Kraus, E. Perlmutter and R. Snively, *Semiclassical Virasoro blocks from AdS$_3$ gravity*, *JHEP* **12** (2015) 077 [`1508.04987`].

[129] A. L. Fitzpatrick and J. Kaplan, *Conformal Blocks Beyond the Semi-Classical Limit*, *JHEP* **05** (2016) 075 [`1512.03052`].

[130] E. Perlmutter, *Virasoro conformal blocks in closed form*, 1502.07742.

[131] M. Beccaria, A. Fachechi and G. Macorini, *Virasoro vacuum block at next-to-leading order in the heavy-light limit*, *JHEP* **02** (2016) 072 [1511.05452].

[132] K. B. Alkalaev and M. Pavlov, *Four-point conformal blocks with three heavy background operators*, *JHEP* **08** (2019) 038 [1905.03195].

[133] A. Bombini, S. Giusto and R. Russo, *A note on the Virasoro blocks at order 1/c*, *Eur. Phys. J. C* **79** (2019) 3 [1807.07886].

[134] C. Cardona, *Virasoro blocks at large exchange dimension*, *Nucl. Phys. B* **963** (2021) 115284 [2006.01237].

[135] A. M. Polyakov, *Nonhamiltonian approach to conformal quantum field theory*, *Zh. Eksp. Teor. Fiz.* **66** (1974) 23.

[136] S. Ferrara, A. F. Grillo and R. Gatto, *Tensor representations of conformal algebra and conformally covariant operator product expansion*, *Annals Phys.* **76** (1973) 161.

[137] D. Simmons-Duffin, *The Conformal Bootstrap*, in *Theoretical Advanced Study Institute in Elementary Particle Physics: New Frontiers in Fields and Strings*, 2, 2016, DOI [1602.07982].

[138] D. Poland, S. Rychkov and A. Vichi, *The Conformal Bootstrap: Theory, Numerical Techniques, and Applications*, *Rev. Mod. Phys.* **91** (2019) 015002 [1805.04405].

[139] R. Rattazzi, V. S. Rychkov, E. Tonni and A. Vichi, *Bounding scalar operator dimensions in 4D CFT*, *JHEP* **12** (2008) 031 [0807.0004].

[140] F. Kos, D. Poland, D. Simmons-Duffin and A. Vichi, *Precision Islands in the Ising and $O(N)$ Models*, *JHEP* **08** (2016) 036 [1603.04436].

[141] D. Z. Freedman and A. Van Proeyen, *Supergravity*. Cambridge Univ. Press, Cambridge, UK, 5, 2012.

[142] M. Duetsch and K.-H. Rehren, *Generalized free fields and the AdS - CFT correspondence*, *Annales Henri Poincare* **4** (2003) 613 [math-ph/0209035].

[143] L. F. Alday and J. M. Maldacena, *Comments on operators with large spin*, *JHEP* **11** (2007) 019 [0708.0672].

[144] Z. Komargodski and A. Zhiboedov, *Convexity and Liberation at Large Spin*, *JHEP* **11** (2013) 140 [1212.4103].

[145] I. Heemskerk, J. Penedones, J. Polchinski and J. Sully, *Holography from Conformal Field Theory*, *JHEP* **10** (2009) 079 [0907.0151].

[146] M. Shigemori, *Superstrata*, *Gen. Rel. Grav.* **52** (2020) 51 [2002.01592].

[147] E. Bakhshaei and A. Bombini, *Three-charge superstrata with internal excitations*, *Class. Quant. Grav.* **36** (2019) 055001 [1811.00067].

[148] J. P. Gauntlett, J. B. Gutowski, C. M. Hull, S. Pakis and H. S. Reall, *All supersymmetric solutions of minimal supergravity in five- dimensions*, *Class. Quant. Grav.* **20** (2003) 4587 [hep-th/0209114].

[149] I. Bena and N. P. Warner, *One ring to rule them all … and in the darkness bind them?*, *Adv.Theor.Math.Phys.* **9** (2005) 667 [hep-th/0408106].

[150] I. Bena and N. P. Warner, *Bubbling supertubes and foaming black holes*, *Phys.Rev.* **D74** (2006) 066001 [hep-th/0505166].

[151] I. Bena, S. Giusto, M. Shigemori and N. P. Warner, *Supersymmetric Solutions in Six Dimensions: A Linear Structure*, *JHEP* **1203** (2012) 084 [1110.2781].

[152] S. Giusto, L. Martucci, M. Petrini and R. Russo, *6D microstate geometries from 10D structures*, *Nucl.Phys.* **B876** (2013) 509 [1306.1745].

[153] O. Lunin, J. M. Maldacena and L. Maoz, *Gravity solutions for the D1-D5 system with angular momentum*, hep-th/0212210.

[154] O. Lunin, S. D. Mathur and A. Saxena, *What is the gravity dual of a chiral primary?*, *Nucl. Phys.* **B655** (2003) 185 [hep-th/0211292].

[155] V. S. Rychkov, *D1-D5 black hole microstate counting from supergravity*, *JHEP* **01** (2006) 063 [hep-th/0512053].

[156] M. Shigemori, *Counting Superstrata*, *JHEP* **10** (2019) 017 [1907.03878].

[157] D. R. Mayerson and M. Shigemori, *Counting D1-D5-P Microstates in Supergravity*, *SciPost Phys.* **10** (2021) 018 [2010.04172].

[158] J. B. Gutowski, D. Martelli and H. S. Reall, *All Supersymmetric solutions of minimal supergravity in six- dimensions*, *Class.Quant.Grav.* **20** (2003) 5049 [hep-th/0306235].

[159] I. Bena, E. Martinec, D. Turton and N. P. Warner, *M-theory Superstrata and the MSW String*, *JHEP* **06** (2017) 137 [1703.10171].

[160] I. Bena, D. Turton, R. Walker and N. P. Warner, *Integrability and Black-Hole Microstate Geometries*, 1709.01107.

[161] N. Čeplak, R. Russo and M. Shigemori, *Supercharging Superstrata*, *JHEP* **03** (2019) 095 [`1812.08761`].

[162] P. Heidmann and N. P. Warner, *Superstratum Symbiosis*, *JHEP* **09** (2019) 059 [`1903.07631`].

[163] P. Heidmann, D. R. Mayerson, R. Walker and N. P. Warner, *Holomorphic Waves of Black Hole Microstructure*, *JHEP* **02** (2020) 192 [`1910.10714`].

[164] D. R. Mayerson, R. A. Walker and N. P. Warner, *Microstate Geometries from Gauged Supergravity in Three Dimensions*, *JHEP* **10** (2020) 030 [`2004.13031`].

[165] Z. Carson, S. Hampton, S. D. Mathur and D. Turton, *Effect of the deformation operator in the D1D5 CFT*, *JHEP* **1501** (2015) 071 [`1410.4543`].

[166] S. Hampton, S. D. Mathur and I. G. Zadeh, *Lifting of D1-D5-P states*, *JHEP* **01** (2019) 075 [`1804.10097`].

[167] S. G. Avery, *Using the D1D5 CFT to Understand Black Holes*, `1012.0072`.

[168] A. Schwimmer and N. Seiberg, *Comments on the N=2, N=3, N=4 Superconformal Algebras in Two-Dimensions*, *Phys.Lett.* **B184** (1987) 191.

[169] S. Giusto, E. Moscato and R. Russo, *AdS$_3$ holography for 1/4 and 1/8 BPS geometries*, *JHEP* **11** (2015) 004 [`1507.00945`].

[170] I. Kanitscheider, K. Skenderis and M. Taylor, *Holographic anatomy of fuzzballs*, *JHEP* **0704** (2007) 023 [`hep-th/0611171`].

[171] J. Garcia i Tormo and M. Taylor, *One point functions for black hole microstates*, *Gen. Rel. Grav.* **51** (2019) 89 [`1904.10200`].

[172] M. Kulaxizi, G. S. Ng and A. Parnachev, *Subleading Eikonal, AdS/CFT and Double Stress Tensors*, *JHEP* **10** (2019) 107 [`1907.00867`].

[173] R. Karlsson, M. Kulaxizi, A. Parnachev and P. Tadić, *Stress tensor sector of conformal correlators operators in the Regge limit*, *JHEP* **07** (2020) 019 [`2002.12254`].

[174] I. S. Gradshteyn and I. M. Ryzhik, *Table of Integrals, Series, and Products (Seventh Edition)*. Academic Press, San Diego; London, 2007.

[175] A. Parnachev and K. Sen, *Notes on AdS-Schwarzschild eikonal phase*, `2011.06920`.

[176] D. Zagier, *The bloch-wigner-ramakrishnan polylogarithm function*, *Mathematische Annalen* **286** (1990) 613.

[177] D. Zagier, *Polylogarithms, dedekind zeta functions, and the algebraic k-theory of fields*, in *Arithmetic algebraic geometry*, pp. 391–430, Springer, (1991).

[178] N. I. Usyukina and A. I. Davydychev, *Exact results for three and four point ladder diagrams with an arbitrary number of rungs*, *Phys. Lett. B* **305** (1993) 136.

[179] S. Sachdev, *Polylogarithm identities in a conformal field theory in three-dimensions*, *Phys. Lett. B* **309** (1993) 285 [`hep-th/9305131`].

[180] E. Filothodoros, A. Petkou and N. Vlachos, *3d fermion-boson map with imaginary chemical potential*, *Phys. Rev. D* **95** (2017) 065029 [`1608.07795`].

[181] D. Dorigoni, M. B. Green and C. Wen, *Exact properties of an integrated correlator in $\mathcal{N} = 4$ $SU(N)$ SYM*, `2102.09537`.

[182] V. Gonçalves, R. Pereira and X. Zhou, *20′ Five-Point Function from $AdS_5 \times S^5$ Supergravity*, *JHEP* **10** (2019) 247 [`1906.05305`].

[183] F. Aprile, J. M. Drummond, P. Heslop and H. Paul, *Unmixing Supergravity*, *JHEP* **02** (2018) 133 [`1706.08456`].

[184] F. Aprile and M. Santagata, *Two-particle spectrum of tensor multiplets coupled to $AdS_3 \times S^3$ gravity*, `2104.00036`.

[185] L. F. Alday, A. Bissi and E. Perlmutter, *Holographic Reconstruction of AdS Exchanges from Crossing Symmetry*, *JHEP* **08** (2017) 147 [`1705.02318`].

[186] M. B. Green and C. Wen, *Maximal $U(1)_Y$-violating n-point correlators in $\mathcal{N} = 4$ super-Yang-Mills theory*, `2009.01211`.

[187] K. Skenderis and M. Taylor, *Fuzzball solutions and D1-D5 microstates*, *Phys.Rev.Lett.* **98** (2007) 071601 [`hep-th/0609154`].

[188] F. Larsen and E. J. Martinec, *U(1) charges and moduli in the D1 - D5 system*, *JHEP* **06** (1999) 019 [`hep-th/9905064`].

[189] M. Baggio, J. de Boer and K. Papadodimas, *A non-renormalization theorem for chiral primary 3-point functions*, *JHEP* **1207** (2012) 137 [`1203.1036`].

[190] D. Zagier, *The dilogarithm function*, in *Frontiers in Number Theory, Physics and Geometry II*, pp. 3–65, Springer-Verlag, Berlin-Heidelberg-New York, (2006).

[191] L. Lewin, *Polylogarithms and associated functions*. North-Holland, New York, NY, 1981.

[192] D. Ramakrishnan, *Analogs of the bloch-wigner function for higher polylogarithms*, *Contemp. Math* **55** (1986) 371.

[193] J. Rhodes, *Polylogarithms*, *Durham University* (2008) .

[194] R. Hain, *Classical Polylogarithms*, `9202022`.

[195] J. Maldacena, D. Simmons-Duffin and A. Zhiboedov, *Looking for a bulk point*, *JHEP* **01** (2017) 013 [`1509.03612`].

[196] D. Z. Freedman, S. D. Mathur, A. Matusis and L. Rastelli, *Comments on 4-point functions in the CFT/AdS correspondence*, *Phys. Lett.* **B452** (1999) 61 [`hep-th/9808006`].

[197] P. Kraus, A. Sivaramakrishnan and R. Snively, *Late time Wilson lines*, *JHEP* **04** (2019) 026 [`1810.01439`].

[198] M. Bianchi, D. Consoli and J. F. Morales, *Probing Fuzzballs with Particles, Waves and Strings*, *JHEP* **06** (2018) 157 [`1711.10287`].

[199] M. Bianchi, D. Consoli, A. Grillo and J. F. Morales, *The dark side of fuzzball geometries*, *JHEP* **05** (2019) 126 [`1811.02397`].

[200] M. Bianchi, A. Grillo and J. F. Morales, *Chaos at the rim of black hole and fuzzball shadows*, *JHEP* **05** (2020) 078 [`2002.05574`].

[201] V. Balasubramanian, J. de Boer, E. Keski-Vakkuri and S. F. Ross, *Supersymmetric conical defects: Towards a string theoretic description of black hole formation*, *Phys. Rev.* **D64** (2001) 064011 [`hep-th/0011217`].

[202] J. M. Maldacena and L. Maoz, *Desingularization by rotation*, *JHEP* **0212** (2002) 055 [`hep-th/0012025`].

[203] B. Craps, M. De Clerck, P. Hacker, K. Nguyen and C. Rabideau, *Slow scrambling in extremal BTZ and microstate geometries*, *JHEP* **03** (2021) 020 [`2009.08518`].

[204] J. Murugan, D. Stanford and E. Witten, *More on Supersymmetric and 2d Analogs of the SYK Model*, *JHEP* **08** (2017) 146 [`1706.05362`].

[205] M. Heydeman, J. H. Schwarz, C. Wen and S.-Q. Zhang, *All Tree Amplitudes of 6D* $(2,0)$ *Supergravity: Interacting Tensor Multiplets and the K3 Moduli Space*, *Phys. Rev. Lett.* **122** (2019) 111604 [`1812.06111`].

[206] J. H. Schwarz and C. Wen, *Unified Formalism for 6D Superamplitudes Based on a Symplectic Grassmannian*, *JHEP* **08** (2019) 125 [`1907.03485`].

[207] O. Aharony, L. F. Alday, A. Bissi and E. Perlmutter, *Loops in AdS from Conformal Field Theory*, *JHEP* **07** (2017) 036 [1612.03891].

[208] L. F. Alday and A. Bissi, *Loop Corrections to Supergravity on $AdS_5 \times S^5$*, *Phys. Rev. Lett.* **119** (2017) 171601 [1706.02388].

[209] L. F. Alday and X. Zhou, *Simplicity of AdS Supergravity at One Loop*, 1912.02663.

[210] F. Aprile, J. Drummond, P. Heslop and H. Paul, *One-loop amplitudes in $AdS_5 \times S^5$ supergravity from $\mathcal{N} = 4$ SYM at strong coupling*, *JHEP* **03** (2020) 190 [1912.01047].

[211] D. E. Berenstein, J. M. Maldacena and H. S. Nastase, *Strings in flat space and pp waves from N = 4 super Yang Mills*, JHEP **04** (2002) 013 [hep-th/0202021].

[212] E. Gava and K. S. Narain, *Proving the PP wave / CFT(2) duality*, *JHEP* **12** (2002) 023 [hep-th/0208081].

[213] J. McGreevy, L. Susskind and N. Toumbas, *Invasion of the giant gravitons from anti-de Sitter space*, JHEP **06** (2000) 008 [hep-th/0003075].

[214] M. Bianchi, D. Consoli, A. Grillo and J. F. Morales, *QNMs of branes, BHs and fuzzballs from Quantum SW geometries*, 2105.04245.

[215] G. Bonelli, C. Iossa, D. P. Lichtig and A. Tanzini, *Exact solution of Kerr black hole perturbations via CFT_2 and instanton counting*, 2105.04483.

[216] M. Alishahiha, A. Davody, A. Naseh and S. F. Taghavi, *On Butterfly effect in Higher Derivative Gravities*, *JHEP* **11** (2016) 032 [1610.02890].

[217] A. Bagchi, S. Chakrabortty, D. Grumiller, B. Radhakrishnan, M. Riegler and A. Sinha, *Non-Lorentzian Chaos and Cosmological Holography*, 2106.07649.

[218] D. R. Mayerson, *Fuzzballs and Observations*, *Gen. Rel. Grav.* **52** (2020) 115 [2010.09736].

[219] A. Bombini and G. Fardelli, *Holographic entanglement entropy and complexity of microstate geometries*, *JHEP* **06** (2020) 181 [1910.01831].

[220] S. Giusto and R. Russo, *Entanglement Entropy and D1-D5 geometries*, *Phys.Rev.* **D90** (2014) 066004 [1405.6185].

[221] C. T. Asplund and S. G. Avery, *Evolution of Entanglement Entropy in the D1-D5 Brane System*, *Phys.Rev.* **D84** (2011) 124053 [1108.2510].

[222] I. Bena and D. R. Mayerson, *Multipole Ratios: A New Window into Black Holes*, *Phys. Rev. Lett.* **125** (2020) 22 [2006.10750].

[223] I. Bena and D. R. Mayerson, *Black Holes Lessons from Multipole Ratios*, *JHEP* **03** (2021) 114 [2007.09152].

[224] M. Bianchi, D. Consoli, A. Grillo, J. F. Morales, P. Pani and G. Raposo, *Distinguishing fuzzballs from black holes through their multipolar structure*, *Phys. Rev. Lett.* **125** (2020) 221601 [2007.01743].

[225] M. Bianchi, D. Consoli, A. Grillo, J. F. Morales, P. Pani and G. Raposo, *The multipolar structure of fuzzballs*, *JHEP* **01** (2021) 003 [2008.01445].

[226] I. Bah, I. Bena, P. Heidmann, Y. Li and D. R. Mayerson, *Gravitational Footprints of Black Holes and Their Microstate Geometries*, 2104.10686.

[227] F. Bacchini, D. R. Mayerson, B. Ripperda, J. Davelaar, H. Olivares, T. Hertog et al., *Fuzzball Shadows: Emergent Horizons from Microstructure*, 2103.12075.

[228] F. C. Eperon, H. S. Reall and J. E. Santos, *Instability of supersymmetric microstate geometries*, *JHEP* **10** (2016) 031 [1607.06828].

[229] D. Marolf, B. Michel and A. Puhm, *A rough end for smooth microstate geometries*, *JHEP* **05** (2017) 021 [1612.05235].

[230] J. Keir, *Wave propagation on microstate geometries*, *Annales Henri Poincare* **21** (2019) 705 [1609.01733].

[231] F. C. Eperon, *Geodesics in supersymmetric microstate geometries*, *Class. Quant. Grav.* **34** (2017) 165003 [1702.03975].

[232] I. Bena, P. Heidmann and D. D. R. Mayerson, *Tidal Love Numbers for Microstate Geometries*, To appear.

[233] V. Dimitrov, T. Lemmens, D. R. Mayerson, V. S. Min and B. Vercnocke, *Gravitational Waves, Holography, and Black Hole Microstates*, 2007.01879.

[234] K. Saraswat and N. Afshordi, *Quantum Nature of Black Holes: Fast Scrambling versus Echoes*, *JHEP* **04** (2020) 136 [1906.02653].

[235] Q. Wang, N. Oshita and N. Afshordi, *Echoes from Quantum Black Holes*, *Phys. Rev. D* **101** (2020) 024031 [1905.00446].

[236] N. Oshita, Q. Wang and N. Afshordi, *On Reflectivity of Quantum Black Hole Horizons*, *JCAP* **04** (2020) 016 [1905.00464].

[237] T. Ikeda, M. Bianchi, D. Consoli, A. Grillo, J. F. Morales, P. Pani et al., *Black-hole microstate spectroscopy: ringdown, quasinormal modes, and echoes*, 2103.10960.

[238] S. G. Avery, B. D. Chowdhury and S. D. Mathur, *Emission from the D1D5 CFT*, *JHEP* **10** (2009) 065 [0906.2015].

[239] S. G. Avery and B. D. Chowdhury, *Emission from the D1D5 CFT: Higher Twists*, *JHEP* **01** (2010) 087 [0907.1663].

[240] B. Chakrabarty, D. Turton and A. Virmani, *Holographic description of non-supersymmetric orbifolded D1-D5-P solutions*, *JHEP* **11** (2015) 063 [1508.01231].

[241] B. Chakrabarty, D. Ghosh and A. Virmani, *Quasinormal modes of supersymmetric microstate geometries from the D1-D5 CFT*, *JHEP* **10** (2019) 072 [1908.01461].

[242] E. Barausse et al., *Prospects for Fundamental Physics with LISA*, *Gen. Rel. Grav.* **52** (2020) 81 [2001.09793].

[243] L. Barack et al., *Black holes, gravitational waves and fundamental physics: a roadmap*, *Class. Quant. Grav.* **36** (2019) 143001 [1806.05195].

[244] I. Bah and P. Heidmann, *Smooth Bubbling Geometries Without Supersymmetry*, 2106.05118.

[245] I. Bah and P. Heidmann, *Topological Stars, Black holes and Generalized Charged Weyl Solutions*, 2012.13407.

[246] A. Houppe and N. P. Warner, *Supersymmetry and Superstrata in Three Dimensions*, 2012.07850.

[247] B. Ganchev, A. Houppe and N. Warner, *Q-Balls Meet Fuzzballs: Non-BPS Microstate Geometries*, 2107.09677.

[248] B. Guo and S. D. Mathur, *To appear*, .

[249] S. G. Avery, B. D. Chowdhury and S. D. Mathur, *Deforming the D1D5 CFT away from the orbifold point*, *JHEP* **06** (2010) 031 [1002.3132].

[250] S. G. Avery, B. D. Chowdhury and S. D. Mathur, *Excitations in the deformed D1D5 CFT*, *JHEP* **06** (2010) 032 [1003.2746].

[251] B. Guo and S. D. Mathur, *Lifting of level-1 states in the D1D5 CFT*, *JHEP* **03** (2020) 028 [1912.05567].

[252] B. Guo and S. D. Mathur, *Lifting at higher levels in the D1D5 CFT*, *JHEP* **11** (2020) 145 [`2008.01274`].

[253] S. S. Gubser, I. R. Klebanov and A. M. Polyakov, *Gauge theory correlators from non-critical string theory*, *Phys. Lett.* **B428** (1998) 105 [`hep-th/9802109`].

[254] F. A. Dolan and H. Osborn, *Conformal four point functions and the operator product expansion*, *Nucl. Phys. B* **599** (2001) 459 [`hep-th/0011040`].

[255] G. Arutyunov, F. Dolan, H. Osborn and E. Sokatchev, *Correlation functions and massive Kaluza-Klein modes in the AdS / CFT correspondence*, *Nucl. Phys. B* **665** (2003) 273 [`hep-th/0212116`].

[256] D. Simmons-Duffin, D. Stanford and E. Witten, *A spacetime derivation of the Lorentzian OPE inversion formula*, *JHEP* **07** (2018) 085 [`1711.03816`].